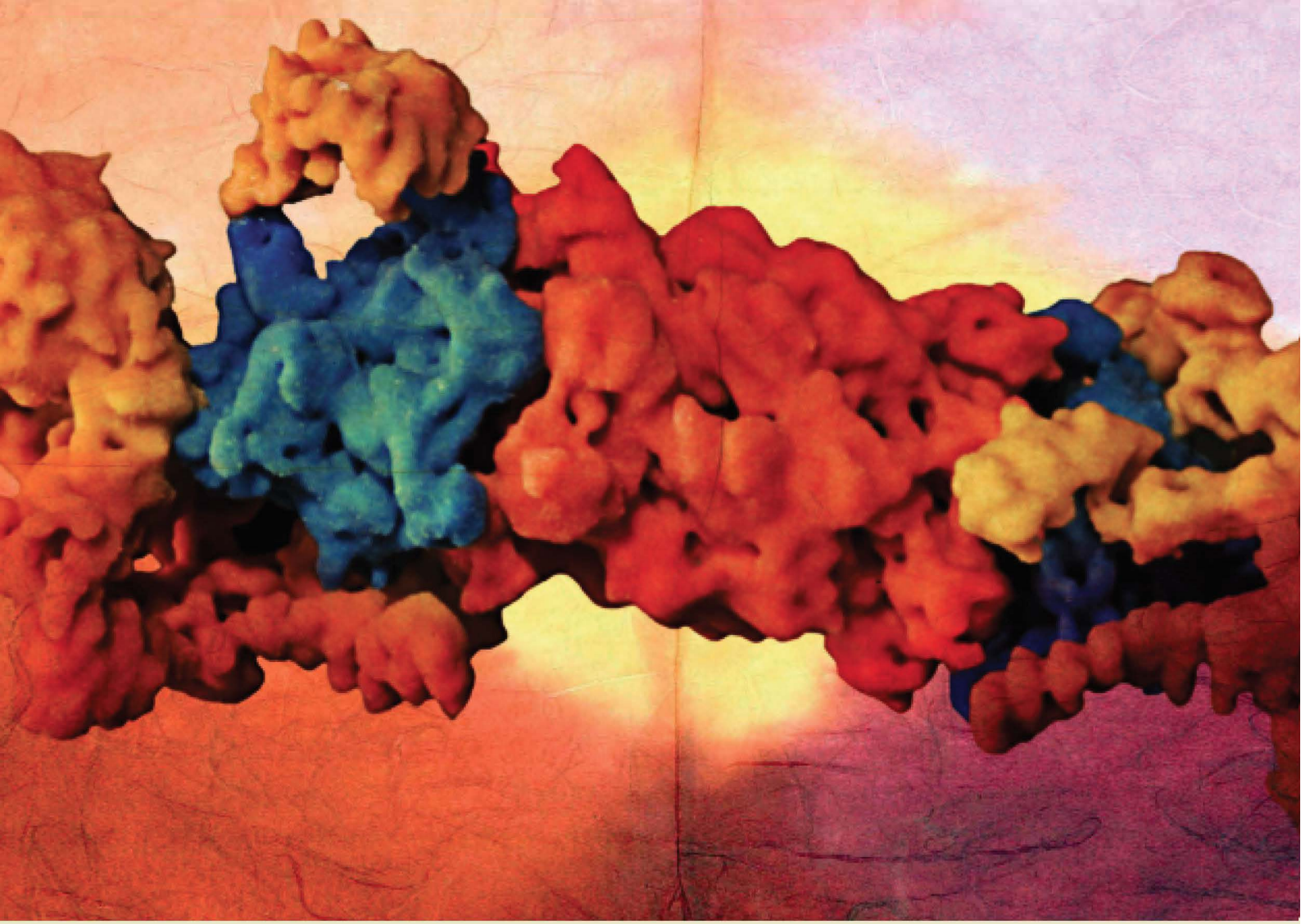

Ivan Lalanda Salazar

Regulation of the Ubiquitin-Proteasome System in brain ischemia: impact on the neuronal proteome

Tese de Doutoramento em Biologia Experimental e Biomedicina, ramo de Neurociências e Doença, orientada pelo Professor Doutor Carlos Bandeira Duarte e pela Doutora Margarida Vaz Caldeira, apresentada ao Instituto de Investigação Interdisciplinar da Universidade de Coimbra.

Novembro 2016

· U C ·

Universidade de Coimbra

Regulation of the Ubiquitin-Proteasome System in brain ischemia:

impact on the neuronal proteome

Regulação do Sistema Ubiquitina-Proteassoma em isquémia cerebral

o impacto no proteoma neuronal

Ivan Lalanda Salazar

November 2016

Regulation of the Ubiquitin-Proteasome System in brain ischemia:

impact on the neuronal proteome

Ivan Lalanda Salazar

PhD thesis presented to the Institute for Interdisciplinary Research of the University of Coimbra (IIIUC) in fulfillment of the requirements for a Doctoral degree in Experimental Biology and Biomedicine, specialization in Neuroscience and Disease

Tese de Doutoramento apresentada ao Instituto de Investigação Interdisciplinar da Universidade de Coimbra (IIIUC), para cumprimento dos requisitos necessários à obtenção do grau de Doutor em Biologia Experimental e Biomedicina, no ramo de Neurociências e Doença

This work was performed at the Center for Neuroscience and Cell Biology, University of Coimbra, Portugal, under the supervision of Professors Carlos Bandeira Duarte and Margarida Vaz Caldeira.

This work was supported by FEDER funds through the Operational Programme Factors Competitiveness - COMPETE 2020 and by National Funds through FCT - Foundation for Science and Technology under the Strategic Project (UID/NEU/04539/2013) and by the PhD scholarship SFRH/BD/51967/2012.

Este trabalho foi realizado no Centro de Neurociências e Biologia Celular da Universidade de Coimbra, Portugal, sob orientação do Professor Doutor Carlos Bandeira Duarte e da Doutora Margarida Vaz Caldeira.

Este trabalho foi financiado por fundos FEDER através do Programa Operacional Fatores de Competitividade – COMPETE, por fundos nacionais, através da FCT - Fundação para a Ciência e Tecnologia pelo projeto estratégico UID/NEU/04539/2013 e pela bolsa de doutoramento SFRH/BD/51967/2012.

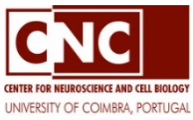

Dedico a tese à minha namorada,

pais e amigos

Cover note

The image presented in the cover of this thesis represent the artistic structure of the 26S Proteasome. Image adapted from Keio J Med. 2013;62(1):1-12.

Agradecimentos

Em primeiro lugar, gostaria de agradecer aos meus pais por me terem educado da melhor forma possível, pela ajuda, e por terem possibilitado que eu prosseguisse os meus estudos até esta etapa final para obtenção do grau de Doutor. Um muito obrigado por tudo. Espero um dia poder retribuir tudo em dobro.

Ao Professor Carlos Duarte, por me ter acolhido desde o tempo longínquo de 2011, na altura para fazer o meu trabalho de dissertação de mestrado. Um muito obrigado por incutir nos seus alunos o espirito critico, o gosto pela Ciência e ainda pela excecional orientação. Espero ter contribuído para mudar um pouco a linha de investigação do seu grupo, um exemplo de pessoa e de chefe. Um muito obrigado pela amizade nestes 5/6 anos que foram realmente marcantes, espero que nunca mude.

À Margarida, um agradecimento muito especial pela ajuda e orientação dada durante este período de tempo. Um muito obrigado pela pessoa que és; carinhosa, afável e amável. Um exemplo para muitos. Fica aqui um pedido de desculpas "quase" público, pelas baboseiras que muitas vezes digo.

Aos elementos do grupo CBD que foram passando, e ficando, gostaria de destacar o Diogo Comprido, pela amizade que irá perdurar, o Pedro Afonso, pelo amigo que é, apesar de nunca se calar, o Graciano Leal, pela calma que o caracteriza, o João Costa, o grande Benfiquista e pessoa incrível que é, e o Michele Curcio, por ser o devorador de bolachas alheias (ou doces em geral!). Foram e sempre serão pessoas que nunca esquecerei. Ao rapper Ricardo Vieira (Smiggers), que apesar de ter estado pouco tempo, deixou marca no laboratório. Foram muitos GB de vídeos parvos e musicas que vimos no Youtube, um connoisseur das grandes artes. À Miranda Mele, um agradecimento especial pela ajuda, amizade e simpatia de pessoa que te é característico. Arrisco-me a dizer marcaste todos os que passaram no laboratório, inclusive a mim. Desculpa também por deixar permanentemente a bancada desarrumada, não é por mal. Podes contar sempre comigo.

Aos colegas e amigos de grupos vizinhos, obrigado Dominique e Tatiana pela verdadeira amizade e por aturarem as minhas parvoíces. Das melhores pessoas que levo daqui. Obrigado ainda Tatiana pela organização de eventos, pelo melhor salame do Mundo e pela encomenda das águas. À Luísa Cortes e à Sandra Santos agradeço a amizade, e a companhia nos almoços e cafés. Sandra, és incrível a tentar resolver problemas relacionado com o toner da impressora. Rui Costa, obrigado por teres casado com a Miranda, pela companhia e pelas conversas de

desporto. Por seres a pessoa mais zen que conheço, considero-te um exemplo para muitos. Vão ser os melhores pais de sempre. Ao Carlos Matos, obrigado por seres quem és, um viciado em anime, e pela tua amizade sempre verdadeira. São todos amigos para a vida.

Ao Luís Ribeiro e Maria Joana, um muito obrigado por me terem dado a oportunidade de partilhar o espaço de laboratório convosco e acima de tudo pela amizade. De todos, são os que vivem mais o papel de Cientista e espero que assim continuem.

Às princesas Mariana Botelho, Marisa Ferreira e Sara Silva, obrigado por me terem ajudado nos momentos mais difíceis. Estou ainda agradecido pela vossa forte tentativa de me ensinarem a dançar quizomba. Escusado será dizer que não funcionou. Foram de facto momentos muito bem passados. São amigas para a vida.

À Professora Ana Luísa, principalmente pela sua simpatia, ao Peça e ao Ramiro, um muito obrigado pela orientação cientifica e questões pertinentes efetuadas nas reuniões.

Um agradecimento especial à Joana Leite e à Mariana Morgado pela amizade que perdura desde os tempos da licenciatura. São destas boas amizades que de facto vão perdurando.

À Mariline Silva, Joana Pedro, Pedro Alves, Marina Rodrigues, Débora, Mário, Calmeiro, Renato, Luis Martins, Joana Fernandes, Rossella Vetrone, Barbara Correia, Marta Vieira, Beatriz Rodrigues (por nunca te calares) e Eduardo, um especial obrigado pela ajuda e apoio que de alguma forma me deram durante estes 4 anos.

Não podia deixar de agradecer à Dona Céu e à grande Elisabete. Ambas contribuíram para o bom funcionamento do laboratório. À Dona Céu, por ser a pessoa mais querida que conheço e, à Beta, por ser uma mulher de armas, apesar do teu feitio por vezes difícil. À Sara Lopes, um muito obrigado pela amizade e pela ajuda que nos dá todos os dias.

Ao meu ano do BEB, um muito obrigado a todos, dando mais enfâse aqueles que partilharam o mesmo espaço de trabalho durante estes últimos 4 anos. Destes, um muito obrigado pela amizade e carinho Mr Mo, Gladys, Lara Franco, Sara Oliveira e Jeannette.

À malta do cross, agradeço a todos pela horita diária em que nos distraímos do trabalho e tentamos levantar algum peso. Seja ele muito ou pouco, é sempre de boa vontade e com muito boa disposição. De forma geral, partilhamos sempre as mesmas lesões. Sejam elas ombros doridos, canelas e mãos em ferida, chichoteadas dos double unders, um quase vómito depois de um cardio demoníaco, entre outras. Um muito obrigado por me ajudarem a esquecer temporariamente os meus problemas. São todos todos incríveis.

À minha gatinha, por seres super autista e estares sempre enfiada no guarda-fatos. Foste uma grande ajuda na escrita e elaboração deste trabalho.

Ao resto da minha família, pela importante contribuição que deram na minha educação e em momentos chave da minha vida. Um agradecimento aos meus avós, tias e primos. Sem vocês nada disto era possível. Gostava de agradecer de forma particular à minha prima Andreia por tudo. Um muito obrigado.

Por ultimo, mas não menos importante, agradeço do fundo do coração à minha namorada Ana Inês Martins, a pessoa mais importante da minha vida. Marcaste de forma muito forte o início do meu percurso académico, já no longínquo ano de 2007, ano em que tudo começou. Um muito obrigado pela tarefa árdua em me aturar, eu sei que é uma missão muito difícil. Espero que assim continuemos. Amo-te.

Ao Departamento de Ciências da Vida da Faculdade de Ciências e Tecnologia da Universidade de Coimbra e ao Centro de Neurociências e Biologia Celular, pelas condições facultadas para a realização deste trabalho.

À Fundação para a Ciência e Tecnologia pelo financiamento.

A todos os que me fazem feliz,

Index

Abbreviations

ADAR- Adenosine deaminase acting on RNA

AIF- Apoptosis inducing factor

AMPAR- α-amino-3-hydroxy-5-methyl-4-isoxazolepropionic acid receptor

APV- D(-)-2-Amino-5-phosphopentanoic acid

APC/C- Anaphase-promoting complex/cyclosome

Arc- Activity-regulated cytoskeleton- associated protein

BBB- Blood-Brain barrier

BCCAo- Bilateral common carotid artery occlusion

BCo- Bilateral carotid occlusion

CamKII- Calcium/calmodulin-dependent protein kinase, type II

CAPNS- Small (30 kDa) regulatory subunit of calpain

CBSW- Calpain-type beta-sandwich domain

Cdk5- Cyclin-dependent kinase 5

CF- Cytosolic fraction

CNS- Central nervous system

CP- Catalytic particle

CREB- cAMP response element-binding protein

CyspC- Calpain-type cysteine protease core

DIV- days in vitro

eEF- eukaryotic elongation factor

eIF- eukaryotic initiation factor

ECM29- Extracellular mutant 29

EAAT- Excitatory amino acid transporter

FMRP- Fragil-X mental retardation protein

GFP- Green fluorescent protein

HECT- Homologous to E6-AP Carboxyl Terminus

KA- Kainic acid/kainate

LDH- Lactate dehydrogenase

LTD- Long-term depression

MDM2- Murine double minute 2

LTP- Long-term potentiation

MTT- 3-(4,5-dimethylthiazol-2-yl)-2,5-diphenyltetrazolium bromide

MCAo- Middle cerebral arterial occlusion

MMF- Microsomal and plasma membrane fraction

Nedd4- Neural-precursor cell-expressed developmentally downregulated gene 4

NF-kB- Nuclear Factor-κappaB

NMF- Nuclear and mitochondrial fraction

NMDAR- N-methyl-D-aspartate receptors

NOS- Nitric oxide synthase

OGD- Oxygen-Glucose Deprivation

PAGE- Polyacrylamide gel electrophoresis

PSD- Post-synaptic density

PHLPP1- PH Domain and Leucine Rich Repeat Protein Phosphatase 1

PKA- Protein kinase A

RING- Really interesting new gene

RP- Regulatory particle

SDS-PAGE- sodium dodecyl sulfate Polyacrylamide gel electrophoresis

SBDP- Spectrin-breakdown product

Siah- Seven in absentia homolog

STEP- Striatal-Enriched protein tyrosine Phosphatase

tPA- tissue plasminogen activator

UCHL- Ubiquitin Carboxy-terminal hydrolase

UIM- Ubiquitin-interacting domain

UPS- Ubiquitin-Proteasome System

USP- Ubiquitin-specific protease

VDCC- Voltage-dependent calcium channels

Abstract

Ischemic stroke is characterized by a decrease in oxygen supply to the brain with a consequent impairment in the metabolic activity. The sudden decrease in the levels of ATP affect the balance between excitatory and inhibitory neurotransmission, and the overactivation of glutamate receptors leads to neuronal death (excitotoxicity). Under these conditions, the $[Ca^{2+}]_i$ overload to the postsynaptic cell induces the activation of calpains, a group calcium-dependent proteases that regulate the function of many substrate proteins through limited proteolysis. In parallel to calpain activation, the Ubiquitin-Proteasome System (UPS), one of the major protein degradation systems in the cells, which also regulate several key and physiological functions, was also shown to be downregulated under energy-depriving conditions. However, how these two proteolytic systems are interconnected under ischemic conditions is currently unknown.

Multiple lines of evidences suggest that proteasome inhibition is beneficial in in vivo models of transient/global ischemia by halting the inflammatory process. However, proteasome activation may also be a powerful tool to prevent cell demise in acute brain injury, and in other disorders of the nervous system, by enhancing the degradation of damaged proteins. In this work, we characterized the alterations in the subcellular distribution of the proteasome in cultured neurons subjected to ischemic conditions, and investigated the mechanisms contributing to the downregulation of the proteasome under the same conditions. In particular, we focused on the putative effects of calpains on the proteasome components, and the impact of the proteasome in neuronal demise. We found that Oxygen-Glucose Deprivation (OGD), a well-known in vitro model mimicking transient global ischemia in cultured neurons, had a differential effect on the dendritic distribution of the proteasome proteins PSMA2 and Rpt6, used as markers of the 20S and 19S proteasome particles, respectively. Non-denaturing polyacrylamide gel electrophoresis (PAGE) followed by immunoblotting with antibodies against the PSMA2 and Rpt6 also showed a disassembly of the proteasome in cortical neurons subjected to in vitro ischemia, further indicating that this is an appropriate model to study the regulation of the proteasome under ischemic conditions.

OGD was also found to enhance calpain activity (assessed by the cleavage of its substrate spectrin) and had the opposite effect on the activity of the proteasome (determined with a fluorogenic substrate). In contrast with the biochemical changes often associated with inhibition of the proteasome, polyubiquitin conjugates were found to be reduced in cortical neurons subjected to OGD, while no changes were detected in free ubiquitin levels. Two non-related assays were used aiming at identifying which subunits of the 19S proteasome may be cleaved by

calpains: (i) cleavage of endogenous proteins in cortical neurons subjected to OGD and (ii) cleavage of green fluorescent protein (GFP) fusion proteins with proteasome subunits in extracts obtained from HEK293t cells incubated with recombinant calpain. We found that the ubiquitin acceptor Rpn10, together with Rpt3 and Rpt5 are calpain substrates, and this may also be the case for Rpt1 and Rpn3.

Finally, here we report that inhibition of USP14, a deubiquitinating enzyme (DUB) associated with the 26S proteasome, provides robust neuroprotection to cerebrocortical neurons subjected to OGD. USP14 inhibition was previously shown to increase the proteolytic activity of the proteasome towards specific substrates, suggesting that increasing degradation of canonical proteasome substrates is sufficient to prevent cell death. Importantly, incubation of cortical neurons with IU1, the USP14 inhibitor, prevented the OGD-induced activation of calpains, but the underlying mechanism remains to be investigated.

Taken together, the results show that OGD induces hypofunction of the proteasome, alongside with an increased activity of calpain against proteasome resident subunits. The mechanism proposed here conciliates the calpain-mediated cleavage of proteasome subunits with the observed disassembly under ischemic conditions. Enhancing the activity of the proteasome prevents cell demise associated with OGD in cultured cerebrocortical neurons, and may represent a novel therapeutic target to restore the deficits observed after stroke.

Keywords: Ubiquitin-Proteasome System (UPS), Calpains, neuroprotection, cleavage, substrate, ischemia, Oxygen and Glucose Deprivation (OGD), Deubiquitinating enzyme (DUB)

Resumo

O acidente vascular cerebral (AVC) é caracterizado pela diminuição da irrigação sanguínea ao nível do cérebro, com consequente alteração da atividade metabólica. O súbito decréscimo dos níveis de ATP afeta toda a neurotransmissão excitatória e inibitória, e a sobreactivação dos recetores para o glutamato levam à morte neuronal (excitotoxicidade). Nestas condições, o aumento excessivo da $[Ca^{2+}]_i$ na célula pós-sináptica é responsável por ativar as calpaínas, um grupo de proteases reguladas por este ião que controla a função de inúmeras proteínas na célula através de proteólise limitada. Paralelamente à ativação das calpaínas, o Sistema Ubiquitina-Proteassoma (UPS), o principal sistema de degradação proteico existente nas células, que tem um papel chave na regulação de vários processos biológicos, encontra-se inibido em condições de deficit de energia na célula. No entanto, a forma como estes dois sistemas proteolíticos interagem não é de todo conhecido.

Várias evidências sugerem que a inibição do proteassoma tem um papel protetor em modelos in vivo de isquémia transiente/global, através da inibição do processo inflamatório. No entanto, a ativação do proteassoma também pode ser benéfica na prevenção da morte celular em várias agressões do tipo agudo/traumáticas ao nível do cérebro, bem como em doenças neurodegenerativas, através do aumento da degradação de proteínas danificadas. Neste trabalho, caracterizámos a alteração na distribuição subcelular do proteassoma em neurónios submetidos a isquémia in vitro, bem como os mecanismos que contribuem para a diminuição da atividade do proteassoma nas mesmas condições. Focámo-nos em particular nos efeitos putativos das calpaínas sobre componentes do proteassoma, bem como no impacto do UPS na morte celular. Observou-se que a deprivação de oxigénio e glucose (OGD) em neurónios em cultura, um modelo in vitro que mimetiza o efeito transitório da isquémia global, tem um efeito diferencial na distribuição dendrítica das proteínas PSMA2 e Rpt6, duas subunidades do proteassoma vulgarmente usadas como marcadores do 20S e do 19S, respetivamente. Eletroforese em géis de poliacrilamida em condições não desnaturantes, seguido de *imunoblot* contra as proteínas PSMA2 e Rpt6, revelou que o proteassoma é desmontado em neurónios corticais submetidos ao modelo in vitro de isquémia cerebral, indicando que se trata de um modelo apropriado para estudar a regulação do proteassoma nestas condições.

A incubação transitória de neurónios em cultura na ausência de oxigénio e glucose induziu a ativação de calpaínas (avaliado através da análise da clivagem da espectrina) e alterou de forma oposta a atividade do proteassoma (determinado através de um ensaio fluorogénico). No entanto, ao contrário das alterações bioquímicas observadas após inibição química do

proteassoma, os níveis de proteínas conjugadas com cadeias de poliubiquitina diminuiu em neurónios corticais em cultura submetidos a OGD, não tendo sido observadas quaisquer alterações nos níveis da ubiquitina livre. Com o objetivo de identificar que proteínas associadas ao 19S podem ser clivadas pelas calpainas, usámos dois ensaios distintos: (i) análise da clivagem de proteínas endógenas em neurónios corticais em cultura submetidos a OGD e (ii) clivagem de proteínas de fusão contendo a sequência de aminoácidos de subunidades do proteassoma associada a GFP (*green fluorescent protein*) em extratos de células HEK293t incubados com calpaína recombinante. Nestes ensaios observou-se a clivagem do recetor para a ubiquitina Rpn10, juntamente com a proteína Rpt3, sendo que o mesmo poderá também acontecer para as proteínas Rpt1 e Rpn3.

Neste trabalho observámos também que a inibição da USP14, uma enzima de desubiquitinação (DUB) associada ao proteassoma 26S, tem um efeito protetor significativo em neurónios corticais submetidos a OGD. Estudos prévios mostraram que a inibição da USP14 estimula a capacidade proteolítica do proteassoma sobre substratos específicos, sugerindo que o aumento da degradação dos seus substratos canónicos é suficiente para prevenir a morte neuronal. Observou-se também que a incubação de neurónios corticais com o inibidor USP14 impede a ativação de calpaínas em resultado da incubação em condições de OGD. No entanto, os mecanismos responsáveis pela inibição das calpaínas nestas condições não estão esclarecidos.

Em conjunto, os resultados obtidos mostram que a atividade do proteassoma se encontra diminuído em condições de OGD, bem como a clivagem de proteínas associadas ao mesmo por parte das calpaínas. O mecanismo aqui proposto concilia a clivagem de proteínas associadas ao proteassoma com a sua desmontagem em condições de isquémia. O aumento da atividade do proteassoma preveniu a morte de neurónios corticais em cultura submetidos a OGD, e pode representar uma nova estratégia terapêutica na recuperação do tecido nervoso após um AVC.

Palavras-chave: Sistema Ubiquitina-Proteassoma (UPS), calpaínas, neuroprotecção, isquémia, deprivação de oxigénio e glucose (OGD), enzima de desubiquitinação (DUB)

Chapter 1

Introduction

Part of the content of this chapter is published in:

Caldeira, M.V., Salazar, I.L., Curcio, M., Canzoniero, L.M., Duarte, C.B., 2014. Role of the ubiquitin-proteasome system in brain ischemia: friend or foe? *Prog Neurobiol* 112**,** 50-69.

Salazar, I.L., Caldeira, M.V., Curcio, M., Duarte, C.B., 2016. The role of proteases in hippocampal synaptic plasticity: putting together small pieces of a complex puzzle. *Neurochem Res* 41**,** 156-182.

Curcio, M., Salazar, I.L., Mele, M., Canzoniero, L.M., Duarte, C.B., 2016. Calpains and neuronal damage in the ischemic brain: The swiss knife in synaptic injury. *Prog Neurobiol* 143**,** 1-35.

1. Introduction

Brain ischemia arises from a disturbance in the blood supply to the brain, mainly due to cardiac arrest or to occlusion of a blood vessel. Atherosclerotic or thrombotic blockade of blood vessels limits blood flow to a discrete area of the brain, while cardiac arrest affects the whole brain. The resulting decrease in oxygen supply and the consequent impairment in the metabolic activity affects the balance between excitatory and inhibitory neurotransmission, due to an upregulation of the glutamatergic activity and a downregulation of the GABAergic neurotransmission (Choi, 1987; Curcio *et al.*, 2016; Mele *et al.*, 2016). The extracellular accumulation of glutamate leads to an overstimulation of glutamate receptors, with a consequent intracellular free calcium concentration ($[Ca^{2+}]_i$) overload, which plays a key role in neuronal demise (excitotoxicity). The toxic effects of glutamate-evoked $[Ca^{2+}]_i$ dysregulation are at least in part mediated by activation of calpains, a group of calcium-dependent proteases present in different neuronal compartments. In addition to the effects on the neuronal proteome mediated by calpains, brain ischemia also alters neuronal proteostasis by inhibition of the ubiquitin-proteasome system and release of cathepsins from the lysosomal compartment (Caldeira *et al.*, 2014).

1.1. Brain ischemia

Cerebral ischemia is one of the most common causes of death and disability worldwide in developed countries, and hypertension has been associated with a higher risk for this malady (Macrez *et al.*, 2011). The lack of oxygen and nutrients in the entire brain (global ischemia, caused by cardiac arrest) or in a specific brain area (focal ischemia, e.g. due to stroke caused by an occlusion of a blood vessel that irrigates the affected region) impairs neuronal metabolism in brain ischemia (Figure 1.1). The subsequent energy depletion is the first step of a complex and intricate process leading to cell demise. Although transient global ischemia affects all forebrain areas, hippocampal neurons are particularly vulnerable to the ischemic insult being pyramidal neurons in the CA1 region the most susceptible (Kirino, 1982; Pulsinelli *et al.*, 1982). Despite their sensitivity to the ischemia-reperfusion injury, CA1 neurons die far later after the insult, in a process known as delayed neuronal injury, which is not yet fully elucidated.

In focal brain ischemia, tissue damage is more severe in the region at the center of the stroke, known as ischemic core, which fully depends on the nutrients provided by the affected blood vessel. Indeed, in this area neurons cannot sustain ATP synthesis because of the shortage of oxygen and glucose. On the other hand, neuronal damage in the surrounding region (penumbra) progresses at a slower rate due to a limited supply of components required for metabolic

activity, provided by collateral circulation (Dirnagl *et al.*, 1999). The limited availability of ATP in the penumbra region induces a delayed apoptotic cell death, while in the core region the impairment of ATP-dependent mechanisms contributes to a rapid necrotic cell death (Lipton, 1999; Broughton *et al.*, 2009). Plasma membrane depolarization (Lipton, 1999), early release of glutamate by exocytosis (Goldberg and Choi, 1993; Dawson *et al.*, 2000), downregulation of Na^+-dependent high-affinity uptake of glutamate by excitatory amino acids transporters (EAAT) in the astrocytic processes (Dallas *et al.*, 2007) as well as their operation in reverse mode (Rossi *et al.*, 2000; Grewer *et al.*, 2008) induce an accumulation of excitatory amino acids in the extracellular space, causing a toxic overactivation of glutamate receptors (excitotoxicity) (Olney, 1969; Choi, 1987). Prolonged activation of ionotropic glutamate receptors, NMDA (N-methyl-D-aspartate) receptors (NMDAR), AMPA (α-amino-3-hydroxy-5-methyl-4-isoxazolepropionic acid) receptors (AMPAR) and kainate receptors (KAR), further contributes to increase the $[Na^+]_i$ and $[Ca^{2+}]_i$ under excitotoxic conditions. The influx of cations via glutamate receptors, particularly Na^+, increases the intracellular water content, resulting in cytotoxic edema (oncotic cell death) (Koh *et al.*, 1990; MacGregor *et al.*, 2003; Song and Yu, 2014)**.** However, Ca^{2+} entry into neurons, rather than sodium entry, has been suggested to be the key event of glutamate toxicity in the ischemic brain (Choi, 1988; Manev *et al.*, 1989; Kristian *et al.*, 1998). According to the *calcium overload hypothesis*, the rise in $[Ca^{2+}]_i$ leads to mitochondrial dysfunction and generation of reactive oxygen species, and overactivates Ca^{2+}-dependent enzymes such as proteases, phospholipases and endonucleases, which breakdown proteins, lipids and nucleic acids, respectively, thereby contributing to cell demise (Choi, 1988; Manev *et al.*, 1989). In the penumbra region, mitochondria were also shown to undergo morphological changes from a tubular/filamentous structure to a more spherical shape; the same was shown in a model of NMDA-induced toxicity (Barsoum *et al.*, 2006; Martorell-Riera *et al.*, 2014). Interestingly, genetic deletion of the OPA1, a protein involved in the fusion of mitochondria, promoted mitochondrial fission and increased GluN1, GluN2B, GluN2B protein levels, as well as the expression of the proapoptotic protein BAX. These results suggest a positive feedback loop between NMDAR overactivation and mitochondrial fragmentation in Retinal ganglion (RGC) cells (Nguyen *et al.*, 2011).

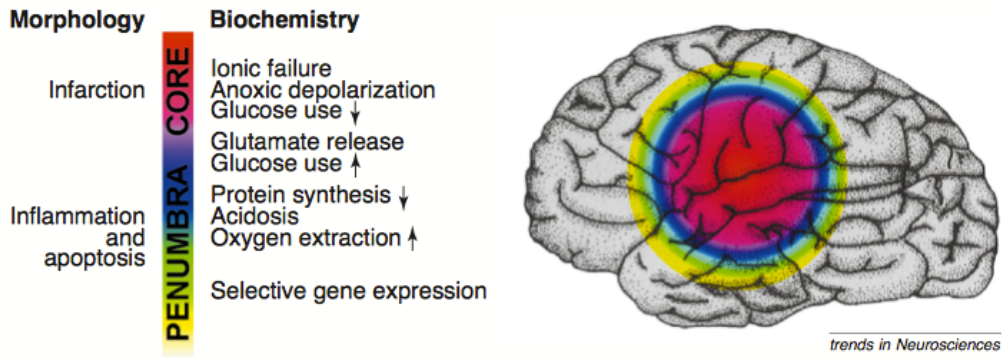

Figure 1.1- The ischemic core and penumbra. The most affected brain region after an ischemic stroke is the core region (red), which under normal conditions depends on the blood supplied by the vessel that was occluded. Cell death is more severe in this region due to an overall failure of the mechanisms responsible to maintain ionic homeostasis, and also due to a severe glucose shortening. On the other hand, in the surrounding region (penumbra) neuronal damage progresses at a slower rate due to a limited supply of components required for metabolic activity, provided by collateral circulations. In the latter region, cell death is not as severe when compared with the ischemic core, and occurs at a later phase if reperfusion does not occur. All the therapeutic strategies aim at preventing cell death in the penumbra region (Dirnagl et al., 1999).

Loss of the Brain-blood barrier (BBB) integrity is another key feature after cerebral ischemia in humans and rats (Belayev *et al.*, 1996; Latour *et al.*, 2004). This is particularly relevant in terms of brain physiology since breakdown of this protective layer allows the entry of peripheral blood molecules into the brain (e.g. proinflammatory molecules), thus promoting an unbalance of brain homeostasis (Obermeier *et al.*, 2013). The BBB breakdown/leakage in the striatum occurs as fast as 30 min after 60 min of middle cerebral arterial occlusion (MCAo) model in mice, and is further extended in the striatum and in cortical areas 1 h after the insult; a broader BBB deterioration and permeability to both small and large tracers is observed 24 h later (Shi *et al.*, 2016b). In fact, after cell death, a strong inflammatory process is observed in the ischemic brain (Iadecola and Anrather, 2011). Natural killer cells were found to be attracted to the lesion site after an acute middle cerebral artery ischemic stroke, and the lack of these cells reduced brain infarct size in a murine model of transient focal ischemia (Gan *et al.*, 2014). Given the importance of the neuron-glia crosstalk in brain plasticity and disease, it is not surprising that astrocytes may represent an additional protective pathway against brain ischemia (Khakh and Sofroniew, 2015). From the molecular point of view, astrocytes can release healthy and functional mitochondria to the extracellular space, which are actively uptaken by neurons thereby amplifying cell survival signals after brain ischemia (upregulated pAKT and BCL-XL), thus promoting cell survival (Hayakawa *et al.*, 2016).

Selective cell death in the mouse striatum starts at 18 h after inducing MCAo for 30 min, further increases at 36 h, with a peak registered at 72 h post-insult (Katchanov *et al.*, 2001). Within the

striatum, different population of neurons are unequally affected. Thus, brain ischemia (30 min MCAo) resulted in a substantial loss of medium spiny projection neurons as seen at day 3, whereas cholinergic, GABAergic, and somatostatin-containing interneurons are not affected 3 and 7 days after the ischemic event (Katchanov *et al.*, 2003). Under these conditions, a high rate of DNA methylation is observed which may induce changes in the gene expression profile favoring cell death. Accordingly, reduction/blockage of DNA methylation using chemical inhibitors/genetic tools of DNA methylfransferases decreased the infarct size evoked by 30 min of MCAo when evaluated 72 h after reperfusion (Endres *et al.*, 2000).

It is widely accepted that the cerebral cortex area (and other brain regions) is more resilient to cerebral ischemia-induced cell death when compared to other brain regions (e.g. CA1 region of the hippocampus). Apoptotic cell death is observed in the CA1 region of hippocampus 3 days (further increasing at day 7) after inducing the 4-vessel occlusion (4-VO) model in adult rat for 15 min, whereas, for instance, the cerebral cortex was not affected under the same conditions (Ayuso *et al.*, 2013). A model of global ischemia in the gerbil [5 min of bilateral common carotid arteries occlusion (BCCAo)] induced substantial cell loss of pyramidal cells in the hippocampal CA1, evident at day 5, whereas no neuronal loss was observed in the CA2 and CA3 regions, or in the dentate gyrus 3 days after the insult [(Calderone *et al.*, 2004) see also (Calderone *et al.*, 2003; Colbourne *et al.*, 2003)].

Intrinsic differences between cell types may explain why the hippocampus is more affected by brain ischemia when compared with other regions, such as the cerebral cortex. Under ischemic conditions, the colocalization (and presumably interaction) between eIF4E (eukaryotic initiation factor (eIF) 4E) and eukaryotic initiation factor 4E-binding protein-2 (4E-BP2), which is critical to control protein synthesis, is decreased in the cerebral cortex and maintained in the CA1 region of the hippocampus. The interaction between the two proteins reduces the rate of protein synthesis and in accordance with the data regarding the interaction of the two proteins a decrease in translation activity was specifically observed in the hippocampus. Preventing translation inhibition, by 4E-BP2 knockdown or with ciclohexamide, decreased apoptotic cell death in the CA1 region under the same conditions, further elucidating the differences between the cerebral cortex and hippocampus in the response to the ischemic injury (Ayuso *et al.*, 2013). Cortical neurons also showed greater spine shrinkage when compared to equivalent hippocampal cultures exposed to an in vitro model of transient global ischemia. The behavior of hippocampal neurons was related with the higher expression of the Rac guanine nucleotide exchange factor (GEF) Tiam1, a protein involved in actin cytoskeleton dynamics (Blanco-Suarez *et al.*, 2014). Therefore, spine shrinkage and active protein synthesis maintenance may be

additional intrinsic neuroprotective mechanisms against brain ischemia present in cortical (but not in hippocampal) neurons.

Neonatal ischemia in P7 rat pups (3 h MCAo followed by 24 h of reperfusion) induces a significant infarct size (Derugin *et al.*, 1998) and very extensive reactive microglia infiltration in the ischemic core (Derugin *et al.*, 2000). Using a similar protocol to induce brain ischemia, the BBB was shown to be undisturbed in the neonatal but not in adult rats, as shown by changes in the permeability to small and large tracers. Expression of occludin and ZO-1, proteins that contribute to the maintenance of the basic structure of BBB by restricting the passage of proteins into the brain, was found to be unchanged (others were found to be upregulated) in both injured and contralateral tissue of neonatal, but were largely reduced in injured adult rats (Fernandez-Lopez *et al.*, 2012).

Oxygen and glucose deprivation (OGD) is a well-known protocol to mimic ischemia-reperfusion in cultured neurons and recapitulates many of the features that characterize the ischemic stroke. In this in vitro model there is also a decrease in ATP levels, similarly to the in vivo condition, but it does not allow distinguishing features characteristic of the penumbra and core regions (Hayakawa *et al.*, 2016). Single cell analysis of neurons subjected or not to OGD gave some refined insights about the individual behavior of each cell. Cortical neurons subjected to 40-45 min of OGD showed an immediate reduction of the ATP levels by about 50 %, reaching a plateau at 20 % when compared with the initial values at 10 min after the insult (Connolly *et al.*, 2014). Two Ca^{2+} waves were also detected, one immediately after the onset of the insult, and a second when the medium was changed to cultured-conditioned medium (reoxygenation), which lasted almost 2.5 h. However, the depolarization of the mitochondrial membrane was only observed during the OGD period, with a full recovery during reperfusion. Importantly, under these conditions, cell death was about 50 % when evaluated 24 h after the insult (Connolly *et al.*, 2014).

OGD was also shown to compromise cell viability in cultured neurons. From the different methods available, Tables 1.1 and 1.2 summarize some of the findings regarding the extent of neuronal death in cerebrocortical neurons and hippocampal neurons, respectively, when exposed to different OGD and post-incubation periods. Although the results obtained varied depending on the experimental conditions used, the developmental stage of both types of cultures have an impact in neuronal death after transient OGD.

Table 1.1- Effect of OGD on the viability of cultured cerebrocortical neurons. The table summarizes the results obtained in studies using different experimental conditions.

OGD	Post-incubation period	Culture information	% cell death	Method	Reference
30 min	24 h	9 DIV Somatosensory cortical neurons	65 % increase	MTT assay	[1]
45 min	24 h	8-11 DIV Cerebrocortical neurons	40 % increase	Hoechst 33342/PI	[2]
1.5 h	24 h	5 DIV Cerebrocortical neurons	20 % increase	AnnexinV	[3]
2 h	24 h	8 DIV Cerebrocortical neurons	4-fold increase	LDH	[4]
2.5 h	24 h	5-6 DIV Cerebrocortical neurons	20 % increase	PI	[5]
3 h	21 h	14-15 DIV Cerebrocortical neurons	50 % increase	PI/calcein-AM	[6]

MTT assay- 3-(4,5-dimethylthiazol-2-yl)-2,5-diphenyltetrazolium bromide assay; PI- Propidium iodide; LDH- Lactate dehydrogenase. [1]- (Wang *et al.*, 2012); [2]- (D'Orsi *et al.*, 2015); [3]- (Lin *et al.*, 2015); [4]- (Guan *et al.*, 2016); [5]- (Choy *et al.*, 2016); [6]-(Beck *et al.*, 2003).

Table 1.2- Effect of OGD on the viability of cultured hippocampal neurons. The table summarizes the results obtained in studies using different experimental conditions.

OGD	Post-incubation period	Culture information	% cell death	Method	Reference
20 min	48 h	15-20 DIV Hippocampal neurons	45 % increase	PI/Hoechst 33342	[1,2]
1.5 h	8 h	15 DIV Hippocampal neurons	30 % increase	Hoechst 33342	[3]
1.5 h	24 h	15 DIV Hippocampal neurons	25 % increase	LDH	[4]
2.5 h	24 h	10 DIV Hippocampal neurons	25 % increase	LDH	[5]

PI- Propidium iodide; LDH- Lactate dehydrogenase. [1,2]- (Blanco-Suarez *et al.*, 2014; Blanco-Suarez and Hanley, 2014); [3]- (Costa *et al.*, 2016), [4]- (Vieira *et al.*, 2016); [5]- (Donath *et al.*, 2016).

This may suggest that the developmental stage in both types of cultures may actually have a profound impact in neuronal death after inducing OGD.

Cell death in ischemia-reperfusion models of brain ischemia is currently under investigation, since the primary route(s) for neuronal cell death remains to be determined. Therefore, a better

understanding of the pathways that lead to neuronal death in brain ischemia is of outmost importance in order to develop therapeutic strategies to halt cell demise. Apoptosis has been widely accepted to be an ATP-dependent mechanism of cell death (Elmore, 2007). Despite the reduced levels of ATP in the ischemic tissue (Lipton, 1999), specially in the core region, it is quite common to find several key features of neuronal apoptosis in neurons subjected to in vitro or in vivo models of transient global/focal ischemia [e.g (Li *et al.*, 2014)]. The proapoptotic Bax protein is a key player in the regulation of the apoptotic cascade acting at the mitochondrial level. $Bax^{-/-}$ mice showed a reduced infarct size when subjected to 60 min of MCAo, and a reduction in propidium iodide incorporation was also observed in $Bax^{-/-}$ cortical neurons exposed to OGD for 45 min followed by 24 h of reoxygenation. These cells also showed a better recovery cytosolic Ca^{2+} increase when compared with neurons expressing Bax (D'Orsi *et al.*, 2015).

Cytochrome c release from the mitochondria, a hallmark of the mitochondrial apoptotic pathway, was observed at day 4 after 5 min of BCCAo in gerbils, and this alteration was prevented by the inhibitor of the Bax channel Bci1, which also prevented the staurosporine-induced apoptosis (Hetz *et al.*, 2005). The apoptotic cascade culminates in the activation of the executioner caspase-3, which is responsible for cleaving a plethora of substrates that are responsible for DNA fragmentation, cell shrinkage, and chromatin condensation among other classical apoptotic features (McIlwain *et al.*, 2015). Caspase-3 is activated after subjecting cultured cerebrocortical neurons to OGD for 2 - 4 h (Meller *et al.*, 2006; Li *et al.*, 2014), and in mice subjected MCAo (2 h) (Li *et al.*, 2014). Initial kinetic studies showed significant caspase-3 activation starting at 9 h after reperfusion and lasting up to 24 h after 30 min of MCAo; a reduction in the infarct volume was obtained even when the caspase-3 inhibitor Z-DEVD-FMK was administered up to 9 h after the insult (Fink *et al.*, 1998). Moreover, rats subjected to 90 min of MCAo showed increased levels of mitochondrial fragmentation (Drp1 marker), apoptosis (cleaved caspase-3), oxidative stress (3-NT) as well as autophagy (LC-3 II/I ratio) in the penumbra region of the ipsilateral cortex, when evaluated 3 days after the insult (Kim *et al.*, 2016). More recent data corroborates in a more integrated way the previous findings, showing that 60 min of MCAo in mice activates caspase-8,9 and-3, enhances Bax protein as well as Bim phosphorylation at day 3 (Donath *et al.*, 2016).

Activation of a mitochondrial apoptotic pathway in brain ischemia is further supported by the results obtained with the BCCAo model (5 min), which showed the mitochondrial accumulation of the apoptotic regulator p53 in a complex with BCL-XL at 8 h after reperfusion, with subsequent release of cytochrome-c to the cytosol; this was evident in the CA1 region of the hippocampus and absent in the CA3 region. At a later point (72 h after the insult), most of the

cells in the CA1 region showed apoptotic morphology and a significant increase in DNA fragmentation, alterations that were prevented by the p53 inhibitor Pifithrin-α (PFT) (Endo *et al.*, 2006a). An upregulation of p53 protein levels was found 12 h after MCAo (for 2 h) in mice, and in cultured primary neurons (11 DIV) subjected to OGD for 4 h followed by 6 h of reoxygenation (Li *et al.*, 2014). In line with these evidence, several other reports showed protection against the ischemic injury upon inhibition/blockade, reduction or even deletion of p53 (Crumrine *et al.*, 1994; Luo *et al.*, 2009; Filichia *et al.*, 2015).

Biochemical alterations in the proteome of cultured neurons subjected transiently to OGD have been reported in several studies. A decrease in the abundance of Nuclear factor (erythroid-derived 2)-like 2 (Nrf2) was reported in primary cultures of rat cortical neurons subjected to 1.5 h of OGD, when evaluated after the insult (starting at 1 h); similar results were obtained in rats submitted to 1 h of MCAo (Chen *et al.*, 2016). Blocking the interaction of Nrf2-Keap1, with a cell-permeable peptide, thus allowing its stabilization and nuclear translocation, was found to afford strong neuroprotection in a model of global cerebral ischemia (Tu *et al.*, 2015). This is of utmost importance since this protein participates in the expression of genes coding for proteins with antioxidant effects (Zhang *et al.*, 2016).

The serine-threonine kinase Akt regulates cell survival pathways by shutting off pro-death genes, and by activating genes associate with cell survival (Kawano *et al.*, 2002). In some studies, the increase in neuronal death in brain ischemia is associated with an upregulation in Akt phosphorylation (e.g. on Ser473) which activates the kinase. These are endogenous neuroprotective mechanisms that may counteract to some extent the demise process. For example, pAkt(Ser473) was increased in the CA1 region of the hippocampus at 8 h after BCCAo (5 min), and the DNA fragmentation observed 3 days after the insult was further exacerbated when Akt phosphorylation was inhibited by administration of the PI3-K inhibitor LY294002 (Endo *et al.*, 2006b). Studies using a different model of brain ischemia (60 min of MCAo) showed increased pAkt(Ser473) protein levels in the territory cortex of the cerebral cortex, but not in core region, when evaluated 4 h after the insult, further suggesting that Akt phosphorylation may regulate cell survival/death (Noshita *et al.*, 2001). Although it was proposed that the severity of the insult may also account for the differential results reported in the literature concerning the effects of ischemic injury on pAkt(Ser473) (Ouyang *et al.*, 1999; Yano *et al.*, 2001), recent data showed an increase in pAkt in both the ischemic core (characterized by a more extensive cell damage) and in the penumbra immediately after the ischemic insult (2 h of MCAo), returning to control levels 60 min later (Zhou *et al.*, 2015). The complexity of the role of Akt in brain ischemia is further shown by the results of experiments using the 4-VO model (10

min). In this model, there was an upregulation of pAkt(Ser473) in post-ischemic neurons in the CA1 region of the hippocampus until 12 h post-insult, which however was not associated with an enhancement in kinase activity. Instead, there was an increase in the expression of the Akt endogenous inhibitor, Carboxyl-terminal modulator protein (CTMP) (Miyawaki *et al.*, 2009). Differently from the in vivo models, OGD for 1.5 h was shown to decrease pAkt as well as the phosphorylated form of PI3K when evaluated 24 h after the insult. Strikingly, further cell death was observed in the presence of the PI3-K inhibitor LY294002, in accordance with the results discussed above (Hansen *et al.*, 2014). Although there is some variability depending on the experimental system used, the available evidence points to a role of the PI3-K/Akt pathway as an endogenous neuroprotective strategy.

1.1.1 Role of glutamate receptors in excitotoxic injury

Under physiological conditions, glutamate release induces a transient increase in the concentration of the neurotransmitter at the synapse, with a consequent short-term activation of glutamate receptors. Glutamate is then rapidly uptaken by the transporters associated with the plasma membrane of the cells surrounding the synaptic cleft, particularly by astrocytes (Zhou and Danbolt, 2014). Activation of AMPAR/KAR allows the influx of Na^+ along its electrochemical gradient, thereby depolarizing the postsynaptic membrane. The AMPAR-mediated depolarization triggers i) the opening of the voltage-dependent calcium channels (VDCC) and ii) the removal of the Mg^{2+} block of Ca^{2+}-permeable NMDAR, allowing the influx of Ca^{2+} into postsynaptic neurons (Kristian and Siesjo, 1998). The difference in $[Ca^{2+}]$ between the intra- and extracellular compartments ($[Ca^{2+}]_e$ is 10000-fold higher than $[Ca^{2+}]_i$) is tightly regulated by mechanisms of Ca^{2+} influx/efflux and Ca^{2+} sequestration (Berridge *et al.*, 2003). Under normal physiological conditions the increase in the postsynaptic $[Ca^{2+}]_i$ following activation of glutamatergic synapses triggers signaling events and activates the machinery that prevents a $[Ca^{2+}]_i$ overload, such as: i) calcium export via the high affinity and low capacity Ca^{2+}-ATPase, and the lower affinity, but with much larger capacity, Na^+/Ca^{2+} exchanger (White and Reynolds, 1995; Guerini *et al.*, 2005), ii) calcium buffering (Gilabert, 2012; Matthews *et al.*, 2013) and iii) calcium sequestration within intracellular organelles, including mitochondria and the endoplasmic reticulum (ER) (Chinopoulos and Adam-Vizi, 2010; Bodalia *et al.*, 2013). In the ischemic brain, the impairment of homeostatic pathways controlling Ca^{2+} influx, efflux and release from intracellular stores induces an accumulation of Ca^{2+} inside the cells, which is deleterious

1.1.2 Role of AMPA receptors in excitotoxic injury

AMPAR are cation channels formed by assembly of four subunits, GluA1-GluA4, and their subunit composition determines their permeability to Ca^{2+}. In the adult brain, AMPAR containing GluA2 subunits are largely impermeable to Ca^{2+}, whereas the lack of this subunit makes the receptors permeable to Ca^{2+} and Zn^{2+} (Hollmann *et al.*, 1991). The low Ca^{2+} permeability of GluA2-containing receptors is due to editing of the pre-mRNA for this AMPAR subunit by the adenosine deaminase acting on RNA [type 2] (ADAR2) at the Q/R site, corresponding to residue 607. In fact, in the adult brain the mature GluA2 proteins contain an arginine residue (R) within the M2 membrane loop region at position 607 in place of the genomically encoded glutamine (Q) (Geiger *et al.*, 1995; Jonas and Burnashev, 1995). This Q/R editing is specific to the GluA2 subunit and the additional positive charge introduced into the pore by the presence of R607 prevents the passage of divalent cations and reduces single-channel conductance (Jonas and Burnashev, 1995; Swanson *et al.*, 1997). Thus, channels containing edited GluA2 subunits are impermeable to Ca^{2+} and exhibit a relatively low single-channel conductance, while those lacking edited GluA2 are Ca^{2+}-permeable and show a higher conductance (Filippini *et al.*, 2016).

In the ischemic brain, the role of AMPAR in excitotoxic injury is primarily (but not exclusively) linked to the depolarization of the membrane which removes the Mg^{2+} block of nearby NMDAR. Several studies using in vivo and in vitro models of brain ischemia showed neuroprotective effects resulting from inhibition of AMPAR and KAR (Buchan *et al.*, 1991; Gill *et al.*, 1992; Schielke *et al.*, 1999; Montero *et al.*, 2007). In the ischemic brain, it was reported a decrease in the expression levels of GluA2 subunits, with a consequent increase in GluA2-lacking AMPAR channels, which contributes to the delayed neurodegeneration following transient forebrain ischemia (Pellegrini-Giampietro *et al.*, 1997). In fact, GluA2 gene expression and protein levels were decreased in pyramidal neurons of the hippocampal CA1 region in gerbils subjected to 5 min of bilateral common artery occlusion (BCAo) followed by 60 or 72 h reperfusion, before the onset of neuronal death (Opitz *et al.*, 2000). In another study it was found that 20 min of OGD decreased GluA2 surface expression at the synaptic sites in cultured hippocampal neurons, via a clathrin-dependent internalization, and facilitated the delivery of GluA2-lacking AMPAR to the synapse, thereby contributing to the synaptic expression of AMPAR lacking this subunit (Liu *et al.*, 2006a). This mechanism was further investigated in a recent study comparing the changes in AMPAR composition in cortical and hippocampal neurons subjected to OGD. Cultured cortical neurons are resistant to an OGD insult that causes hippocampal neuronal death, due to the rapid endocytosis of the GluA2 subunit in hippocampal neurons subjected to the ischemic injury,

a mechanism absent in cortical neurons; concurrently, GluA1 was inserted in both neuronal cell types in response to OGD (Blanco-Suarez and Hanley, 2014).

Since GluA2-lacking AMPAR allow toxic influx of Ca^{2+} and Zn^{2+}, the contribution of the change in AMPAR subunit composition to ischemia-induced neuronal death was investigated using 1-naphthyl acetyl spermine (Naspm), a specific blocker of GluA2-lacking AMPAR. Stereotaxic intrahippocampal injection of Naspm, at different time points of reperfusion after transient global ischemia in rats, reduced the accumulation of Zn^{2+} and neuronal death in the hippocampal CA1 region (Noh *et al.*, 2005), showing a role for GluA2-lacking AMPAR in ischemia-induced delayed cell death. Likewise, excitotoxic stimulation of cultured cortical neurons with glutamate induced an NMDAR- and calpain-dependent downregulation of ADAR2 which correlated with the loss of GluA2 Q/R site editing (Mahajan *et al.*, 2011). Moreover, 15 min of transient forebrain ischemia in rats followed by 6 days of reperfusion decreased the expression of the nuclear enzyme ADAR2 and therefore disrupted GluA2 Q/R site editing in vulnerable neurons (Peng *et al.*, 2006). This downregulation of ADAR2 is expected to contribute to neuronal demise by inducing the expression of Ca^{2+}-permeable GluA2(Q) receptors.

1.1.3 Role of NMDA receptors in excitotoxic injury

Differently from AMPAR, NMDAR are found in the brain as di- or tri-heteromeric complexes. The GluN1 subunit, four different GluN2 subunits (GluN2A, GluN2B, GluN2C, GluN2D) encoded by four different genes, and two GluN3 subunits (GluN3A and GluN3B, obtained from two distinct genes) assemble to form functional NMDAR (Kutsuwada *et al.*, 1992; Ishii *et al.*, 1993; Traynelis *et al.*, 2010). NMDAR are activated when the depolarization of the plasma membrane induces the removal of Mg^{2+} from the receptor channel. The depolarization of the membrane is mediated primarily by AMPARs (Mayer *et al.*, 1984; Nowak *et al.*, 1984), and the activity of NMDAR also requires the binding of two different agonists, namely glutamate and glycine (or D-serine) (Johnson and Ascher, 1987). The obligatory GluN1 subunit forms the co-agonist glycine (D-serine) binding site, whereas GluN2 subunits provide the glutamate binding sites (Monyer *et al.*, 1992; Kuryatov *et al.*, 1994; Laube *et al.*, 1997). Functional NMDAR typically require assembly of two GluN1 subunits together with two GluN2 subunits (forming di- or tri-heteromeric receptors depending on GluN2 subtypes), displaying different biophysical and pharmacological properties based on their molecular composition (Paoletti *et al.*, 2013). Di-heteromeric NMDAR composed of GluN1/GluN2A and GluN1/GluN2B display lower agonist and co-agonist potencies, higher sensitivity to the Mg^{2+} block, higher Ca^{2+} permeability and higher single-channel conductance when compared with GluN1/GluN2C and GluN1/GluN2D NMDAR

(Stern *et al.*, 1992; Wyllie *et al.*, 1996; Erreger *et al.*, 2007; Chen *et al.*, 2008b). Tri-heteromeric NMDAR composed of GluN1/GluN2A/GluN2B, which hold distinct pharmacological and kinetic properties from di-heteromeric receptors (Hatton and Paoletti, 2005; Hansen *et al.*, 2014), are highly expressed in the adult brain, especially in hippocampal synapses (Rauner and Kohr, 2011).

NMDAR subunits are differentially distributed in the brain and their expression profile also changes during development, giving rise to distinct receptors with different biophysical and pharmacological properties (Monyer *et al.*, 1994; Lau and Zukin, 2007; Paoletti *et al.*, 2013). In addition to GluN1, which is virtually expressed in all neurons, the most expressed NMDAR isoforms in the adult brain are GluN2A and GluN2B (Monyer *et al.*, 1994; Paoletti *et al.*, 2013). Nevertheless, in the adult forebrain, GluN2B containing NMDAR are fourfold more expressed when compared with GluN2A-NMDAR; the same trend is observed in the hippocampus, thalamus, olfactory bulb among other regions (Frank *et al.*, 2016). There is evidence that GluN2A is mainly expressed at the synapses of neurons in the adult brain whereas GluN2B-containing NMDAR are found in extra- and peri-synaptic sites (Groc *et al.*, 2006). However, more recent data suggest that GluN2B is not only found out of the synapse, because it can also form di- or tri-heteromers at synaptic sites (Storey *et al.*, 2011; Wyllie *et al.*, 2013).

Pharmacological studies showed that NMDAR activity and function plays a key role in the survival of different types of neurons, through activation of signaling pathways coupled to the induction of survival genes and suppression of death genes (Hardingham, 2006; Hardingham and Bading, 2010). This hypothesis is also supported by studies with transgenic animal models showing that mice lacking GluN1 gene expression die soon after birth (Forrest *et al.*, 1994), and by early studies showing that NMDAR antagonist induces cell death in the developing brain (Gould *et al.*, 1994). On the other hand, GluN2A or GluN2B knockdown had different effects on mice viability, suggesting a distinct role for these two NMDAR subunits. Mice lacking GluN2A gene expression are viable but display impaired learning and memory, whereas GluN2B knockout mice showed a reduced viability (Sakimura *et al.*, 1995; Kutsuwada *et al.*, 1996). The differential functional role of GluN2A and GluN2B NMDAR subunits has been attributed, at least in part, to their distinct distribution on the plasma membrane.

In the ischemic brain, the spillover of glutamate from the synapse due to the low activity of the glutamate uptake systems allows the stimulation of synaptic and extrasynaptic populations of NMDAR, which is longer lasting than the transient activation under normal physiological conditions (Figure 1.2). The sustained activation of extrasynaptic NMDAR has been shown to play a key role in neuronal demise in the ischemic brain due to the recruitment of specific signaling pathways. Studies with a chemical inhibitor of GluN2B-containing NMDAR, which are

mainly extrasynaptic, showed a reduction in the infarct volume following transient MCAo, whereas blocking GluN2A-containing receptors was without effect (Liu *et al.*, 2007). Furthermore, the GluN2B subtype antagonist ifenprodil attenuated 4-VO-induced cell death (Chen *et al.*, 2008a). Similarly, ifenprodil was more effective than NVP-AAM077, a preferential GluN2A inhibitor, in reducing OGD-induced excitotoxicity as well as NMDAR-mediated elevation of $[Ca^{2+}]_i$ in cultured cortical neurons (Zhou *et al.*, 2013). In addition, the NMDA-induced cell death in hippocampal slices and cultured cerebrocortical neurons was found to be mediated by NMDAR containing GluN2B subunits, and insensitive to antagonists of GluN2A subunits (Zhou and Baudry, 2006; Liu *et al.*, 2007). Together, these results point to a key and specific role of GluN2B-containing NMDAR in excitotoxic damage.

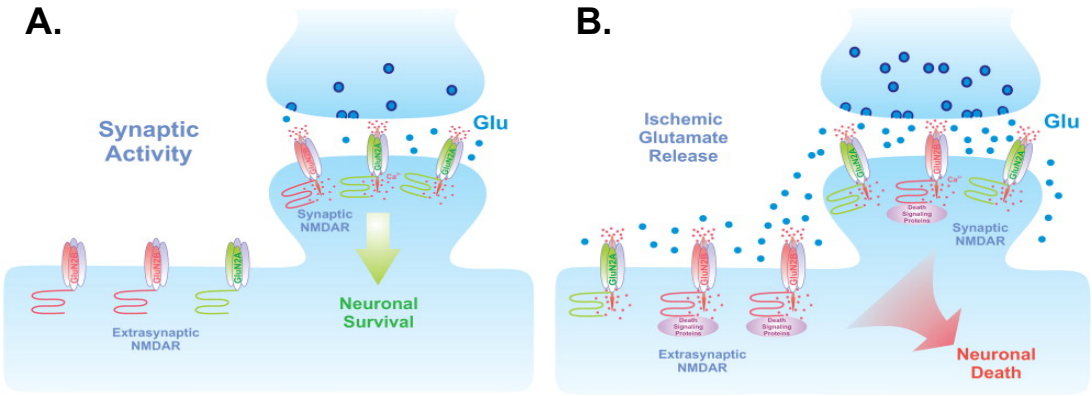

Figure 1.2- Overview of the glutamatergic synapse under normal and ischemic conditions. A) Under normal physiological conditions, glutamate release from the presynaptic terminal activates synaptic NMDAR, which are coupled to the regulation of the expression of genes that are often associated with neuronal survival. Because NMDAR of different compositions show a dynamic distribution in the plasma membrane, it is also common to find NMDAR at extrasynaptic sites. **B)** Brain ischemia promotes a massive release of the neurotransmitter glutamate which is accumulated at the synaptic cleft. Under the latter conditions, glutamate spillover is observed and an overall excessive activation of NMDAR is associated with cell demise (Lai et al., 2014).

Clinically, NMDAR antagonists have been developed in order to halt the excitotoxic cell death after brain ischemia (Cheng *et al.*, 2004). The vast majority of the NMDAR antagonists/inhibitors developed and tested have failed due to a lack of neuroprotection or to their adverse cognitive side effects in healthy individuals (Hoyte *et al.*, 2004; Gonzalez-Burgos and Lewis, 2012). However, the current view proposing a role for the excessive activity of NMDAR in excitotoxic injury, and the use of drugs targeting these channels to prevent cell death, has been challenged. Recent studies proposed a different model based on the evidence showing that pharmacological blockade of the NMDAR channel with MK801 prevents the NMDAR current but it does not prevent the excitotoxic dendritic-blebing, as well as cell lysis induced by transient OGD. The

authors proposed an unidentified metabotropic function for the NMDAR-Src-Panx1 signaling pathway in regulating cell death after ischemia (Weilinger *et al.*, 2016) [for ineffectiveness of NMDAR inhibition in preventing cell death after ischemia see also (D'Orsi *et al.*, 2012; Saver *et al.*, 2015)].

Together, the available evidence suggests that NMDAR composition, in particular the presence of GluN2B subunits, and their localization, are the link between excitotoxicity and cell death pathways.

1.1.4 Activation of extrasynaptic vs synaptic NMDAR in cell death

NMDAR-mediated Ca^{2+} entry is much more effective in killing neurons than the influx through other channels, pointing to a source specificity in this signaling pathway (Curcio et al., 2016). The relative role of synaptic and extrasynaptic NMDAR in excitotoxic injury remains controversial, since contradictory results have been obtained using different experimental approaches. Discrepancies were found in studies performed i) in distinct preparations, ii) using the same models and/or iii) with the same protocol to stimulate the two populations of receptors (see below).

Hardingham and co-workers were pioneers in addressing the relative contribution of extrasynaptic NMDAR in inducing cell death in cultured hippocampal neurons (DIV 10-12). They found that activation of the extrasynaptic population of NMDAR is coupled to excitotoxic neuronal death, whereas activation of the synaptic population was often associated with cell survival (Hardingham *et al.*, 2002). Maturation of hippocampal neurons in culture (to 21-28 DIV) is accompanied by an upregulation of NMDAR GluN2A subunits (Zhou and Baudry, 2006), which represents an additional extrasynaptic route for excitotoxic Ca^{2+} signaling (Stanika *et al.*, 2009).

Several studies have characterized the mechanisms underlying the differential responses to activation of synaptic *vs* extrasynaptic NMDAR in cultured neurons, and showed that Ca^{2+}-entry through extrasynaptic NMDA receptors is selectively coupled to downregulation of pro-survival signaling pathways and to the loss of mitochondrial membrane potential (Figure 1.3). Mitochondrial Ca^{2+} unbalance under the same conditions is linked with generation of reactive oxygen species, which contribute to excitotoxic cell death (D'Orsi *et al.*, 2012). In contrast, synaptic NMDAR selectively increase the cAMP [(Cyclic adenosine monophosphate) response element-binding protein (CREB)] activity and the expression of neuroprotective genes, thereby promoting resistance to oxidative insults, and downregulate pro-death genes (Hardingham *et al.*, 2002; Papadia *et al.*, 2005; Papadia *et al.*, 2008; Zhang *et al.*, 2011; Baxter *et al.*, 2015).

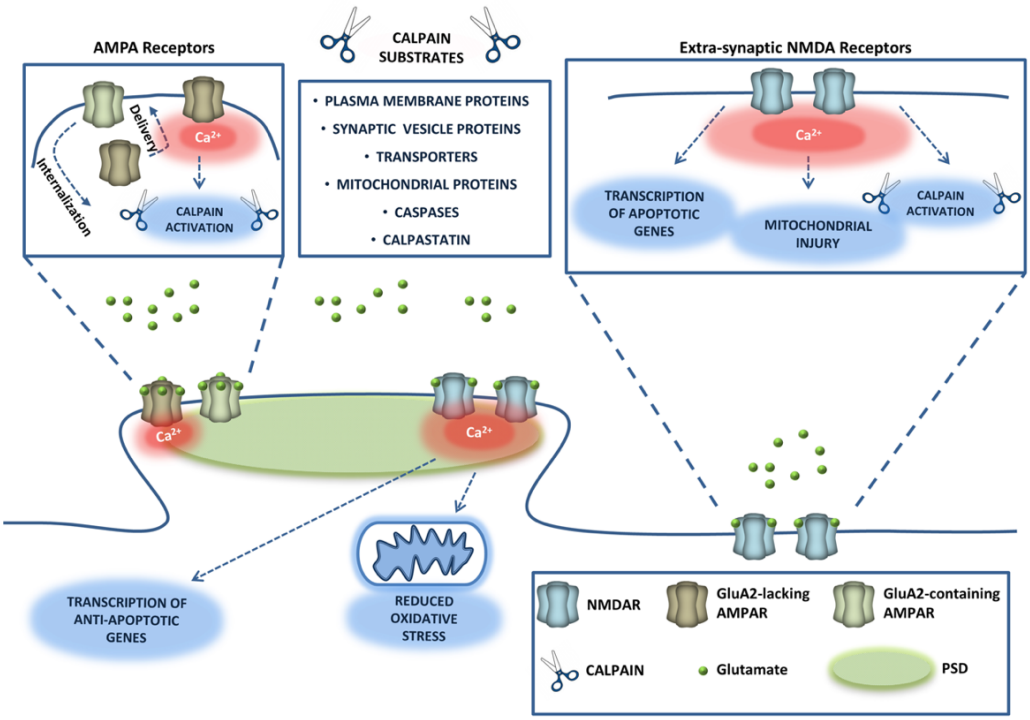

Figure 1.3- Activation of ionotropic glutamate receptors and downstream responses in brain ischemia. The increased release of glutamate and the inhibition of glutamate uptake mechanisms in brain ischemia induces glutamate spillover from the synapse which overactivate synaptic and extrasynaptic ionotropic glutamate receptors. The downregulation of GluA2 mRNA and protein expression, associated with the internalization of GluA2-containing AMPAR and synaptic delivery of Ca^{2+} permeable-AMPAR (lacking GluA2) observed in post-ischemic neurons, contribute to the increase in $[Ca^{2+}]_i$. The $[Ca^{2+}]_i$ overload increases calpain activity with consequent cleavage of several proteins, which contributes to cell death. Calcium influx through synaptic NMDAR induces signaling pathways which upregulate the transcription of anti-apoptotic genes and genes involved in antioxidant defenses. In contrast, the excessive activation of extrasynaptic NMDAR induces signaling pathways promoting transcription of pro-apoptotic genes and mitochondrial injury, contributing to excitotoxic cell death. Moreover, extrasynaptic NMDAR activity induces calpain-mediated cleavage of Myocyte enhancer factor 2 (MEF2), glutamic acid decarboxylase (GAD65/67), α-spectrin, Sodium-calcium exchanger 3(NCX3), and STEP (Caldeira et al., 2014).

Despite the extensive evidence favoring the selective role of extrasynaptic NMDAR in excitotoxic death, this hypothesis has been questioned by several studies. Thus, the synaptic population of NMDAR was shown to mediate the excitotoxic damage in cultured hippocampal neurons subjected to hypoxic conditions and no protection was observed when extrasynaptic NMDAR were blocked (Wroge *et al.*, 2012). A different set of studies, performed in cultured cortical neurons, showed no preferential coupling of synaptic or extrasynaptic NMDAR to excitotoxic injury (Zhou *et al.*, 2013). In the latter culture system, activation of synaptic or extrasynaptic NMDAR alone did not cause measurable cell death, but instead stimulated pro-survival signaling mechanisms (CREB, ERK, Akt). Furthermore, excessive stimulation with glutamate, NMDA,

kainate or AMPA was not coupled to neuronal death in cell types that only possess extrasynaptic NMDAR (e.g retinal ganglion cells) (Ullian *et al.*, 2004). Additionally, PSD95 and PSD93 downregulation were shown to protect neurons from NMDAR-induced cell death and MCAo, respectively (Cui *et al.*, 2007; Rong *et al.*, 2016).

The relative role of synaptic and extrasynaptic NMDAR in excitotoxic injury and neuronal survival was also investigated in more complex settings, which reproduce the in vivo condition to a larger extent. Recent studies using hippocampal slices subjected to OGD showed glutamate spillover from the synapse which induced the activation of extrasynaptic NMDAR. Under the same conditions, there was an increase in Ca^{2+} activity in astrocytes which mediated the OGD-induced upregulation in the frequency of extrasynaptic NMDAR-mediated currents. These results show an important cross-talk between astrocytes and neurons in the activation of extrasynaptic NMDAR (Dong *et al.*, 2013).

Based on these evidences it was proposed that neuronal damage may arise from the co-activation of synaptic and extrasynaptic NMDAR. The lack of compartmental specificity in the NMDAR coupling to excitotoxic injury reported in these studies was correlated with the similarity in the responses induced by NMDAR containing GluN2A and GluN2B subunits in cultured cerebrocortical neurons: i) GluN2A or GluN2B mediated prosurvival signaling induced by synaptic or extrasynaptic NMDAR and ii) both subunits contributed to the pro-death signaling triggered by co-activation of synaptic and extrasynaptic receptors. Together, these data suggest that both subunits mediate the function of synaptic and extrasynaptic NMDAR, and indicate that they play similar roles in the activation of prosurvival and death pathways in cultured cortical neurons (Zhou *et al.*, 2013). Additional studies are required to determine i) whether and how distinct NMDAR, with different cellular distributions and/or subunit compositions, are differentially coupled to excitotoxic neuronal damage, and ii) the molecular mechanisms involved.

1.2. The calpain-calpastatin system

1.2.1. Calpains

Calpains are a family of calcium-dependent neutral cysteine proteases ubiquitously expressed. When active, these enzymes modify the structure and activity of their protein targets by limited proteolysis. This mechanism is distinct from the complete protein degradation mediated by proteasomes and lysosomes, and regulates different cellular processes such as tissue regeneration, cell development, proliferation, differentiation, gene expression, signal

transduction, synaptic plasticity and apoptosis (Ono and Sorimachi, 2012; Ono *et al.*, 2016; Salazar *et al.*, 2016). Given the sequence homology in the human genome, 15 calpain members have been so far identified (Campbell and Davies, 2012; Ono and Sorimachi, 2012) and are classified as classical and non-classical depending on the conserved protein domains linked to the calpain-type cysteine protease core [Figure 1.4A; (CysPc, see below)]. The classical calpains contain the calpain-type beta-sandwich domain (CBSW), a domain known to interact with Ca^{2+} and phospholipids, and the 5 EF-hand domain on the C-terminus of CysPc (Figure 1.4A) (Goll *et al.*, 2003; Tompa *et al.*, 2004; Ono *et al.*, 2016). However, it was shown that the cation does not interact with this region in the crystal structures of Ca^{2+}-bound calpain in complex with calpastatin (Hanna *et al.*, 2008; Moldoveanu *et al.*, 2008). Calpains 1, 2, 3, 8, 9, 11, 12, 13 and 14 were found to be expressed in humans, with calpain 1 and calpain 2 being ubiquitously expressed and the best studied [for extensive reviews see (Goll *et al.*, 2003; Curcio *et al.*, 2016; Ono *et al.*, 2016)].

In the nervous system, calpain 1 and calpain 2 are highly expressed and are present in neurons and glial cells, but their relative abundance differs. Calpain 1 is more expressed in neurons while calpain 2 is more abundant in glial cells (Hamakubo *et al.*, 1986). Calpain 1 and calpain 2 share ~60 % homology and their catalytic activity is modulated by interaction with a small (30 kDa) regulatory subunit (CAPNS1), giving rise to heterodimers known as μ- and m-calpain, respectively [Figure 1.4A; (Goll *et al.*, 2003; Sorimachi *et al.*, 2011a)]. They are so called due to the Ca^{2+} concentration required for their activity: for half maximal in vitro activity, μ-calpain requires 3-50 μM Ca^{2+} whereas 0.4-0.8 mM is necessary to activate m-calpain (Goll *et al.*, 2003).

The 80 kDa catalytic large subunit of μ- and m-calpain contains four domains/regions (Sorimachi *et al.*, 2011b). The anchor helix (formerly called domain I) at the N-terminus of the protein stabilizes the structural arrangement of the heterodimers and undergoes autolysis during calpain activation by Ca^{2+} (Khorchid and Ikura, 2002). The catalytic CysPc domain is made up of two protease core domains (PC1 and PC2), which form the active cysteine catalytic region and physically interact with the endogenous inhibitor calpastatin or with the substrate (Strobl *et al.*, 2000; Melloni *et al.*, 2006; Ono and Sorimachi, 2012).

The C-terminal domain (previously called domain IV) of calpain contains 5 EF-hand motifs and it is also referred to as penta-EF hand (PEF) domain of the large subnit [PEF(L)], and represents the Ca^{2+}-binding domain (Khorchid and Ikura, 2002; Campbell and Davies, 2012). The regulatory subunit of μ- and m-calpain is composed of two domains/regions, the glycine-rich hydrophobic N-terminus domain and the calcium-binding domain (previously called domain V and VI,

respectively), which contains 5 EF-hand motifs similarly to the PEF domain of the catalytic subunit [also called PEF(S)] (Goll *et al.*, 2003; Sorimachi *et al.*, 2011a).

Calpain 1 and calpain 2 differ in the catalytic residues of their active sites, which makes the conformation of μ-calpain closer to the active state when compared with m-calpain. The higher sensitivity of μ-calpain to Ca^{2+} when compared with m-calpain also results from the PEF domain of calpain 1 (Pal *et al.*, 2003; Campbell and Davies, 2012). The two calpain isoforms are also characterized by a distinct interaction with the small regulatory subunits. In the CNS there are two different small regulatory subunit proteins (CAPNS1 and CAPNS2) which are significantly similar. One major structural difference is the presence of a 20 amino acid sequence in the N-terminus of CAPNS1, which is thought to be involved in the interaction with membrane-phospholipids, and is absent in CAPNS2. Moreover, CAPNS2 interacts transiently with the catalytic subunit of calpain 1 and 2, with a lower affinity than CAPNS1, and does not undergo autolytic cleavage in the presence of Ca^{2+} (Schad *et al.*, 2002; Friedrich *et al.*, 2004).

Calpains cleave their substrates generating two or more fragments, depending on the calpain cleavage site(s) present in the target protein. The position of the cleavage site(s) is the most important parameter in the calpain-mediated modulation of substrate functions. Therefore, the prediction of calpain cleavage sites is the key to understand how calpain activity modulates cellular mechanisms through substrate proteolysis. Several studies have tried to predict calpain cleavage sites by analysis of substrate primary structure (Tompa *et al.*, 2004; DuVerle *et al.*, 2011; Liu *et al.*, 2011; Fan *et al.*, 2013). However, only a limited number of these substrates are currently known (Kim *et al.*, 2013a; Shinkai-Ouchi *et al.*, 2016), with the exact mechanism of substrate recognition and cleavage by calpain still to be determined. The impact of the presence of sequences rich in proline, glutamic acid, serine and threonine (also known as PEST sequences), and the target recognition by calpains (Molinari *et al.*, 1995; Wang *et al.*, 2003), remains to be fully elucidated. Moreover, it has been suggested that calpain cleavage depends on the substrate conformation rather than on its primary structure (Sorimachi *et al.*, 2012). In fact, the tertiary/quaternary structure of a substrate determines the accessibility of calpains to the target sequence because a putative calpain cleavage site might be hidden in the folded substrate (Sorimachi *et al.*, 2012). Therefore, a correct and precise prediction of a calpain cleavage site in a putative calpain substrate requires the analysis of the amino acid composition as well as the tertiary/quaternary structure of the substrate itself.

1.2.2. Calpastatin

Calpastatin is the only endogenous inhibitor of calpains known. Heterogeneity in the size of the calpastatin protein has been observed among different species, as well as in different tissues of the same species (Takano *et al.*, 1984). This protein contains four inhibitory units, each one of them interacting with one molecule of calpain with different kinetics (Hanna *et al.*, 2007). Furthermore, each of the four calpastatin inhibitory units is composed of three well-conserved subdomains: A, B and C [Figure 1.4B; (Tompa *et al.*, 2002; Hanna *et al.*, 2007)]. The subdomains A and C interact respectively with the PEF(L) and with the PEF(S) (Yang *et al.*, 1994; Takano *et al.*, 1995). Expression of subdomains A and C of calpastatin domain I can sensitize both μ-calpain and m-calpain to Ca^{2+}; in this case, calpastatin was found to reduce the Ca^{2+} concentration required for half-maximal activity of μ- and m-calpain (Tompa *et al.*, 2002). Subdomain B is responsible for calpain inhibition, but weakly interacts with its substrate when expressed in absence of the A and C regions. These results suggest a role for subdomains A and C as enhancers in the inhibition of calpains (Ma *et al.*, 1993; Takano *et al.*, 1995; Tompa *et al.*, 2002). In addition to the four inhibitory domains, calpastatin contains an N-terminus domain (domain L) which was proposed to have no inhibitory effects (Maki *et al.*, 1987; Hanna *et al.*, 2007). A different work has shown that this domain recognizes and binds a sequence within the catalytic domain of calpain in the absence of Ca^{2+}, or at physiological Ca^{2+} concentrations, suggesting a mechanism to control the degree of calpain activation potentially generated in response to an influx of Ca^{2+} (Melloni *et al.*, 2006).

Calpastatin alone is not able to bind Ca^{2+}, but the protein binds and inhibits calpains following an increase in the $[Ca^{2+}]_i$. Accordingly, calpastatin associates in large aggregates under resting conditions, and is redistributed into the cytosol in response to an increase in $[Ca^{2+}]_i$. This shift in localization increases the inhibitory capacity against calpains and is linked to mechanisms of negative feedback that downregulate calpastatin gene expression. On the other hand, calpain-mediated calpastatin cleavage is followed by an increase in the expression of the mRNA of calpastatin (Averna *et al.*, 2003). Therefore, the calpain-calpastatin system is highly interconnected in terms of their expression levels.

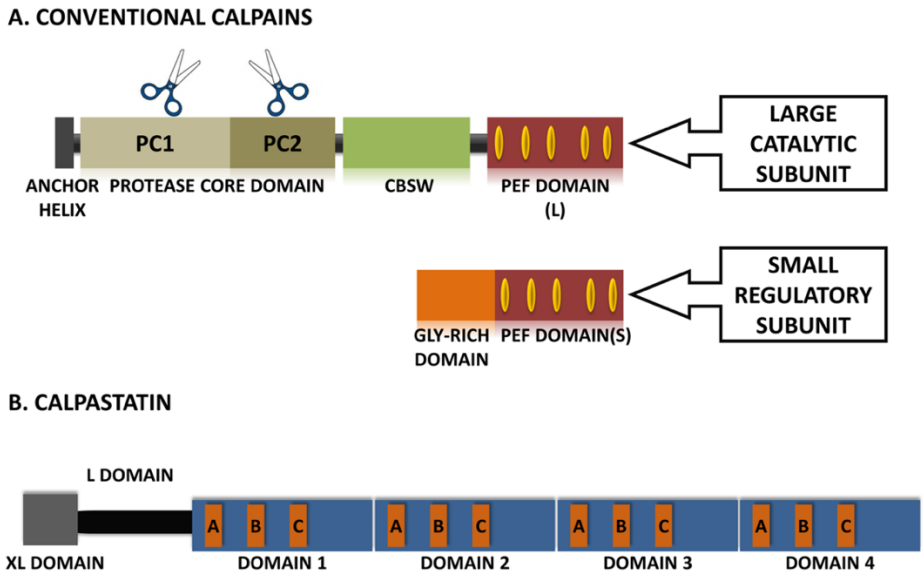

Figure 1.4- Domain structure of conventional calpains and calpastatin. A) Schematic representation of conventional calpains, which are made of a large catalytic subunit and a small regulatory subunit. The large subunit contains the anchor helix at the N-terminus, the catalytic CysPc domain (made up of two Protease Core domains), which represents the active catalytic region (scissors), the CBSW domain and the PEF domain, which forms the calcium-binding domain. The small subunit contains a PEF domain, similarly to the large subunit, and a Glycine-rich N-terminus domain. **B)** Schematic representation of the longest isoform of human calpastatin: the XL and L domains lack inhibitory activity; the four inhibitory units/domains (each one binding to one molecule of calpain) are composed of subdomains A, B and C. Subdomain B mediates calpain inhibition, whereas subdomains A and C interact with the PEF(L) and PEF(S), respectively (Curcio *et al.*, 2016).

1.2.3. Calpains and brain ischemia

Calpains are present in dendritic spines and have been shown to regulate synaptic plasticity in the hippocampus through limited proteolysis of a plethora of intracellular effectors [for recent reviews see (Briz and Baudry, 2016; Salazar *et al.*, 2016)]. In fact, synaptic activity was shown to induce calpain activation which may lead to the cleavage of several proteins (Wang *et al.*, 2013b). In contrast with this effect on the cleavage of specific substrates, characteristic of conditions of controlled calpain activation, the excessive activation of the protease in brain ischemia leads to the uncontrolled cleavage of a large number of target proteins. Therefore, it is not surprising that calpains play a role in several neurodegenerative diseases and in neuronal damage after acute brain injury. A common feature of many of these disorders is the excitotoxic response resulting from the excessive influx of Ca^{2+} through NMDAR channels, with a consequent $[Ca^{2+}]_i$ overload and excessive activation of calpains [reviewed in (Camins *et al.*, 2006; Bevers and Neumar, 2008; Curcio *et al.*, 2016)].

Early evidence regarding calpain activation in the brain induced by occlusion of blood vessels that irrigate the brain date from the 90´s. In these early studies, it was also found that α-spectrin can be cleaved by calpain, giving rise to truncated fragments (Lee *et al.*, 1991; Rami and Krieglstein, 1993; Saido *et al.*, 1993). Concomitant studies showed that 5 min of BCCAo increases the immunolabeling for the calpain-specific fragment of α-spectrin, as fast as 30 min after the insult, in the hippocampus, cortex, thalamus, and striatum of the gerbil; staining confined to the vulnerable hippocampal CA1 region was still observed at day 2 (Roberts-Lewis *et al.*, 1994). Moreover, the authors found that the severity of the insult is largely correlated with the degree of calpain activation; no calpain activation was seen when cell death was absent (1 min BCCAo), and massive calpain activation was detected in regions outside the hippocampus after a severe ischemic insult (10 min BCCAo) (Roberts-Lewis *et al.*, 1994). Similar results were obtained, although with a distinct kinetics of calpain activation in the hippocampal CA1 region, in experiments using 10 min of transient global ischemia in gerbils (15 min after the insult and 4-24 h after) (Saido *et al.*, 1993). Subsequent work reported a third wave of calpain activation in the cytoplasm of CA1 neurons, between day 3-7, which correlate with the delayed cell death observed in this subpopulation of the hippocampus (Yokota *et al.*, 1995). μ-Calpain autolysis was also observed in the brain after cardiac arrest (Neumar *et al.*, 1996). This bimodal pattern of calpain activation was later on confirmed and extended to other brain regions (Neumar *et al.*, 2001).

Since calpain activation occurs at an early time point after the ischemic insult, when cell death is not observed (e.g CA1 region of the hippocampus), inhibition of these proteases represents an interesting strategy to prevent cell death. Leupeptin infusion into the gerbil right lateral ventricule, 3 days before inducing of BCCAo (10 min), reduced the cell loss observed in the CA1 region of the hippocampus, as well as the truncation of α-spectrin, when evaluated 2 weeks after the insult (Lee *et al.*, 1991). The calpain inhibitor I (two doses given intracisternally 30 min and 2 h before the insult) also reduced necrotic cell death in the CA1 subfield when evaluated 7 days after ischemia in rats submitted to 10 min of BCCAo; protection was also afforded in an in vitro model of cytotoxic hypoxia (Rami and Krieglstein, 1993). Furthermore, similar results were obtained using the calpain inhibitor ALLN, in a model of transient forebrain ischemia (5-min) (Yokota *et al.*, 1999). Additionally, neuroprotective effects of the calpain inhibitor MDL28170 were reported in several models of ischemia-reperfusion, when the compound was administered immediately after (Kawamura *et al.*, 2005), 3 h (Li *et al.*, 1998), and 6 h after the insult (Markgraf *et al.*, 1998).

Given the poor specificity of calpain inhibitors, due to specific off-side targets, other strategies were required to confirm the role of the protease in neuronal death after brain ischemia. Initial studies addressing this issue were performed by overexpression of calpastatin, the endogenous calpain inhibitor. Transgenic mice overexpressing the human calpastatin gene were protected against kainate-mediated excitotoxicity in the hippocampus, and show decreased dendritic and axonal degeneration (Higuchi *et al.*, 2005). These studies showed reduced number of TUNEL positive cells, decreased nuclear translocation of the apoptosis-inducing factor (AIF) and endonuclease G, as well as decreased levels of truncated α-spectrin (Takano *et al.*, 2005). Similar results were obtained in studies using a model of traumatic brain injury, which also promotes calpain activation, and calpastatin overexpression reduced neuronal damage (Schoch *et al.*, 2013). Calpain activity was indeed shown in several studies to contribute to the demise process upon exposure of different types of neurons to toxic concentrations of NMDA (Xu *et al.*, 2007; D'Orsi *et al.*, 2012; Wang and Huang, 2012).

Changes in the subcellular distribution of calpains 1 and 2, in addition to calpastatin, were evaluated in three different fractions prepared form the rabbit brain under control conditions and following 90 minutes hypoxia: nuclear and mitochondrial (NMF), microsomal and plasma membrane (MMF), and cytosolic fractions (CF). All three proteins showed a low distribution in the MMF (5-7 %) and the highest distribution in the CF (50-66 %) under control conditions. The hypoxic paradigm used induced a downregulation of the three proteins in the CF, whereas an increased expression was found in the MMF, suggesting that after the insult calpain and calpastatin translocate to the plasma membrane, where calpain substrates are cleaved (Ostwald *et al.*, 1994).

Calpain 1 was also detected in the intermembrane space of mitochondria purified from mouse brain and cultured rat hippocampal/cortical neurons (Cao *et al.*, 2007). However, upon OGD, the active protease translocates to the inner mitochondrial membrane and to a lower extent to the outer membrane. The shift of calpain 1 to the inner mitochondrial membrane was followed by the calpain 1-mediated cleavage and release of AIF (Cao *et al.*, 2007). Because calpain inhibitors can also preserve mitochondrial function in cardiac tissue subjected to ischemia-reperfusion, and given the fact that calpains can cleave the Bax protein leading to cytochrome c release, and convert the antiapoptotic protein BcL-xL to become proapoptotic, it is safe enough to hypothesize that calpains may also regulate the apoptotic cascade in brain ischemia (Nakagawa and Yuan, 2000; Choi *et al.*, 2001). Another layer of complexity may result from the cleavage of certain members of the caspase family by calpains. Indeed, calpain was also proposed to

truncate caspase- 9,7 and-3, although with distinct functions in terms of cell fate (McGinnis *et al.*, 1999; Ruiz-Vela *et al.*, 1999; Chua *et al.*, 2000; Blomgren *et al.*, 2001).

Recent evidence suggests that not all NMDAR are coupled to calpain activation but it is mainly the extrasynaptic subpopulation of this class of glutamate receptors that, once stimulated, activates calpain and induces cell death [Figure 1.5; (Xu *et al.*, 2009a; Wei *et al.*, 2012; Wang *et al.*, 2013b)]. These results support the model proposing a preferential role for Ca^{2+} entry via extrasynaptic NMDAR in excitotoxic injury (Hardingham *et al.*, 2002). The first strong evidence for a mechanism underlying the selective role of extrasynaptic NMDAR in activating calpain was obtained in studies investigating the post-translational modifications of the phosphatase Striatal-Enriched protein tyrosine Phosphatase (STEP) (Xu *et al.*, 2009a). This protein phosphatase dephosphorylates and inactivates many synaptic signaling proteins, including Fyn, ERK and the stress-activated protein kinase p38. STEP also dephosphorylates GluN2B, thereby facilitating internalization of NMDAR (Xu *et al.*, 2009a; Goebel-Goody *et al.*, 2012). The activity of STEP isoforms ($STEP_{61}$ and $STEP_{46}$) is upregulated in the initial period following excitotoxic injury, with a consequent dephosphorylation of target proteins. Although the disruption in p38 signaling may provide neuroprotection in the early phase after transient focal ischemia, dephosphorylation of ERK and CREB impairs their role in neuronal survival (Paul *et al.*, 2003; Deb *et al.*, 2013).

Synaptic NMDAR are coupled to the activation of μ-calpain and through controlled proteolysis of intermediate proteins (a negative regulator) they are able to keep Akt in the phosphorylated form. In contrast, extrasynaptic NMDAR activation is coupled to m-calpain activation and degradation of the STEP protein (Figure 1.5). Consistent with this model, acute mouse hippocampal slices were protected against NMDA-induced neurotoxicity when m-calpain was inhibited, and showed an exacerbation of cell death in the absence of μ-calpain (Wang *et al.*, 2013b). This fits with the model in which Akt dephosphorylation may represent an endogenous mechanism that further exacerbate cell death.

Cyclin-dependent kinase 5 (Cdk5) is a serine/threonine kinase that is ubiquitous in the nervous system, participating in synaptic plasticity, although it is also involved in neurodegeneration (Barnett and Bibb, 2011). The Cdk5-activating cofactor p35 is cleaved by calpain, giving rise to p25, a more stable form of the protein, which lacks the amino-terminal myristoylation site and mislocalizes in the cell body and nucleus, thus inducing a sustained activation of Cdk5 (Patrick *et al.*, 1999; O'Hare *et al.*, 2005). Although the complex p25/Cdk5 is not more active than p35/Cdk5 (Peterson *et al.*, 2010), the longer half-life of the truncated isoform extends the activity of the complex. Accumulation of p25, translocation of the complex p25/Cdk5 to the nucleus and

aberrant activation of Cdk5 have been shown to have an important role in excitotoxic and ischemic neuronal death; cdk5 conditional-knockout mice show reduced infarct size after transient MCAo (O'Hare *et al.*, 2005; Meyer *et al.*, 2014). Cdk5 knockdown in mice submitted to MCAo (60 min) increased pAkt (S473) and prevented p38 up-regulation. Additionally, amelioration in the cognitive defects brought by brain ischemia, as well as Brain-derived neurotrophic factor (BDNF) release and subsequent activation of the TrKB-CREB pro-survival signaling pathway, was detected [(Gutierrez-Vargas *et al.*, 2016) see also (Gutierrez-Vargas *et al.*, 2015)].

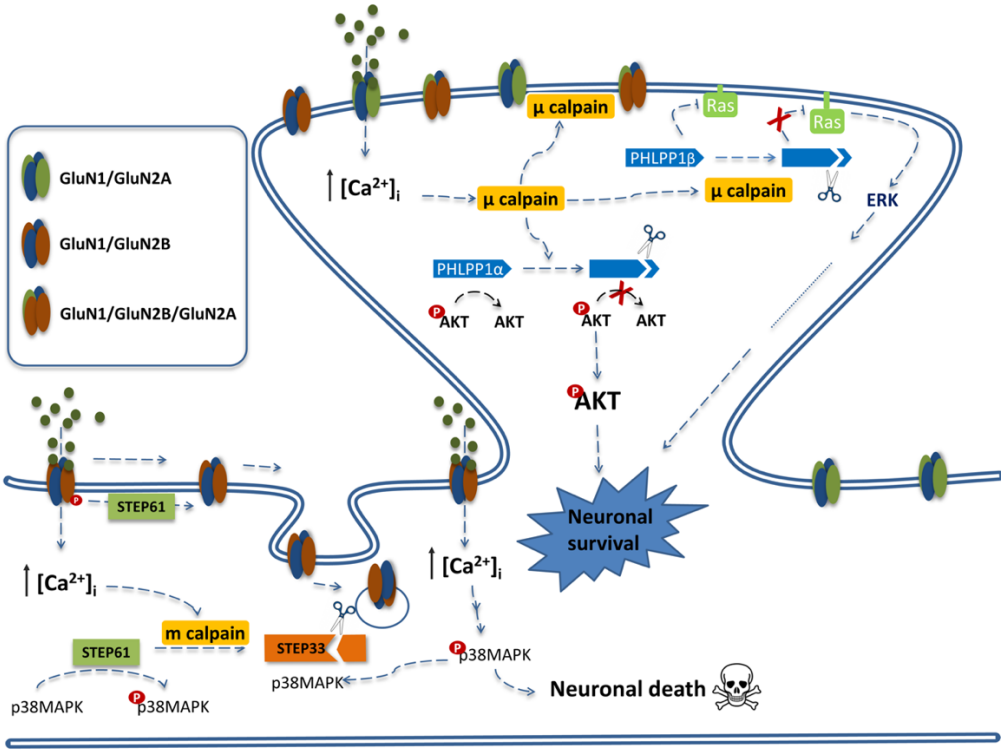

Figure 1.5- Differential effects of synaptic and extrasynaptic NMDAR on calpain activation and on downstream signaling mechanisms. Extrasynaptic NMDAR are preferentially coupled to activation of m-calpain, whereas the entry of Ca^{2+} through the synaptic population of NMDAR induces the activity of μ-calpain. Stimulation of the former population of NMDAR leads to the cleavage of STEP61 to STEP33. The truncated phosphatase is unable to bind and dephosphorylate its substrates, including p38 MAPK and GluN2B. In the phosphorylated (active) form, p38 MAPK contributes to neuronal death induced by excitotoxic stimulation of glutamate receptors. Active STEP also dephosphorylates GluN2B, thereby facilitating the internalization of NMDAR. Calpain-mediated cleavage of STEP may therefore upregulate the surface expression of GluN2B-containing NMDAR by impairing the internalization mechanisms, contributing to exacerbate the excitotoxic damage. In contrast, activation of μ-calpain following activation of synaptic NMDAR promotes neuronal survival by different mechanisms. μ-calpain cleaves PHLPP1α, a protein involved in the dephosphorylation (inactivation) of Akt, a pro-survival protein kinase. At the synapse, μ-calpain also cleaves PHLPP1β, a protein that binds and traps Ras in its inactive form, inhibiting ERK phosphorylation. Therefore, cleavage of PHLPP1β upregulates Ras/ERK signaling. Stimulation of synaptic NMDAR leads to the translocation of μ-calpain to the synapse, where the protease interacts with GluN2A subunits (Curcio *et al.*, 2016).

Calpain activation also plays a role in the reduction of protein synthesis observed in the CA1 region of the hippocampus, where neurons are destined to die after the ischemic injury (described previously). The activation of calpains after OGD and in the 4-VO model downregulates the eIF4G1 protein, which may contribute to cell death by reducing physiological protein synthesis [(Vosler *et al.*, 2011) see also (Ayuso *et al.*, 2013)].

Hence, calpains may regulate cell death and intracellular signaling under physiological conditions and during acute injury to the brain.

1.3. The Ubiquitin-Proteasome System (UPS)

Eukaryotic cells need to dispose continuously of unwanted or damaged biomolecules (e.g. proteins and organelles). Two major proteolytic systems play pivotal roles in the destruction of those biomolecules: (i) the Ubiquitin-Proteasome System (UPS), which is responsible for the turnover of small cytosolic proteins, and (ii) the autophagic-lysosomal system. The latter system is involved in the turnover of proteins, in addition to engulfing and degrading entire organelles (Cohen-Kaplan *et al.*, 2016). The UPS roles in the cell are transversal and particularly relevant in research areas ranging from cancer to brain disorders (Dennissen *et al.*, 2012; Caldeira *et al.*, 2014; Grigoreva *et al.*, 2015; Yerbury *et al.*, 2016).

The concerted action of ubiquitinating enzymes and the proteasome allows the degradation of many soluble proteins, and, under basal conditions, is responsible for regulating several homeostatic and important processes such as cell division, cell death, signal transduction, and membrane transport, among others.

1.3.1. Ubiquitin

Ubiquitin is a small, heat-stable and highly conserved 76-amino acid protein with 8.5 kDa, which can be covalently attached to other proteins (Hershko and Ciechanover, 1998). Ubiquitin was first described as a thymic hormone and to have lymphocyte-differentiation properties (Goldstein *et al.*, 1975; Schlesinger *et al.*, 1975; Hershko and Ciechanover, 1998), before its role in selective degradation of proteins was finally uncovered. Additional studies were required to identify a small protein, named APF-1 (ATP-dependent proteolysis factor 1), which was shown to play an important role in the selective degradation of APF-1 modified proteins (Ciehanover *et*

al., 1978; Ciechanover *et al.*, 1980). Later on, given the similarities on the amino acid sequence and physical properties, it was found that APF-1 was indeed ubiquitin (Wilkinson *et al.*, 1980).

Substrate proteins can be modified either by addition of one ubiquitin molecule (monoubiquitin), multiple monoubiquitin (multi-ubiquitination) or by a polyubiquitin chain (polyubiquitination). In the latter process, any of the seven lysine residues (Lys6, Lys11, Lys27, Lys29, Lys33, Lys48, Lys63) of ubiquitin can be linked to the previous one, resulting in a sizeable increase of the chains with different configurations [Figure 1.6; (Grabbe *et al.*, 2011)]. In an early attempt to quantify the relative abundance of polyubiquitin chains, using an yeast model, it was found that Lys48 polyubiquitin chains are the most abundant ones (29 %), followed by Lys11 (28 %), Lys63 (16 %), Lys6 (10.9 %), Lys27 (9 %), Lys33 (3.5 %) and Lys29 (3.2 %) [Figure1.6; (Xu *et al.*, 2009b)], which contrasts with another study in specific points (Ziv *et al.*, 2011). In the latter work, about 80 – 90 % of the polyubiquitin chains were formed via Lys48 or Lys63 (Ziv *et al.*, 2011).

The myriad of polyubiquitin modifying possibilities is responsible for the high complexity of this system, thus regulating different outcomes in the modified protein. While Lys48 polyubiquitin chains target proteins for proteasomal degradation in a process requiring at least four ubiquitin molecules (Chau *et al.*, 1989; Thrower *et al.*, 2000; Lander *et al.*, 2012), non-canonical Lys63 polyubiquitin chains are often associated with non-proteolytic functions such as DNA repair, kinase activity modulation (Hoege *et al.*, 2002; Chandrasekharan *et al.*, 2009), and protein sorting (Lauwers *et al.*, 2009; Lin *et al.*, 2011). Nevertheless, under certain conditions (e.g *in vitro* reactions with purified proteasomes), Lys63 polyubiquitin chains can also serve as degradative signal for the proteasome (Saeki *et al.*, 2009), which was not observed *in vivo* (Nathan *et al.*, 2013). A relatively large fraction of newly synthesized proteins arise as defective ribosomal products, being more than 30 % of them ubiquitinated (Schubert *et al.*, 2000; Ha *et al.*, 2016). Using the yeast as a model, it was found that ubiquitination occurs in 12-15 % of newly synthetized proteins while translation is occurring, being the effect enhanced by misfolding agents and HSP70 inhibitors, and prevented by ubiquitin mutants lacking Lys48 (Wang *et al.*, 2013a). Proteins involved in translation, ribosome biogenesis, nuclear transport and amino acid metabolism are more frequently subjected to this quality control mechanism; the same trend was also observed for longer polypeptides (Ha *et al.*, 2016).

Accumulation of Lys11,48-linked polyubiquitin chains (heterotypic polyubiquitin chains) has been associated with cell division, as they target important cell cycle regulators for proteasomal degradation (Castaneda *et al.*, 2013; Grice *et al.*, 2015; Min *et al.*, 2015), and along with Lys6, Lys27, Lys29, and Lys33-linked polyubiquitin chains, they may also direct proteins for

proteasomal degradation (Xu *et al.*, 2009b; Kim *et al.*, 2011). Additionally, some substrates (e.g NOXA, retinoblastoma protein (Rb), p53, p73, Rpn4 among others) have also been reported to be degraded by the proteasome (20S or 26S) in a manner independent of ubiquitination (Kalejta and Shenk, 2003; Ju and Xie, 2004; Asher *et al.*, 2005; Craxton *et al.*, 2012). Surprisingly, in some cases, mono- and multi-monoubiquitination can also act as proteasomal degradative signals (Boutet *et al.*, 2007; Dimova *et al.*, 2012; Braten *et al.*, 2016).

Ubiquitin itself is also a target of phosphorylation (e.g Ser65) by the PINK1 kinase, which in turn may serve as an autoregulatory mechanism of polyubiquitin chain assembly and function (Kane *et al.*, 2014; Swaney *et al.*, 2015). This adds an additional layer of complexity to this rather intricate proteolytic system that awaits further investigation in the context of the disease state.

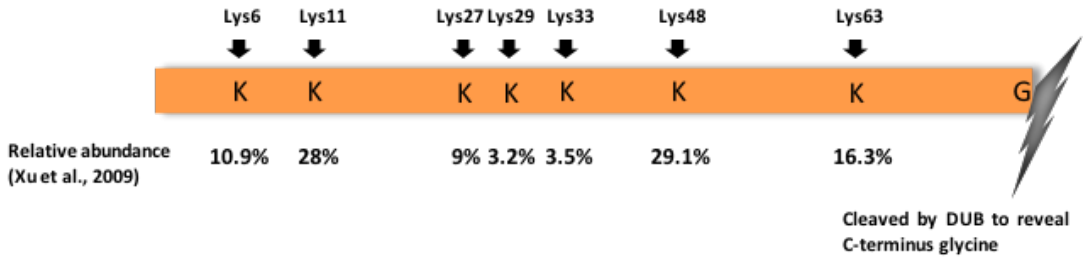

Figure 1.6- Ubiquitin structure. Ubiquitin is synthesized as a large precursor protein, whose C- terminus is cleaved by a deubiquitinating enzyme (DUB) to reveal a C-terminus glycine residue. Seven lysine residues are present in the primary amino acid structure of ubiquitin, which allow multiple potential polyubiquitin chain linkages. From all types of polyubiquitin chains, Lys48 (29.1 %), Lys11 (28 %) and Lys63 (16.3 %) are the most abundant (adapted from Xu et al., 2009).

1.3.2. Ubiquitination machinery

As a post-translational modification, the ubiquitination process, i.e., the process of adding ubiquitin to a substrate protein, and the removal of these ubiquitin molecules at a later point, is a finely tuned process governed by a cascade of ubiquitination enzymes and by deubiquitinating enzymes (DUBs), respectively.

Protein ubiquitination occurs through a sequential action of three different classes of enzymes: E1 or ubiquitin activating enzyme, E2 or ubiquitin conjugating enzyme and E3 or ubiquitin ligase. The human genome encodes for one E1, ~40 E2s and ~650 E3s [Figure 1.7; (Ye and Rape, 2009; de Bie and Ciechanover, 2011)]. E1 is the first enzyme involved in the ubiquitination cascade. It binds to Mg^{2+}-ATP and subsequently to ubiquitin to activate its C-terminal glycine residue. ATP hydrolysis generates an ubiquitin adenylate, followed by ubiquitin transference to a cysteine

residue of E1 through a thiol-ester linkage, with the release of adenosine monophosphate (AMP)(Ciechanover *et al.*, 1981; Haas *et al.*, 1982; Jin *et al.*, 2007; Olsen and Lima, 2013). Since this activating step is sequentially repeated, each fully loaded E1 carries two molecules of ubiquitin, one as a thiol-ester and the other as an adenylate (Fang and Weissman, 2004; Finley *et al.*, 2012). Activated ubiquitin is then transferred to a conserved core domain of ~150 residues (ubiquitin-conjugating (UBC) domain) of an E2 conjugating enzyme that includes an invariant cysteine residue responsible for accepting ubiquitin from E1 (Fang and Weissman, 2004; Ye and Rape, 2009). In the third step, ubiquitin is transferred, specifically, to a substrate protein by an E3 ligase. Two different classes of E3 ligases are responsible for the interaction with the E2 conjugating enzymes and can serve either as catalytic intermediates, or mediate the direct transfer of ubiquitin to the substrate: 1) Homologous to E6-AP Carboxyl Terminus (HECT) E3 ligases serves as intermediate ubiquitin acceptors through the formation of a thiol-ester linkage between ubiquitin and the cysteine residue in the HECT domain before ubiquitin is attached to the substrate ; 2) Really Interesting New Gene (RING) E3 ligases act only as "scaffold" proteins forming an E2-substrate protein complex that allows the direct transfer of ubiquitin to the target protein. Both types of E3 ligases lead to the formation of an isopeptide bond between the C-terminal glycine of ubiquitin and a ε-NH_2 group of an internal Lys of the substrate [for very recent review about the E3 ligase biology, please see (Buetow and Huang, 2016)].

1.3.3. Deubiquitinating enzymes

The ubiquitination process can be counteracted by deubiquitinating enzymes (DUBs). Six major classes of DUBs have been described: Ubiquitin C-terminal hydrolases (UCHs), Ubiquitin-specific proteases (USPs), Machado-Joseph disease protein domain proteases, ovarian tumor proteases and JAMM motif proteases (Love *et al.*, 2007; Sahtoe and Sixma, 2015), in addition to the newly discovered Motif Interacting with Ub-containing Novel DUB family (MINDY-1) (Abdul Rehman *et al.*, 2016). Almost all DUBs are cysteine proteases, except those belonging to the JAMM family which are metalloproteases (Todi and Paulson, 2011). DUBs may be intrinsic to the 26S proteasome (e.g. Rpn11), or may associate reversibly with the proteasome (e.g. Uch37 and USP14) (Koulich *et al.*, 2008; Tai *et al.*, 2010; Liu and Jacobson, 2013), and most of them have a cytosolic localization. Nevertheless, the *modus operandi* of ubiquitin removal is quite different: while Rpn11 remove polyubiquitin chains *en bloc* (from the proximal end), Uch37 and USP14 remove ubiquitin chains from the distal end, thus allowing the regeneration of free monomeric ubiquitin for re-utilization (Lam *et al.*, 1997; Yao *et al.*, 2006; Lee *et al.*, 2011a); a model was also proposed according to which USP14 can cleave ubiquitin chains *en bloc* (Lee *et al.*, 2016).

The overall function of DUBs is to cleave ubiquitin-linked molecules after the C-terminus of the last residue of ubiquitin (Gly76), being essential to: i) the maintenance of monomeric ubiquitin pool, either by cleaving the ubiquitin precursor (UCHL3, USP9X, USP7, USP5 and Otulin/Gumby/FAM105b) or by trimming polyubiquitin chains; ii) rescuing of proteins targeted for degradation, allowing the cell to adapt quickly to physiological changes, and iii) prevent ubiquitin-proteasome dependent protein degradation (Guterman and Glickman, 2004; Komander *et al.*, 2009; Grou *et al.*, 2015). Activation of the DUBs USP14 and Uch37, either by polyubiquitin chains or their chemical mimetics, stimulates the 19S associated ATPases thereby opening the 20S closed gate and thus promoting peptide hydrolysis (Peth *et al.*, 2009; Peth *et al.*, 2013). Recently, it was proposed a structural model in which the DUB USP14 controls the activity of the proteasome. Ubiquitin-bound USP14 prevents protein deubiquitination by Rpn11 allowing their stabilization in a proteasome-bound state; this is followed by translocation of the proteins into the proteasome where they are degraded (Bashore *et al.*, 2015).

1.3.4. Proteasome

The 26S proteasome is a 2.5 MDa multisubunit complex responsible for the controlled ATP-dependent degradation of polyubiquitinated proteins. It is composed of a catalytic 20S core particle (CP or 20S proteasome) associated with one (26S or RP_1CP) or two (30S or RP_2CP) 19S regulatory particles (RP or 19S proteasome), that are responsible for detecting, deubiquitinating and unfolding ubiquitinated proteins (da Fonseca *et al.*, 2012; Djakovic *et al.*, 2012). The 26S proteasome consists of at least 66 resident subunits and associated proteins, e.g. E3 ligases and assembling factors, such as molecular chaperones and others (Tai *et al.*, 2010; Fabre *et al.*, 2014). Although some ambiguity exists regarding proteasome subcellular localization, due to the different experimental approaches used, there are compelling evidence showing its nuclear and cytoplasmic expression (Lehmann *et al.*, 2002; Weberruss *et al.*, 2013; Yedidi *et al.*, 2016), in addition to proteasome storage granules (Yedidi *et al.*, 2016). However, recent data fostered the idea that only cytoplasmic proteasomes are catalytically active, and the nucleus is devoid of 26S proteasomes (Dang *et al.*, 2016).

Proteins committed for proteasomal degradation, labeled with a polyubiquitin chain with the appropriate size and topology, bind to the 26S proteasome (Lander *et al.*, 2012). Subsequent deubiquitination promotes the translocation of the proteins and their degradation by the proteasome. At the end, small peptides ranging from 2 to 24 amino acids (variable length), but short enough to diffuse out of the proteasome, and free ubiquitin are regenerated for reutilization; limited proteolysis has also been proposed [Figure 1.7; (Kisselev *et al.*, 1998;

Kisselev *et al.*, 1999; Emmerich *et al.*, 2000; Beinke and Ley, 2004)]. The interplay between ubiquitin and the 26S proteasome is further supported by a study showing increased catalytic activity of the 26S proteasome, in the presence of ubiquitinated substrates, and no changes were observed in the activity of the 20S proteasome (Peth et al., 2009).

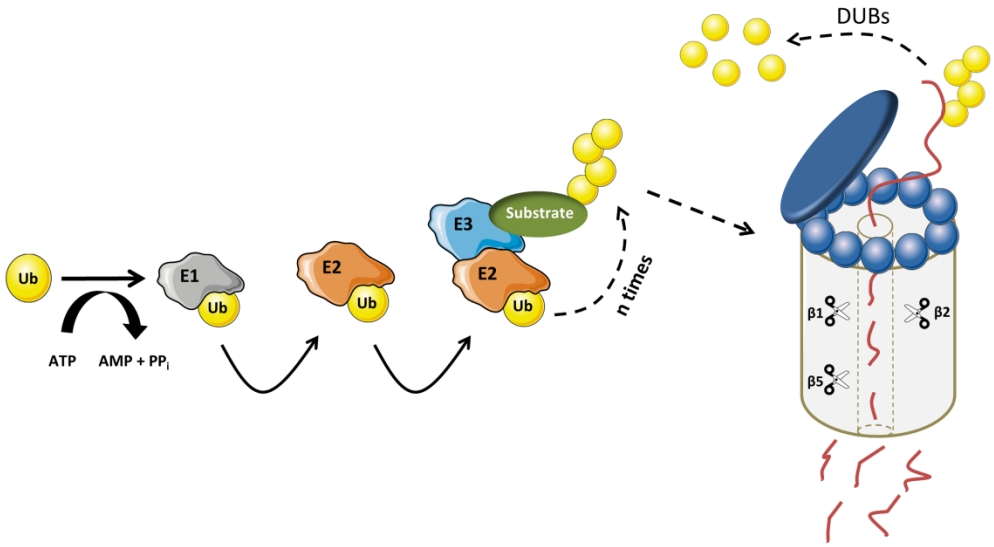

Figure 1.7- Main components of the Ubiquitin-Proteasome System. In order to be attached to the substrate protein, ubiquitin is first activated by the E1-activating enzyme in an ATP-dependent manner, and further transferred to the E2-conjugating enzyme. The substrate-specificity of this pathway is given by the E3 ligase, which allows the ubiquitination of a specific substrate. When a proper chain is assembled, with at least four ubiquitin moieties, it is recognized, unfolded and deubiquitinated by the 19S regulatory particle. This unfolding process allows the protein to enter the 20S catalytic particle where it is degraded by the β1 (trypsin-like activity), β2 (caspase-like activity) and β5 (chymotrypsin-like activity) subunits. At the end, small peptides are generated and ubiquitin is regenerated (Caldeira *et al.*, 2014).

The 20S proteasome is a ~670 kDa barrel-shaped structure composed of 28 subunits arranged in a four stacked ring structure: two α1-7 outer rings and two β1-7 inner rings [Figure 1.8; (da Fonseca and Morris, 2008)]. In the center of the ring there is a narrow pore, of about 12-18 Å, where a protein targeted for degradation can enter in an unfolded state (Huang *et al.*, 2016). Although the proteasome pore is closed by the N-terminus of the α2-4-subunits in free CP, truncation of the α3 N-terminal is enough to keep the pore open and increases the degradation of small peptides (Peth *et al.*, 2009). The resulting α3ΔN proteasomes showed increased activity in the degradation of the fluorogenic peptides and many established proteasome substrates (Choi *et al.*, 2016). Besides closing the pore, α-subunits are also responsible for compartmentalizing the catalytic β-subunits, thereby preventing uncontrolled cleavage of cytosolic proteins. Similarly, the β ring also forms a central chamber where the peptidylglutamyl-like (cleaving after acidic residues), trypsin-like (cleaving after basic residues) and chymotrypsin-

like (cleaving after hydrophobic residues) activities of the 20S proteasome are mediated by the β1, β2 and β5 subunits, respectively (Groll *et al.*, 1997; Orlowski and Wilk, 2000).

The other component of the 26S proteasome, the 19S regulatory particle, is a ~700 kDa multisubunit complex composed of at least 18 subunits. The 19S proteasome serves to recognize ubiquitinated proteins, deubiquitinate them and unfold the substrates in order to make them suitable to enter into the 20S catalytic pore. Biochemically, it is further divided in two distinct sub-complexes: the lid and the base [Figure 1.8; (Tomko and Hochstrasser, 2013)]. The lid consists of eight non-ATPase subunits, Rpn3, Rpn5-9, Rpn12 and Rpn11 (a DUB enzyme). The base contains six distinct AAA+ ATPases, Rpt1-6, and four non-ATPase subunits, the large scaffolding proteins Rpn1 and Rpn2, and the intrinsic ubiquitin acceptors Rpn10 and Rpn13 (Lander *et al.*, 2012; Tomko and Hochstrasser, 2013). Both proteins are apically located for a better capturing of ubiquitinated substrates through their ubiquitin binding domains Ubiquitin-Interacting Motif (UIM) and pleckstrin-like receptor for ubiquitin (Pru) domain, respectively (Hamazaki *et al.*, 2007; Schreiner *et al.*, 2008; Sakata *et al.*, 2012). Additionally, it was also proposed a role for these ubiquitin acceptors in the binding of a shuttling factor for the proteasome (e.g mHR23B and ubiquilin) (Hamazaki *et al.*, 2015). For the two large scaffolding proteins, it was shown that Rpn1 binds the shuttling factors Rad23 and Dsk2, the non-obligatory deubiquitinating enzyme Ubp6/USP14 and even ubiquitin, whereas Rpn2 serves as docking site for the ubiquitin acceptor Rpn13 (Elsasser *et al.*, 2002; Elsasser *et al.*, 2004; Rosenzweig *et al.*, 2012; Shi *et al.*, 2016a).

The ATPase ring of the 19S proteasome exhibits a spiral-staircase-like arrangement, resulting in some asymmetry in the Rpt subunits, predicting an even more complex mechanism for regulating polypeptide-substrate unfolding and translocation through the axial pore to the catalytic core by using ATP as energy source (Lander *et al.*, 2012; Kim *et al.*, 2015; Huang *et al.*, 2016). Conflicting results exist regarding the model for gate opening and substrate degradation. One study reported the importance of the Rpt2 subunit as the solely one responsible for CP opening and substrate entry (Köhler *et al.*, 2001), whereas others proposed a more complex mechanism, which also included the Rpt5 subunit (Smith *et al.*, 2007). Nevertheless, a more recent study has shown that the interaction of Rpt6 tail with the catalytic particle is essential for the Rpt3-mediated gate opening and maturation of the proteasome holonzyme (Sokolova *et al.*, 2015). All these studies are in accordance with atomic structure studies of human 26S proteasome showing insertion of the C-terminal tails of Rpt3 and Rpt5 subunits into surface pockets of the α-subunits in the CP, and the structural flexibility of the Rpt2 subunit which may regulate the function of others Rpt proteins (Huang *et al.*, 2016; Schweitzer *et al.*, 2016).

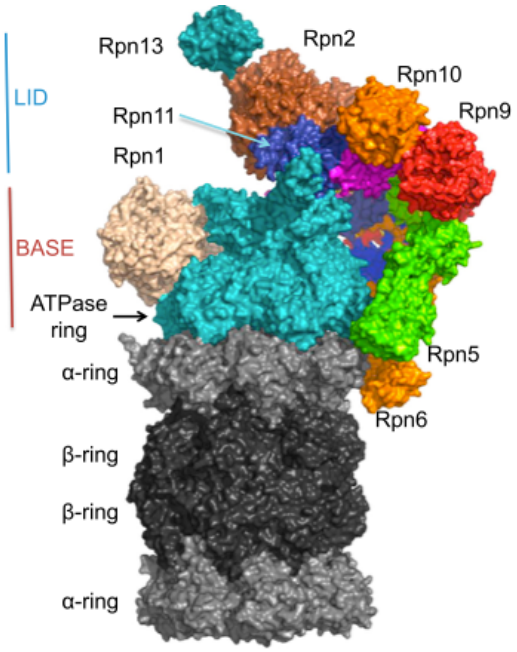

Figure 1.8- Current structural model for 26S proteasome. The 20S proteasome (bottom part) consists of two inner β-rings and two outer α-rings juxtaposed, forming a barrel-shaped structure. Each ring is composed by seven subunits (α1-7 and β1-7). While the only function of the α-ring is to close the pore through its N-terminus region, the β-ring is responsible to the degradative function of this catalytic particle. The peptidylglutamyl-like, trypsin-like and chymotrypsin-like activities of the 20S proteasome are catalyzed by the β1, β2 and β5 subunits, respectively. The 19S proteasome (top part) is further subdivided in two distinct biochemical entities; the base and the lid. They are composed by the AAA+ ATPase Ring (Rpt_{1-6}), and by subunits that have primarly a structural function (Rpn1-2,5-6,9) or participate actively in the ubiquitin-dependent recognition (Rpn10,13) and removal (Rpn11) (Spyracopoulos, 2016).

1.4. Role of the UPS in the nervous system

Neurons are very specialized post-mitotic cells unable to dilute the cellular content through cell division. As a result, the intracellular biochemical milieu is relatively constant throughout the life of the neuron. This makes neurons particularly vulnerable to diseases where aggregation-prone proteins are accumulated, leading ultimately to cell death (Dennissen *et al.*, 2012; Yerbury *et al.*, 2016). Thus, neurons rely on the degradative machineries that cells evolved, for instance the UPS, to maintain proper protein homeostasis thus preventing the unwanted accumulation of misfolded proteins. In the nervous system, the UPS is responsible for the regulation of numerous physiological aspects of synaptic function and architecture, ranging from spinogenesis (Hamilton *et al.*, 2012), presynaptic function and differentiation (Jiang *et al.*, 2010; Pinto and Almeida, 2016), apical dendrite outgrowth/polarization (Hamilton and Zito, 2013; Miao *et al.*, 2013), synapse formation and elimination (Yi and Ehlers, 2007), and learning and memory-associated processes such as Long-term potentiation (LTP), Long-term depression (LTD) and homeostatic plasticity, among others [for extensive reviews see (Leal *et al.*, 2015; Salazar *et al.*, 2016)] .

Rat cerebrocortical cell extracts possess a higher proportion of RP_1CP and RP_2CP (~57 %), when compared to HeLa (~39 %) and to rat liver/kidney cell extracts (~51 %) (Tai *et al.*, 2010). In the rodent brain tissue, the mean levels of unconjugated ubiquitin (122.6 pmol/mg) are comparable to the conjugated form (111.6 pmol/mg), and the proportion of polyubiquitin chains are to a certain extent similar to those observed in yeast cell extracts (Lys48 > Lys63 > Lys11 > Lys6 > Lys33 > Lys27 > Lys29) (Na *et al.*, 2012). All the above mentioned evidence point towards the importance of the UPS in the nervous system, and suggests that selective protein degradation is a highly controlled process.

1.4.1. Proteolysis and regulation of the UPS by synaptic activity

Synaptic activity can alter significantly the neuronal proteome within minutes after postsynaptic receptor activation. In fact, several components of the UPS can also be regulated upon NMDAR activation (Ehlers, 2003; Bingol and Schuman, 2006). Studies performed in cultured hippocampal neurons showed that increasing synaptic activity enhances proteasome activity, and induces a redistribution of the 26S proteasome from dendritic shafts to dendritic spines, as shown using the degradation reporter Ub^{G76V}-GFP and the proteasome reporter Rpt1-GFP, respectively (Bingol and Schuman, 2006). These alterations require Ca^{2+} influx through NMDAR and L-type voltage-gated calcium channels, followed by activation of the Ca^{2+}- and calmodulin-dependent protein kinase II alpha (CamKIIα), and subsequent phosphorylation of the 19S ATPase subunit Rpt6 on Ser120 (Djakovic *et al.*, 2009; Bingol *et al.*, 2010). In accordance with the role of CamKII in sequestering the proteasome at the synapse, and with the well-established interaction GluN2B-CamKII (Zhou *et al.*, 2007; Hamilton *et al.*, 2012), a recent report showed a decrease in the abundance of several proteasome subunits in purified postsynaptic densities (PSD) from hippocampal cultures obtained from $GluN2B^{-/-}$ mice (e.g Psmb1, Psmb2, Usp31 and others), providing the missing link between NMDAR activation and ulterior changes in the UPS (Ferreira *et al.*, 2015). Similarly, activation of NMDAR also stimulates the Ubiquitin C-terminal Hydrolase L1 (UCH-L1), thereby increasing free ubiquitin levels (Cartier *et al.*, 2009). NMDA application also promotes the accumulation of the deubiquitination enzyme CYLD (cylindromatosis) at the PSD, and its phosphorylation by CaMKII increases the activity of the enzyme towards Lys63-polyubiquitin chains (Thein *et al.*, 2014), suggesting that NMDAR are coupled to the activation of multiple deubiquitinating enzymes in parallel, which allow targeting a broader spectra of substrates.

In addition to the dynamics of the proteasomes in dendritic spines, several components of the synaptic proteome undergo ubiquitination in response to neuronal activity. Therefore, it is not

surprising that modulation of the excitability status of the neuronal networks can have differential effects in the proteins present in the PSD; overall ubiquitination in the PSD is increased and decreased in response to bath application of biccuculine and Tetrodotoxin (TTX), respectively (Ehlers, 2003). These results indicate that the neuronal proteome is finely regulated if the *status quo* of the neuronal network is challenged. Together, the multitude of actions on this complex proteolytic system following an increase in synaptic activity contributes to the regulation of proper synaptic remodeling and transmission.

1.4.2. Regulation of the synaptic proteasome through the UPS

Postsynapticaly, the UPS is responsible for regulating the levels and/or localization of several proteins present in the PSD (Figure 1.9). The GluN2B subunit of NMDAR was shown to be ubiquitinated by the E3 ligase Mib2, in a manner requiring the Fyn kinase, and overexpression of Mib2 was shown to decrease NMDAR-mediated currents (Jurd *et al.*, 2008). Furthermore, the NMDAR obligatory GluN1 subunit is ubiquitinated by the Fbxo2 E3 ligase when this subunit is translocated back to the endoplasmic reticulum, being degraded by cytosolic proteasomes (Kato *et al.*, 2005). Not surprisingly, Fbxo2 loss in vivo is associated with an increased surface expression of GluN1. Under the same conditions there is an upregulation in cell surface GluN2A, as well as in the abundance of the synaptic markers PSD-95 and VGlut1 (vesicular glutamate transporter type 1) (Atkin *et al.*, 2015), but whether Fbxo2 acts as a ligase for VGlut1, GluN2A and PSD95 remains to be further tested. Knockdown of the E3 ligase TRIM3 prevented the loss of both GKAP and Shank, suggesting that they may share the same ubiquitin ligase, or even that they can be co-degraded (Hung *et al.*, 2010). The removal of GKAP from the synapse is dependent on Ser54 phosphorylation by CamKIIα which induces its ubiquitination (Shin *et al.*, 2012). Nonetheless, Trim3$^{-/-}$ mice showed increased levels of γ-actin at hippocampal synapses, higher spine densities, increased LTP, and enhanced short-term contextual fear memory consolidation, while no changes were observed in Shank1 and GKAP total protein levels, suggesting that this E3 ligase may not be responsible for the turnover of both proteins (Schreiber *et al.*, 2015). For PSD95, both Siah (seven in absentia homolog) and Mdm2 (Murine double minute 2 homolog) were shown to act as E3 ligases to induce its ubiquitination (Tsai *et al.*, 2012; Mir *et al.*, 2014). The E3 ligase Ube3A, a protein associated with the Angelman Syndrome, is responsible for the turnover of Arc (activity-regulated cytoskeleton-associated protein; also known as Arg3.1), a protein involved in AMPAR endocytosis (Greer *et al.*, 2010).

Initial studies showed that AMPA-induced internalization of AMPAR was abolished by the proteasome inhibitor MG132, but no ubiquitination of AMPAR subunits was observed at that

time (Patrick *et al.*, 2003). Later, it was found that the activity-dependent ubiquitination (Lys63 polyubiquitin chains) of the GluA1 C-terminal tail is dependent on the Neural-precursor cell-expressed developmentally downregulated gene 4-1 (Nedd4-1) E3 ligase (Schwarz *et al.*, 2010; Widagdo *et al.*, 2015), and knockdown of the ligase prevented GluA1 ubiquitination, the interaction with the endocytic adaptor Eps15, and subsequent internalization of the subunit (Lin *et al.*, 2011). This process is counteracted by the DUB USP8 in its dephosphorylated state (active), in response to NMDAR activation, which promotes AMPAR reinsertion (Scudder *et al.*, 2014). Additionally, USP46 can also act as a DUB towards Lys63 polyubiquitin chains added to AMPAR by Nedd4 (Huo *et al.*, 2015). The AMPAR GluA2 subunit is also ubiquitinated in response to bicuculline treatment (Lussier *et al.*, 2011). The available evidence suggests that the RNF167 E3 ligase is involved in GluA2 ubiquitination and, accordingly, knockdown of this ligase was shown (i) to increase AMPAR mediated currents by increasing the surface expression of GluA2 and (ii) to prevent GluA2 ubiquitination in response to bicuculline treatment (Lussier *et al.*, 2012). The ubiquitination sites were identified in the C-terminal residues Lys868, and Lys870/882 for GluA1 and GluA2 subunits, respectively (Lin *et al.*, 2011; Widagdo *et al.*, 2015). Nevertheless, it is worthwhile to mention that all the studies were conducted using an experimental set up that rely almost exclusively in using proteasome inhibitors. These inhibitors were shown very recently also to have an effect in suppressing the expression of several synaptic proteins, as well as to have an effect in the expression levels of Nedd4 (Hakim *et al.*, 2016).

Thus, although the UPS may be responsible for the turnover of most soluble proteins, it also exerts an effect in the trafficking of glutamate receptors which in turn can affect synaptic strength.

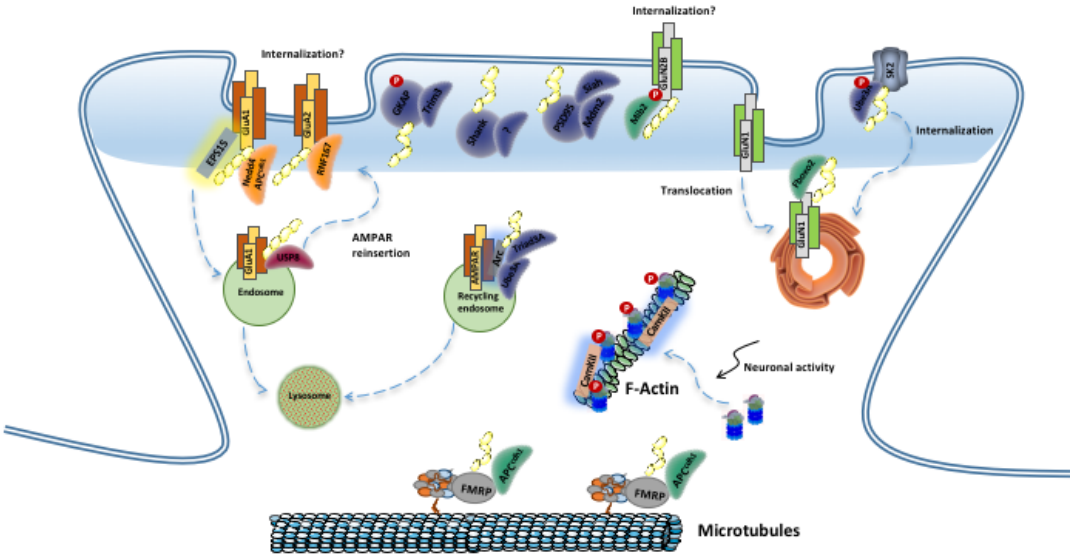

Figure 1.9- Regulation of the synaptic proteome by the Ubiqutin-Proteasome System. Several synaptic proteins undergo selective ubiquitination is response to increased neuronal activity. 1. AMPAR, especially GluA1 and GluA2 subunits, were shown to be ubiquitinated in response to AMPA treatment. The Nedd4 and APCCdh1 complex of E3 ligases ubiquitinates GluA1 while the RNF167 E3 ligase is the putative ligase for GluA2 subunit. GluA1 internalization and subsequent lysosomal degradation is halted if the DUB USP8 is activated, in a NMDA-dependent manner; the DUB removes the ubiquitin tag allowing the recycling of the AMPA receptor subunit. 2. The E3 ligases Ube3A and Triad3A are responsible for the ubiquitination of Arc, a protein involved in AMPAR endocytosis, thus regulating, in a indirect manner, AMPAR trafficking. 3. Neuronal activity induces the sequestration of proteasomes into dendritic spines through interaction with the actin cytoskeleton. 4. Furthermore, the postsynaptic proteins PSD-95 and GKAP are ubiquitinated by the Mdm2/Siah and Trim3E3 ligases, respectively. Removal of GKAP from synaptic sites and subsequent ubiquitination of the protein is mediated by CamKIIα-dependent phosphorylation. Shank is also ubiquitinated, but the E3 ligase remanins to be identified. 5. The NMDAR subunits GluN1 and GluN2B are ubiquitinated by the Fboxo2 and Mib2 E3 ligases, respectively. 6. Recently, Additional E3 ligases were recently identified. The activity of the Ube3A E3 ligase, which is regulated by protein kinase A (PKA), promotes SK2 channel endocytosis, by ubiquitinating its C-terminal domain. 8. Fraxil-X mental retardation protein (FMRP) was also shown to be ubiquitinated by the APC/Cdh1 E3 complex followed by its degradation, allowing the translation of the FMRP-repressed mRNAs important for synaptic plasticity (Salazar *et al.*, 2016).

1.5. UPS in Ischemic conditions

Despite recent advances, there are still major gaps in the understanding of the pathogenesis of cerebral ischemic injury and therapeutic options for stroke patients are limited (Moskowitz *et al.*, 2010). Transient cerebral ischemia is associated with an inflammatory response and a rapid and excessive production of various misfolded proteins due to oxidative stress among other mechanisms (Caldeira *et al.*, 2014). Overproduction of damaged proteins following ischemia is reflected in a pronounced upregulation in the conjugation of target proteins with ubiquitin (Hayashi *et al.*, 1992; Caldeira *et al.*, 2014). Therefore, the accumulation of ubiquitin-containing protein aggregates following ischemia is a general feature. However, the factors leading to

deposition of these aggregates and their consequences for stroke outcome remain poorly understood.

1.5.1. UPS and *in vivo* ischemia models

Transient cerebral ischemia induces the formation of irreversible misfolded protein aggregates (Figure 1.10). The first reports showed that brief rat forebrain ischemia, induced by bilateral common carotid occlusion combined with a reduction of the mean arterial blood pressure to 50 mmHg, evoked a selective and sustained loss of ubiquitin immunoreactivity in rat hippocampal CA1 neurons (Magnusson and Wieloch, 1989). However, a few years later, it was shown that the loss of ubiquitin immunoreactivity in gerbil hippocampal CA1 neurons after ischemia induced by BCo was a result of free ubiquitin depletion and did not arise from ubiquitin conjugation (Morimoto *et al.*, 1996). BCo-induced transient ischemia in gerbils promotes a transient consumption of free ubiquitin associated with an increase of conjugated multiubiquitin chains in hippocampal CA3 and dentate gyrus regions, where neurons survive, but these changes are persistent in the CA1 region, where neurons are more vulnerable and destined to die after 5 min of ischemia (Ide *et al.*, 1999). Under the same experimental conditions, a transient upregulation of the ubiquitin mRNA was observed in all hippocampal neurons and in the cerebral cortex, with maximal effects observed after 6 h of reperfusion, which then decreased to control levels at 48 h (Ide *et al.*, 1999). In the 2-VO model of global ischemia in rats, dying neurons in the hippocampal CA1 region also exhibited an accumulation of high-molecular weight ubiquitin-conjugated proteins, which were found in clusters around nuclei and close to the dendritic membrane during 4–24 h reperfusion after 15 min ischemia; this was not observed in CA1 neurons destined to survive or in the dentate gyrus (Hu *et al.*, 2000). Similar results were obtained at 1, 4, and 24 h of reperfusion after 2 h MCAo in rats, a model of focal ischemia (Hu *et al.*, 2001). The ubiquitin-positive immunoclusters of misfolded/damaged protein aggregates were also found in postsynaptic densities from hippocampal neurons of rats subjected to 15 min of 2-VO model followed by 4 and 24 h of reperfusion (Liu *et al.*, 2004). In summary, these results suggest that ubiquitin-containing clusters of misfolded or damaged proteins are formed in all post-ischemic neurons, primarily during reperfusion.

The clusters of ubiquitinated proteins formed after brain ischemia may give rise to protein aggregates by an unknown process, possibly through translation arrest, but the aggregates are maintained exclusively in CA1 neurons until their death (Hu *et al.*, 2000; Hu *et al.*, 2001; Liu *et al.*, 2004; Liu *et al.*, 2005a). In fact, translational complex components are irreversibly clumped into large abnormal protein aggregates after transient brain ischemia (Liu *et al.*, 2005a) or focal

brain ischemia (Zhang *et al.*, 2006a), suggesting that the irreversible inhibition of translation in neurons destined to die after ischemia is caused by irreversible aggregation of translational complex components, chaperones and protein folding enzymes. An enrichment of ubiquitinated proteins in insoluble fractions was observed 4 h after 10 min of BCCAo, particularly Lys6, Lys11, Lys48 and Lys63 modified polyubiquitin chains (Iwabuchi *et al.*, 2014). The same study found selective accumulation of ubiquitinated proteins responsible to regulate LTP, neurotransmission, initiation and elongation factors among others (Iwabuchi *et al.*, 2014). CamKII is one of the proteins present in aggregates after brain ischemia, with 27 out of the 28 lysine residues being ubiquitinated, consistent its aggregation after brain ischemia (Mengesdorf *et al.*, 2002; Iwabuchi *et al.*, 2014). Moreover, proteasomes, particularly the 19S RP, are also sequestered into these protein aggregates in post-ischemic brains (Ge *et al.*, 2007). Furthermore, cytoplasmic ubiquitin-containing aggregates and stress granules are clustered together in CA1 neurons at day 2-3 of reperfusion following global forebrain ischemia and may contribute to sustained translation arrest and CA1 pyramidal neuron vulnerability (DeGracia *et al.*, 2007).

Recent work also demonstrates that reperfusion, rather than ischemia, leads to the accumulation of ubiquitin aggregates in the neocortex, an area of more intense reperfusion, as well as in the striatum after MCAo (Hochrainer *et al.*, 2012). However, no ubiquitin aggregates were found in permanent ischemia and surprisingly proteasome impairment was greatest under these conditions (Hochrainer *et al.*, 2012), suggesting that the two events are independent. The formation of ubiquitin-protein aggregates may thus reflect a greater potential for tissue survival in the immediate postischemic period. The cause and effect relationship between protein aggregation and subsequent neuronal death remains to be determined and further studies are needed to uncover the roles of ubiquitinated protein aggregation after brain ischemia.

Accumulation of ubiquitin conjugated proteins and depletion of free ubiquitin following an ischemic injury suggest an impairment of proteasome function. In fact, transient global brain ischemia impairs 26S proteasome function by promoting proteasome disassembly, both in rats (Ge *et al.*, 2007) and gerbils (Kamikubo and Hayashi, 1996; Asai *et al.*, 2002). However, while the 26S proteasome activity recovers in many regions after reperfusion (e.g. CA3, dentate gyrus, and frontal cortex), in more vulnerable areas, such as CA1 region of the hippocampus, the 19S and 20S proteasomes do not fully reassociate, and the proteasome is irreversibly inhibited (Asai *et al.*, 2002). A time-dependent decrease in proteasome activity has also been detected in ipsilateral cortex and hippocampus during 1–24 h reperfusion after transient focal ischemia (Keller *et al.*, 2000), and this downregulation of proteasome activity was partly attributed to oxidative stress (Keller *et al.*, 2000).

Transient forebrain ischemia induced by BCAo in mongolian gerbils and transient focal brain ischemia induced by MCAo in mice were without effect on the expression of proteasome subunits, although a downregulation of the proteasome activity was found in both cases (Kamikubo and Hayashi, 1996; Keller *et al.*, 2000). These evidences suggest that posttranslational mechanisms are involved in the downregulation of the proteasome in the ischemic brain.

In summary, brain ischemia induces an excessive accumulation of ubiquitinated proteins, which are in excess to be degraded by the proteasome. The accumulation of ubiquitinated proteins may be further exacerbated due to the impairment of the proteasome activity, giving rise to aggregates that also contain other unfolded/damaged proteins or organelles, as observed in delayed neuronal death after brain ischemia.

1.5.2. Changes in the UPS in *in vitro* models of global ischemia

OGD, an in vitro model for transient global ischemia, was shown to induce hippocampal neuronal death, through activation of NMDAR, and to downregulate proteasome activity in a NMDAR activation-dependent manner (Caldeira *et al.*, 2013). This OGD induced decline on proteasome activity may be due to a rapid ATP depletion. A decrease in ATP content was in fact observed in cultured cortical neurons exposed to OGD followed by reoxygenation (Chen *et al.*, 2010) and in cultured hippocampal neurons subjected to excitotoxic stimulation (Caldeira *et al.*, 2013). However, irreversible ATP-independent inhibition of proteasome activity was detected in hippocampal CA1 neurons after transient forebrain ischemia (Asai *et al.*, 2002), suggesting that two different mechanisms may be involved in the regulation of proteasome activity after in vitro ischemia.

OGD followed by incubation of cells in culture conditioned medium (to mimic reperfusion) induces oxidative damage of the proteins, and the upregulation of oxidized proteins increases protein degradation after OGD in cultured cortical neurons (Weih *et al.*, 2001). However, a rapid increase in protein degradation was also observed even during OGD. Inhibition of proteasome was shown to prevent proteolysis of oxidized proteins after OGD (Weih *et al.*, 2001), suggesting a role for the UPS in the clearance of oxidized proteins in neuronal cells. Moreover, proteasomal activity was shown to be similar immediately after OGD and in sham-washed cultured cortical neurons (Weih *et al.*, 2001), in agreement with the relative resistance of the proteasome against oxidative stress (Reinheckel *et al.*, 1998). However, these results contrast with the protein aggregation and reduced cytosolic and nuclear free ubiquitin distribution reported in the

organotypic hippocampal slice culture model of OGD (Ouyang *et al.*, 2005). OGD followed by reoxygenation was also found to induce a time-dependent ubiquitination of misfolded proteins and aggregate formation, specially clustered near nuclei of cultured cortical neurons (Chen *et al.*, 2010). These effects seem to be mediated by a dysregulation of endoplasmic reticulum Ca^{2+} concentration, which affects protein folding. Interestingly, endoplasmic reticulum Ca^{2+} dysregulation also partially affects proteasome activity after OGD (Chen *et al.*, 2010). These findings point to the UPS as an active component of the cellular defense system against oxidative stress after cerebral ischemia.

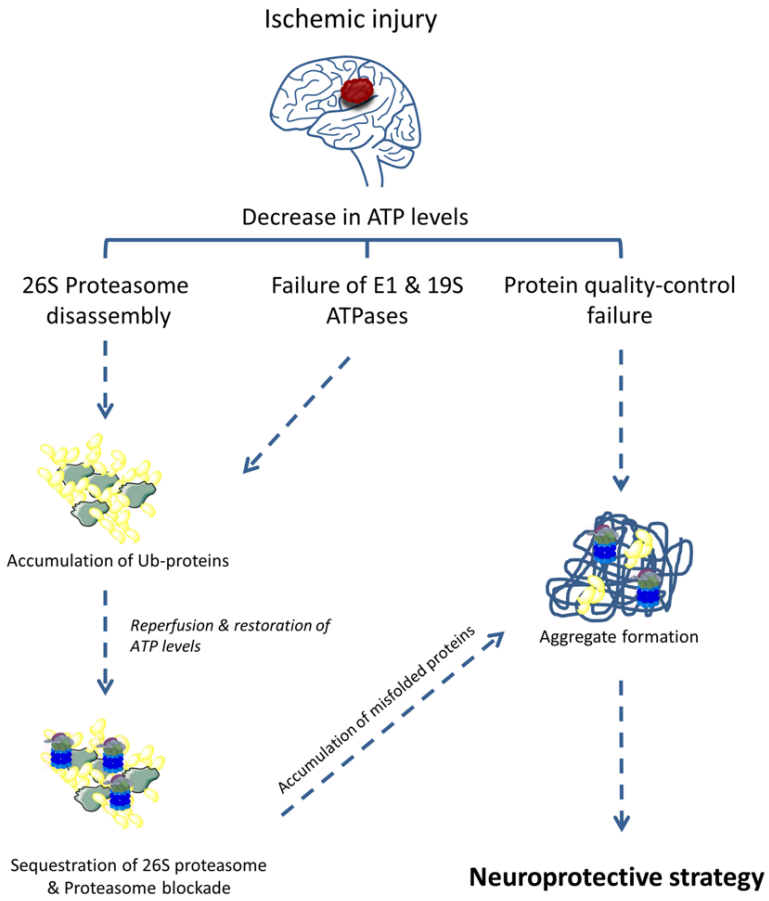

Figure 1.10- Overview of the consequences of brain ischemia on the Ubiquitin-Proteasome System. Transient ischemia decreases the ATP content of the affected areas, which contributes to 26S proteasome disassembly, leading to accumulation of ubiquitinated proteins and/or failure of the ubiquitin activating enzyme (E1), thus decreasing the overall efficiency of protein degradation by the UPS. After reperfusion of the injured area, 26S proteasomes are requested to degrade the accumulated ubiquitin conjugates and become sequestered. Since there is a large amount of 26S targeted proteins, proteasome also become blocked. The accumulation of new misfolded proteins will lead to the formation of aggregates. ATP decrease after ischemic injury may also contribute to the failure of quality-control mechanisms, which also contribute to aggregate formation. Aggregate formation is a protective response of the cell against abnormal proteins (Caldeira *et al.*, 2014).

1.5.3. UPS in glutamate-induced excitotoxicity

Activation of NMDAR plays a role in neuronal death induced by transient OGD in different neuronal culture systems (Martinez-Sanchez *et al.*, 2004; Bonde *et al.*, 2005; Ahlgren *et al.*, 2011), similarly to the role of glutamate receptors in neuronal damage in the ischemic brain [for review see (Kostandy, 2012)]. The activation of NMDA-type glutamate receptors is a mediator of neuronal death in OGD and may play a role in ischemia-induced downregulation of the proteasome activity, as shown in experiments where cultured hippocampal neurons were subjected to excitotoxic stimulation with glutamate or with NMDA (Caldeira *et al.*, 2013). The downregulation of the proteasome activity after excitotoxic stimulation with glutamate is specifically mediated by activation of extrasynaptic NMDAR (Caldeira *et al.*, 2013), in agreement with their role in excitotoxic neuronal death (Bengtson *et al.*, 2008). In particular, the entry of calcium through NMDAR channels is actively involved in the downregulation of the proteasome activity, possibly due to activation of downstream signaling pathways that target proteasome proteolytic activity. The effects of excitotoxic stimulation with glutamate on the activity of the proteasome, as measured with fluorogenic substrates, correlate with a disassembly of the 26S proteasome, by a mechanism that may be related with the decrease in the ATP content (Caldeira *et al.*, 2013). These structural changes in the proteasome resemble the alterations in the proteasome structure observed in brain ischemia (Kamikubo and Hayashi, 1996; Asai *et al.*, 2002; Ge *et al.*, 2007), further suggesting that overactivation of glutamate receptors plays a key role in the downregulation of the proteasome in the ischemic brain.

Although it is still unknown which are the signaling cascades that mediate the downregulation of the proteasome activity in brain ischemia, the activation of calpains and lysosomal cathepsins are good candidates, given the fact that the toxic effects of glutamate are partially mediated by the Ca^{2+}-dependent activation of calpains (Takano *et al.*, 2005), and these proteases were shown to be activated before downregulation of the proteasome in hippocampal neurons subjected to excitotoxic stimulation (Melo *et al.*, 2013). Recently, using cortical neurons with compromised ATP production, it was shown that the calpain-mediated cleavage of the S5a/Rpn10 ubiquitin acceptor protein within the proteasome may account for the decrease in the abundance of fully-assembled proteasomes (Huang *et al.*, 2013). The lysosomal cysteine proteases, cathepsin-B and cathepsin-L, are also involved in ischemic cerebral damage (Seyfried *et al.*, 2001) and in proteasomal subunit degradation (Cuervo *et al.*, 1995). Accordingly, it was shown that the excitotoxicity-induced proteasome inhibition was partially prevented by inhibition of cathepsin-L (Caldeira *et al.*, 2013), and more recent data demonstrated the role of macroautophagy in the degradation of proteasomes, a process called proteophagy (Waite *et al.*, 2016). This suggests

that the cross-talk between several family of proteases with the proteasome may occur thus regulating many aspects of the cell fate.

The studies performed concerning the effect of excitotoxic stimulation on the activity of the proteasome in cultured hippocampal neurons show that the nuclear proteasomes are preferentially targeted when compared with the cytosolic pool, which is not fully understood (Caldeira *et al.*, 2013). Impaired trafficking might be an attractive hypothesis that should be considered. The lack of substrate degradation by the UPS does not necessary correlate with proteasome dysfunction. Cell death brought by excessive NMDAR activation (100μM, 25min) was promoted by c-Jun elevation due to its impaired nuclear degradation. Synaptonuclear translocation of the synaptic component Proline rich 7 (PRR7) was shown to halt c-Jun degradation by interacting with the FBW7 E3 ligase, thus promoting a c-Jun transcriptional response (e.g induction of cell death associated genes) (Kravchick *et al.*, 2016).

Excessive NMDAR stimulation promotes the nuclear accumulation of cyclin B1 inducing apoptotic cell death by abnormal S-phase entry (Almeida *et al.*, 2005; Maestre *et al.*, 2008). Biochemically, this is due to the calpain-mediated generation of the Cdk5-p25, hyperphosphorylation of the Anaphase-Promoting complex/cyclosome (APC/C) Cdh1 activator protein, and subsequent entrapment of this E3 ligase in the cytosol, failing in the degradation of the cyclin B1 protein (Maestre *et al.*, 2008). Furthermore, excitotoxic stimulation with glutamate also downregulates total DUB activity but it was without effect on the activity of UCH-L1, showing that not all deubiquitinating enzymes are affected (Caldeira *et al.*, 2013). Taken together, these evidences suggest that the UPS is subjected to regulation at different levels in brain ischemia, and differential effects may be expected in distinct subcellular compartments.

Given the results pointing to a role of the UPS in the regulation of glutamatergic synapses, the downregulation of the proteasome observed in brain ischemia may have important implications at this level. A neurotoxic insult with glutamate (100 μM during 4 h) was shown to decrease the number of PDS-95 puncta and to cause PSD loss, which was accompanied by spine loss in cultured hippocampal neurons (Waataja *et al.*, 2008). These effects were attenuated by NMDAR antagonists, but protective effects were also observed in the presence of a proteasome inhibitor and by a genetic approach expressing p14ARF (which binds and inhibits Mdm2, cognate E3 ligase for PSD-95). This study suggests that glutamate activates NMDARs to stimulate a Ca^{2+}-dependent E3 ligase leading to PSD-95 ubiquitination and degradation through proteasome, with consequent loss of PSD-95 clustering (Waataja *et al.*, 2008). These results suggest that some of the alterations resulting from proteasome inhibition in brain ischemia may be protective.

Taken together, the available evidence show that excitotoxic stimulation with glutamate has multiple effects on the UPS which may contribute to the demise process in brain ischemia and in other neurological disorders.

1.5.4. UPS in ischemic tolerance

Ischemic tolerance is a neuroprotective mechanism in the brain, whereby prior exposure to brief periods of ischemia induces protection to subsequent harmful ischemic events (for review see (Meller, 2009)). Two mechanisms of ischemic tolerance have been described: i) classical or delayed ischemic tolerance, which requires protein synthesis and changes in the genomic response, resulting in protection after 24-72 h after the preconditioning stimulus (Barone *et al.*, 1998), and ii) rapid ischemic tolerance, independent of de novo protein synthesis, and producing neuroprotection within 30 min to 1 h following the preconditioning event (Meller *et al.*, 2006), suggesting that is regulated by posttranslational mechanisms.

UPS has been shown to play an important role in both types of ischemic tolerance. In fact, after delayed tolerant ischemia (5 min of BCCAo at 48 h of reperfusion period after a preconditioning stimulus of 2 min) the abundance of free ubiquitin was found to be restored above the normal values, in contrast with the ischemia-induced moderate and transient reduction of free ubiquitin. Although the results suggest *de novo* ubiquitin synthesis, no changes were observed in the ubiquitin mRNA (Ide *et al.*, 1999). A role for the UPS on rapid tolerance to ischemia was also described. A proteomic analysis of ubiquitinated proteins showed an upregulation of 17 proteins in cultured cerebrocortical neurons after a preconditioning ischemic event in vitro (OGD-pre-treated cells) and 7 proteins were exclusive of control samples. The authors found a cell death-associated protein, Bcl-2-interacting mediator of cell death (Bim), which is selectively ubiquitinated and degraded by the proteasome in cultured cortical neurons preconditioned with 30 min of OGD and 1 h of recovery, followed by 120 min of OGD and 24 h of post-incubation in culture conditioned medium (Meller *et al.*, 2006). These results suggest a rapid degradation of cell death promoting proteins and rapid neuroprotection by the UPS. Moreover, the UPS was found to increase neuronal resistance to excitotoxicity through rapid modulation of postsynaptic densities after preconditioning ischemia (Meller *et al.*, 2008). Ubiquitination and degradation of proteins involved in the structure and function of the PSD, namely MARCKS and fascin (actin binding proteins), result in the reorganization of actin cytoskeleton after preconditioning ischemia. These alterations result in the loss of NMDAR from the PSD and a concomitant selective attenuation of toxic NMDAR-mediated signaling at the time when tolerance to ischemia is acquired (Meller *et al.*, 2008). Accordingly, inhibition of the proteasome activity was

found to block the rapid ischemic tolerance-induced neuroprotection (Meller *et al.*, 2008). Moreover, previous studies have also shown a decrease of synaptic NMDAR during tolerance to OGD (Sattler *et al.*, 2000) and PSD-95 degradation by the UPS together with a loss of dendritic spines upon NMDAR activation (Waataja *et al.*, 2008). The neuroprotective effects (cerebral infarct size, memory and motor performance) induced by both acute and delayed ischemia preconditioning are also attenuated when the proteasome is inhibited with Z-Leu-Leu-Phe-CHO (Rehni *et al.*, 2010), further suggesting that immediate as well as prolonged beneficial effects of ischemic preconditioning in global cerebral ischemia and reperfusion (17 min BCAO followed by 24 h reperfusion) may be attributed to UPS activity.

1.5.5. Protective effects of proteasome inhibitors in brain ischemia

The experimental evidences described above point to a downregulation of the UPS in brain ischemia, as observed for example by an increase in the accumulation of ubiquitinated proteins, which correlates with neuronal death. Furthermore, injection of a proteasome inhibitor into the lateral ventricle of rats significantly decreased Nuclear Factor-κappaB (NF-kB) activity and resulted in apoptotic neuronal death in various CNS areas, suggesting that proteasome inhibition induces apoptotic neuronal death (Taglialatela *et al.*, 1998). Also, incubation of different types of neurons with proteasome inhibitors was shown to induce cell death (Qiu *et al.*, 2000; Bobba *et al.*, 2002; Ding *et al.*, 2006). These evidences would further suggest that proteasome inhibition contributes to neuronal death in brain ischemia. However, in contrast with the results described above, proteasome inhibitors were shown to provide neuroprotection in various models of stroke.

CVT-634, the first proteasome inhibitor to be tested in a rat model of focal brain ischemia, reduced infarction without affecting regional cerebral blood flow (Buchan *et al.*, 2000). A more detailed characterization of the neuroprotective properties of proteasome inhibitors in brain ischemia was provided with studies using MLN519, a compound structurally similar to lactacystin (Williams *et al.*, 2003). The effect of MLN519 was tested using transient MCAo (Williams *et al.*, 2004; Williams *et al.*, 2005), and the cardioembolic stroke model (Zhang *et al.*, 2001), and a therapeutic window of 6-10 h after ischemia/reperfusion brain injury was observed using the former model. The neuroprotective effects of MLN519 were attributed to a decrease in inflammation after the ischemic injury, through downregulation of NF-κB and downstream inflammatory genes, as well as inhibition of the infiltration of inflammatory cells into the brain (Phillips *et al.*, 2000; Zhang *et al.*, 2001; Williams *et al.*, 2003; Williams *et al.*, 2004; Williams *et al.*, 2005). In addition to the effects in reducing the brain pathology, MLN519 also improved the

neurological outcome after MCAo (Williams *et al.*, 2005). Furthermore, when combined with tissue plasminogen activator (tPA), MLN519 reduced the infarct volume and improved the neurological outcome as determined 1 week after stroke (Zhang *et al.*, 2001). Similarly, the proteasome inhibitor bortezomib combined with low doses of tPA showed additional neuroprotective effects when tested in a model of embolic stroke in rats (Zhang *et al.*, 2006b). Single administration of bortezomib within 2-4 h after injury also showed neuroprotective effects, and the proteasome inhibitor was proposed to act by promoting Endothelial nitric oxide synthase (eNOS)-dependent vascular protection and to prevent NF-κB-dependent vascular disruption (Zhang *et al.*, 2006b; Zhang *et al.*, 2006c; Zhang *et al.*, 2010). However, opposing results regarding the contribution of NF-κB in mediating cell death also exist. Deletion of the NF-κB p50 gene increased the number of TUNEL-positive cells in mice submitted to barrel cortex ischemic stroke when compared with the wild-type counterparts (Li *et al.*, 2013). Furthermore, the same trend was also observed for blood-brain barrier damage, suggesting that the NF-κB protein may have dual effects in mediating cell death and cell survival (Li *et al.*, 2013).

Although bortezomib has been approved by the Food and Drug Administration for the treatment of multiple myeloma and mantle cell lymphoma, the clinical use of this proteasome inhibitor is limited because of severe side effects (Ruschak *et al.*, 2011). A novel proteasome inhibitor, BSc2118, which is putatively better tolerated, was shown to provide protection in mice subjected to MCAo, when injected intrastriatally no later than 12h post-stroke. A single injection of BSc2118 provided long-term neuroprotection, reduced functional impairment, stabilized the blood-brain barrier by decreasing Matrix metallopeptidase 9 (MMP9) activity and enhanced angioneurogenesis. The upregulation of the Hypoxia-Inducible Factor 1A (HIF1A) transcription factor is also an important mediator in BSc2118-induced neuroprotection (Doeppner *et al.*, 2012). The same group also showed a reduction in infarct volume even when the compound was administered up to 9 h post-stroke. Although the inhibitor was administered in a different manner (systemic intraperitoneal delivery), the effect was also attributed to the preservation of the blood-brain-barrier integrity; neuronal survival persisted up to 28 days post-stroke (Doeppner *et al.*, 2016).

This apparent contradiction between the toxic effects resulting from proteasome inhibition in neurons and the effect of proteasome inhibitors in brain ischemia may be explained by an effect of proteasome inhibition in the secondary phase of brain injury and in neuroinflammation after stroke, which are reduced by proteasome inhibitors. Although neurons are sensitive to proteasome inhibition, they may be able to tolerate relatively long periods of intracellular accumulation of ubiquitinated proteins, allowing the control of neuroinflammation with the

proteasome inhibitors. Although therapy with proteasome inhibitors may be tolerated, it may exacerbate to some extent the response to ischemia due to an accumulation of ubiquitinated proteins that must be then removed by autophagic mechanisms.

Contrasting with all the results discussed above, the activity of the proteasome is enhanced after ischemic-reperfusion injury in the rat retina, and the proteasome inhibitor Bortezomib reduced the cell death by reducing the inflammatory mediators, pro-apoptotic proteins and oxidative makers (Chen *et al.*, 2013). Moreover, the IU1 compound, which acts as a USP14 inhibitor, a DUB that acts as a negative regulator of the 26S proteasome (Lee et al., 2010), was shown to reduce brain infarct volume in a mouse model of transient focal cerebral ischemia at day 4 after the insult (Doeppner et al., 2013), contrasting with the role of proteasome inhibition in promoting cell survival. The apparent contradiction between the effects of IU1 and proteasome inhibitors in brain ischemia should be further studied.

Objectives of the work

As discussed in the previous sections, the Ubiquitin-Proteasome System was shown to be impaired in several models of transient global/focal ischemia in the brain, as well as in models of NMDA-induced excitotoxicity (Sections 1.5.1, 1.5.2, 1.5.3). Under the same conditions there is an excessive activation of calpains due to the $[Ca^{2+}]_i$ overload. Little is known about the intimate relationship between these two proteolytic systems in a brain ischemia scenario. The main objective of the present work was to investigate the role of calpains in the dysregulation of the proteasome in brain ischemia, focusing in proteins of the 19S regulatory particle. As secondary objective, we aimed at characterizing the changes in subcellular localization of endogenous proteasomes in low-density cultured cerebrocortical neurons exposed to transient oxygen-glucose deprivation (OGD), which mimics global ischemia in vitro.

In the work described in Chapter 3 we established a low-density culture system to perform immunocytochemistry experiments in cerebrocortical neurons exposed to OGD, and analysed the dendritic distribution of the proteasome proteins PSMA2 and Rpt6 as markers of the 20S and 19S proteasome particles, respectively.

Moreover, we report OGD-induced changes in the chymotrypsin-like activity and in the assembly of the proteasome that mimic the alterations that have been described in vivo, indicating that OGD is a good in vitro model to investigate the dysregulation of the proteasome in brain ischemia. Under the same experimental conditions, we report evidences showing calpain activation. Since the decreased activity of the proteasome correlates with activated calpains, we investigated whether calpains may play a role in cleaving subunits belonging to the 26S proteasome which in turn may impair 26S proteasome. Herein we reported changes in several proteasome subunits in cultured cortical neurons subjected to transient OGD.

Because proteasome inhibition is a common feature observed in chronic neurodegenerative diseases and after acute brain injury, the effect of a proteasome activator in preventing cell demise will be also addressed. Thus, the neuroprotective effect of the DUB inhibitor USP14 in protecting cultured cortical neurons against the toxic effects of OGD was studied, in preventing calpain activation in the former conditions, and also in restoring normal polyubiquitination.

Chapter 2

Experimental Procedures

2. Experimental Procedures

2.1. Cerebrocortical cultures (high density and low density cultures)

Primary cultures of rat cortical neurons were prepared from the cortices of E17-E18 Wistar rat embryos. Briefly, cortices where washed with ice-cold HBSS three and five times, prior and after trypsin (0.06 %, 10 min at 37 °C) treatment, respectively. Cells were mechanically dissociated, no more than 10-15 times with HBSS. After counting, the cells were plated with Neuronal Plating Medium (MEM supplemented with 10 % horse serum, 0.6 % glucose and 1mM pyruvic acid) for 2-3 h in 6- or 24-well plates ($92.8x10^3$ cells/cm^2) coated with poly-D-lysine (0.1 mg/mL). After this period, the plating medium was removed and replaced by Neurobasal medium supplemented with SM1 supplement (1:50 dilution), without glutamate, 0.5 mM glutamine and 0.12 mg/mL gentamycin. For imaging purposes, low-density cortical cells were plated at a final density of $1.0x10^4$ cells/cm^2 on poly-D-lysine-coated coverslips, in 60 mm culture dishes, in neuronal plating medium. After 2-3 h, coverslips were flipped over an astroglial feeder layer. After 2-3 days in culture, division of glial cells was halted by addition of 10 µM 5-FdU-NOAC (5-FDU) to the medium. Cultures were fed twice a week and maintained in Neurobasal medium supplemented with SM1 supplement, and kept in a humidified incubator of 5 % CO_2, at 37 °C, for 14-15 days.

2.2. HEK293t cells maintenance and transfection

HEK293t cells were grown for 2 days in MW6 culture boxes until they reached about 60 % confluence. A solution of $CaCl_2$ (115 uM) and DNA (2-5 ug or 10 ug, for low yield and high yield DNA) was added drop-wise to a solution of 2x HEPES buffered saline (HBS) (50 mM HEPES, 280 mM NaCl, 1.5 mM Na_2HPO_4, pH 7.0). The precipitates were immediately then distributed evenly over the HEK293t cultures. The cells were allowed to incorporate the precipitates for 6 h and were further incubated for about 48 h to express the plasmid content. During these periods cells were maintained at 37 °C, with saturating humidity and 5 % CO_2 /95 % air. HEK293t cells were then washed twice with ice-cold PBS and the cells were then lysed in 100 µl of 50 mM Tris-HCl pH 7.5, 10 % Glycerol, 5 mM $MgCl_2$, 2 mM DTT, 2 mM ATP. The extracts were then centrifuged at 16,100 x g for 10 min at 4°C, and the protein content in the supernatants was quantified using the Bradford method.

2.3. Oxygen-Glucose Deprivation (OGD) Assays

Cultured cerebrocortical neurons (14-15 DIV) were incubated for 45 min or 1h30min (see figure captions) in a solution containing 10 mM Hepes, 116 mM NaCl, 5.4 mM KCl, 0.8 mM $MgSO_4$, 1 mM NaH_2PO_4, 25 mM $NaHCO_3$, 1.8 mM $CaCl_2$, pH 7.3, and supplemented with 25 mM glucose (Sham cells) or with 25 mM sucrose (OGD) at 37°C. Sham cells were maintained in an incubator with 5 % CO_2/95 % air, whereas the latter group was incubated in an oxygen deprived chamber (5 % CO_2, 7.5 % H_2, 87.5 % N_2; OGD cells) (Thermo Forma Anaerobic System Model 1029). Cells were further incubated in culture conditioned medium for 4 h (for extracts), or for the period of time indicated in figure captions (for proteasome activity). When appropriate, 50 µM MDL 28170 (Calbiochem) or 100 µM APV (Enzo Lifesciences) were added to the culture medium 30 min before OGD and were present throughout the experimental procedure. The DUB USP14 inhibitor IU1 (20 µM; Focus Biomolecules) was added to the culture medium 30 min before OGD, or immediately after, and was present throughout the experiment.

2.4. Immunocytochemistry

Cerebrocortical neurons (low-density cultures) were fixed in 4 % sucrose/paraformaldehyde (in PBS) for 15 min at room temperature and permeabilized with 0.3 % Triton X-100 in PBS. Neurons were then incubated with 10 % BSA in PBS, for 30 min at 37°C, to block non-specific staining, and incubated overnight at 4°C with the primary antibodies diluted in 3 % BSA in PBS. The following primary antibodies and dilutions were used: anti-PSMA2 (1:300 dilution [rabbit]; Cell Signaling #2455), anti-Rpt6 (1:400 dilution [mouse]; Enzo #BML-PW9265), anti-MAP2 (1:10,000 dilution [chicken], Abcam #ab5392), anti-PSD95 (1:200 dilution [rabbit]; Cell Signaling # 1673450S) and anti-PSD95 (1:200 [mouse]; Thermo Scientific #MA1-045). The cells were washed 6 times with PBS for 2 min and incubated with Alexa Fluor 568- (1:500 dilution, Invitrogen), Alexa Fluor 488- (1:500 dilution; Invitrogen) and AMCA- (1:200 dilution; Jackson ImmunoResearch) conjugated secondary antibodies, for 45 min at 37°C. After washing the cells 6 times with PBS for 2 min, the coverslips were mounted with a fluorescence mounting medium (DAKO).

2.5. Flurorescence Microscopy and quantitative fluorescence analysis

Imaging was performed in an Axio Observer Z1 fluorescence microscope, coupled to an Axiocam HRm digital camera, using a Plan-Apochromat 63x/1.4 oil objective. Images were quantified using the ImageJ image analysis software. For quantitation, independent sets of cells were cultured and stained simultaneously, and imaged using identical settings. The immunoreactivity signals were analysed after setting the thresholds, and the recognizable clusters under those

conditions were included in the analysis. The number, area and the integrated intensity of PSMA2 or Rpt6 particles in dendrites were determined and represented per dendritic area. For colocalization analysis, regions around thresholded puncta were overlaid as a mask in the PSD95 (or MAP2) channel, and the integrated intensity, area and number of colocalized particles determined.

2.6. Nuclear morphology staining

Cerebrocortical neurons were cultured for 14 days on poly-D-lysine-coated glass coverslips, at a density of $94.7x10^3$ cells/cm^2. After the appropriate stimulus (see figure captions), cells were fixed in 4 % sucrose/ 4 % paraformaldehyde (in PBS), for 15 min at room temperature, washed once with ice-cold PBS and the nuclei were then stained with Hoechst 33342 (1 µg/mL), for 10 min, protected from the light, at room temperature. After this, cells were washed once with ice-cold PBS and the coverslips were mounted with a fluorescent mounting medium (DAKO). Images were captured using a Zeiss Axiovert 200 fluorescent microscope coupled to an Axiocam camera. Three independent coverslips were prepared for each experimental condition, and at least 200 cells were counted in each case.

2.7. Preparation of extracts and quantification of proteasome activity

Hippocampal neurons were washed twice with ice-cold phosphate-buffered saline (PBS). The cells were then lysed in 1 mM EDTA, 10 mM Tris-HCl pH 7.5, 20 % Glycerol, 4 mM dithyothreitol (DTT) and 2 mM ATP (100 µl/well). Whole cell extracts were centrifuged at 16,100 x g for 10 min at 4°C, total protein content in the supernatants was quantified using the Bio-Rad method, and the concentration of the samples was equalized with lysis buffer.

The peptidase activity of the proteasome was assayed by monitoring the production of 7-amino-4-methylcoumarin (AMC) from a fluorogenic peptide: Suc-LLVY-AMC (for chymotrypsin-like activity; Peptide Institute, Inc). Samples (5-10 µg) were incubated with the fluorogenic substrate, 50 µM Suc-LLVY-AMC, in 50 mM Tris-HCl (pH 8.0) and 0.5 mM EDTA buffer, in a final volume of 100 µl. The release of fluorescent AMC was measured at 37°C using a SPECTRAmax Gemini EM (Molecular Devices) microplate reader, at an excitation wavelength of 360 nm and an emission wavelength of 460 nm, for 60 min at 5 min intervals. All the experiments were performed in the presence of 2 mM ATP. Specific activity was determined by subtracting the activity measured in the presence of 10 µM MG-132 (Calbiochem), a reversible proteasome inhibitor.

2.8. Native Gel Electrophoresis

Cerebrocortical neurons (14 DIV) were washed twice with ice-cold PBS and the cells were then lysed in 100 µl of 50 mM Tris-HCl pH 7.5, 10 % Glycerol, 5 mM $MgCl_2$, 2 mM DTT and 2 mM ATP. The extracts were then centrifuged at 16,100 x g for 10 min at 4°C, and the protein content in the supernatants was quantified using the Bradford method. The protein concentration in the samples was equalized with lysis buffer before separation in 4 % polyacrylamide native gels, under non-denaturing conditions, at 90 V for 8 h (4°C) as described elsewhere (Elsasser et al., 2005; Caldeira et al., 2013). The proteins in the gel were then electrotransferred to polyvinylidene (PVDF) membranes and immunoblotted using an antibody against PSMA2 (Cell Signaling) or Rpt6 (Enzo).

2.9. Western Blotting

Cerebrocortical neurons (14 DIV) were washed with ice-cold PBS buffer and then lysed with RIPA buffer (150 mM NaCl, 50 mM Tris-HCl, pH 7.4, 5 mM EGTA, 1 % Triton, 0.5 % DOC and 0.1 % SDS at a final pH 7.5), supplemented with 50 mM NaF, 1.5 mM sodium orthovanadate and the cocktail of protease inhibitors. After centrifugation at 16,100 x g for 10 min, protein in the supernatants was quantified using the bicinchoninic acid (BCA) assay, and the samples were diluted with a 2x concentrated denaturating buffer (125 mM Tris, pH 6.8, 100 mM glycine, 4 % SDS, 200 mM DTT, 40 % glycerol, 3 mM sodium orthovanadate, and 0.01 % bromophenol blue).

Protein samples were separated by sodium dodecyl sulfate polyacrylamide gel electrophoresis (SDS-PAGE), in 6.5-11 % polyacrylamide gels, transferred to PVDF membranes (Millipore), and immunoblotted. Blots were incubated with primary antibodies (overnight at 4°C), washed and exposed to alkaline phosphatase-conjugated secondary antibodies (1:20,000 dilution; Jackson Immunoresearch; 1 h at room temperature). The following primary antibodies were used: Anti-PSMA2 (1:1000 dilution [rabbit]; Cell Signaling #2455), Anti-Rpt6 (1:1000 dilution [mouse]; Enzo #BML-PW9265), Anti-GFP (1:1000 dilution [mouse]; Roche #11814460001), Anti-Rpn10 (1:1000 dilution [mouse]; Enzo # BML-PW9250), Anti-Ubiquitin (1:1000 dilution [rabbit]; DAKO #Z0458), Anti-Spectrin (1:1000 dilution [mouse]; Millipore # MAB1622), Anti-Rpt3 (1:100 dilution [mouse]; Santa Cruz Biotechnology #sc-166115), Anti-Rpn1 (1:100 dilution [mouse]; Santa Cruz Biotechnology #sc-271775), Anti-Rpt1 (1:100 dilution [mouse]; Santa Cruz Biotechnology #sc-166972), Anti-Rpn3 (1:200 dilution [mouse]; Santa Cruz Biotechnology #sc-393588) and Anti-Calpain1 (1:1000 dilution [rabbit]; Abcam # ab28258). Alkaline phosphatase activity was visualized by ECF on the Storm 860 Gel and Blot Imaging System (GE Healthcare) or the ChemiDoc Touch Imaging System (BioRad).

2.10. Stripping and reprobing of the membranes

In order to reprobe membranes with additional primary antibodies, namely those used against β-tubulin, used as experimental loading control, ECF was removed by washing the membranes with TBS-T for 30-40 min. After this washing step, the membranes were washed for 5 min with 0.2 M NaOH and washed again, abundantly with water for 30 min. Membranes were again blocked for 45 min, with 5 % non-fat milk in TBS-T, and incubated with the anti-β-tubulin antibody (1:600 000). Secondary antibodies were incubated for 1 h at room temperature as previously mentioned.

2.11. Incubation of HEK293t cell extracts with human recombinant calpain

HEK293t cell extracts were diluted in a buffer containing 50 mM Tris-HCl, pH 7.4, 100 mM KCl, 2 mM DTT and 2mM ATP, and incubated with 2.5 U/mL recombinant calpain I (human erythrocytes, Calbiochem), in the presence or in the absence of 4 mM $CaCl_2$, for 1 h at 37°C and with constant agitation (Gomes et al., 2011; Lobo et al., 2011). Incubation was stopped by addition of concentrated denaturating buffer followed by boiling the samples for 5 min at 95°C.

2.12. Evaluation of putative PEST sequences in proteasome subunits

The amino acid sequence of 26S proteasome subunits was analysed for the presence of putative PEST sequences. The subunit composition of the 26S proteasome was published in (Bousquet-Dubouch *et al.*, 2009), and the Uniprot ID for the proteins from *Rattus novergicus* is indicated Table 2.1. The amino acid sequence of each protein, obtained from the UniProt Database (http://www.uniprot.org), was analysed using the EPESTFIND proteolytic sequence finder (http://emboss.bioinformatics.nl/cgi-bin/emboss/help/epestfind). The threshold was set to +5.00, and only proteins with a score higher than this were considered to be putative targets for proteolytic cleavage by the proteasome.

2.13. Lactate dehydrogenase (LDH) assay

After the OGD insult, the cells were further incubated in culture conditioned medium for the period of time mentioned in the figure captions. The LDH leakage to the extracellular medium was evaluated by a colorimetric assay, using the CyoTox 96 Non-Radioactive assay kit (Promega), according to the manufacturer´s instructions. Briefly, the extracellular medium was removed and diluted with an equal volume of H_2O to a final volume of 100 µl, and 50 µl of substrate mix was added to the diluted sample, at room temperature, protected from the light. Incubation with the substrate was performed for 15-30 min and the reaction was stopped with 50 µl of stop

solution. The activity of LDH was measured using a SPECTRAmax Gemini EM (Molecular Devices) microplate reader, at an excitation wavelength of 490 nm. The percentage of LDH released to the medium was determined as the ratio between LDH activity in the extracellular medium and total LDH activity (100 % cell death) obtained by cell lysis.

Table 2.1 - Proteasomal proteins analysed for the presence of putative PEST sequences using the EPESTFIND software. The Uniprot IDs correspond to the *Rattus novergicus* proteins. Adapted from (Bousquet-Dubouch et al., 2009).

	Uniprot ID	Gene	Protein	Uniprot ID	Gene	Protein
20S Core particle	P60901	PSMA6	α1	P28073	PSMB6	β1
	P17220	PSMA2	α2	Q95HWO	PSMB7	β2
	P21670	PSMA4	α3	P40112	PSMB3	β3
	P48004	PSMA7	α4	P40307	PSMB2	β4
	P34064	PSMA5	α5	P28075	PSMB5	β5
	P18420	PSMA1	α6	P18421	PSMB1	β6
	P18422	PSMA3	α7	P34067	PSMB4	β7
19S Core particle	Q63347	PSMC2	Rpt1	Q4FZT9	PSMD2	Rpn1
	P62193	PSMC1	Rpt2	O88761	PSMD1	Rpn2
	P43686	PSMC4	Rpt3	Q5U2S7	PSMD3	Rpn3
	G3V6W6	PSMC6	Rpt4	Q5XIC6	PSMD12	Rpn5
	Q63569	PSMC3	Rpt5	F1LMZ8	PSMD14	Rpn6
	P62198	PSMC5	Rpt6	Q6DCT9	PSMD6	Rpn7
	Q5U2N2	USP14	Usp14	D4AEH3	PSMD7	Rpn8
	BOBN93	PSMD13	Rpn9	Q9ESH1	PSMD4	Rpn10
	Q4V8E2	PSMD14	Rpn11	F1LMQ3	PSMD8	Rpn12
	Q95MB5	ADRM1	Rpn13			

2.14. Total RNA isolation, RNA quality and RNA concentration

Total RNA from 14 DIV cultured cerebrocortical neurons was extracted with NZyol (Nzytech), following the manufacturer's specifications. The full content of a 6-well cluster plate, with a density of $94.7x10^3$ cells/cm^2, was collected for each experimental condition. After the addition of chloroform and phase separation, the RNA was precipitated by the addition of isopropanol. The precipitated RNA was washed once with 75 % ethanol, centrifuged, air-dried and resuspended in 60 µl of RNase-free water (GIBCO Invitrogen). The whole procedure was performed at 4°C. RNA quality and integrity was assessed using the Experion automated gel-electrophoresis system (Bio-Rad). A virtual gel was created for each sample, to estimate the degradation of the reference markers, RNA 18S and 28S. Samples showing RNA degradation or contamination by DNA were discarded. RNA concentration was determined using the Nanodrop System (ThermoScientific). The samples were aliquoted and stored at -80°C until further use.

2.15. Reverse Transcription reaction

For first strand cDNA synthesis 1 µg of total RNA was mixed with Random Hexamer Primer $p(dN)_6$ followed by 10 min denaturation at 65°C to ensure loss of secondary structures that may interfere with the annealing step. The samples were chilled on ice, and the template-primer mix was then supplemented with Reaction Buffer (50 mM Tris/HCl, 30 mM KCl, 8 mM $MgCl_2$, pH 8.5), Protector RNase Inhibitor (20 U), dNTPs (1 mM each) and finally AMV Reverse Transcriptase (10U; Roche), in a 20 µl final volume. The reaction was performed at 25°C for 10 min, followed by 30 min at 55°C, for primer annealing to the template and cDNA synthesis, respectively. The Reverse Transcriptase was then denatured during 5 min at 85°C, and the samples were cooled to 4°C for 5 min, and finally stored at -80°C until further use.

2.16. Primer Design

Primers for real-time PCR were designed using the "Beacon Designer 7" software (Premier Biosoft International), and the following considerations were taken: (1) GC content about 50 %; (2) annealing temperature (T_a) between 55 ± 5°C; (3) secondary structures and primer-dimers were avoided; (4) primers length between 18-24 bp; (5) final product length between 100-200 bp. The following primers for UbiquitinC gene were used: Forward sequence (5'-3') CTTTGTGAAAACCTTAACTG; Reverse sequence (5'-3') ATCTTTGCCTTGACATTT.

2.17. Real-Time PCR

For gene expression analysis 2 µl of 1:100 diluted cDNA were added to 10 µl 2x SYBR Green Master Mix (Bio-Rad) and the final concentration of each primer was 250 nM in 20 µl total volume. The thermocycling reaction was initiated with activation of the Taq DNA Polymerase by heating at 95°C during 30 s, followed by 45 cycles of a 10 s denaturation step at 95°C, a 30 s annealing step at the optimal annealing temperature for each set of primers, and a 30 s elongation step at 72°C. The fluorescence was measured after the extension step, using the iQ5 Multicolor Real-Time PCR Detection System (BioRad). After the thermocycling reaction the melting step was performed with slow heating, starting at 55°C and with a rate of 0.5°C per 10 s, up to 95°C, with continuous measurement of fluorescence, allowing detection of possible non-specific products. The assay included a non-template control and a standard curve (in 10-fold steps) of cDNA for assessing the efficiency of each set of primers. All reactions were run in duplicate to reduce confounding variance.

The threshold cycle (C_t) represents the detectable fluorescence signal above background resulting from the accumulation of amplified product, and is a proportional measure of the

starting target sequence concentration. C_t was measured in the exponential phase and, therefore, was not affected by possible limiting components in the reaction. For every run performed C_t was set at the same fluorescence value. Data analysis was performed using the GenEx (MultiD Analyses) software for real-time PCR expression profiling.

2.18. Statistical Analysis

Statistical analysis was performed using one-way ANOVA analysis of variance followed by the Dunnett's or Bonferroni test, or using the two-tailed Student´s *t* test, as indicated in the figure captions.

Chapter 3

Results

3.1. Proteasome Dynamics during OGD in cortical neurons

The ubiquitin-proteasome system (UPS) is responsible for the turnover of many cytosolic proteins, and under resting conditions they show a widespread distribution in neurons, which includes nuclei, cytoplasm, dendrites, axons and synaptic buttons (Mengual *et al.*, 1996). Furthermore, proteasomes were shown to be recruited to dendritic spines in response to neuronal activity (Bingol and Schuman, 2006). Lewi body formation in Alzheimer´s disease also show positive staining for the regulatory particle of the proteasome, consistent with its sequestration in proteins aggregates (Fergusson *et al.*, 1996). Entrapment of proteasomes in large protein aggregates was also proposed during the reperfusion period after brain ischemia (Ge *et al.*, 2007). This suggests that the proteasome trafficking may me impaired in the disease state, thus promoting an unbalance in several neuronal homeostatic mechanisms.

Since little is known about the proteasome dynamics after brain ischemia, namely the subcellular localization of the two components of the 26S proteasome, we evaluated the effect of oxygen and glucose deprivation (OGD) on the distribution of the proteasome in low density cultures of cerebrocortical neurons. OGD is a well-known protocol used to mimic global brain ischemia-reperfusion in cultured neurons, and was previously validated by many authors (Caldeira *et al.*, 2013; Fernandes *et al.*, 2014; Mele *et al.*, 2014; Curcio *et al.*, 2015; D'Orsi *et al.*, 2015; Costa *et al.*, 2016). However, these experiments are commonly performed in high density cultures, which do not allow assessing accurately the subcellular distribution of proteins in immunocytochemistry experiments. Therefore, in the first part of the work we adapted the OGD protocol of *in vitro* global ischemia to low density cultures ($1.0x10^4$ cells/cm^2). Cultured cerebrocortical neurons were subjected to 30 min of OGD, in the presence or absence of glial cells, and were further incubated in the original conditioned medium for 6 h in the presence of the glial cell feeder layer (Figure 3.1A). Cell death was evaluated by analysis of nuclear morphology after staining with Hoechst 33342. Cortical neurons subjected to OGD (30 min) in the absence of glial cells showed a significant increase in cell death when determined at 6 h after the insult, to about 38 % (Figure 3.1A, *$p<0.05$). In contrast, the same ischemic insult did not induce significant cell death when performed in the presence of glial cells and cortical neurons were further incubated in culture conditioned medium for 6 h (Figure 3.1A).

Given the protective effect provided by glial cells when present during the period of OGD, in additional experiments we tested the effect of longer OGD periods on cell viability by exposing the cells to ischemic conditions in the absence of the glial cell feeder layer. After OGD, cortical neurons were further incubated in culture conditioned medium and in the presence of glial cells.

A significant increase in cell death was observed after ischemic insults of 45 min (~54 %) and 60 min (~57 %) when analysed 8 h after the OGD period (Figure 3.1B, ***p<0.001). Based on these observations, all subsequent experiments were performed using 45 minutes of OGD in absence of glia cells.

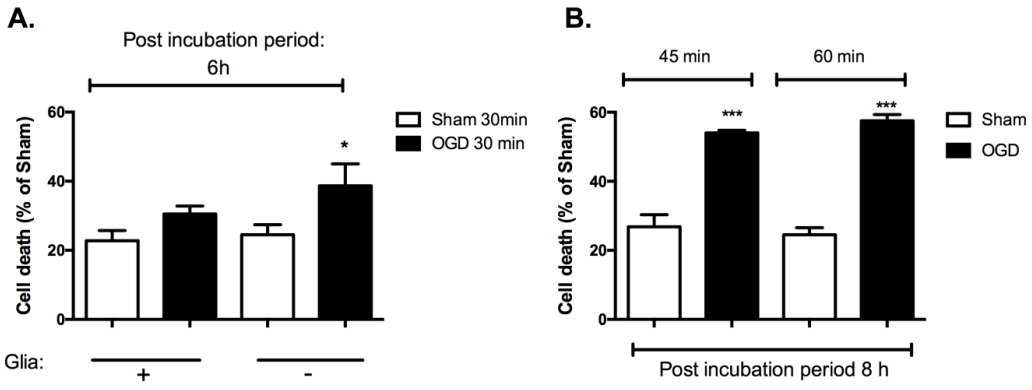

Figure 3.1- Effect of OGD on the viability of cortical neurons cultured at a low-density. A. Cultured cortical neurons (15 DIV) were subjected to OGD for 30 min in presence or absence of glia and were further incubated in culture-conditioned medium for 6 h. **B.** Cultured cortical neurons (15 DIV) were subjected to OGD for the indicated periods of time (45 min, 60 min), and were further incubated in culture-conditioned medium for 8 h (post-incubation). Cell death was analysed after nuclei staining with Hoechst 33342. The results are average ± SEM of 3 different experiments performed in duplicate and in independent preparations. Statistical analysis was performed by one-way ANOVA, followed by the Bonferroni's test. *p<0.05, ***p<0.001.

The 26S proteasome is composed by a 20S catalytic core and a 19S regulatory particle. Although biochemically distinct, they participate in the concerted action of recognition, binding, unfolding and subsequent degradation of the target protein (Lander *et al.*, 2012; Huang *et al.*, 2016). Despite the clear heterogeneity in their subunit composition, it is possible to label the two proteasomal particles, the 20S and the 19S, by means of using antibodies recognizing PSMA2 (α2) and Rpt6 proteins, respectively (da Fonseca and Morris, 2008; Lander *et al.*, 2012). Therefore, to analyse the effect of OGD on the subcellular distribution of the 20S and 19S proteasomes, we performed immunocytochemistry experiments with specific antibodies for PSMA2 and Rpt6 in low density cultures of cortical neurons. Both proteins are found in the soma and in dendrites of cultured neurons as evaluated by the colocalization with the dendritic marker MAP2 (data not shown). The results of Figure 3.2 show a significant increase of the area (Figure $3.2A_2$ 1.42 fold; ***p<0.001) and intensity (Figure $3.2A_3$ 1.62 fold; ***p<0.001) of PSMA2 puncta in neurites after 45 min of OGD followed by 2h of post-incubation. These effects were transient since 4 h after OGD these differences were no longer observed. At a later time point, i.e. 6 h after OGD, there was a secondary increase in the puncta intensity (Figure $3.2A_3$ 1.99 fold;

**p<0.01), without further changes in the other parameters evaluated. OGD was without effect on the number of PSMA2 puncta present in the dendritic compartment (Figure 3.2A_1).

Further analysis of the OGD-induced changes in the PSMA2 distribution along dendrites showed a significant, although transient, increase in the number (Figure 3.2A_4 1.41 fold; ***p<0.001) and area (Figure 3.2A_5 1.52 fold; **p<0.01) of puncta that colocalized with the post-synaptic density marker PSD95, when analysed 2 h after the ischemic insult. In addition, the percentage of total PSMA2 immunoreactivity that colocalized with PSD95 was also increased at 2 h after OGD, but no similar effects were observed when the PSMA2 distribution was analysed at later time points after the ischemic insult (Figure 3.2A_6 1.24 fold; **p<0.01).

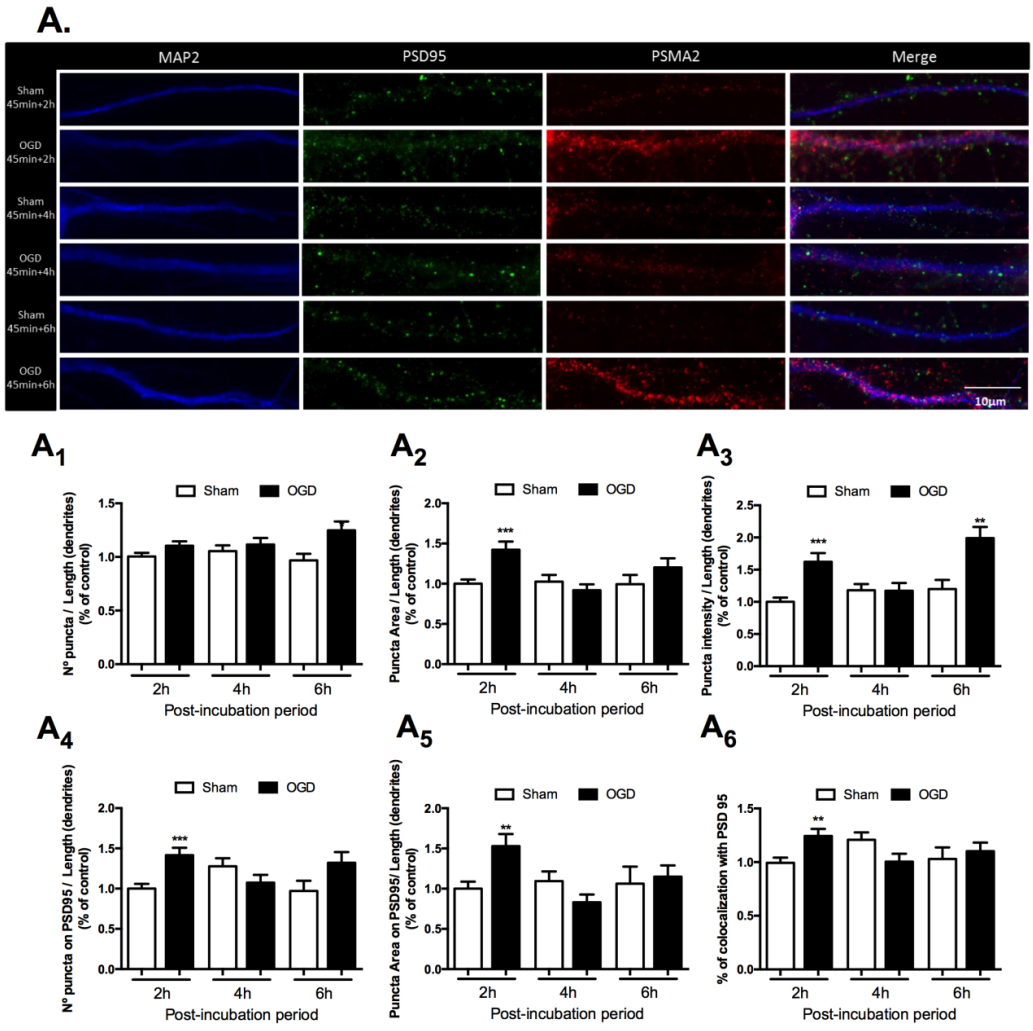

Figure 3.2- Alterations in the dendritic distribution of PSMA2 in cortical neurons subjected to OGD. PSMA2 protein expression was evaluated by immunocytochemistry in neurons subjected to 45 min of OGD and further incubated in culture conditioned medium for 2, 4 or 6 h. The number (A_1), area (A_2), and intensity (A_3) of PSMA2 puncta were analysed in the dendritic compartment through colocalization with MAP2, and normalized for its length. The number (A_4) and area (A_5) of PSMA2 puncta colocalizing with PSD95, as well as the percentage of colocalization (A_6), were also calculated. Imaging was performed in an Axio Observer Z1 fluorescence microscope, coupled to an Axiocam HRm digital camera, using a Plan-Apochromat 63x/1.4 oil objective. Results are means ± SEM of at least 3 independent

experiments (30 cells). Statistical analysis was performed by one-way ANOVA, followed by Dunnett's test. **p<0.01; ***p<0.001 - significantly different when compared to control conditions.

In contrast with the observations for PSMA2 protein, OGD did not affect the number (Figure 3.3A_1), area (Figure 3.3A_2) and intensity (Figure 3.3A_3) of Rpt6 puncta along dendrites when evaluated 2 h and 6 h after the insult. Furthermore, no changes were detected in the number and area of Rpt6 puncta that colocalized with PSD95 (Figure 3.3A_4-A_5), as well as in the total protein fraction that colocalized with PSD95 (Figure 3.3A_6). Alterations in the subcellular distribution of Rpt6 were only observed at 4 h after the insult, with a decrease in the area (Figure 3.3A_2 0.74 fold; *p<0.05) and intensity of puncta (Figure 3.3A_3 0.85 fold; *<0.05), as well as in the puncta number (Figure 3.3A_4 0.86 fold; **p<0.01) and area (Figure 3.3A_5 0.69 fold; **p<0.01) that colocalized with PSD95.

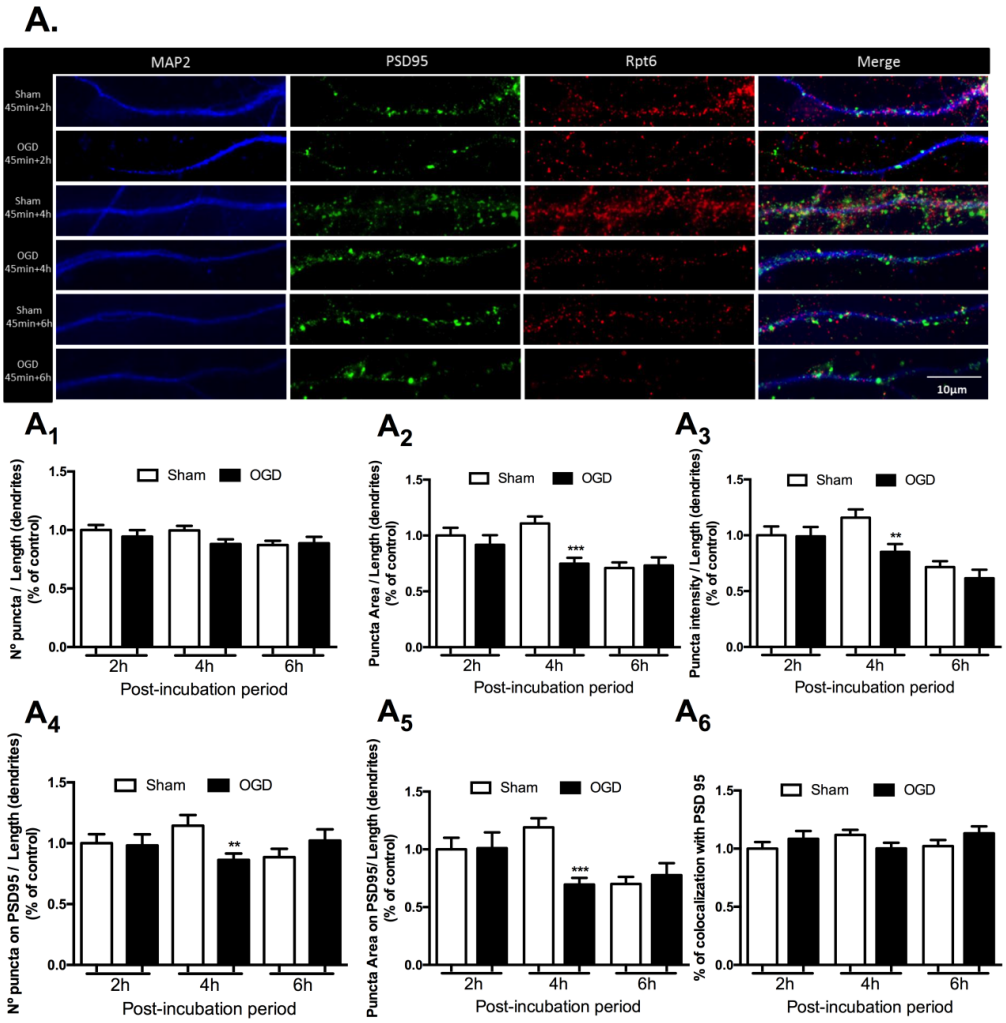

Figure 3.3- Alterations in the dendritic distribution of Rpt6 in cortical neurons subjected to OGD. Rpt6 expression was evaluated by immunocytochemistry in neurons subjected to 45 min of OGD and further incubated in culture conditioned medium for 2, 4 and 6 h. The number (A_1), area (A_2), and intensity (A_3) of Rpt6 puncta were analysed in the dendritic compartment through colocalization with MAP2, and normalized for its length. The number (A_4) and

area (A_5) of Rpt6 puncta colocalizing with PSD95, as well as the percentage of colocalization (A_6), were also calculated. Imaging was performed in an Axio Observer Z1 fluorescence microscope, coupled to an Axiocam HRm digital camera, using a Plan-Apochromat 63x/1.4 oil objective. Results are mean ± SEM of at least 3 independent experiments (30 cells) performed in distinct preparations. Statistical analysis was performed by one-way ANOVA, followed by Dunnett's test *p<0.05 **p<0.01 - significantly different when compared to control conditions.

Together, these results show differential effects of OGD in the localization Psma2 and Rpt6, which were used to label the 20S and 19S proteasome, respectively. The distribution of PSMA2 was more affected at 2 h after the insult, while the localization of Rpt6 only showed changes at 4 h of recovery. Additional experiments are required to better characterize the subcellular distribution of both proteins and to understand how the localization and composition of proteasome is affected upon an ischemic insult.

3.2. Effect of OGD on proteasome activity and assembly

Proteasome activity was shown to be downregulated under ischemic conditions by numerous authors. The two-vessel occlusion model (15 min) induces a persistent decrease in the chymotrypsin-like activity of the proteasome when analysed up to 72 h after the insult, with a concomitant increase in polyubiquitin conjugates (Ge *et al.*, 2007). OGD for 1.5 h also decreases the chymotrypsin-like activity of the proteasome when evaluated 4 h after the insult in cultured hippocampal neurons, and similar results were obtained in cultured hippocampal neurons subjected to excitotoxic stimulation with glutamate (Caldeira *et al.*, 2013). In addition to the decrease in proteasome activity, the 26S proteasome was found to be disassembled into its major constituents, the 19S and the 20S particles, in models of transient forebrain ischemia and global ischemia (Asai *et al.*, 2002; Ge *et al.*, 2007). An increase in polyubiquitin conjugates (a biochemical marker for proteasome activity impairment) in large protein aggregates was also reported in cerebrocortical neurons exposed to OGD for 2 h followed by different periods of post-incubation (Chen *et al.*, 2010).

To characterize the effect of OGD on proteasome activity, cerebrocortical neurons were subjected transiently to OGD and the chymotrypsin-like activity of the proteasome was evaluated after incubation of the cells for different periods in culture conditioned medium. Exposure of cerebrocortical neurons to OGD for 2 h reduced the activity of the proteasome, with the maximal effect obtained immediately after injury (52 % of the control) (Figure 3.4A). The inhibition of the proteasome induced by OGD was maintained even after incubation of cortical neurons in culture conditioned medium for up to 5 h (***p<0.001 for all time points). A shorter

period of OGD (1.5 h) also reduced the chymotrypsin-like activity of the proteasome, but to a lower extent when compared with the results obtained when the insult was performed for 2 h (Figure 3.4B). Under the former conditions, the activity of the proteasome was reduced to 47 - 62 % of the control. Based on these observations, subsequent experiments were performed using 1.5 h of OGD and 4 h of post incubation period, unless stated otherwise.

Since a well-characterized effect of chemical proteasome inhibition in cells is the accumulation of high-molecular weight polyubiquitin conjugates, with subsequent depletion of free ubiquitin, we investigated ubiquitin homeostasis in cultured cortical neurons subjected to OGD. Surprisingly, a decrease of about 24 % in the amount of polyubiquitin conjugates was observed after OGD when compared to the Sham condition (Figure 3.4C; *p<0.05). No changes were observed for free ubiquitin levels under the same experimental conditions (Figure 3.4D). Instead, we observed a significant decrease of about 28 % in ubiquitinC mRNA levels (Figure 3.4E,F).

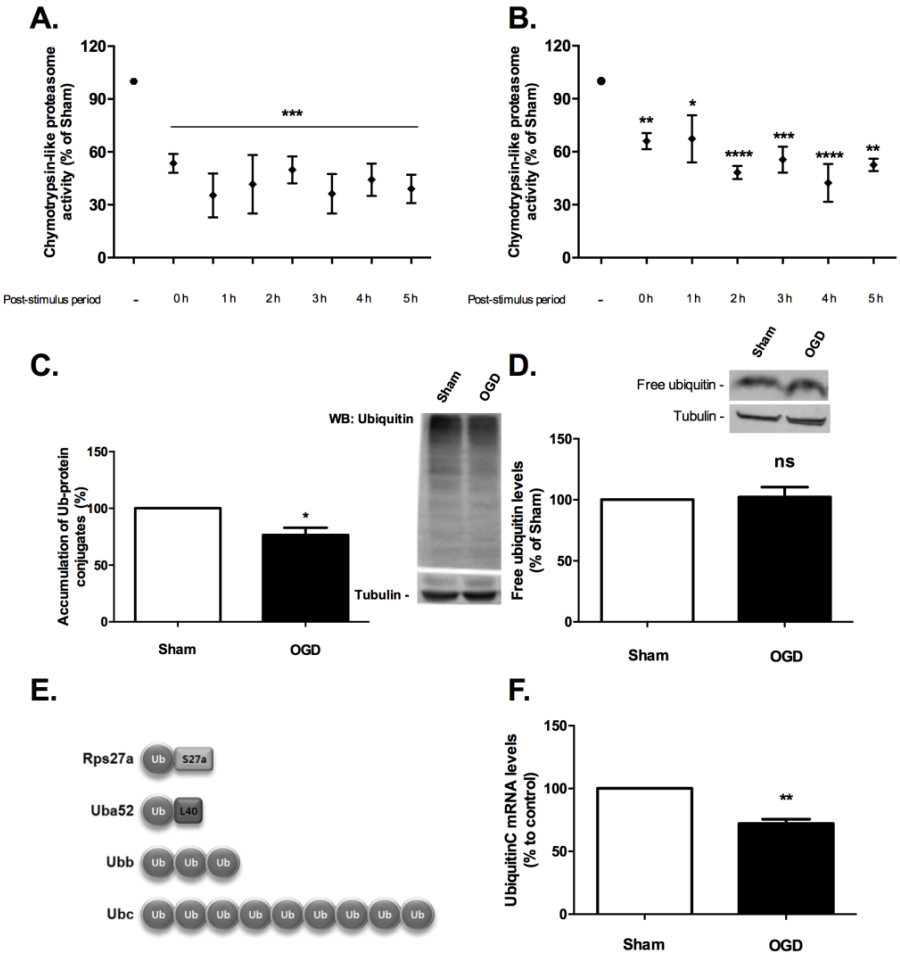

Figure 3.4- Changes in proteasome activity and ubiquitin homeostasis in response to OGD. A, B. Fifteen DIV cerebrocortical neurons were subjected to 2 h (A) or 1.5 h (B) of OGD and were further incubated in culture conditioned medium for 0, 1, 2, 3, 4 or 5 h. The chymotrypsin-like activity of the proteasome was evaluated with a

fluorogenic substrate (25µM Suc-LLVY-AMC) using cell extracts. **C, D, F.** Fifteen DIV cerebrocortical neurons subjected to 1.5 h of OGD were further incubated in culture conditioned medium for 4 h. Examples of the encoding transcripts found for ubiquitin (Oh *et al.*, 2013) **(E).** Total **(C)** and free **(D)** ubiquitin levels were evaluated with an antibody that recognizes both forms of the protein. Tubulin protein levels was used as a loading control. **F.** UbiquitinC mRNA expression was evaluated by qPCR and normalized using *Gapdh* as a reference gene. The results obtained in cells subjected to OGD were normalized to those obtained under Sham conditions (100 %). The results are the average ± SEM of 3–4 independent experiments performed in independent preparations. Statistical analysis was performed by one-way ANOVA, followed by the Dunnett's test, comparing all conditions with the control (A, B), or using the Student's *t* test (C, D and F) (ns, p>0.5; *p< 0.05; **p< 0.01; ***p< 0.001; ****p< 0.0001).

The results of Figure 3.4C showing the decrease in polyubiquitin conjugates following incubation of cortical neurons under conditions of OGD contrast with the evidence from previous reports, where an increase in protein ubiquitination was observed in in vivo and in vitro ischemia (Chen *et al.*, 2010). In the latter studies, ubiquitin immunoblotting was performed in samples containing the proteins present in aggregates, which are characterized by their insolubility in Triton-X100 (Chen *et al.*, 2010; Hochrainer *et al.*, 2012). Using this and a different protocol (Matos *et al.*, 2016), we did not detect ubiquitinated proteins in western blot experiments (not shown).

A disassembly of the proteasome after OGD may account for the observed decrease in activity. To address this hypothesis, we evaluated the assembly status of the 26S proteasome under non-denaturing conditions, by native polyacrylamide gel electrophoresis (PAGE), as previously reported (Elsasser *et al.*, 2005; Caldeira *et al.*, 2013), followed by immunoblotting of the native gels with the antibodies against the proteasome subunit PSMA2, which belongs to the catalytic core, and against the Rpt6 regulatory particle protein. Cerebrocortical neurons exposed to OGD for 2 h, followed by 4 h of incubation in culture conditioned medium, showed a dramatic decrease in the fully-assembled proteasomes as observed by the changes in the immunoreactivity for PSMA2 and Rpt6. Thus, a decrease was observed in the catalytic core particle PSMA2 immunoreactivity in the high molecular weight fraction (26S/30S proteasomes), to 19 % (26S, single capped) or 13 % (30S, double capped) (Figure 3.5A. left panel; ***p<0.001), and similar results were obtained for the regulatory particle protein Rpt6 (Figure 3.5B; ***p<0.001). As a result the proteasome disassembly, an increase of about to 240 % was observed in the immunoreactivity of PSMA2 associated with 20S proteasomes (low molecular weight fraction) (Figure 3.5A, right panel; ***p<0.001). Control experiments to evaluate total levels of PSMA2 and Rpt6 under the same conditions, showed no changes in total abundance of both proteins, further corroborating the evidence pointing to a proteasome disassembly following OGD (Figure 3.5C and D; ns p>0.05).

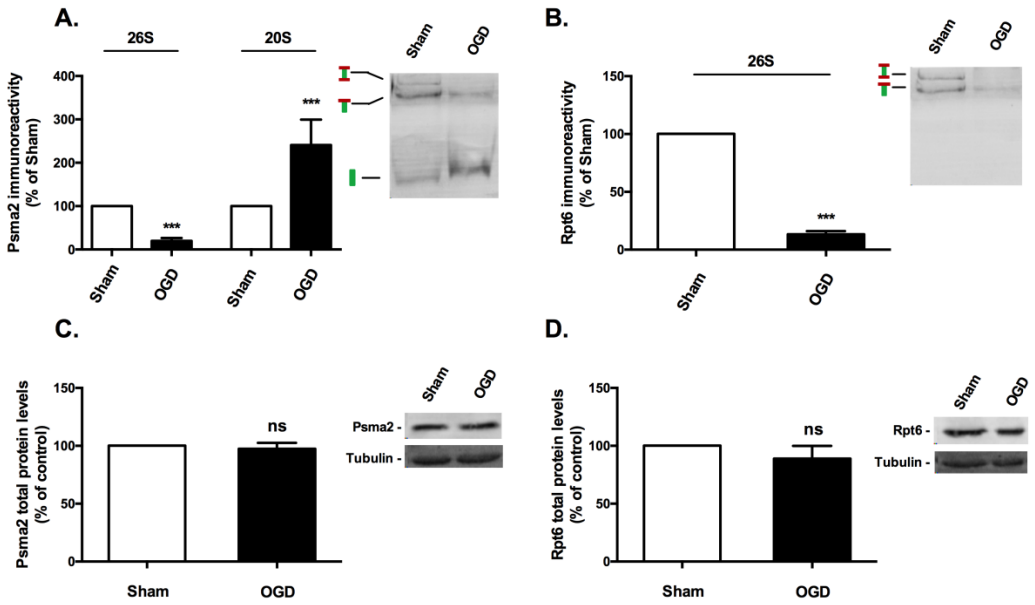

Figure 3.5- Effect of OGD on proteasome assembly under non-denaturing conditions in neurons submitted to 2 h of OGD. Fifteen DIV cerebrocortical neurons were subjected to OGD for 2 h and were further incubated in culture conditioned medium for 4 h. The abundance of Psma2 **(A)** and Rpt6 **(C)** was determined under non-denaturating conditions after immunoblotting the native gel (Native-PAGE) with antibodies against Psma2, to probe the 26S and the 20S proteasomes, and against Rpt6, to identify 26S proteasomes. Total abundance of Psma2 **(C)** and Rpt6 **(D)** was also evaluated under denaturing conditions (SDS-PAGE) as control experiments, and β-tubulin was used as loading control. Control (Sham) protein levels of Pmsa2 **(C)** or Rpt6 **(D)** subunits were set to 100 %. The results are the average ± SEM of 3-4 independent experiments. Statistical analysis was performed by the Student's *t* test (ns, p>0.5; ***p< 0.001).

The results of Figure 3.4 (A, B), comparing the effects of OGD for 2h and 1.5 h on the activity of the proteasome, show more robust effects under the former conditions. Therefore, in additional experiments we compared the alterations in the assembly of the proteasome in cultured cortical neurons subjected to OGD for 2 h (Figure 3.5) and 1.5 h (Figure 3.6), and further incubated in culture conditioned medium for 4 h. The latter conditions reduced the population of fully-assembled proteasomes (26S; single and double capped) to about 10 %, as shown by a decrease in the catalytic core particle PSMA2 immunoreactivity in the high molecular weight fraction (10 %) (Figure 3.6A left panel; ***p<0.001), as well as in the regulatory particle protein Rpt6 (8 %) (Figure 3.6B ****p<0.0001). Similarly, the 20S proteasomes were upregulated to about 467 %, as shown by an increase in the PSMA2 immunoreactivity in the low molecular weight fraction (Figure 3.6A right panel; **p<0.01). Control experiments to evaluate total levels PSMA2 and Rpt6 proteins, showed no changes in total abundance of both proteins, further indicating a proteasome disassembly under these conditions (Figure 3.6C and D; ns p>0.05).

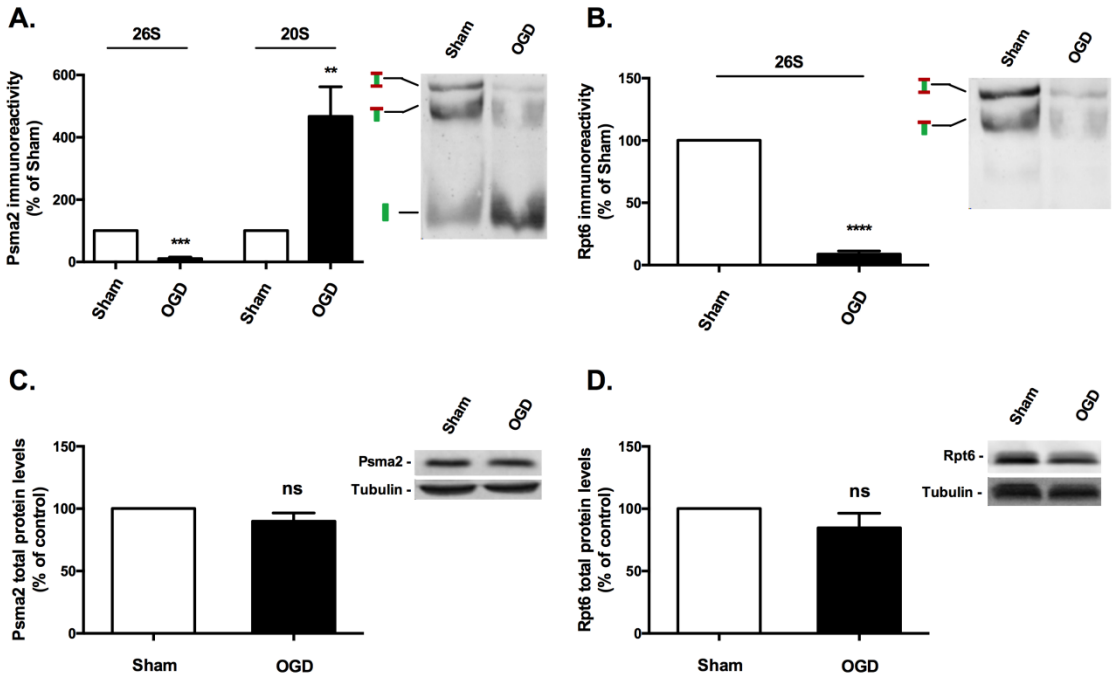

Figure 3.6- Effect of OGD on proteasome assembly under non-denaturing conditions in neurons submitted to 1.5 h of OGD. Fifteen DIV cerebrocortical neurons were subjected to 1.5 h of OGD and were further incubated in culture conditioned medium for 4 h. The abundance of Psma2 **(A)** and Rpt6 **(C)** was determined under non-denaturating conditions after immunoblotting the native gel (Native-PAGE) with antibodies against Psma2, to probe the 26S and the 20S proteasomes, and against Rpt6, to identify 26S proteasomes. Total abundance of Psma2 **(C)** and Rpt6 **(D)** was also evaluated under denaturing conditions (SDS-PAGE) as control experiments, and β-tubulin was used as loading control. Control (Sham) protein levels of Pmsa2 **(C)** or Rpt6 **(D)** subunits were set to 100 %. The results are the average ± SEM of 3-4 independent experiments. Statistical analysis was performed by the Student's *t* test (ns, p>0.5; **p<0.01; ***p< 0.001; *** p<0.0001).

Taken together, these results indicate that 1.5 h or 2 h of OGD induces 30/26S proteasome disassembly into its major constituents, which may account for the observed decrease in proteasome activity. No 19S regulatory particles were observed in these experiments, which would be expected following disassembly of the proteasome. This is in agreement with the labile properties of the free 19S proteasome, which makes difficult its visualization (Liu *et al.*, 2005b; Wang *et al.*, 2011).

3.3. OGD induces calpain activation: a possible link leading to proteasome dysfunction

The $[Ca^{2+}]_i$ overload followed by activation of calpains, a group of Ca^{2+}-dependent cysteine proteases, is a hallmark of ischemia/reperfusion, both in *in vivo* and *in vitro* models, as is also characteristic of NMDAR-dependent excitotoxicity (Neumar *et al.*, 2001; Fernandes *et al.*, 2014; Curcio *et al.*, 2015). One strategy to assess calpain activation is through analysis of the cleavage of a well-known substrate, α-spectrin, which exists as a protein with a molecular weight of 280

kDa under control conditions (Figure 3.7A). Following calpain activation, the full-length protein is cleaved to form spectrin-breakdown products (SBDP) with 150 and 145 kDa [Figure 3.7A) (Wang, 2000)].

Cerebrocortical neurons subjected to OGD for 1.5 h exhibited a 4-fold increase in the calpain-mediated SBDP150/145, when compared to the control situation (Figure 2.6B left panel; $^{++++}p<0.0001$). The abundance of SBDP150/145 was reduced to basal levels in the presence of the calpain inhibitor MDL28170 (Figure 3.7B; ns - $p>0.05$, when compared with the control), or NMDAR antagonist APV (Figure 3.7B; ns - $p>0.05$). Both inhibitors completely abrogated the increase of SBDP145/150 observed in cortical neurons subjected to OGD (Figure 3.7B; ****$p<0.0001$). Furthermore, in the absence of the inhibitors there was no apparent formation of the SBDP120, further suggesting that caspase-3 is not active under these experimental conditions.

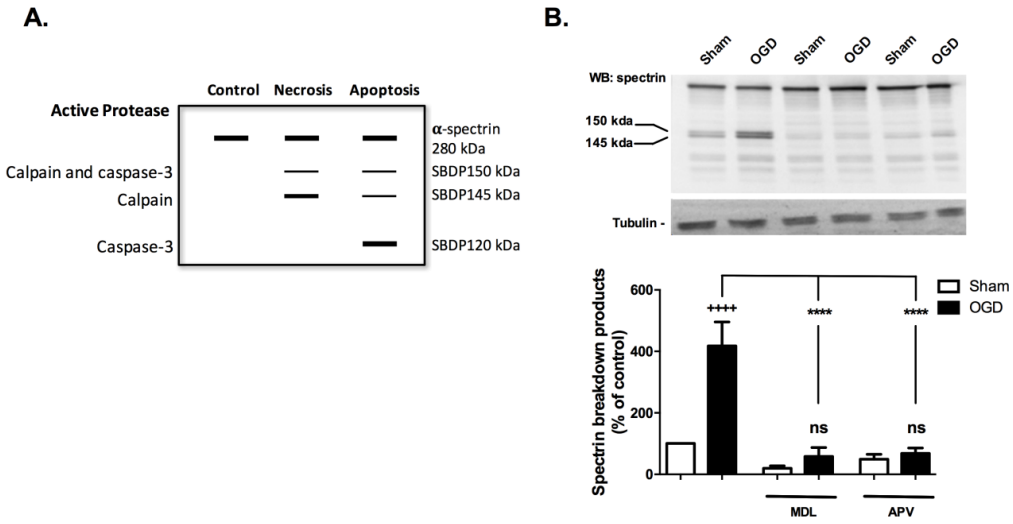

Figure 3.7- Calpain activation after OGD in cultured cerebrocortical neurons. A. Schematic representation of an immunoblot for α-spectrin with samples from control neurons, neurons undergoing either necrosis (with only calpain-mediated formation of SBDP150 and SBDP145) or apoptosis (with both caspase- and calpain-generated SBDPs). The distinct fragment sizes and patterns of α-spectrin fragmentation are illustrated (adapted from Wang et al., 2000). **B.** Fifteen DIV cerebrocortical neurons were subjected to OGD for 1.5 h and were further incubated in culture conditioned medium for 4 h. Spectrin full-length (280 kDa) and SBDPs were analysed by western blot using an antibody recognizing both the N- and C-terminal regions of the protein. When 100 µM APV or 50 µM MDL28170 were used, the inhibitors were added 30 min prior and during OGD, and were also present during the post-incubation period. β-tubulin was used as loading control. Control (Sham without MDL or APV) protein levels of spectrin were set to 100 %. The results are the average ± SEM of 3 independent experiments. Statistical analysis was performed by one-way ANOVA, followed by the Bonferroni´s multiple comparison test, comparing all the conditions with the respective control (ns, $p>0.5$; $^{++++}p< 0.0001$; ****$p< 0.0001$).

The abundance of the proteasome can be regulated by several ways, in cells destined to die. For instance, apoptotic Jurkat T cells showed a cleavage of several proteasome subunits by caspase-3, namely Rpt5, Rpn2, Rpn1, Rpn10 subunits (Adrain *et al.*, 2004; Sun *et al.*, 2004), while α2, α4, ß4 and Rpt1 were truncated by caspase-7 (Jang *et al.*, 2007). Therefore, we hypothesized that calpains may have also a role in the inactivation of the proteasome in ischemic conditions, by limited proteolysis of certain proteasomal subunits. Accordingly, it was already reported in the literature that the Rpn10 protein can be cleaved by calpains in the presence of mitochondrial toxins in cultured cortical neurons (Huang *et al.*, 2013).

Although controversial, the presence of PEST sequences has been associated with calpain-mediated proteolysis (Molinari *et al.*, 1995; Wang *et al.*, 2003). PEST sequences are rich in proline, glutamic acid, serine and threonine amino acids, and has been suggested to be an effective signal for protein destruction, as several short-lived proteins arbor this motif (Rogers *et al.*, 1986). Thus, we analysed the presence of putative PEST sequences in all proteins belonging to the 26S proteasomes, using the online software EPESTFIND (http://emboss.bioinformatics.nl/cgi-bin/emboss/epestfind). From all proteasome subunits tested (Table 2.1), only six proteins were found with scores above the threshold of 5.00. The following scores were obtained: Rpn1 - 5.04 (Figure 3.10A), Rpn3 - 10.66 (Figure 3.11A), Rpn5 - 14.97 (Figure 3.8A), Rpn12 - 8.28 (Figure 3.8B) and USP14 - 10.89 (Figure 3.8C). However, the presence of this sequence is not a strict requirement for calpain-mediated cleavage of proteins, neither its absence discards a possible calpain-mediated cleavage; false-positive and false-negative results may also be expected. All these putative calpain targets should be then further confirmed by immunoblotting in order to evaluate their relative abundance in the experimental conditions used.

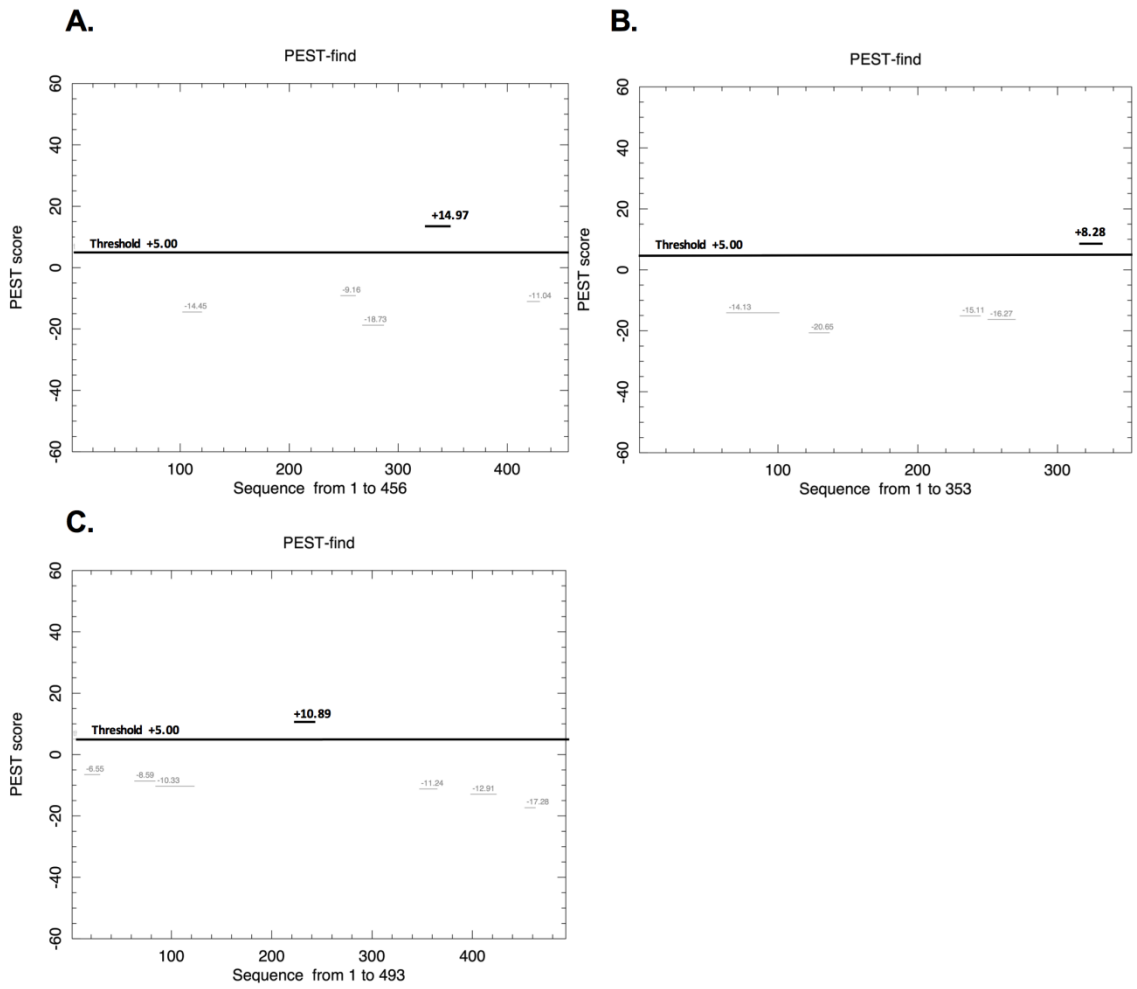

Figure 3.8- Analysis of the putative presence of PEST sequences in the Rpn5, Rpn12 and USP14 proteasome subunits using EPESTFIND. The following accession numbers were used to retrieve the amino acid sequences of the proteasome subunits: Rpn5 (A) (Uniprot; Q5XIC6), Rpn12 (B) (Uniprot; F1LMQ3) and USP14 (C) (Uniprot; Q5U2N2). The threshold was set to 5.00, and the results above this value were considered good putative calpain substrates. Rpn5 arbors a putative PEST sequence between the amino acid sequences 330-349 with a score of 14.97. Rpn12 arbors a putative PEST sequence between the amino acid sequences 327-340 with a score of 8.28. Usp14 arbors a putative PEST sequence between the amino acid sequences 224-238 with a score of 10.89.

Given the evidence suggesting that several proteasome subunits may be cleaved by calpains, and considering the activation of these proteases under ischemic conditions (e.g. Figure 3.7), we further investigated the role of calpains in the cleavage of several proteasome subunits in cultured cerebrocortical neurons exposed or not to OGD. OGD (1.5 h) significantly decreased (35 %) Rpn10 protein levels (a regulatory subunit) in cultured cortical neurons, when evaluated after 4 h of reoxygenation (Figure 3.9B; $^{++}p<0.001$), but the antibody used did not detect the truncated protein (not shown). The effect of OGD was completely abolished in the presence of the calpain inhibitor MDL28170 (Figure 3.9B; ns $p>0.05$), and by the NMDAR antagonist APV (Figure 3.9B right part; ns $p>0.05$). However, negative results were obtained when the Rpn10

amino acid sequence was analysed for the presence of putative PEST sequences using EPESTFIND (Figure 3.9A).

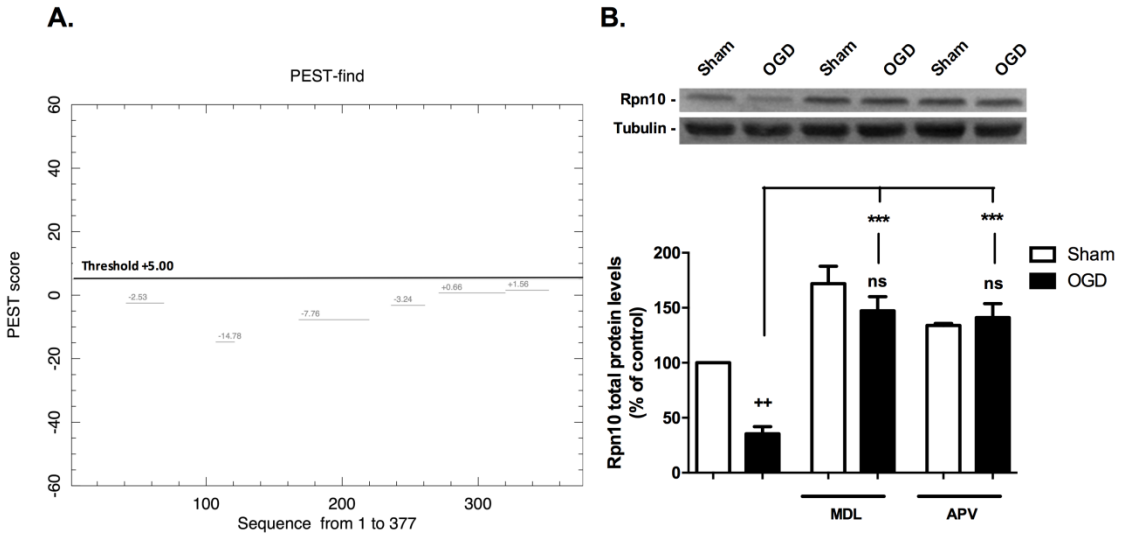

Figure 3.9- Total abundance of Rpn10 protein levels in cerebrocortical neurons exposed to OGD. A. Analysis of the putative presence of PEST sequences in the Rpn10 protein using EPESTFIND. The accession number Q9ESH1 (Uniprot) was used to retrieve the Rpn10 amino acid sequence used to search for putative PEST sequences. The threshold was set to 5.00, and the results above this value were considered good putative calpain substrates. **B.** Total abundance of Rpn10 protein levels in cerebrocortical neurons (15 DIV) exposed to 1.5 h of OGD and further incubated in cultured conditioned medium for 4 h. When 100 µM APV or 50 µM MDL28170 were used, the cells were incubated with the inhibitors prior (30 min) and during OGD, and the drugs were also present during the post-incubation period. Control (Sham without MDL or APV) Rpn10 protein levels were set to 100 %. β-tubulin was used as loading control. The results are the average ± SEM of 4 independent experiments, performed in different preparations. Statistical analysis was performed by one-way ANOVA, followed by the Bonferroni´s multiple comparison test, comparing all the conditions with the respective control (ns, $p>0.5$; $^{++}p< 0.01$; ***$p< 0.001$).

To further investigate the role of calpains on the cleavage of proteasome subunits in cerebrocortical neurons subjected to OGD, and taking into account the results of the EPESTFIND anaysis, changes in the abundance of the regulatory particle subunits Rpn1 and Rpn3 (two regulatory subunits) were evaluated by western blot. OGD for 1.5 h did not change Rpn1 total protein levels when evaluated 4 h after the insult (Figure 3.10B; ns >0.05), as compared with the Sham condition, suggesting that Rpn1 is not cleaved. This finding contrasts with the prediction by the EPESTFIND algorithm, which identified an amino acid sequence in Rpn1 with a score of 5.04 (Figure 3.10A).

Rpn3 total protein levels showed a slight reduction (14 %) in cortical neurons subjected to OGD, when evaluated 4 h after the insult, while no effect was observed when the experiments were performed in the presence of MDL28170 or with APV. However, additional experiments should

be performed to determine whether the effect of OGD on Rpn3 protein levels is statistically significant (Figure 3.11B; two independent experiments). If this is the case, the results will be in accordance with the score of 10.66 obtained in EPESTFIND using the amino acid sequence of Rpn3 protein (Figure 3.11A).

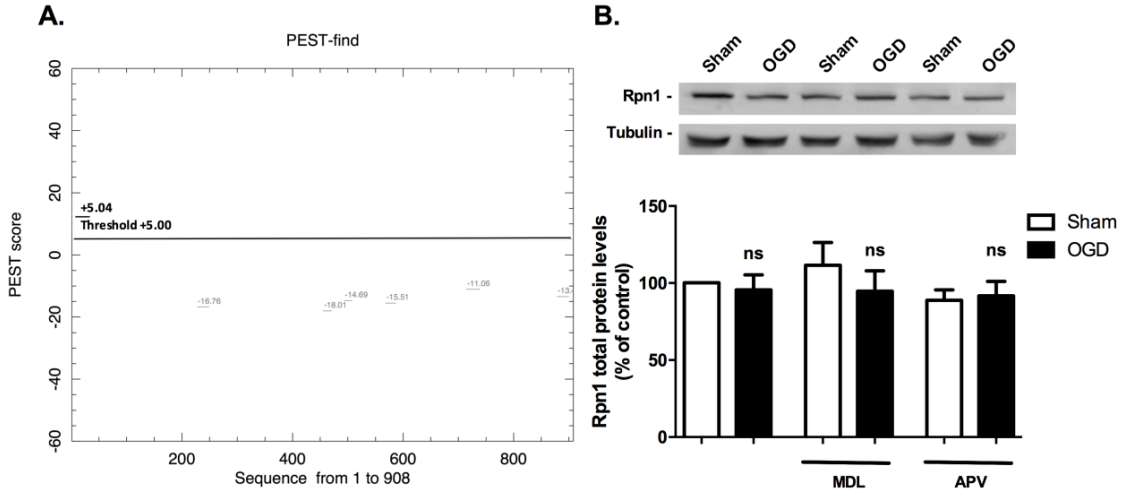

Figure 3.10- Total abundance of Rpn1 protein levels in cerebrocortical neurons exposed to OGD. A. Analysis of the putative presence of PEST sequences in the Rpn1 protein using EPESTFIND. The accession number Q4FZT9 (Uniprot) was used to retrieve the Rpn1 amino acid sequence used to search for putative PEST sequence on the EPESTFIND online tool. The threshold was set to 5.00, and the results above this value were considered good putative calpain substrates. Rpn1 arbors a putative PEST sequence within the amino acid sequence 8-27 with a score of 5.04. **B.** Total abundance of Rpn1 protein levels in cerebrocortical neurons (15 DIV) exposed to OGD for 1.5 h and further incubated in culture conditioned medium for 4 h. When 100 µM APV or 50 µM MDL28170 were used, the cells were incubated with the inhibitors prior (30 min) and during OGD, and the drugs were also present during the post-incubation period. Control (Sham without MDL or APV) protein levels of Rpn1 were set to 100 %. β-tubulin was used as loading control. The results are the average ± SEM of 4 independent experiments, performed in different preparations. Statistical analysis was performed by one-way ANOVA, followed by the Bonferroni´s multiple comparison test, comparing all the conditions with the respective control (ns, p>0.5).

In additional experiments, we investigated the stability of the proteasomal regulatory subunits belonging to the AAA+ ATPase ring in cortical neurons subjected to OGD (1.5 h) followed by incubation in culture conditioned medium for 4 h. Under these conditions there was a reduction in Rpt1 protein levels by 24 %, which however was not statistically significant (Figure 3.12B; ns >0.05), and this effect was abrogated in the presence of MDL28170 or APV. However, analysis of the Rpt1 amino acid sequence using the EPESTFIND tool showed no PEST sequences in this proteasome regulatory subunit (Figure 3.12A).

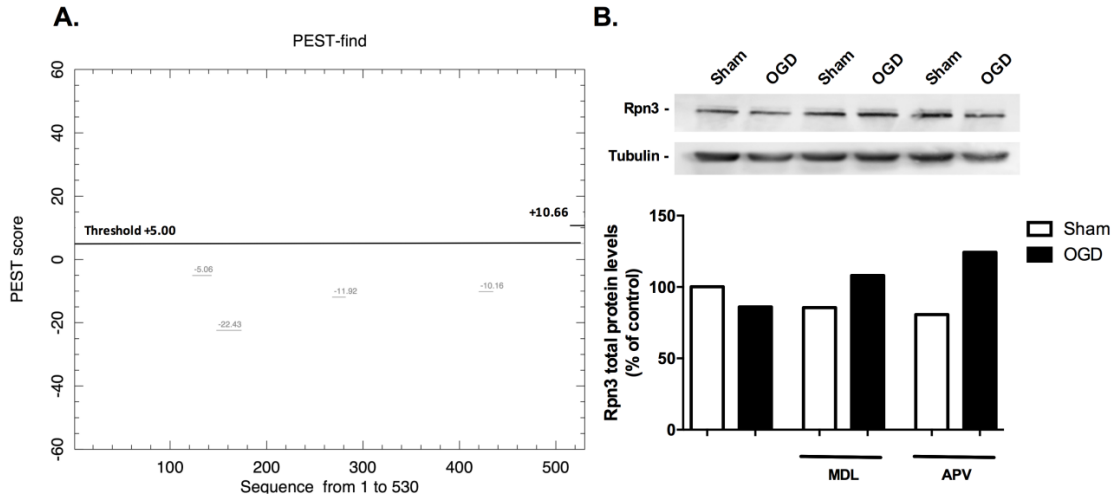

Figure 3.11- Total abundance of Rpn3 protein levels in cerebrocortical neurons exposed to OGD. A. Analysis of the putative presence of PEST sequences in the Rpn3 protein using EPESTFIND. The accession number Q5U2S7 (Uniprot) was used to retrieve the amino acid sequence used to search for putative PEST sequence on the EPESTFIND online tool. The threshold was set to 5.00, and the results above this value were considered good putative calpain substrates. Rpn3 arbors a putative PEST sequence within the amino acid sequence 519-530 with a score of 10.66. **B.** Total abundance of Rpn3 protein levels in cerebrocortical neurons (15 DIV) exposed to OGD for 1.5 h and further incubated in culture conditioned medium for 4 h. When 100 µM APV or 50 µM MDL28170 were used, the cells were incubated with the inhibitors prior (30 min) and during OGD, and the drugs were also present during the post-incubation period. Control (Sham without MDL or APV) protein levels of Rpn3 were set to 100 %. β-tubulin was used as loading control. The results are the average of 2 independent experiments, performed in different preparations.

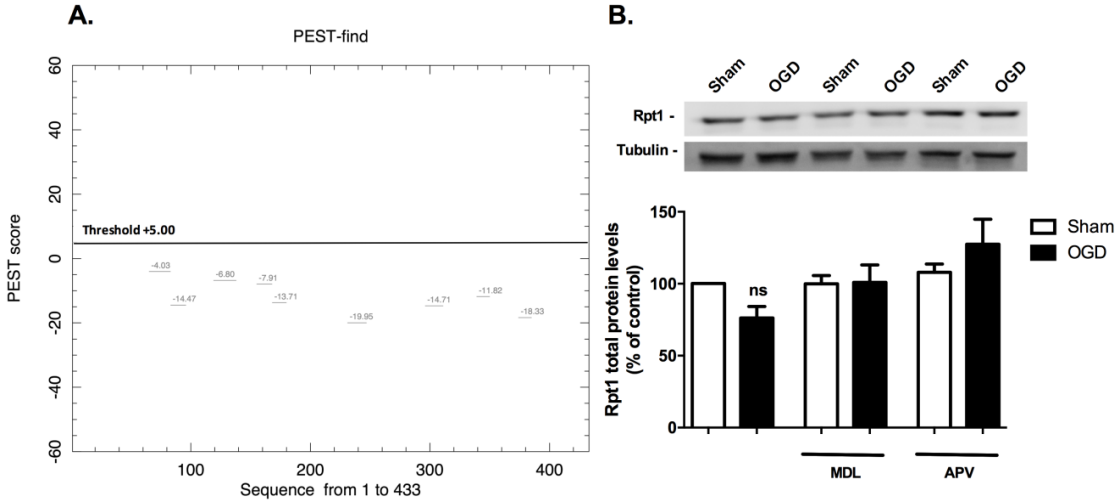

Figure 3.12- Total abundance of Rpt1 protein levels in cerebrocortical neurons exposed to OGD. A. Analysis of the putative presence of PEST sequences in the Rpt1 protein using EPESTFIND. The Q63347 (Uniprot) accession number was used to find for putative PEST sequence on the EPESTFIND online tool. The threshold was set to 5.00, and the results above this value were considered good putative calpain substrates. **B.** Total abundance of Rpt1 protein levels in cerebrocortical neurons (15 DIV) exposed to OGD for 1.5 h and further incubated in culture conditioned medium for 4 h. When 100 µM APV or 50 µM MDL28170 were used, the cells were incubated with the inhibitors prior (30 min) and during OGD, and the drugs were also present during the post-incubation period. Control (Sham without MDL or APV) protein levels of Rpt1 were set to 100 %. β-tubulin was used as loading control. The results are the average ± SEM of 4 independent experiments, performed in different preparations. Statistical analysis was performed by one-

way ANOVA, followed by the Bonferroni´s multiple comparison test, comparing all the conditions with the respective control (ns, p>0.5).

Lastly, cerebrocortical neurons subjected to OGD for 1.5 h showed a significant decrease of about 36 % in total Rpt3 protein abundance (Figure 3.13B; *p<0.01). This decrease was prevented when neurons were pre-incubated with the calpain inhibitor MDL28179 (Figure 3.13B; ns p>0.05), and with the NMDAR antagonist APV (Figure 3.13B; ns p>0.05). Surprisingly, analysis of the Rpt3 protein amino acid sequence showed no potential PEST sequences in its (Figure 3.13A).

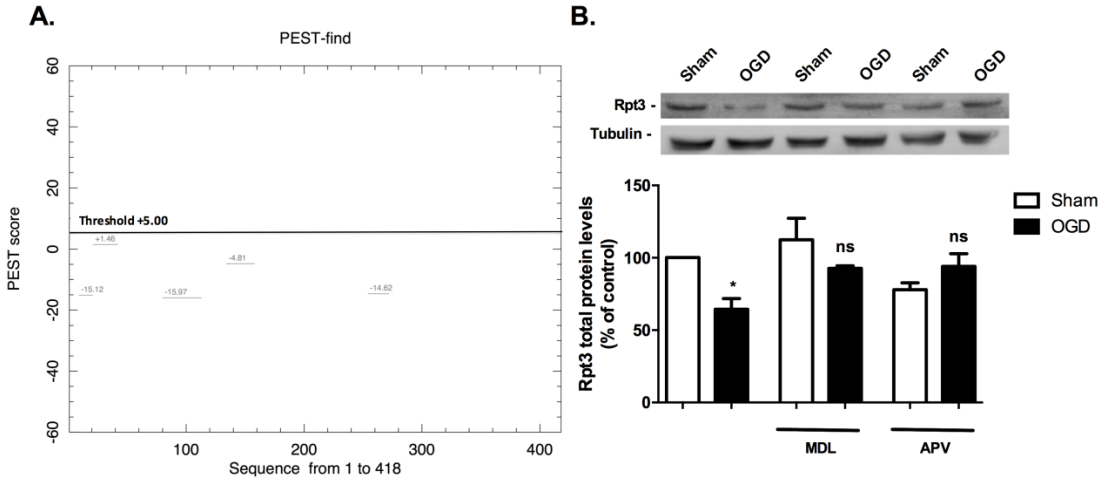

Figure 3.13- Total abundance of Rpt3 protein levels in cerebrocortical neurons exposed to OGD. A. Analysis of the putative presence of PEST sequences in the Rpt3 protein using EPESTFIND . The Q63570 (Uniprot) accession number was used to find for putative PEST sequence on the EPESTFIND online tool. The threshold was set to 5.00, and the results above this value were considered good calpain substrates. **B.** Total abundance of Rpt3 protein levels in cerebrocortical neurons (15 DIV) exposed to OGD for 1.5 h and further incubated in culture conditioned medium for 4 h. When 100 µM APV or 50 µM MDL28170 were used, the cells were incubated with the inhibitors prior (30 min) and during OGD, and the drugs were also present during the post-incubation period. Control (Sham without MDL or APV) protein levels of Rpt1 were set to 100 %.. β-tubulin was used as loading control. The results are the average ± SEM of 4 independent experiments, performed in different preparations. Statistical analysis was performed by one-way ANOVA, followed by the Bonferroni´s multiple comparison test, comparing all the conditions with the respective control (ns, p>0.5).

Because the AAA+ ATPase ring, composed by the proteins Rpt1-6, resides at the interface between the 20S and the 19S, its components are more exposed to proteases present in the cytoplasmic and nuclear compartments. Therefore, we tested the ability of purified recombinant calpain to cleave these subunits. For this purpose, HEK293t were transiently transfected with plasmids encoding the GFP-Rpt1-6 fusion proteins (a kind gift from Shigeo Murata, Graduate School of Pharmaceutical Sciences, The University of Tokyo), and the resulting cell extracts were incubated with recombinant calpain (37°C for 1.5 h), in the presence or in the absence of Ca^{2+} (4

mM), under non-denaturating conditions to preserve the structure of the proteasome. The calpain-mediated alterations in proteasome subunits were analysed by western blot, with an antibody against GFP; cleavage of the proteasome subunits should decrease the abundance of the full-length GFP-fusion proteins, and this effect may be correlated with an upregulation of truncated forms. Figure 3.14 shows that calpain decreased the total protein levels of the GFP fusion proteins with Rpt1, Rpt3 and Rpt5. Furthermore, incubation with the protease in a Ca^{2+} containing medium generated low molecular weight cleavage products of Rpt1 and Rpt 5. In these experiments no Rpt3 cleavage product was detected, suggesting the cleavage products may degraded by other mechanisms. Because the same extract sample was divided for the two experimental conditions, the difference between the Rpt3-GFP immunoreactivity in the experiments performed in the presence and in the absence of Ca^{2+} cannot be attributed to the loading of different amounts of protein in the gel, but may instead reflect the degradation of the protein. These results suggest that calpain may act directly on the Rpt1, 3 and 5 regulatory particles of the proteasome, and are in agreement with the role for calpain as mediator of the downregulation of Rpt1 and Rpt3 protein levels in cortical neurons subjected to OGD (Figure 3.12 and 3.13).

Taken together, the results described in this section suggest that calpain activation under ischemic conditions is responsible for cleaving a plethora of effectors in the cell. This is the first time that calpain activation under ischemic conditions was shown to have a role in cleaving several proteasome proteins. From the proteasome subunits tested, Rpn10 and Rpt3 were validated as being calpain substrates in cortical neurons subjected to OGD, and the same may also apply to Rpt1. In addition, Rpn3 may also pose a good candidate for calpain-dependent proteolysis which awaits further confirmation. Other proteins with putative PEST sequences are Rpn5, Rpn12 and USP14, which should also be tested for calpain-mediated cleavage in cortical neurons subjected to ischemic conditions.

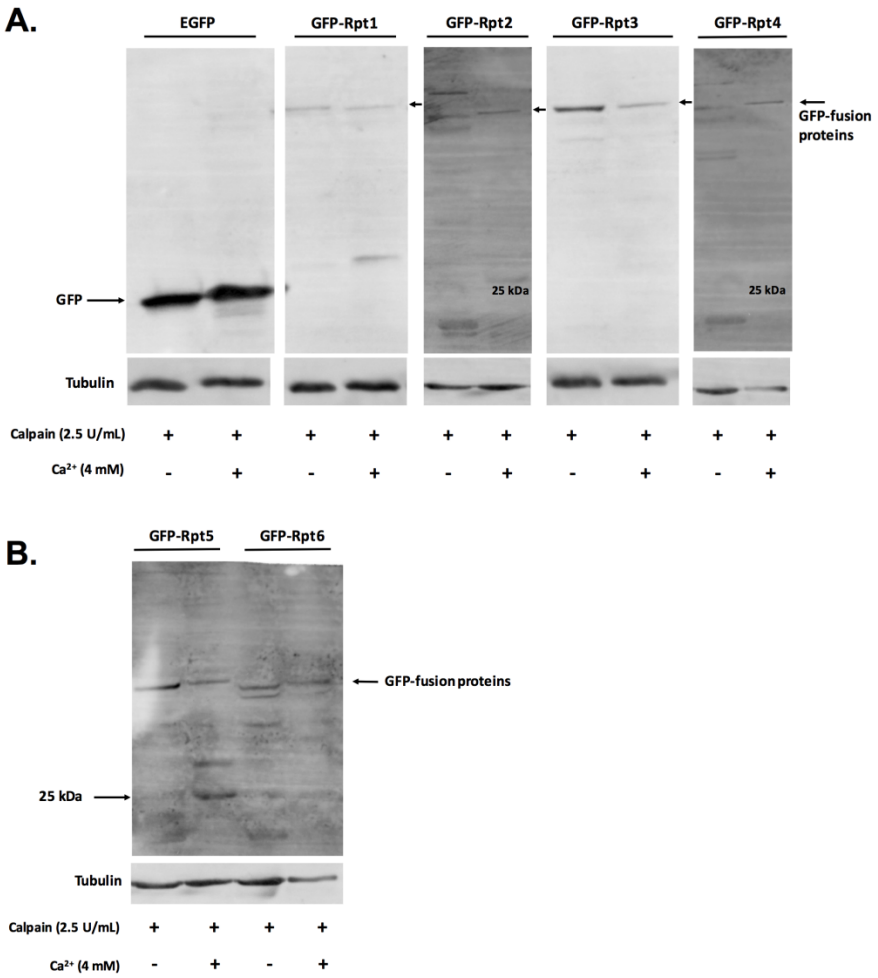

Figure 3.14- Effect of calpain on GFP-Rpt1-6 subunits. HEK293t cells were transfected with plasmids encoding GFP fusion proteins with the proteasome subunits Rpt1-6, and were further incubated for 48 h in culture conditioned medium. Cell lysis was performed in a buffer that allows maintaining the integrity of the 26S proteasome (see Native-PAGE preparation). In all conditions, cell extracts were incubated with calpain (2.5 U/mL) for 1.5 h at 37°C, in the presence or in the absence of 4 mM Ca^{2+}, with constant agitation. The fusion-proteins and truncated fragments were analysed by Western Blot using an antibody against the GFP protein. **A.** Anti-GFP immunoblot in cell extracts obtained from HEK293t cells transfected with a low DNA concentration (2-5 µg/well), for the plasmids GFP and GFP-Rpt1-4. **B.** Anti-GFP immunoblot in cell extracts obtained from HEK293t cells transfected with a high DNA concentration (10 µg/well) for the plasmids GFP-Rpt5 and 6.

3.4. Proteasome activation as a protective strategy to prevent cell death evoked by OGD in cultured cerebrocortical neurons

Proteasome downregulation as well as its disassembly is a common feature observed in models of transient global/focal ischemia, and also in in vitro models (Hu *et al.*, 2000; Asai *et al.*, 2002; Ge *et al.*, 2007; Hochrainer *et al.*, 2012; Caldeira *et al.*, 2013). In fact, proteasome inhibition *per se* is capable to induce apoptotic cell death in cultured neurons (Keller and Markesbery, 2000; Ding *et al.*, 2006). However, these observations contrast with the neuroprotective effects

resulting from proteasome inhibition in several *in vivo* models if brain ischemia (Williams *et al.*, 2003; Williams *et al.*, 2004; Williams *et al.*, 2005).

To determine whether inhibition of the proteasome activity contributes to neuronal death in cortical neurons subjected to OGD, the cells were exposed to in vitro ischemia in the presence of IU1, an inhibitor of USP14 (a DUB associated with the 26S proteasome). IU1 was shown to enhance the degradation of mutant proteins associated with several neurodegenerative disorders such as Tau, Ataxin-3 and TDP-43 in cell lines (Lee *et al.*, 2010). Since little is known about its effect in the nervous system, we first characterized the effect of IU1 on the viability of cortical neurons and on ubiquitin homeostasis. The effect of IU1 on the accumulation of polyubiquitin conjugates was tested at different concentrations of the drug, and protein ubiquitination was analysed by immunoblot using an anti-ubiquitin antibody (Figure 3.15A). Incubation of cerebrocortical neurons with IU1 for 4 h was sufficient to enhance the accumulation of polyubiquitin conjugates (Figure 3.15A), and maximal effects were observed with 12 µM IU1 (Figure 3.15A). This is in accordance with previous results showing an increase in polyubiquitin conjugates in MEFs incubated with IU1 (Lee *et al.*, 2010). The toxicity of IU1 on cerebrocortical neurons was also addressed, by analysis of nuclear morphology after staining of the cells with Hoechst 33342. Incubation with IU1 up to 30 µM for 24 h did not affect cell viability, but at 50 µM the drug significantly increased cell death (29 %) (Figure 3.15B; ****p<0.0001). Taking into account these results, together with previous reports (Lee *et al.*, 2010), 20 µM of the IU1 was used for subsequent experiments.

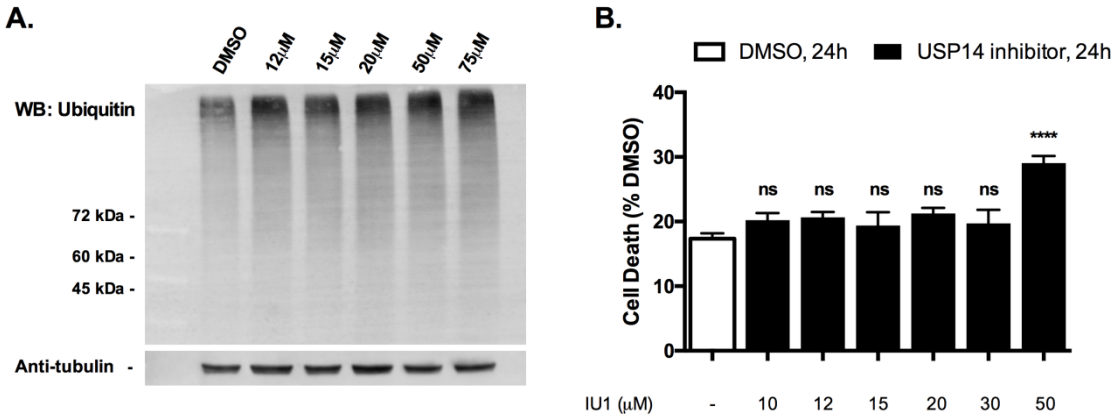

Figure 3.15- Effect of IU1 on ubiquitin homeostasis and cell viability. A. Cerebrocortical neurons (15 DIV) were incubated with increasing concentrations of the USP14 inhibitor IU1, from 10 to 75 µM, for 4 h as indicated in the figure. Total polyubiquitin conjugates were assessed using an antibody that recognizes ubiquitin. β-tubulin was used as loading control. The assay was performed only once as a proof of concept. **B.** Effect of IU1 on cell viability. Cortical neurons were incubated with IU1 at the indicated concentrations, for 24 h. Cell death was analysed by nuclear morphology after nuclei staining with Hoechst 33342, with at least 200 cells counted for each condition and in

duplicates (400 per condition). The results are the average ± SEM of 4 independent experiments. Statistical analysis was performed by one-way ANOVA, followed by the Bonferroni´s multiple comparison test, comparing all the conditions with the respective control (ns, p>0.5;****p< 0.0001).

To access if an increased proteasome activity is protective in cerebrocortical neurons subjected to OGD, we tested the effect of the UPS activator IU1 on the release of LDH, a cytosolic enzyme, to the extracellular medium. OGD for 1.5 h increased cell death by about 16 % when compared to the Sham condition, as evaluated 24 h after the insult (Figure 3.16A; ***p<0.001). When 20 μM IU1 was added 30 minutes before OGD, and maintained thought the experiment, cell death was brought back to control levels (Figure 3.16B; ns p>0.05). Moreover, OGD-induced cell death in cerebrocortical neurons that were previously incubated with 20 μM IU1 was significantly decreased when compared with non-treated cells also subjected to OGD (Figure 3.16A, black bars; ***p<0.001), indicating that pre-incubation of cerebrocortical neurons with IU1 protects neurons against OGD-induced cell death.

In order to be considered as a putative therapeutic strategy in brain ischemia, and since patients do not arrive at the clinics in the acute phase of injury, activation of the proteasome has to be effective when tested after the insult. Therefore, we checked whether IU1 can still exert neuroprotective effects when administered immediately after OGD. Preliminary results show that the neuroprotective effect of proteasome activation may be lost when IU1 is administered immediately after the insult (postOGD) (Figure 3.16B). Additional experiments are needed to confirm these results.

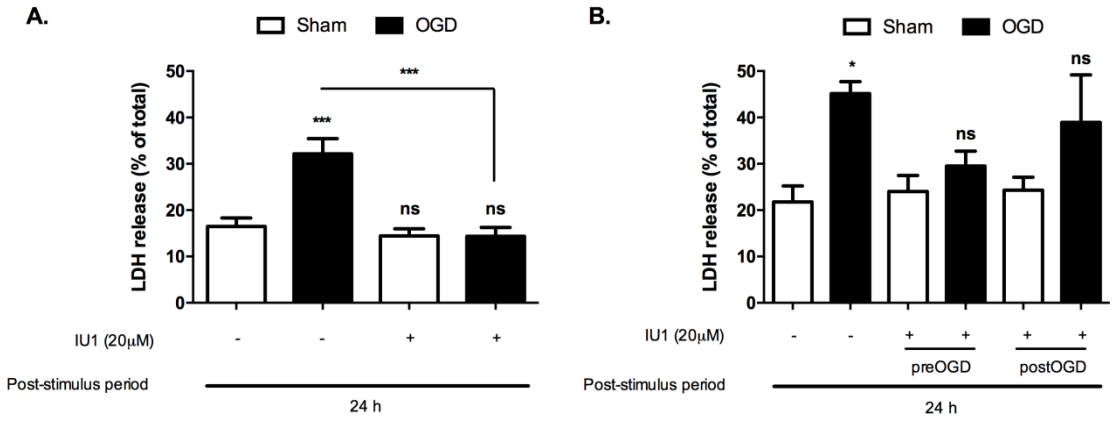

Figure 3.16- Cell death evoked by OGD is prevented by the USP14 inhibitor IU1. Cell death was evaluated after exposing cerebrocortical neurons (15 DIV) to OGD for 1.5 h, and the cells were further incubated in culture conditioned medium for 24 h. The LDH activity in the extracellular medium was evaluated according to the manufacturer protocol with slight modifications. The percentage of cell death was normalized to the full-kill (100 %). **A.** The DUB USP14 inhibitor IU1 (20 μM) was added 30 min prior and during OGD, and was present during the post-incubation period. **B.** The DUB USP14 inhibitor IU1 (20 μM) was added 30 min prior and during OGD (preOGD), or

immediately after (postOGD), and was present during the post-incubation period. The results are the average ± SEM of 3-4 independent experiments. Statistical analysis was performed by one-way ANOVA, followed by the Bonferroni´s multiple comparison test, comparing all the conditions with the respective control (ns, p>0.5; ***p< 0.001).

The neuroprotective effects of IU1 in cortical neurons subjected to OGD is likely to arise from alterations in the proteome following the increase in protein ubiquitination with a consequent activation of the proteasome. To investigate whether incubation with IU1 affects calpain activation following OGD, the activity of the protease was analysed by measuring the cleavage of spectrin (see also Figure 3.7). Cerebrocortical neurons exposed to OGD for 1.5 h and further incubated in culture conditioned medium for 24 h showed a 1.9-fold increase of the SBDP145/150 (Figure 3.17A; *p<0.05 [see also Figure 3.7]), which is indicative of calpain activation. However, when 20 µM of IU1 was present there was no increase in SBDPs 145/150 kDa when the Sham and OGD conditions were compared, indicating that there was no calpain activation (Figure 3.17A; ns p>0.05). A significant decrease in the SBDP levels was therefore observed in cortical neurons subjected to OGD with pre-treatment with IU1 when compared with the same ischemic insult but in the absence of the DUB inhibitor (Figure 3.17A; **p<0.001). The decrease in polyubiquitin conjugates observed at 4 h after the insult (Figure 3.4C) was also observed at 24 h after OGD, although it was not statistically significant under the latter conditions (Figure 3.17B; ns p>0.05). This alteration was no longer observed when cortical neurons were subjected to OGD in the presence of the USP14 inhibitor (Figure 3.17B; ns p>0.05).

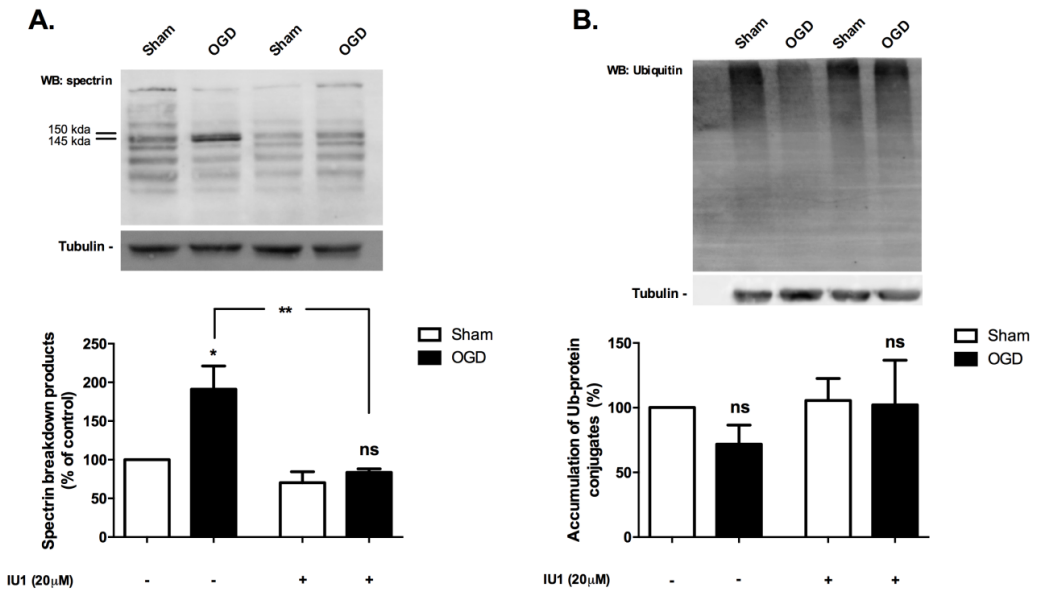

Figure 3.17- Effect of IU1 on the cleavage of α-spectrin and on the abundance of polyubiquitin conjugates. Fifteen DIV cerebrocortical neurons were subjected to OGD for 1.5 h and were further incubated in culture conditioned

medium for 24 h. **A.** Full-length (280 kDa) and proteolytic fragments of α-spectrin (SBDPs) were analysed by western blot using an antibody recognizing both N- and C-terminal regions of the protein. **B.** Total polyubiquitin conjugates were analysed by western blot using an antibody that recognizes all types of polyubiquitin chains. When indicated, the USP14 inhibitor IU1 (20 μM) was added 30 min prior and during OGD, and the drug was also present during the post-incubation period. The results obtained in cells subjected to OGD were normalized to those obtained under Sham condition without IU1 (100 %). β-tubulin was used as loading control. The results are the average ± SEM of 3 independent experiments, performed in distinct preparations. Statistical analysis was performed by one-way ANOVA, followed by the Bonferroni´s multiple comparison test, comparing all the conditions with the respective control (ns, P>0.5; *p<0.05; **p< 0.01).

The results described above suggest that calpain activity is decreased in cortical neurons incubated with IU1, and/or their abundance might be reduced. Indeed, calpains 1 and 2 were shown to be ubiquitinated in a very recent proteomic study (Gao *et al.*, 2016). Given the effect of IU1 in inducing the ubiquitin-dependent degradation of its cognate substrates, we hypothesized that the decreased calpain activity might be correlated with a downregulation of the protease abundance. However, no changes in total calpain-1 protein levels were observed in cortical neurons subjected to OGD (1.5 h), in the presence or in the absence of IU1 (Figure 3.18A), ruling out the contribution of calpain-1 downregulation for the effects of IU1 on the cleavage if spectrin.

Putative non-specific effects of the USP14 inhibitor on calpain activity were also tested, by measuring the activity of human purified calpain-1 in the presence of 20 μM of IU1. Calpain activity was measured using the proteasome substrate Suc-LLVY-AMC, which is also known to be a calpain fluorogenic substrate (Campbell and Quadrilatero, 2016), and the specific activity was calculated as the difference between the fluorescence signal obtained in the absence and in the presence of the calpain inhibitor MDL28170. The results showed that calpain-1 activity was virtually the same in the presence (dashed line) or absence (full line) of the IU1 (Figure 3.18B). Together, these results suggest that the neuroprotective effects of IU1 may be correlated with a decrease in calpain activation. Since total calpain-1 protein levels were not changed, and the USP14 inhibitor did not effect on the activity of calpain-1, there must be other players that contribute to the inhibition of calpain following incubation of cortical neurons with the DUB inhibitor.

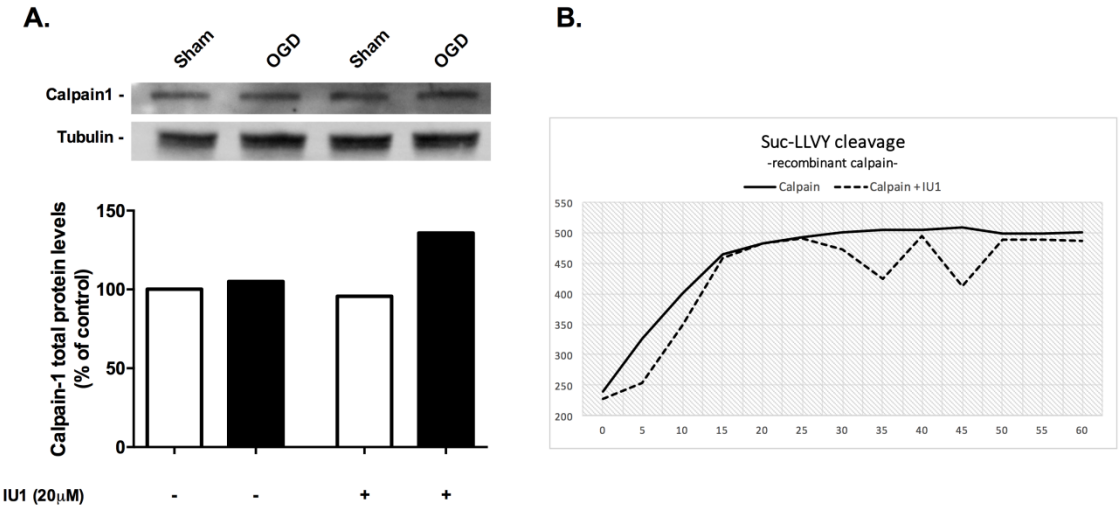

Figure 3.18- Effect of IU1 on total Calpain-1 protein levels in cortical neurons subjected to OGD. A. Total abundance of Calpain-1 protein levels in cerebrocortical neurons (15 DIV) exposed to OGD for 1.5 h and further incubated in culture conditioned medium for 24 h. Where indicated, the USP14 inhibitor IU1 (20 μM) was added 30 min prior and during OGD, and the drug was also present during the post-incubation period. The results obtained in cells subjected to OGD were normalized to those obtained under Sham conditions in the absence of IU1 (100 %). β-tubulin was used as loading control. The results are the average of 2 independent experiments, performed in different preparations. **B.** Activity of recombinant calpain-1. Recombinant calpain-1 (7.5 U/mL) enzyme activity was measured using a fluorogenic substrate (25 μM Suc-LLVY-AMC) for 1 h and in the presence of 10 mM of Ca^{2+}.

Chapter 4

General Discussion and Conclusions

4. General Discussion and Conclusions

In the present work we further investigated the alterations in the Ubiquitin-Proteasome System (UPS) in brain ischemia, using an in vitro model of transient global ischemia. Cultured cortical neurons exposed transiently to Oxygen and Glucose Deprivation (OGD) showed: (i) differential changes in the subcellular distribution of the 19S and 20S proteasomes in the dendritic compartment; (ii) a decrease in the chymotrypsin-like activity of the proteasome, as well as in the fully assembled proteasomes (single-26S and double capped-30S proteasome); iii) in parallel to proteasome inhibition, calpains were activated and cleaved several resident proteasomal subunits, adding a new layer of complexity to the alterations observed in the UPS under ischemic conditions, by limited proteolysis of proteasome subunits; iv) boosting proteasome activity, prevented cell demise induced by in vitro ischemia. The latter results suggest that enhancing the activity of the proteasome may represent a novel therapeutic target to restore the neuronal deficits observed after stroke.

4.1. OGD induces subcellular changes in endogenous proteasomes

Using immunocytochemistry and antibodies specific for PMSA2 and Rpt6, commonly used as markers of the 20S catalytic particle and the 19S regulatory particle, respectively, we found that OGD has a differential effect on the dendritic distribution of the two proteasomal components. This is also in accordance with the results showing a disassembly of the proteasome in cultured hippocampal neurons subjected transiently to OGD. Previous work from our laboratory also showed that the nuclear and cytoplasmic population of proteasomes are differentially affected by excitotoxic glutamate stimulation, with the nuclear fraction being more affected under these conditions (Caldeira *et al.*, 2013). Furthermore, depriving yeast cells from nitrogen, but not glucose, induces proteasome disassembly followed by nuclear export and targeting to the vacuoles. However, the core and regulatory particles were targeted to the vacuoles in a differential manner, since only the former proteasomal component depended on the deubiquitinating enzyme Ubp3 (Waite et al., 2016). Despite the differences between neurons and yeast cells, it may be hypothesized that the clustering of PSMA2 along dendrites early after OGD (2 h), in regions close to the synapse, may result from an increased trafficking of 20S proteasomes (without discarding possible effects on 26S proteasomes) to hotspots where there is an increased formation of reactive oxygen species. This may be relevant from the functional point of view since the 20S proteasomes are more effective in degrading oxidatively damaged proteins, another common hallmark of the ischemic brain (Davies, 2001; Weih *et al.*, 2001; Li *et*

al., 2014). It will be important to determine whether the sites of 20S accumulation also contain a high density of mitochondria, the major ROS producers after brain ischemia (Li *et al.*, 2014; D'Orsi *et al.*, 2015). The delayed increase in the Rpt6 puncta intensity after OGD in cortical neurons may suggest that regulatory mechanisms are induced to restoring normal and basal ubiquitin-dependent proteolysis after the 20S degrade the oxidatively damaged proteins.

Analysis of the PSMA2 and Rpt6 protein levels in cultured cortical neurons subjected to OGD showed no significant changes, when assessed by western blot at 4 h after injury. Although a higher cell density was used in the latter experiments, which may influence the demise process, the results suggest that OGD does not induce an autophagic degradation of 26S proteasomes components (19S and 20S), as reported in yeast deprived from nitrogen (Waite *et al.*, 2016). This difference may be due to an impairment of autophagy, as observed in the 2-VO model in rats. Whether a strategy to enhance autophagy after OGD would also affect the abundance of proteasomes along dendrites deserves further investigation (Liu *et al.*, 2010). Colocalization studies between the proteins markers of the 19S and 20S proteasome particles are required to better elucidate the alterations in the molecular structure of the proteasome after OGD, along with their colocalization with classical lysosomal/endosomal and mitochondrial markers.

To the best of our knowledge, this is the first time that the OGD protocol was adapted to low-density cultures (Figure 3.1), which allows evaluating the alterations in the subcellular distribution of proteins after brain ischemia. We found that 30 min of OGD in the presence of glial cells did not affect cell viability when evaluated 6 h after the insult, in contrast with the results obtained in similar experiments when the ischemic injury was performed in the absence of glial cells (Figure 3.1). This is consistent with the results showing neuroprotective effects of astrocytes (Li *et al.*, 2008), possibly due to an upregulation of EAAT2 that is responsible for removing excessive glutamate from the medium (Zhang *et al.*, 2007; Gong *et al.*, 2012; Bacigaluppi *et al.*, 2016). In contrast, prolonged hypoxia in cultured astrocytes (exposure to 2.5% and 1% O_2 for 24 h) showed an opposite effect, decreasing glutamate uptake due to a downregulation of the EAAT1,2 proteins (Dallas *et al.*, 2007). Under the experimental conditions used in this work, OGD may have increased glutamate uptake by glial cells since there was a decrease in the rate of cell death as evaluated by the nuclear morphology (Figure 3.1). It is also relevant to consider the hypothesis proposing that cultured astrocytes may release healthy mitochondria which may be accumulated into neurons. These mitochondria may restore the ATP levels, thereby preventing neuronal cell death (Hayakawa *et al.*, 2016).

4.2. OGD impairs the proteolytic activity of the proteasome and induces its disassembling

In the present study we found that incubation of cortical neurons under OGD for 1.5 h reduced the chymotrypsin-like activity of the proteasome by about 58%, when evaluated 4 h after the insult. An additional decrease in proteasome activity (about 80%) was reported in cerebrocortical neurons subjected to 2 h of OGD, followed by 2-8 h of reperfusion (Chen *et al.*, 2010). Cultured hippocampal neurons may be more resistant to the stress induced by OGD since in this case 1.5 h of in vitro ischemia was found to decrease the chymotrypsin-like activity of the proteasome about 20% when determined 4 h after the insult (Caldeira *et al.*, 2013). In the latter model, the effect of OGD on the activity of the proteasome was mediated by activation of NMDA receptors for glutamate (Caldeira *et al.*, 2013).

The decreased proteolytic activity of the proteasome after OGD correlates with its disassembly, as observed in cultured cortical neurons exposed to the same conditions (Figure 3.4). The disassembly of the proteasome was observed at 4 h after OGD but it may last longer since a sustained inhibition of the proteasome activity was also observed in cortical neurons subjected to OGD. The decrease in the proteasome stability may result from the excessive stimulation of glutamate receptors, as suggested in experiments with hippocampal neurons subjected to excitotoxic stimulation (Caldeira *et al.*, 2013). In accordance with the results obtained in in vitro experiments, transient global brain ischemia in rats was shown to impair the 26S proteasome activity by promoting proteasome disassembly (Ge et al., 2007). In the latter study the disassembly of the proteasome after the ischemic insult was detected after isolation of the proteasomes by glycerol-density centrifugation which also allows the separation of the 26S and 20S proteasomes. Together, these findings show that transient incubation of cultured neurons under conditions of OGD is a valuable model to investigate the molecular mechanisms involved in the disassembly of the proteasome in brain ischemia.

In several brain regions (e.g. CA3, dentate gyrus, and frontal cortex), the dissociation of the 19S and 20S particles of the proteasome after the ischemic insult is followed by reassembly of the 26S proteasome. However, in the CA1 region of the hippocampus, which is highly sensitive to the ischemic injury, the regulatory and catalytic particles of the proteasome fail to reassociate and the activity is kept low (Asai et al., 2002). The proteasome disassembly may allow the degradation of unfolded and oxidized proteins, which was shown to be carried out more effectively by 20S proteasomes, by a mechanism that does not require ubiquitination (Shringarpure *et al.*, 2003; Aiken *et al.*, 2011). Given the rather short post-incubation period

used in this work, we cannot exclude the possibility that the disassembled proteasomes may reassemble at later time points, along with a recovery in the proteolytic activity.

The mechanisms underlying the differential effect of the ischemic insult on the activity and assembly of the proteasome in the CA1 region *vs* the other brain regions are not fully understood. However, the expression levels of the chaperone Hsp70 may account, at least in part, for the differential stability of the proteasomes in distinct brain regions. The expression of Hsp70 is increased in the motor cortex, but is downregulated in the hippocampus, due to calpain-mediated cleavage, in a model of transient global ischemia in monkeys (Zhu *et al.*, 2012). This protein participates actively in the dissociation of the 26S proteasome into its constituents (20S and 19S), by binding to the 19S regulators (Grune *et al.*, 2011). The transient upregulation of Hsp70 in the cerebral cortex after ischemia may contribute to the disassembly of the proteasome observed in this brain region during the early period of reperfusion after transient brain ischemia (Ge *et al.*, 2007). However, additional experiments should be performed in order to validate this hypothesis since the analysis of the alterations in the Hsp70 protein levels in the motor cortex were performed in a model of transient global brain ischemia in *Macaca fuscata* (Zhu et al., 2012), while the alterations in proteasome assembly were investigated in the cerebral cortex using the BCCAo in gerbils as a model (Asai *et al.*, 2002). The use of distinct models of brain ischemia in distinct species may also account for the differences in the kinetics of the two events reported in the literature. As stated above, Hsp70 expression in the CA1 region is limited due to the calpain-dependent cleavage (Zhu *et al.*, 2012), in conditions also reported to induce a permanent 26S proteasome disassembly (Asai *et al.*, 2002). It remains to be determined whether Hsp70 is actively involved in proteasome disassembly under these conditions.

Mutations in the AAA+ ATPase ring proteins (Rpt1-6), namely those that interfere with binding of ATP, cause defects in the assembly of the 26S proteasomes and impair ubiquitin binding and peptide hydrolysis (Kim *et al.*, 2013b). Accordingly, early evidence showed that biochemical isolation of 26S proteasomes in the absence of ATP causes the dissociation of the 26S proteasome into the 19S and 20S particles. Furthermore, a re-association of the proteasomes was observed when ATP was added back to the medium (Hendil *et al.*, 2002). ATP is essential not only to the assembly of the 26S proteasome but is also important for peptide hydrolysis (Liu *et al.*, 2006b). Given the role of ATP in the stability and function of the proteasome, it is not surprising that the drop in ATP levels during ischemia, (Chen *et al.*, 2010; Connolly *et al.*, 2014; Hayakawa *et al.*, 2016) is associated with a decreased proteasome assembly and activity.

Proteasome disassembly was also reported in models of oxidative stress and impaired mitochondrial ATP production (Huang *et al.*, 2013; Livnat-Levanon *et al.*, 2014), which are characteristics of the ischemic brain cascade. Furthermore, the proteasome assembly was shown to be regulated by the redox molecule NADH. Thus, in the absence of ATP the stability of the 26S proteasome was not affected in cell lines where the $NADH/NAD^+$ ratio was artificially increased, and cell death induced by mitochondrial function inhibition was halted under the same conditions (Tsvetkov *et al.*, 2014). Alongside with the available data for ATP levels after brain ischemia, the $NADH/NAD^+$ ratio was shown to be decreased in brain slices exposed to brain ischemia, which may also contribute to the disassembly of the proteasome (Kannurpatti and Joshi, 1999). Proteasome hypofunction and disassembly is also relevant in other forms of acute brain injury [(e.g traumatic brain injury) (Yao *et al.*, 2007, 2008)] as well as in several neurodegenerative disorders (Im and Chung, 2016).

Given the information presented here, we can conclude that proteasome disassembly may have a dual impact in cell survival. The concomitant increase in 20S proteasomes may represent an elegant strategy to efficiently degrade oxidatively damaged proteins, in an unregulated and energy-independent manner. However, overall hypofunction of the proteasome may have deleterious consequences contributing to neuronal cell death. Additional experiments modulating the assembly status of endogenous proteasomes are required to elucidate its relative contribution to cell demise. This will also allow to dissect and distinguish the relative importance of the activity of disassembled proteasomes, which contribute to protein degradation in the presence of diminished ATP levels under ischemic conditions.

4.3. Ubiquitin homeostasis is altered in brain ischemia

In this work we observed that transient OGD decreases the chymotrypsin-like activity of the proteasome in cultured cortical neurons and induces its disassembly into the 19S and 20S particles. Under the same conditions we found a decrease in total polyubiquitin conjugates and in the expression of one of the ubiquitin encoding genes, the ubiquitinC mRNA, but no alterations were found in monomeric ubiquitin (Figure 3.4). This is in contrast with previous reports showing an upregulation in polyubiquitin protein conjugates in conditions of in vivo and in vitro ischemia (Ge *et al.*, 2007; Chen *et al.*, 2010; Hochrainer *et al.*, 2012). Thus, accumulation of polyubiquitin conjugates was observed during the reperfusion period (starting at 1 h) after 30 min of MCAo, and a decrease in monomeric ubiquitin levels was also observed (Hochrainer *et al.*, 2012). Furthermore, 2 h of OGD in cerebrocortical neurons, which resemble the experimental conditions used in this work, was shown to induce a dramatic increase in

polyubiquitin conjugates, starting after 2 h of reperfusion (Chen *et al.*, 2010). In these studies, protein ubiquitination was evaluated in fractions containing the precipitated proteins, while in the present study we used cell lysates depleted of the heavy membrane fraction. However, no protein ubiquitination was observed in experiments in protein precipitates isolated from cultured cortical neurons subjected to OGD, suggesting that the differences in sample preparation do not account for the differential results obtained.

Immunohistochemical staining of brain slices obtained from mice subjected to 45 min of MCAo showed a sharp decrease in ubiquitin reactivity in ischemic core, when compared to the peri-ischemic infarct area, suggesting that the severity of the insult is positively correlated with ubiquitin expression (Li *et al.*, 2016). This resembles the pattern of change in protein ubiquitination observed in the present work which may, therefore, reflect the response to a more severe ischemic injury. It will be important to determine in future experiments whether the duration of the OGD insult affects the pattern of changes in protein ubiquitination. A decrease in protein polyubiquitination as observed in the present work after OGD may reflect alterations in the activity of ligases in addition to the reduction in protein degradation by the proteasome. Accordingly, in cerebrocortical neurons exposed to mitochondrial toxins that compromise ATP production, there was a reduction in fully-assembled proteasomes together with a downregulation in the total polyubiquitin conjugates, which the authors correlated with a decreased ubiquitin conjugation at the E1 activating enzyme level (Huang *et al.*, 2013). Since in the present work we observed a decrease in polyubiquitination in cultured neurons subjected to OGD, the results may be explained based on a reduction in the activity of the E1 activating enzyme (or the downstream ubiquitin conjugating enzymes). This is in contrast with the results obtained in lens cells exposed to oxidative stress; H_2O_2 increased the activity of the E1 activating enzyme (Shang *et al.*, 1997).

The ubiquitin protein is the result of the expression of four independent genes (UBC, UBB, UBA52, and RPS27A). In this work we evaluated the expression of the UBC gene because it is regulated by stress, together with UBB (Ryu *et al.*, 2007; Kimura and Tanaka, 2010). The results obtained showed a decrease in UbiquitinC expression in cortical neurons subjected transiently to OGD (Figure 3.4). A reduction in UbiquitinC/UBC mRNA expression levels was also found in a model of traumatic brain injury when evaluated 1-2 days after the insult, along with a decrease in free ubiquitin levels (Yao *et al.*, 2007). The alterations in the expression of ubiquitin genes has also been investigated in different models of brain ischemia: (i) UBC mRNA showed a delayed increase in the hippocampus and in the cerebral cortex of rats, at 4-6 h after 4-VO (20 min) (Noga and Hayashi, 1996); (ii) an increase in the mRNA for ubiquitin (it is not clear which gene

was used) was observed in the hippocampus up to 24 h after BCCAo (5 min) in gerbils, returning to basal levels at 48 h after the lesion (Ide *et al.*, 1999); (iii) 15 min of spinal cord ischemia in rabbits increased in ubiquitin protein, as well as to the DUB UCH-L1 during the early stage of reperfusion (Yamauchi *et al.*, 2008). It remains to be determined whether there is a fundamental difference in the brain ischemia-induced alteration in the expression of ubiquitin genes between the in vitro and in vivo models, since the effects described above contrast with the downregulation in UBC gene expression observed in cortical neurons exposed transiently to OGD. Alternatively, the differential results may be explained based on the distinct time points of reperfusion after injury tested in the present work *vs* the in vivo studies.

Based on the evidence here reported, we can hypothesize that the effect of OGD on the reduction of polyubiquitination may be the result of a decrease in ubiquitin conjugation due to the low ATP levels. Alterations in ubiquitin deconjugation may not contribute to the OGD-induced alterations in ubiquitin conjugation since no alteration in total free ubiquitin was observed.

4.4. Calpain activation under ischemic conditions have an impact in the Ubiquitin-Proteasome System components

Herein, we provide evidence showing calpain activation in cerebrocortical neurons subjected to OGD (1.5 h), when evaluate 4 h after the insult (Figure 3.7), as determined by an increase in the levels of spectrin-breakdown products of 145/150 kDa. The apparent absence of the 120 kDa SBDP under the same conditions discards the possible contribution of caspase-3 to the cellular responses to the injury. The results are in accordance with other reports showing calpain activation in cultured hippocampal neurons subjected to OGD (1.5 h and 2 h), when evaluated at different post-incubation periods after the insult (Fernandes *et al.*, 2014; Curcio *et al.*, 2015). As a proof of concept, we also showed that NMDAR acts upstream of calpain activation in cerebrocortical neurons subjected to OGD, by using pharmacological tools to inhibit NMDAR and calpains. Under these conditions, no spectrin cleavage was observed, corroborating previous in vitro and in vivo findings (Roberts-Lewis *et al.*, 1994; Neumar *et al.*, 2001; Kawamura *et al.*, 2005; Fernandes *et al.*, 2014; Curcio *et al.*, 2015). Furthermore, proteasome activity was severely diminished and its assembly was compromised (Figures 3.4 and 3.6).

Evaluation of the presence of putative PEST sequence in all subunits of the proteasome using the EPESTFIND online tool to find potential targets of calpains suggested that several proteasome subunits could be cleaved by this protease. From all candidates tested, we identified Rpn3, Rpn5, Rpn12, Rpn1 and USP14 as putative calpain targets (Figure 3.8, 3.10, 3.11). Additionally,

using a simple assay with recombinant calpain and extracts prepared from HEK293t cells expressing GFP fusion proteins with proteasomal AAA+ ATPase proteasome subunits, we also indentified Rpt1, Rpt3 and Rpt5 as putative calpain targets (Figure 3.14). In accordance with previous reports, we also observed the calpain-mediated cleavage of the Rpn10 ubiquitin acceptor in cerebrocortical neurons subjected to OGD [Figure 3.9 (Huang *et al.*, 2013)]. From those 8 putative calpain substrates, we validated Rpt3 as a calpain substrate, using western blot experiments, along with Rpn10, and showed strong evidence that both Rpt1 and Rpn3 can also be substrates of the protease (Figure 3.9, 3.11, 3.12, 3.13). Remarkably, in the various proteomic studies conducted so far, aiming at identifying potential calpain substrates, none of these studies showed cleavage of proteasomal subunits (Kim *et al.*, 2013a; Shinkai-Ouchi *et al.*, 2016).

The results obtained in this work indicate that some of the proteasome subunits are specifically targeted by calpains, while other proteasome components were not cleaved by the protease. Furthermore, the screening for putative calpain targets using the EPESTFIND online tool confirmed the present difficulty in predicting calpain substrates. Although some amino acid sequences appear to be preferential calpain targets, the protease is thought to recognize the overall 3D, rather than the primary, structures of their substrates (Sorimachi *et al.*, 2011a; Sorimachi *et al.*, 2012; Ono *et al.*, 2016).

4.5. Role of calpain-mediated cleavage of proteasome subunits in regulating proteasome assembly/activity

Although we have not investigated the functional impact of the calpain-mediated cleavage of proteasome subunits, there are several lines of evidence suggesting that it may affect the degradation of UPS substrates as indicated below. Although several of the studies that have addressed these questions were conducted in yeast cells, or using the Drosophila as a model, the mechanism is thought to be highly conserved between eukaryotic cell types (Murata *et al.*, 2009).

Pioneer studies have shown that knockdnown of the Rpt1, Rpn10, Rpn2 and Rpn12 proteasome subunits among others, reduced the viability of Schneider 2 (S2) cells, as well as the chymotrypsin-like activity (Wojcik and DeMartino, 2002). However, after glycerol-gradient centrifugation to isolate the different subpopulations of proteasomes, the activity of the 26S proteasome was only impaired when Rpn2, Rpt1 and Rpn12 were downregulated, whilst Rpn10 knockdown showed the opposite effect (Wojcik and DeMartino, 2002). Therefore, a reduction in Rpt1, Rpn2 and Rpn12 total protein levels has a profound effect on proteasome assembly.

Additionally, the C-terminal region of the Rpt3 protein is essential for a proper assembly of the proteasome [(Kumar *et al.*, 2010); see (Smith *et al.*, 2007) for results showing the effect of point mutations and peptide entry], and proper polyubiquitinated proteins turnover (Sokolova *et al.*, 2015), whereas the Rpn6 protein was shown to interact with both α2 and Rpt6 protein, thus tethering the base of the 19S particle to the 20S (Pathare *et al.*, 2012). In fact, its absence in yeast cells results in a severe impairment in the ubiquitin-proteasome pathway as shown by compromised assembled proteasomes and accumulation of polyubiquitin chains (Santamaria *et al.*, 2003), whereas its overexpression was shown to increase proteasome assembly in embryonic stem cells (Vilchez *et al.*, 2012a). Rpn2 along with Rpn1 were proposed to act as a platform for base assembly, assuming also a vital role in interacting with extraproteasomal partners involved in protein degradation (Rosenzweig *et al.*, 2008). Additionally, Rpn12 also participates in the 19S regulatory particle maturation (Tomko and Hochstrasser, 2011), whereas the C-terminal domain of Rpt1 interacts transiently with the protein Hsm3/S5b, a chaperone involved in the base subcomplex formation, both in humans and yeast cells (Le Tallec *et al.*, 2009; Takagi *et al.*, 2012). Interestingly, loss of this protein also have a profound impact in 26S/30S proteasome assembly (Le Tallec *et al.*, 2009). Rpn3 temperature sensitive mutants also show also distinct defects in proteasome assembly, as well as accumulation of polyubiquitin conjugates (Joshi *et al.*, 2011).

Rpn10-deficient mice showed embryonic lethality, and UIM domain deletion in this protein impaired the ubiquitin-dependent degradation of proteins in the mice liver (Hamazaki *et al.*, 2007). Studies using a similar mice model with the UIM domain of Rpn10 genetically deleted showed an impaired interaction of polyubiquitinated substrates with the proteasome, as shown with purified proteasomes immunoblotted with an antibody against ubiquitin (Hamazaki *et al.*, 2015). Furthermore, RNAi for Rpn10 was without effect on total polyubiquitinated proteins using total cell extracts obtained for HEK293t cells (Hamazaki *et al.*, 2015). Distinct results were obtained using a very distant organism in terms of polyubiquitin conjugates accumulation. Genetic deletion of the Rpn10 ortholog in *Drosophila melanogaster* showed a dramatic increase in polyubiquitinated proteins, larval lethality along with an increase in 26S proteasomes [(Szlanka *et al.*, 2003); see also (Wojcik and DeMartino, 2002)]. The available evidence, including the result showing Rpn10 cleavage by calpains (Huang *et al.*, 2013), suggest that the stability/abundance of Rpn10 may not be the only factor responsible for controlling proteasome stability/assembly given the increase in proteasome activity when the protein is downregulated (Wojcik and DeMartino, 2002; Huang *et al.*, 2013). However, the differential effects observed

may be organism-and tissue-dependent, and may also involve the degradation/interaction of other proteins

The experimental setup used in this work allowed the identification of putative proteasome subunits that may be cleaved by calpains, providing an insight about the molecular mechanism contributing to proteasome hypofunction in cortical neurons exposed transiently to OGD. Given the effects described above (Wojcik and DeMartino, 2002), the cleavage of Rpn10 alone is unlikely to account for the observed downregulation of proteasome activity. On the other hand, the cleavage of Rpt1, Rpt3 and Rpn3 may contribute to the decrease in the stability of the proteasome after OGD (Le Tallec *et al.*, 2009; Kumar *et al.*, 2010; Joshi *et al.*, 2011; Takagi *et al.*, 2012). Additional experiments are also required to evaluate if calpains physically interact with proteasome subunits. It should also be considered that calpains cleave but do not degrade target proteins. Therefore, the formation of truncated proteasome subunits may have an effect on the proteasome structure and activity that is distinct from that obtained after deletion of the protein. Other factors that may also contribute to the regulation of the proteasome activity/stability after OGD include: (i) ATP, which is important for the assembly of the 26S proteasome (Hendil *et al.*, 2002; Liu *et al.*, 2006b); (ii) phosphorylation state of proteasome subunits (Bingol *et al.*, 2010; Lokireddy *et al.*, 2015).

4.6. Proteasome activation as a tool to prevent cell death induced by brain ischemia

As discussed above, in this work we showed the disassembly of the proteasome and a decrease in its chymotrypsin-like activity in cerebrocortical neurons exposed to OGD for 1.5 h (Figures 3.4 and 3.6). The impairment of the proteasome activity associated with neuronal death after OGD is in apparent contradiction with the reports pointing to a neuroprotective effect of proteasome inhibitors in several in vivo models of transient global/focal ischemia (Williams *et al.*, 2003; Williams *et al.*, 2005; Zhang *et al.*, 2010; Doeppner *et al.*, 2012; Doeppner *et al.*, 2016). However, the latter results have been attributed mainly to the inhibition of the inflammatory responses resulting from the ischemic insult and to the stabilization of the blood-brain barrier. In fact, chemical proteasome inhibition is sufficient to increase neuronal cell death by inducing ER stress and activating the mitochondrial apoptotic pathway (Nishitoh *et al.*, 2002; Guo *et al.*, 2016). Therefore, therapeutic strategies to augment the degradative capacity of the UPS may also afford protection in several brain disorders.

The DUB USP14 acts as a brake in the degradation of proteasome substrates in vivo since its genetic deletion increased the turnover in yeast cells (Hanna *et al.*, 2006) and similar results were obtained upon inhibition of the enzyme in cultured mammalian cells (Lee *et al.*, 2010;

Ponnappan *et al.*, 2013). We found that preincubation of cortical neurons with the USP14 inhibitor IU1 abrogates OGD-induced cell death. Interestingly, there was a decrease in calpain activity and a maintenance of ubiquitin homeostasis under the same conditions (Figure 3.15-3.17). This suggests that IU1 may act upstream of calpain activation, or it may reduce its activity through post-transcriptional regulation. The concentration used here (20 µM) is within the range of concentrations that affect the degradation of endogenous substrates without compromising cell viability (up to 100 µM) in human-derived cell lines (Lee *et al.*, 2010; Nag and Finley, 2012). Indeed, IU1 was also shown to have a cytoprotective effect in Rat glomerular epithelial cells subjected to the ER stressor tunicamycin, and to a transient anoxia protocol similar to OGD (Sareen-Khanna *et al.*, 2016). Furthermore, IU1 was reported to reduce brain infarct volume in a mouse model of transient focal cerebral ischemia at day 4 after the insult. In the latter study, elevation of the microRNA124 was found to downregulate USP14, and inhibition of this DUB mimicked the effect obtained under the former conditions (Doeppner et al., 2013). However, the possibility of an increased ubiquitin-dependent protein turnover was not considered in this study.

More recently, two studies addressed the role of USP14 in controlling proteolysis in the cells, and showed an even more complex mechanism than initially proposed. USP14 is responsible for trimming both Lys48 and Lys63 polyubiquitin chains, which is in accordance with the consequent increase in the overall accumulation of polyubiquitin conjugates [(Lee *et al.*, 2010; Vaden *et al.*, 2015; Xu *et al.*, 2015; Lee *et al.*, 2016); Figure 3.15]. The neuroprotective effects of the USP14 inhibition may also be attributed to increased autophagy (Xu *et al.*, 2016), being consistent with the effect of autophagy in neuroprotection in in vivo and in vitro ischemia/reperfusion models (Zhang *et al.*, 2013). Because IU1 increases the turnover of proteins degraded in the UPS, identifying the putative candidates that are downregulated and contribute to the observed neuroprotective effects may provide an additional strategy for treating brain injury in ischemia/reperfusion models. This list is currently limited to a few proteins, but mTOR emerged as a candidate in cell lines with compromised USP14 levels/activity (Xu *et al.*, 2015). mTOR inhibition with rapamycin was shown to improve cell survival following OGD (Fletcher *et al.*, 2013), suggesting that its increased degradation of this protein may account, at least in part, for the protective effects of USP14 inhibition. In addition, increased degradation of Bim by the proteasome was also shown to mediate ischemic tolerance in cerebrocortical neurons exposed to OGD (Meller *et al.*, 2006). Because Bim is an apoptotic protein, and the UPS was shown to regulate this form of cell death (Wojcik, 2002), the degradation of other apoptotic proteins by the UPS may also contribute to the protective effects of USP14 inhibition. Therefore,

identification of which substrates display alterations in stability/activity in cultured neurons exposed to IU1 before the ischemic insult will provide additional information.

We also found that the neuroprotective effects of IU1 are extended to the magnitude of calpain activation, without affecting calpain-1 total protein levels (Figures 3.16 and 3.17). In future studies, it will be important to determine whether incubation with IU1 affects calpain-2 protein levels. If no alteration in calpain protein levels is observed in cortical neurons incubated with IU1, the effects of the DUB inhibitor may result from changes in an upstream event. Since calpains are activated downstream of glutamate receptors stimulation in OGD, a decrease in the surface expression of NMDA and AMPA receptors would decrease the $[Ca^{2+}]_i$ overload after the ischemic insult. Interestingly, there are several reports indicating that the synaptic abundance and traffic of NMDA and AMPA receptors can be regulated by ubiquitination [for review see (Salazar *et al.*, 2016)]. Furthermore, it will be relevant to investigate whether the protein levels of a common modulatory subunit (calpain4), which regulates both calpain1- and 2, is altered in the presence of IU1 (Amini *et al.*, 2013). Because USP14 also shows deubiquitinating activity towards Lys63 polyubiquitin chains, calpain-1/2 polyubiquitination (most likely Lys63; consistent with its non-proteolytic function) may also represent a novel regulatory mechanism controlling the magnitude of its own activation, as shown, for instance, for phosphorylation (Glading *et al.*, 2004; Zadran *et al.*, 2010). This should represent a novel mechanism of regulation of calpain, since the protease was not found in previous proteomic studies in which Lys63- polyubiquitin chains were isolated (Silva *et al.*, 2015). Whether USP14 inhibition affects $[Ca^{2+}]_i$ homeostasis is also an open question that may influence the degree of calpain activation after brain ischemia.

Numerous reports have identified calpain targets which are cleaved in brain ischemia thereby contributing to neuronal demise (Bevers and Neumar, 2008; Curcio *et al.*, 2016). Therefore, the results showing an inhibition of calpain activation by IU1 in cortical neurons subjected to OGD suggest that the modulation of this proteolytic pathway may contribute to the protective effects of the DUB inhibitor. Since calpains cleave several proteasome subunits, as shown in this work, inhibition of these proteases in cells pretreated with IU1 may enhance proteasome stability and protein degradation by the UPS, thereby stabilizing the proteostasis mechanisms. The protective effects of IU1 were only observed when the drug was present during OGD, which makes this approach less relevant from the therapeutic point of view. However, the time required to achieve an effective concentration of IU1 inside the cells may prevent the effect of the DUB inhibitor when administered after OGD.

In conclusion, we hereby propose a mechanism in which proteasome disassembly and downregulation may be an event downstream of calpain activation following transient brain ischemia. Calpain cleaves specific proteasome resident proteins which in turn are responsible for the regulation of its assembly state and, consequently, affect the ubiquitin-dependent protein turnover. However, it is difficult to experimentally evaluate proteasome activity in the presence of calpain inhibitors due to their poor specificity. In line of these results, 19S and the 20S proteasome particles may be differentially regulated after OGD. This hypothesis is supported by the observed differential changes in the distribution of PSMA2 and Rpt6 following OGD. We also hypothesized that the decrease in polyubiquitin conjugates in cortical neurons subjected to OGD is the result of an impairment in ubiquitin conjugation, although this should be experimentally addressed to rule out the effect of increased deconjugation. Consistent with the proteasome disassembly under ischemia conditions, inhibition of the DUB USP14, which is expected to boost the activity of the proteasomes that remain assembled, is sufficient to inhibit cell death following OGD. Therefore, IU1 acts through a preconditioning effect by a mechanism that involve the preservation of the overall levels of protein polyubiquitination and a decrease in calpain activity by a yet unidentified mechanism. For a graphical view about the mechanism proposed please see Figure 4.1.

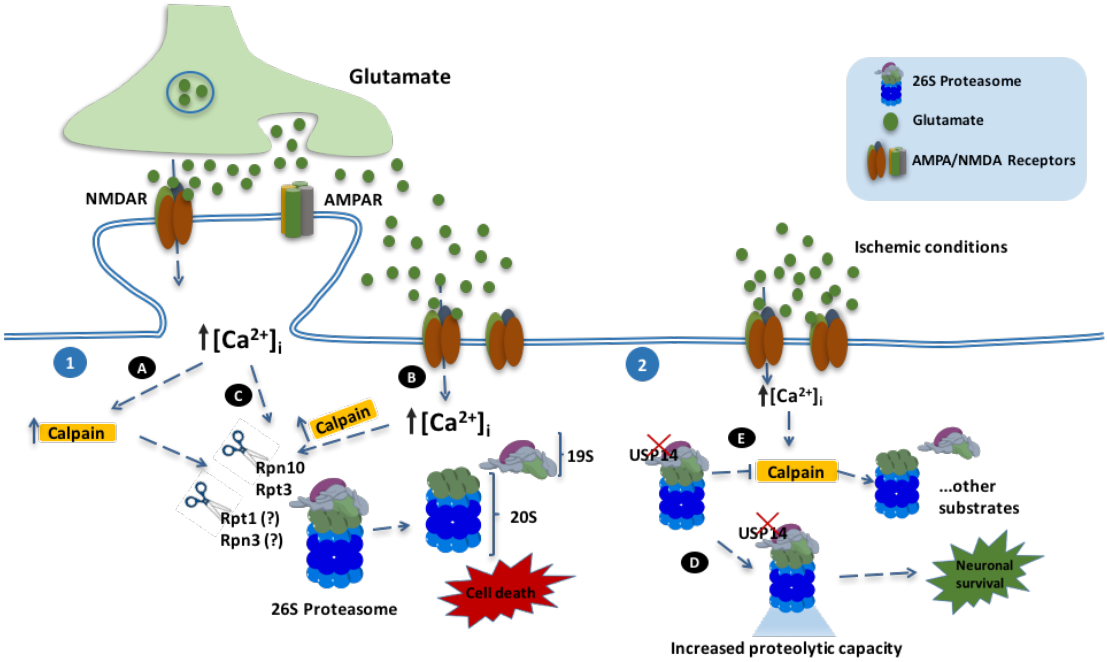

Figure 4.1- Proposed model for alterations in the stability of the UPS after brain ischemia. (1) An early event is the excessive activation of NMDAR located at the synaptic and extrasnaptic sites, which induces a massive increase in the $[Ca^{2+}]_i$. As a consequence of the excessive accumulation of Ca^{2+}, calpains are activated **(A,B)** with the consequent cleavage of several proteins associated with the proteasome resulting in the disassembly of the proteolytic structure (shown by the scissors). Proteasome disassembly may also result from the activation of other pathways independent

of calpain activation: e.g lack of ATP and oxidative stress **(C)**. The disassembly of the 26S proteasome into its major components is thought to induce cell death in cultured neurons subjected to transient ischemia. Proteasome activation **(2**) by means of inhibiting the DUB USP14 with a chemical inhibitor increases the overall function of the UPS through degradation of its canonical substrates. Under these conditions, neuronal cell death is halted in neurons subjected to ischemic conditions **(D)**. Furthermore, USP14 inhibition also abrogates OGD-evoked calpain activation by an unknown mechanism **(E)**, which may then prevent the cleavage of the proteasome subunits (and other subunits) and the disassembly of its structure. Therefore, USP14 inhibition may have dual function in regulating cell survival after OGD, (i) by halting calpain activation and (ii) boosting the overall activity of the UPS.

Chapter 5

Future Perspectives

Future Perspectives

In this work, we showed an overall hypofunction of the Ubiquitin-Proteasome System (UPS) in an in vitro model of brain ischemia, in accordance with the available in vivo evidence. Under the same experimental conditions, calpain activation contributed to the selective cleavage of several proteins of the 26S proteasome. In addition, boosting the activity of the proteasome was found to afford neuroprotection against the cell demise observed following transient incubation of cultured neurons under conditions of Oxygen-Glucose Deprivation (OGD). Although several important points that are worth to further investigate were discussed in the previous sections, in this section we will point out some of the open questions remaining in the field.

General questions

Although we obtained compelling evidence pointing to a cross-talk between calpains and the proteasome in response to ischemic injury, a detailed understanding of the molecular mechanisms involved is still lacking at this point. Furthermore, additional studies are required to determine whether the alterations in the components of the proteasome are indeed associated with cell demise. Finally, complementary experiments should elucidate how IU1 protects cerebrocortical neurons against OGD. The latter studies will also provide a clearer insight about the biochemical changes that are associated with the neuroprotective effect resulting from the activation of the UPS under ischemic conditions. Together, these questions can be addressed as follows:

i) whether other proteasome proteins, besides those identified in this study, can be cleaved by calpains, can be investigated by incubating purified proteasomes with recombinant calpain, and using proteomics tools to identify the substrates of the protease; ii) identifying the calpain cleavage sites in the proteasome subunits is of utmost importance since they may be correlated with proteasome disassembly; iii) analysis of the physical interaction of calpains with endogenous proteasomes may contribute to understand why specific subunits are cleaved; iv) calpastatin overexpression will provide a valuable tool to better dissect the involvement of calpains in regulating the proteasome after transient brain ischemia, thus avoiding the non-specific effects of chemical calpain inhibitors; v) other timepoints after OGD should also be considered to investigate if the alterations in the proteasome activity are transient or not; vi) to further evaluate polyubiquitin conjugates in Triton-X100 insoluble fractions, given the discrepancy of the results obtained in this work and the reports in the literature; vii) evaluation of the changes in E1 activity after OGD will allow determining whether the decreased ubiquitin

conjugation may be due to an impaired function of the ligase; viii) to evaluate the proteome modifications (ubiquitin-modificated) in the presence of IU1 and correlate the decreased protein(s) level(s) with the associated neuroprotective effects; ix) to address the role of IU1 in maintaining 26S proteasome integrity; x) to investigate whether calpain-1 is a target of polyubiquitin modification in the presence of the IU1 (due to the overall stabilization of polyubiquitin bound substrates); xi) to evaluate total protein levels of both calpain-2 and the small regulatory subunit (calpain4).

Is the UPS a valid target for inducing neuroprotection?

It is well established that the UPS function is downregulated after brain ischemia, and several studies have reported the proteasome disassembly under these conditions [this study; (Asai *et al.*, 2002; Ge *et al.*, 2007; Caldeira *et al.*, 2013; Caldeira *et al.*, 2014). The mechanisms involved in the disassembly of the proteasome in brain ischemia are still not understood, in part due to the plethora of regulators that contribute to its stability. A detailed characterization of the biochemical changes that contribute to the disassembly of the 26S proteasome in brain ischemia will allow designing novel strategies to preserve its stability/assembly (in addition to proteasome activators), thereby increasing protein degradation. These tools may be the basis of future neuroprotective strategies.

Overexpression of Rpn6, a protein that we reported as a candidate for calpain-mediated cleavage, was found to increase the relative abundance of 26S and 30S proteasome in human embryonic stem cells (Vilchez *et al.*, 2012a). In line with this evidence, overexpression of the Rpn6 proteasome subunit in *Caenorhabditis elegans* increased the resistance to heat and to oxidative stress, and extended their lifespan (Vilchez *et al.*, 2012b). The Rpn6 protein is phosphorylated by protein kinase A (PKA) on Ser14, and this phosphorylation is sufficient to increase the degradation of short-lived and aggregation prone proteins by the proteasome (Lokireddy *et al.*, 2015). Supporting this evidence, rolipram, which increases the activity of the proteasome by acting on cyclic-AMP levels, resulting in PKA activation (Lokireddy *et al.*, 2015), was also shown to have profound neuroprotective effects after brain ischemia (Soares *et al.*, 2016). However, based on these experiments it is not possible to attribute the effects of PKA to the modulation of the proteasome activity, since there are many other substrates of the kinase. Therefore, in future studies it will be important to evaluate how the modulation of the Rpn6 protein phosphorylation regulate neuronal cell death after OGD. This question may be

addressed by expressing in neurons phosphomimetic (S14A) and the phosphodead (S14A) mutants of Rpn6.

Additionally, USP14 activation by Akt-dependent phosphorylation on Ser432 was shown to inhibit the activity of the proteasome (Xu *et al.*, 2015). Considering the alterations in AKT phosphorylation status under ischemic conditions discussed previously [see section 1.1] modulation of USP14 phosphorylation status may also represent another potential strategy to protect cultured cerebrocortical neurons against OGD, by increasing the overall activity of the proteasome. Similarly to the experiments proposed above to investigate how Rpn6 phosphorylation modulates neuronal damage in brain ischemia, the usage of USP14 phosphomutants may contribute to further elucidate the response of neurons when exposed to ischemic conditions.

The USP14 inhibitor IU1 has been shown to have a dicotomic effect on the UPS. In addition to its role in activating the UPS, inhibition of USP14 was also shown to increase the autophagic pathway (Xu *et al.*, 2015; Xu *et al.*, 2016). Therefore, distinguishing the relative contribution of these two proteolytic systems in the observed neuroprotective effects after OGD will allow pinpointing which degradation system(s) is involved in protecting cultured neurons against the OGD insult. The use of specific chemical inhibitors of the two systems will help addressing this question.

Is there an endogenous proteasome inhibitor?

Proteasome assembly/activity is highly regulated by complex mechanisms. Therefore, faulty proteasomes are actively degraded (Waite *et al.*, 2016) or repressed (Lee *et al.*, 2011b), and these are important mechanism of quality-control in eukaryotic cells. The extracellular mutant 29 (Ecm29) protein was shown to interact with the proteasomes and to repress their activity in vitro and in vivo (Lee *et al.*, 2011b; De La Mota-Peynado *et al.*, 2013). Mice deficient for the KIAA0368 gene, the mammalian orthologue of Ecm29, showed no alterations in the peptidase activity and in proteasome formation under control conditions (Haratake *et al.*, 2016). However, KIAA0368-deficient cells showed increased resilience to proteasome disassembly under oxidative stress conditions when compared with wild-type cells (Haratake *et al.*, 2016). This suggests that the Ecm29 protein plays an active role in inducing proteasome disassembly under the latter conditions. Therefore, it will be important to investigate the role of Ecm29 in cultured cerebrocortical neurons subjected to OGD.

Chapter 6

References

Abdul Rehman, S.A., Kristariyanto, Y.A., Choi, S.Y., Nkosi, P.J., Weidlich, S., Labib, K., Hofmann, K., Kulathu, Y., 2016. MINDY-1 Is a Member of an Evolutionarily Conserved and Structurally Distinct New Family of Deubiquitinating Enzymes. *Mol Cell* 63**,** 146-155.

Adrain, C., Creagh, E.M., Cullen, S.P., Martin, S.J., 2004. Caspase-dependent inactivation of proteasome function during programmed cell death in Drosophila and man. *J Biol Chem* 279**,** 36923-36930.

Ahlgren, H., Henjum, K., Ottersen, O.P., Runden-Pran, E., 2011. Validation of organotypical hippocampal slice cultures as an ex vivo model of brain ischemia: different roles of NMDA receptors in cell death signalling after exposure to NMDA or oxygen and glucose deprivation. *Cell Tissue Res* 345**,** 329-341.

Aiken, C.T., Kaake, R.M., Wang, X., Huang, L., 2011. Oxidative stress-mediated regulation of proteasome complexes. *Mol Cell Proteomics* 10**,** R110 006924.

Almeida, A., Bolanos, J.P., Moreno, S., 2005. Cdh1/Hct1-APC is essential for the survival of postmitotic neurons. *J Neurosci* 25**,** 8115-8121.

Amini, M., Ma, C.L., Farazifard, R., Zhu, G., Zhang, Y., Vanderluit, J., Zoltewicz, J.S., Hage, F., Savitt, J.M., Lagace, D.C., Slack, R.S., Beique, J.C., Baudry, M., Greer, P.A., Bergeron, R., Park, D.S., 2013. Conditional disruption of calpain in the CNS alters dendrite morphology, impairs LTP, and promotes neuronal survival following injury. *J Neurosci* 33**,** 5773-5784.

Asai, A., Tanahashi, N., Qiu, J.H., Saito, N., Chi, S., Kawahara, N., Tanaka, K., Kirino, T., 2002. Selective proteasomal dysfunction in the hippocampal CA1 region after transient forebrain ischemia. *J Cereb Blood Flow Metab* 22**,** 705-710.

Asher, G., Tsvetkov, P., Kahana, C., Shaul, Y., 2005. A mechanism of ubiquitin-independent proteasomal degradation of the tumor suppressors p53 and p73. *Genes Dev* 19**,** 316-321.

Atkin, G., Moore, S., Lu, Y., Nelson, R.F., Tipper, N., Rajpal, G., Hunt, J., Tennant, W., Hell, J.W., Murphy, G.G., Paulson, H., 2015. Loss of F-box only protein 2 (Fbxo2) disrupts levels and localization of select NMDA receptor subunits, and promotes aberrant synaptic connectivity. *J Neurosci* 35**,** 6165-6178.

Averna, M., De Tullio, R., Capini, P., Salamino, F., Pontremoli, S., Melloni, E., 2003. Changes in calpastatin localization and expression during calpain activation: a new mechanism for the regulation of intracellular Ca^{2+}-dependent proteolysis. *Cell Mol Life Sci* 60**,** 2669-2678.

Ayuso, M.I., Martinez-Alonso, E., Cid, C., Alonso de Lecinana, M., Alcazar, A., 2013. The translational repressor eIF4E-binding protein 2 (4E-BP2) correlates with selective delayed neuronal death after ischemia. *J Cereb Blood Flow Metab* 33**,** 1173-1181.

Bacigaluppi, M., Russo, G.L., Peruzzotti-Jametti, L., Rossi, S., Sandrone, S., Butti, E., De Ceglia, R., Bergamaschi, A., Motta, C., Gallizioli, M., Studer, V., Colombo, E., Farina, C., Comi, G., Politi, L.S., Muzio, L., Villani, C., Invernizzi, R.W., Hermann, D.M., Centonze, D., Martino, G., 2016. Neural Stem Cell Transplantation Induces Stroke Recovery by Upregulating Glutamate Transporter GLT-1 in Astrocytes. *J Neurosci* 36**,** 10529-10544.

Barnett, D.G., Bibb, J.A., 2011. The role of Cdk5 in cognition and neuropsychiatric and neurological pathology. *Brain Res Bull* 85**,** 9-13.

Barone, F.C., White, R.F., Spera, P.A., Ellison, J., Currie, R.W., Wang, X., Feuerstein, G.Z., 1998. Ischemic preconditioning and brain tolerance: temporal histological and functional outcomes, protein synthesis requirement, and interleukin-1 receptor antagonist and early gene expression. *Stroke* 29**,** 1937-1950; discussion 1950-1931.

Barsoum, M.J., Yuan, H., Gerencser, A.A., Liot, G., Kushnareva, Y., Graber, S., Kovacs, I., Lee, W.D., Waggoner, J., Cui, J., White, A.D., Bossy, B., Martinou, J.C., Youle, R.J., Lipton, S.A., Ellisman, M.H., Perkins, G.A., Bossy-Wetzel, E., 2006. Nitric oxide-induced mitochondrial fission is regulated by dynamin-related GTPases in neurons. *EMBO J* 25**,** 3900-3911.

Bashore, C., Dambacher, C.M., Goodall, E.A., Matyskiela, M.E., Lander, G.C., Martin, A., 2015. Ubp6 deubiquitinase controls conformational dynamics and substrate degradation of the 26S proteasome. *Nat Struct Mol Biol* 22**,** 712-719.

Baxter, P.S., Bell, K.F., Hasel, P., Kaindl, A.M., Fricker, M., Thomson, D., Cregan, S.P., Gillingwater, T.H., Hardingham, G.E., 2015. Synaptic NMDA receptor activity is coupled to the transcriptional control of the glutathione system. *Nat Commun* 6**,** 6761.

Beck, J., Lenart, B., Kintner, D.B., Sun, D., 2003. Na-K-Cl cotransporter contributes to glutamate-mediated excitotoxicity. *J Neurosci* 23**,** 5061-5068.

Beinke, S., Ley, S.C., 2004. Functions of NF-kappaB1 and NF-kappaB2 in immune cell biology. *Biochem J* 382**,** 393-409.

Belayev, L., Busto, R., Zhao, W., Ginsberg, M.D., 1996. Quantitative evaluation of blood-brain barrier permeability following middle cerebral artery occlusion in rats. *Brain Res* 739**,** 88-96.

Bengtson, C.P., Dick, O., Bading, H., 2008. A quantitative method to assess extrasynaptic NMDA receptor function in the protective effect of synaptic activity against neurotoxicity. *BMC Neurosci* 9**,** 11.

Berridge, M.J., Bootman, M.D., Roderick, H.L., 2003. Calcium signalling: dynamics, homeostasis and remodelling. *Nat Rev Mol Cell Biol* 4**,** 517-529.

Bevers, M.B., Neumar, R.W., 2008. Mechanistic role of calpains in postischemic neurodegeneration. *J Cereb Blood Flow Metab* 28**,** 655-673.

Bingol, B., Schuman, E.M., 2006. Activity-dependent dynamics and sequestration of proteasomes in dendritic spines. *Nature* 441**,** 1144-1148.

Bingol, B., Wang, C.F., Arnott, D., Cheng, D., Peng, J., Sheng, M., 2010. Autophosphorylated CaMKIIalpha acts as a scaffold to recruit proteasomes to dendritic spines. *Cell* 140**,** 567-578.

Blanco-Suarez, E., Fiuza, M., Liu, X., Chakkarapani, E., Hanley, J.G., 2014. Differential Tiam1/Rac1 activation in hippocampal and cortical neurons mediates differential spine shrinkage in response to oxygen/glucose deprivation. *J Cereb Blood Flow Metab* 34**,** 1898-1906.

Blanco-Suarez, E., Hanley, J.G., 2014. Distinct subunit-specific alpha-amino-3-hydroxy-5-methyl-4-isoxazolepropionic acid (AMPA) receptor trafficking mechanisms in cultured cortical and hippocampal neurons in response to oxygen and glucose deprivation. *J Biol Chem* 289**,** 4644-4651.

Blomgren, K., Zhu, C., Wang, X., Karlsson, J.O., Leverin, A.L., Bahr, B.A., Mallard, C., Hagberg, H., 2001. Synergistic activation of caspase-3 by m-calpain after neonatal hypoxia-ischemia: a mechanism of "pathological apoptosis"? *J Biol Chem* 276**,** 10191-10198.

Bobba, A., Canu, N., Atlante, A., Petragallo, V., Calissano, P., Marra, E., 2002. Proteasome inhibitors prevent cytochrome c release during apoptosis but not in excitotoxic death of cerebellar granule neurons. *FEBS Lett* 515**,** 8-12.

Bodalia, A., Li, H., Jackson, M.F., 2013. Loss of endoplasmic reticulum Ca^{2+} homeostasis: contribution to neuronal cell death during cerebral ischemia. *Acta Pharmacol Sin* 34**,** 49-59.

Bonde, C., Noraberg, J., Noer, H., Zimmer, J., 2005. Ionotropic glutamate receptors and glutamate transporters are involved in necrotic neuronal cell death induced by oxygen-glucose deprivation of hippocampal slice cultures. *Neuroscience* 136**,** 779-794.

Bousquet-Dubouch, M.P., Baudelet, E., Guerin, F., Matondo, M., Uttenweiler-Joseph, S., Burlet-Schiltz, O., Monsarrat, B., 2009. Affinity purification strategy to capture human endogenous proteasome complexes diversity and to identify proteasome-interacting proteins. *Mol Cell Proteomics* 8**,** 1150-1164.

Boutet, S.C., Disatnik, M.H., Chan, L.S., Iori, K., Rando, T.A., 2007. Regulation of Pax3 by proteasomal degradation of monoubiquitinated protein in skeletal muscle progenitors. *Cell* 130**,** 349-362.

Braten, O., Livneh, I., Ziv, T., Admon, A., Kehat, I., Caspi, L.H., Gonen, H., Bercovich, B., Godzik, A., Jahandideh, S., Jaroszewski, L., Sommer, T., Kwon, Y.T., Guharoy, M., Tompa, P., Ciechanover, A., 2016. Numerous proteins with unique characteristics are degraded by the 26S proteasome following monoubiquitination. *Proc Natl Acad Sci U S A* 113**,** E4639-4647.

Briz, V., Baudry, M., 2016. Calpains: Master Regulators of Synaptic Plasticity. *Neuroscientist*. (in press)

Broughton, B.R., Reutens, D.C., Sobey, C.G., 2009. Apoptotic mechanisms after cerebral ischemia. *Stroke* 40**,** e331-339.

Buchan, A.M., Li, H., Blackburn, B., 2000. Neuroprotection achieved with a novel proteasome inhibitor which blocks NF-kappaB activation. *Neuroreport* 11**,** 427-430.

Buchan, A.M., Xue, D., Huang, Z.G., Smith, K.H., Lesiuk, H., 1991. Delayed AMPA receptor blockade reduces cerebral infarction induced by focal ischemia. *Neuroreport* 2**,** 473-476.

Buetow, L., Huang, D.T., 2016. Structural insights into the catalysis and regulation of E3 ubiquitin ligases. *Nat Rev Mol Cell Biol* 17**,** 626-642.

Caldeira, M.V., Curcio, M., Leal, G., Salazar, I.L., Mele, M., Santos, A.R., Melo, C.V., Pereira, P., Canzoniero, L.M., Duarte, C.B., 2013. Excitotoxic stimulation downregulates the ubiquitin-proteasome system through activation of NMDA receptors in cultured hippocampal neurons. *Biochim Biophys Acta* 1832**,** 263-274.

Caldeira, M.V., Salazar, I.L., Curcio, M., Canzoniero, L.M., Duarte, C.B., 2014. Role of the ubiquitin-proteasome system in brain ischemia: friend or foe? *Prog Neurobiol* 112**,** 50-69.

Calderone, A., Jover, T., Mashiko, T., Noh, K.M., Tanaka, H., Bennett, M.V., Zukin, R.S., 2004. Late calcium EDTA rescues hippocampal CA1 neurons from global ischemia-induced death. *J Neurosci* 24**,** 9903-9913.

Calderone, A., Jover, T., Noh, K.M., Tanaka, H., Yokota, H., Lin, Y., Grooms, S.Y., Regis, R., Bennett, M.V., Zukin, R.S., 2003. Ischemic insults derepress the gene silencer REST in neurons destined to die. *J Neurosci* 23**,** 2112-2121.

Camins, A., Verdaguer, E., Folch, J., Pallas, M., 2006. Involvement of calpain activation in neurodegenerative processes. *CNS Drug Rev* 12**,** 135-148.

Campbell, R.L., Davies, P.L., 2012. Structure-function relationships in calpains. *Biochem J* 447**,** 335-351.

Campbell, T.L., Quadrilatero, J., 2016. Data on skeletal muscle apoptosis, autophagy, and morphology in mice treated with doxorubicin. *Data Brief* 7**,** 786-793.

Cao, G., Xing, J., Xiao, X., Liou, A.K., Gao, Y., Yin, X.M., Clark, R.S., Graham, S.H., Chen, J., 2007. Critical role of calpain I in mitochondrial release of apoptosis-inducing factor in ischemic neuronal injury. *J Neurosci* 27**,** 9278-9293.

Cartier, A.E., Djakovic, S.N., Salehi, A., Wilson, S.M., Masliah, E., Patrick, G.N., 2009. Regulation of synaptic structure by ubiquitin C-terminal hydrolase L1. *J Neurosci* 29**,** 7857-7868.

Castaneda, C.A., Kashyap, T.R., Nakasone, M.A., Krueger, S., Fushman, D., 2013. Unique structural, dynamical, and functional properties of k11-linked polyubiquitin chains. *Structure* 21**,** 1168-1181.

Chandrasekharan, M.B., Huang, F., Sun, Z.W., 2009. Ubiquitination of histone H2B regulates chromatin dynamics by enhancing nucleosome stability. *Proc Natl Acad Sci U S A* 106**,** 16686-16691.

Chau, V., Tobias, J.W., Bachmair, A., Marriott, D., Ecker, D.J., Gonda, D.K., Varshavsky, A., 1989. A multiubiquitin chain is confined to specific lysine in a targeted short-lived protein. *Science* 243**,** 1576-1583.

Chen, F.T., Yang, C.M., Yang, C.H., 2013. The protective effects of the proteasome inhibitor bortezomib (velcade) on ischemia-reperfusion injury in the rat retina. *PLoS One* 8**,** e64262.

Chen, M., Lu, T.J., Chen, X.J., Zhou, Y., Chen, Q., Feng, X.Y., Xu, L., Duan, W.H., Xiong, Z.Q., 2008a. Differential roles of NMDA receptor subtypes in ischemic neuronal cell death and ischemic tolerance. *Stroke* 39**,** 3042-3048.

Chen, P.E., Geballe, M.T., Katz, E., Erreger, K., Livesey, M.R., O'Toole, K.K., Le, P., Lee, C.J., Snyder, J.P., Traynelis, S.F., Wyllie, D.J., 2008b. Modulation of glycine potency in rat recombinant NMDA receptors containing chimeric NR2A/2D subunits expressed in Xenopus laevis oocytes. *J Physiol* 586**,** 227-245.

Chen, X., Kintner, D.B., Baba, A., Matsuda, T., Shull, G.E., Sun, D., 2010. Protein aggregation in neurons following OGD: a role for Na^{+} and Ca^{2+} ionic dysregulation. *J Neurochem* 112**,** 173-182.

Chen, X., Liu, Y., Zhu, J., Lei, S., Dong, Y., Li, L., Jiang, B., Tan, L., Wu, J., Yu, S., Zhao, Y., 2016. GSK-3beta downregulates Nrf2 in cultured cortical neurons and in a rat model of cerebral ischemia-reperfusion. *Sci Rep* 6**,** 20196.

Cheng, Y.D., Al-Khoury, L., Zivin, J.A., 2004. Neuroprotection for ischemic stroke: two decades of success and failure. *NeuroRx* 1**,** 36-45.

Chinopoulos, C., Adam-Vizi, V., 2010. Mitochondrial Ca^{2+} sequestration and precipitation revisited. *FEBS J* 277**,** 3637-3651.

Choi, D.W., 1987. Ionic dependence of glutamate neurotoxicity. *J Neurosci* 7**,** 369-379.

Choi, D.W., 1988. Calcium-mediated neurotoxicity: relationship to specific channel types and role in ischemic damage. *Trends Neurosci* 11**,** 465-469.

Choi, W.H., de Poot, S.A., Lee, J.H., Kim, J.H., Han, D.H., Kim, Y.K., Finley, D., Lee, M.J., 2016. Open-gate mutants of the mammalian proteasome show enhanced ubiquitin-conjugate degradation. *Nat Commun* 7**,** 10963.

Choi, W.S., Lee, E.H., Chung, C.W., Jung, Y.K., Jin, B.K., Kim, S.U., Oh, T.H., Saido, T.C., Oh, Y.J., 2001. Cleavage of Bax is mediated by caspase-dependent or -independent calpain activation in dopaminergic neuronal cells: protective role of Bcl-2. *J Neurochem* 77**,** 1531-1541.

Choy, F.C., Klaric, T.S., Leong, W.K., Koblar, S.A., Lewis, M.D., 2016. Reduction of the neuroprotective transcription factor Npas4 results in increased neuronal necrosis, inflammation and brain lesion size following ischaemia. *J Cereb Blood Flow Metab* 36**,** 1449-1463.

Chua, B.T., Guo, K., Li, P., 2000. Direct cleavage by the calcium-activated protease calpain can lead to inactivation of caspases. *J Biol Chem* 275**,** 5131-5135.

Ciechanover, A., Heller, H., Elias, S., Haas, A.L., Hershko, A., 1980. ATP-dependent conjugation of reticulocyte proteins with the polypeptide required for protein degradation. *Proc Natl Acad Sci U S A* 77**,** 1365-1368.

Ciechanover, A., Heller, H., Katz-Etzion, R., Hershko, A., 1981. Activation of the heat-stable polypeptide of the ATP-dependent proteolytic system. *Proc Natl Acad Sci U S A* 78**,** 761-765.

Ciehanover, A., Hod, Y., Hershko, A., 1978. A heat-stable polypeptide component of an ATP-dependent proteolytic system from reticulocytes. *Biochem Biophys Res Commun* 81**,** 1100-1105.

Cohen-Kaplan, V., Livneh, I., Avni, N., Cohen-Rosenzweig, C., Ciechanover, A., 2016. The ubiquitin-proteasome system and autophagy: Coordinated and independent activities. *Int J Biochem Cell Biol* 79**,** 403-418.

Colbourne, F., Grooms, S.Y., Zukin, R.S., Buchan, A.M., Bennett, M.V., 2003. Hypothermia rescues hippocampal CA1 neurons and attenuates down-regulation of the AMPA receptor GluR2 subunit after forebrain ischemia. *Proc Natl Acad Sci U S A* 100**,** 2906-2910.

Connolly, N.M., Dussmann, H., Anilkumar, U., Huber, H.J., Prehn, J.H., 2014. Single-cell imaging of bioenergetic responses to neuronal excitotoxicity and oxygen and glucose deprivation. *J Neurosci* 34**,** 10192-10205.

Costa, J.T., Mele, M., Baptista, M.S., Gomes, J.R., Ruscher, K., Nobre, R.J., de Almeida, L.P., Wieloch, T., Duarte, C.B., 2016. Gephyrin Cleavage in In Vitro Brain Ischemia Decreases GABAA Receptor Clustering and Contributes to Neuronal Death. *Mol Neurobiol* 53**,** 3513-3527.

Craxton, A., Butterworth, M., Harper, N., Fairall, L., Schwabe, J., Ciechanover, A., Cohen, G.M., 2012. NOXA, a sensor of proteasome integrity, is degraded by 26S proteasomes by an ubiquitin-independent pathway that is blocked by MCL-1. *Cell Death Differ* 19**,** 1424-1434.

Crumrine, R.C., Thomas, A.L., Morgan, P.F., 1994. Attenuation of p53 expression protects against focal ischemic damage in transgenic mice. *J Cereb Blood Flow Metab* 14**,** 887-891.

Cuervo, A.M., Palmer, A., Rivett, A.J., Knecht, E., 1995. Degradation of proteasomes by lysosomes in rat liver. *Eur J Biochem* 227**,** 792-800.

Cui, H., Hayashi, A., Sun, H.S., Belmares, M.P., Cobey, C., Phan, T., Schweizer, J., Salter, M.W., Wang, Y.T., Tasker, R.A., Garman, D., Rabinowitz, J., Lu, P.S., Tymianski, M., 2007. PDZ protein interactions underlying NMDA receptor-mediated excitotoxicity and neuroprotection by PSD-95 inhibitors. *J Neurosci* 27**,** 9901-9915.

Curcio, M., Salazar, I.L., Inacio, A.R., Duarte, E.P., Canzoniero, L.M., Duarte, C.B., 2015. Brain ischemia downregulates the neuroprotective GDNF-Ret signaling by a calpain-dependent mechanism in cultured hippocampal neurons. *Cell Death Dis* 6**,** e1645.

Curcio, M., Salazar, I.L., Mele, M., Canzoniero, L.M., Duarte, C.B., 2016. Calpains and neuronal damage in the ischemic brain: The swiss knife in synaptic injury. *Prog Neurobiol* 143**,** 1-35.

D'Orsi, B., Bonner, H., Tuffy, L.P., Dussmann, H., Woods, I., Courtney, M.J., Ward, M.W., Prehn, J.H., 2012. Calpains are downstream effectors of bax-dependent excitotoxic apoptosis. *J Neurosci* 32**,** 1847-1858.

D'Orsi, B., Kilbride, S.M., Chen, G., Perez Alvarez, S., Bonner, H.P., Pfeiffer, S., Plesnila, N., Engel, T., Henshall, D.C., Dussmann, H., Prehn, J.H., 2015. Bax regulates neuronal Ca^{2+} homeostasis. *J Neurosci* 35**,** 1706-1722.

da Fonseca, P.C., He, J., Morris, E.P., 2012. Molecular model of the human 26S proteasome. *Mol Cell* 46**,** 54-66.

da Fonseca, P.C., Morris, E.P., 2008. Structure of the human 26S proteasome: subunit radial displacements open the gate into the proteolytic core. *J Biol Chem* 283**,** 23305-23314.

Dallas, M., Boycott, H.E., Atkinson, L., Miller, A., Boyle, J.P., Pearson, H.A., Peers, C., 2007. Hypoxia suppresses glutamate transport in astrocytes. *J Neurosci* 27**,** 3946-3955.

Dang, F.W., Chen, L., Madura, K., 2016. Catalytically Active Proteasomes Function Predominantly in the Cytosol. *J Biol Chem* 291**,** 18765-18777.

Davies, K.J., 2001. Degradation of oxidized proteins by the 20S proteasome. *Biochimie* 83**,** 301-310.

Dawson, L.A., Djali, S., Gonzales, C., Vinegra, M.A., Zaleska, M.M., 2000. Characterization of transient focal ischemia-induced increases in extracellular glutamate and aspartate in spontaneously hypertensive rats. *Brain Res Bull* 53**,** 767-776.

de Bie, P., Ciechanover, A., 2011. Ubiquitination of E3 ligases: self-regulation of the ubiquitin system via proteolytic and non-proteolytic mechanisms. *Cell Death Differ* 18**,** 1393-1402.

De La Mota-Peynado, A., Lee, S.Y., Pierce, B.M., Wani, P., Singh, C.R., Roelofs, J., 2013. The proteasome-associated protein Ecm29 inhibits proteasomal ATPase activity and in vivo protein degradation by the proteasome. *J Biol Chem* 288**,** 29467-29481.

Deb, I., Manhas, N., Poddar, R., Rajagopal, S., Allan, A.M., Lombroso, P.J., Rosenberg, G.A., Candelario-Jalil, E., Paul, S., 2013. Neuroprotective role of a brain-enriched tyrosine phosphatase, STEP, in focal cerebral ischemia. *J Neurosci* 33**,** 17814-17826.

DeGracia, D.J., Rudolph, J., Roberts, G.G., Rafols, J.A., Wang, J., 2007. Convergence of stress granules and protein aggregates in hippocampal cornu ammonis 1 at later reperfusion following global brain ischemia. *Neuroscience* 146**,** 562-572.

Dennissen, F.J., Kholod, N., van Leeuwen, F.W., 2012. The ubiquitin proteasome system in neurodegenerative diseases: culprit, accomplice or victim? *Prog Neurobiol* 96**,** 190-207.

Derugin, N., Ferriero, D.M., Vexler, Z.S., 1998. Neonatal reversible focal cerebral ischemia: a new model. *Neurosci Res* 32**,** 349-353.

Derugin, N., Wendland, M., Muramatsu, K., Roberts, T.P., Gregory, G., Ferriero, D.M., Vexler, Z.S., 2000. Evolution of brain injury after transient middle cerebral artery occlusion in neonatal rats. *Stroke* 31**,** 1752-1761.

Dimova, N.V., Hathaway, N.A., Lee, B.H., Kirkpatrick, D.S., Berkowitz, M.L., Gygi, S.P., Finley, D., King, R.W., 2012. APC/C-mediated multiple monoubiquitylation provides an alternative degradation signal for cyclin B1. *Nat Cell Biol* 14**,** 168-176.

Ding, Q., Dimayuga, E., Markesbery, W.R., Keller, J.N., 2006. Proteasome inhibition induces reversible impairments in protein synthesis. *FASEB J* 20**,** 1055-1063.

Dirnagl, U., Iadecola, C., Moskowitz, M.A., 1999. Pathobiology of ischaemic stroke: an integrated view. *Trends Neurosci* 22**,** 391-397.

Djakovic, S.N., Marquez-Lona, E.M., Jakawich, S.K., Wright, R., Chu, C., Sutton, M.A., Patrick, G.N., 2012. Phosphorylation of Rpt6 regulates synaptic strength in hippocampal neurons. *J Neurosci* 32**,** 5126-5131.

Djakovic, S.N., Schwarz, L.A., Barylko, B., DeMartino, G.N., Patrick, G.N., 2009. Regulation of the proteasome by neuronal activity and calcium/calmodulin-dependent protein kinase II. *J Biol Chem* 284**,** 26655-26665.

Doeppner, T.R., Doehring, M., Bretschneider, E., Zechariah, A., Kaltwasser, B., Muller, B., Koch, J.C., Bahr, M., Hermann, D.M., Michel, U., 2013. MicroRNA-124 protects against focal cerebral ischemia via mechanisms involving Usp14-dependent REST degradation. *Acta Neuropathol* 126**,** 251-265.

Doeppner, T.R., Kaltwasser, B., Kuckelkorn, U., Henkelein, P., Bretschneider, E., Kilic, E., Hermann, D.M., 2016. Systemic Proteasome Inhibition Induces Sustained Post-stroke Neurological Recovery and Neuroprotection via Mechanisms Involving Reversal of Peripheral Immunosuppression and Preservation of Blood-Brain-Barrier Integrity. *Mol Neurobiol* 53**,** 6332-6341.

Doeppner, T.R., Mlynarczuk-Bialy, I., Kuckelkorn, U., Kaltwasser, B., Herz, J., Hasan, M.R., Hermann, D.M., Bahr, M., 2012. The novel proteasome inhibitor BSc2118 protects against cerebral ischaemia through HIF1A accumulation and enhanced angioneurogenesis. *Brain* 135**,** 3282-3297.

Donath, S., An, J., Lee, S.L., Gertz, K., Datwyler, A.L., Harms, U., Muller, S., Farr, T.D., Fuchtemeier, M., Lattig-Tunnemann, G., Lips, J., Foddis, M., Mosch, L., Bernard, R., Grittner, U., Balkaya, M., Kronenberg, G., Dirnagl, U., Endres, M., Harms, C., 2016. Interaction of ARC and Daxx: A Novel Endogenous Target to Preserve Motor Function and Cell Loss after Focal Brain Ischemia in Mice. *J Neurosci* 36**,** 8132-8148.

Dong, Q.P., He, J.Q., Chai, Z., 2013. Astrocytic Ca^{2+} waves mediate activation of extrasynaptic NMDA receptors in hippocampal neurons to aggravate brain damage during ischemia. *Neurobiol Dis* 58**,** 68-75.

DuVerle, D.A., Ono, Y., Sorimachi, H., Mamitsuka, H., 2011. Calpain cleavage prediction using multiple kernel learning. *PLoS One* 6**,** e19035.

Ehlers, M.D., 2003. Activity level controls postsynaptic composition and signaling via the ubiquitin-proteasome system. *Nat Neurosci* 6**,** 231-242.

Elmore, S., 2007. Apoptosis: a review of programmed cell death. *Toxicol Pathol* 35**,** 495-516.

Elsasser, S., Chandler-Militello, D., Muller, B., Hanna, J., Finley, D., 2004. Rad23 and Rpn10 serve as alternative ubiquitin receptors for the proteasome. *J Biol Chem* 279**,** 26817-26822.

Elsasser, S., Gali, R.R., Schwickart, M., Larsen, C.N., Leggett, D.S., Muller, B., Feng, M.T., Tubing, F., Dittmar, G.A., Finley, D., 2002. Proteasome subunit Rpn1 binds ubiquitin-like protein domains. *Nat Cell Biol* 4**,** 725-730.

Elsasser, S., Schmidt, M., Finley, D., 2005. Characterization of the proteasome using native gel electrophoresis. *Methods Enzymol* 398**,** 353-363.

Emmerich, N.P., Nussbaum, A.K., Stevanovic, S., Priemer, M., Toes, R.E., Rammensee, H.G., Schild, H., 2000. The human 26S and 20S proteasomes generate overlapping but different sets of peptide fragments from a model protein substrate. *J Biol Chem* 275**,** 21140-21148.

Endo, H., Kamada, H., Nito, C., Nishi, T., Chan, P.H., 2006a. Mitochondrial translocation of p53 mediates release of cytochrome c and hippocampal CA1 neuronal death after transient global cerebral ischemia in rats. *J Neurosci* 26**,** 7974-7983.

Endo, H., Nito, C., Kamada, H., Nishi, T., Chan, P.H., 2006b. Activation of the Akt/GSK3beta signaling pathway mediates survival of vulnerable hippocampal neurons after transient global cerebral ischemia in rats. *J Cereb Blood Flow Metab* 26**,** 1479-1489.

Endres, M., Meisel, A., Biniszkiewicz, D., Namura, S., Prass, K., Ruscher, K., Lipski, A., Jaenisch, R., Moskowitz, M.A., Dirnagl, U., 2000. DNA methyltransferase contributes to delayed ischemic brain injury. *J Neurosci* 20**,** 3175-3181.

Erreger, K., Geballe, M.T., Kristensen, A., Chen, P.E., Hansen, K.B., Lee, C.J., Yuan, H., Le, P., Lyuboslavsky, P.N., Micale, N., Jorgensen, L., Clausen, R.P., Wyllie, D.J., Snyder, J.P., Traynelis, S.F., 2007. Subunit-specific agonist activity at NR2A-, NR2B-, NR2C-, and NR2D-containing N-methyl-D-aspartate glutamate receptors. *Mol Pharmacol* 72**,** 907-920.

Fabre, B., Lambour, T., Garrigues, L., Ducoux-Petit, M., Amalric, F., Monsarrat, B., Burlet-Schiltz, O., Bousquet-Dubouch, M.P., 2014. Label-free quantitative proteomics reveals the dynamics of proteasome complexes composition and stoichiometry in a wide range of human cell lines. *J Proteome Res* 13**,** 3027-3037.

Fan, Y.X., Zhang, Y., Shen, H.B., 2013. LabCaS: labeling calpain substrate cleavage sites from amino acid sequence using conditional random fields. *Proteins* 81**,** 622-634.

Fang, S., Weissman, A.M., 2004. A field guide to ubiquitylation. *Cell Mol Life Sci* 61**,** 1546-1561.

Fergusson, J., Landon, M., Lowe, J., Dawson, S.P., Layfield, R., Hanger, D.P., Mayer, R.J., 1996. Pathological lesions of Alzheimer's disease and dementia with Lewy bodies brains exhibit

immunoreactivity to an ATPase that is a regulatory subunit of the 26S proteasome. *Neurosci Lett* 219**,** 167-170.

Fernandes, J., Vieira, M., Carreto, L., Santos, M.A., Duarte, C.B., Carvalho, A.L., Santos, A.E., 2014. In vitro ischemia triggers a transcriptional response to down-regulate synaptic proteins in hippocampal neurons. *PLoS One* 9**,** e99958.

Fernandez-Lopez, D., Faustino, J., Daneman, R., Zhou, L., Lee, S.Y., Derugin, N., Wendland, M.F., Vexler, Z.S., 2012. Blood-brain barrier permeability is increased after acute adult stroke but not neonatal stroke in the rat. *J Neurosci* 32**,** 9588-9600.

Ferreira, J.S., Schmidt, J., Rio, P., Aguas, R., Rooyakkers, A., Li, K.W., Smit, A.B., Craig, A.M., Carvalho, A.L., 2015. GluN2B-Containing NMDA Receptors Regulate AMPA Receptor Traffic through Anchoring of the Synaptic Proteasome. *J Neurosci* 35**,** 8462-8479.

Filichia, E., Shen, H., Zhou, X., Qi, X., Jin, K., Greig, N., Hoffer, B., Luo, Y., 2015. Forebrain neuronal specific ablation of p53 gene provides protection in a cortical ischemic stroke model. *Neuroscience* 295**,** 1-10.

Filippini, A., Bonini, D., La Via, L., Barbon, A., 2016. The Good and the Bad of Glutamate Receptor RNA Editing. *Mol Neurobiol*.

Fink, K., Zhu, J., Namura, S., Shimizu-Sasamata, M., Endres, M., Ma, J., Dalkara, T., Yuan, J., Moskowitz, M.A., 1998. Prolonged therapeutic window for ischemic brain damage caused by delayed caspase activation. *J Cereb Blood Flow Metab* 18**,** 1071-1076.

Finley, D., Ulrich, H.D., Sommer, T., Kaiser, P., 2012. The ubiquitin-proteasome system of Saccharomyces cerevisiae. *Genetics* 192**,** 319-360.

Fletcher, L., Evans, T.M., Watts, L.T., Jimenez, D.F., Digicaylioglu, M., 2013. Rapamycin treatment improves neuron viability in an in vitro model of stroke. *PLoS One* 8**,** e68281.

Forrest, D., Yuzaki, M., Soares, H.D., Ng, L., Luk, D.C., Sheng, M., Stewart, C.L., Morgan, J.I., Connor, J.A., Curran, T., 1994. Targeted disruption of NMDA receptor 1 gene abolishes NMDA response and results in neonatal death. *Neuron* 13**,** 325-338.

Frank, R.A., Komiyama, N.H., Ryan, T.J., Zhu, F., O'Dell, T.J., Grant, S.G., 2016. NMDA receptors are selectively partitioned into complexes and supercomplexes during synapse maturation. *Nat Commun* 7**,** 11264.

Friedrich, P., Papp, H., Halasy, K., Farkas, A., Farkas, B., Tompa, P., Kasa, P., 2004. Differential distribution of calpain small subunit 1 and 2 in rat brain. *Eur J Neurosci* 19**,** 1819-1825.

Gan, Y., Liu, Q., Wu, W., Yin, J.X., Bai, X.F., Shen, R., Wang, Y., Chen, J., La Cava, A., Poursine-Laurent, J., Yokoyama, W., Shi, F.D., 2014. Ischemic neurons recruit natural killer cells that accelerate brain infarction. *Proc Natl Acad Sci U S A* 111**,** 2704-2709.

Gao, Y., Li, Y., Zhang, C., Zhao, M., Deng, C., Lan, Q., Liu, Z., Su, N., Wang, J., Xu, F., Xu, Y., Ping, L., Chang, L., Gao, H., Wu, J., Xue, Y., Deng, Z., Peng, J., Xu, P., 2016. Enhanced Purification of Ubiquitinated Proteins by Engineered Tandem Hybrid Ubiquitin-binding Domains (ThUBDs). *Mol Cell Proteomics* 15**,** 1381-1396.

Ge, P., Luo, Y., Liu, C.L., Hu, B., 2007. Protein aggregation and proteasome dysfunction after brain ischemia. *Stroke* 38**,** 3230-3236.

Geiger, J.R., Melcher, T., Koh, D.S., Sakmann, B., Seeburg, P.H., Jonas, P., Monyer, H., 1995. Relative abundance of subunit mRNAs determines gating and Ca^{2+} permeability of AMPA receptors in principal neurons and interneurons in rat CNS. *Neuron* 15**,** 193-204.

Gilabert, J.A., 2012. Cytoplasmic calcium buffering. *Adv Exp Med Biol* 740**,** 483-498.

Gill, R., Nordholm, L., Lodge, D., 1992. The neuroprotective actions of 2,3-dihydroxy-6-nitro-7-sulfamoyl-benzo(F)quinoxaline (NBQX) in a rat focal ischaemia model. *Brain Res* 580**,** 35-43.

Glading, A., Bodnar, R.J., Reynolds, I.J., Shiraha, H., Satish, L., Potter, D.A., Blair, H.C., Wells, A., 2004. Epidermal growth factor activates m-calpain (calpain II), at least in part, by extracellular signal-regulated kinase-mediated phosphorylation. *Mol Cell Biol* 24**,** 2499-2512.

Goebel-Goody, S.M., Baum, M., Paspalas, C.D., Fernandez, S.M., Carty, N.C., Kurup, P., Lombroso, P.J., 2012. Therapeutic implications for striatal-enriched protein tyrosine phosphatase (STEP) in neuropsychiatric disorders. *Pharmacol Rev* 64**,** 65-87.

Goldberg, M.P., Choi, D.W., 1993. Combined oxygen and glucose deprivation in cortical cell culture: calcium-dependent and calcium-independent mechanisms of neuronal injury. *J Neurosci* 13**,** 3510-3524.

Goldstein, G., Scheid, M., Hammerling, U., Schlesinger, D.H., Niall, H.D., Boyse, E.A., 1975. Isolation of a polypeptide that has lymphocyte-differentiating properties and is probably represented universally in living cells. *Proc Natl Acad Sci U S A* 72**,** 11-15.

Goll, D.E., Thompson, V.F., Li, H., Wei, W., Cong, J., 2003. The calpain system. *Physiol Rev* 83**,** 731-801.

Gomes, J.R., Lobo, A.C., Melo, C.V., Inacio, A.R., Takano, J., Iwata, N., Saido, T.C., de Almeida, L.P., Wieloch, T., Duarte, C.B., 2011. Cleavage of the vesicular GABA transporter under excitotoxic conditions is followed by accumulation of the truncated transporter in nonsynaptic sites. *J Neurosci* 31**,** 4622-4635.

Gong, S.J., Chen, L.Y., Zhang, M., Gong, J.X., Ma, Y.X., Zhang, J.M., Wang, Y.J., Hu, Y.Y., Sun, X.C., Li, W.B., Zhang, Y., 2012. Intermittent hypobaric hypoxia preconditioning induced brain ischemic tolerance by up-regulating glial glutamate transporter-1 in rats. *Neurochem Res* 37**,** 527-537.

Gonzalez-Burgos, G., Lewis, D.A., 2012. NMDA receptor hypofunction, parvalbumin-positive neurons, and cortical gamma oscillations in schizophrenia. *Schizophr Bull* 38**,** 950-957.

Gould, E., Cameron, H.A., McEwen, B.S., 1994. Blockade of NMDA receptors increases cell death and birth in the developing rat dentate gyrus. *J Comp Neurol* 340**,** 551-565.

Grabbe, C., Husnjak, K., Dikic, I., 2011. The spatial and temporal organization of ubiquitin networks. *Nat Rev Mol Cell Biol* 12**,** 295-307.

Greer, P.L., Hanayama, R., Bloodgood, B.L., Mardinly, A.R., Lipton, D.M., Flavell, S.W., Kim, T.K., Griffith, E.C., Waldon, Z., Maehr, R., Ploegh, H.L., Chowdhury, S., Worley, P.F., Steen, J., Greenberg, M.E., 2010. The Angelman Syndrome protein Ube3A regulates synapse development by ubiquitinating arc. *Cell* 140**,** 704-716.

Grewer, C., Gameiro, A., Zhang, Z., Tao, Z., Braams, S., Rauen, T., 2008. Glutamate forward and reverse transport: from molecular mechanism to transporter-mediated release after ischemia. *IUBMB Life* 60**,** 609-619.

Grice, G.L., Lobb, I.T., Weekes, M.P., Gygi, S.P., Antrobus, R., Nathan, J.A., 2015. The Proteasome Distinguishes between Heterotypic and Homotypic Lysine-11-Linked Polyubiquitin Chains. *Cell Rep* 12**,** 545-553.

Grigoreva, T.A., Tribulovich, V.G., Garabadzhiu, A.V., Melino, G., Barlev, N.A., 2015. The 26S proteasome is a multifaceted target for anti-cancer therapies. *Oncotarget* 6**,** 24733-24749.

Groc, L., Heine, M., Cousins, S.L., Stephenson, F.A., Lounis, B., Cognet, L., Choquet, D., 2006. NMDA receptor surface mobility depends on NR2A-2B subunits. *Proc Natl Acad Sci U S A* 103**,** 18769-18774.

Groll, M., Ditzel, L., Lowe, J., Stock, D., Bochtler, M., Bartunik, H.D., Huber, R., 1997. Structure of 20S proteasome from yeast at 2.4 A resolution. *Nature* 386**,** 463-471.

Grou, C.P., Pinto, M.P., Mendes, A.V., Domingues, P., Azevedo, J.E., 2015. The de novo synthesis of ubiquitin: identification of deubiquitinases acting on ubiquitin precursors. *Sci Rep* 5**,** 12836.

Grune, T., Catalgol, B., Licht, A., Ermak, G., Pickering, A.M., Ngo, J.K., Davies, K.J., 2011. HSP70 mediates dissociation and reassociation of the 26S proteasome during adaptation to oxidative stress. *Free Radic Biol Med* 51**,** 1355-1364.

Guan, J., Du, S., Lv, T., Qu, S., Fu, Q., Yuan, Y., 2016. Oxygen-glucose deprivation preconditioning protects neurons against oxygen-glucose deprivation/reperfusion induced injury via bone morphogenetic protein-7 mediated ERK, p38 and Smad signalling pathways. *Clin Exp Pharmacol Physiol* 43**,** 125-134.

Guerini, D., Coletto, L., Carafoli, E., 2005. Exporting calcium from cells. *Cell Calcium* 38**,** 281-289.

Guo, F., He, X.B., Li, S., Le, W., 2016. A Central Role for Phosphorylated p38alpha in Linking Proteasome Inhibition-Induced Apoptosis and Autophagy. *Mol Neurobiol*.

Guterman, A., Glickman, M.H., 2004. Complementary roles for Rpn11 and Ubp6 in deubiquitination and proteolysis by the proteasome. *J Biol Chem* 279**,** 1729-1738.

Gutierrez-Vargas, J.A., Moreno, H., Cardona-Gomez, G.P., 2016. Targeting CDK5 post-stroke provides long-term neuroprotection and rescues synaptic plasticity. *J Cereb Blood Flow Metab*.

Gutierrez-Vargas, J.A., Munera, A., Cardona-Gomez, G.P., 2015. CDK5 knockdown prevents hippocampal degeneration and cognitive dysfunction produced by cerebral ischemia. *J Cereb Blood Flow Metab* 35**,** 1937-1949.

Ha, S.W., Ju, D., Hao, W., Xie, Y., 2016. Rapidly Translated Polypeptides Are Preferred Substrates for Cotranslational Protein Degradation. *J Biol Chem* 291**,** 9827-9834.

Haas, A.L., Warms, J.V., Hershko, A., Rose, I.A., 1982. Ubiquitin-activating enzyme. Mechanism and role in protein-ubiquitin conjugation. *J Biol Chem* 257**,** 2543-2548.

Hakim, V., Cohen, L.D., Zuchman, R., Ziv, T., Ziv, N.E., 2016. The effects of proteasomal inhibition on synaptic proteostasis. *EMBO J* 35**,** 2238-2262.

Hamakubo, T., Kannagi, R., Murachi, T., Matus, A., 1986. Distribution of calpains I and II in rat brain. *J Neurosci* 6**,** 3103-3111.

Hamazaki, J., Hirayama, S., Murata, S., 2015. Redundant Roles of Rpn10 and Rpn13 in Recognition of Ubiquitinated Proteins and Cellular Homeostasis. *PLoS Genet* 11**,** e1005401.

Hamazaki, J., Sasaki, K., Kawahara, H., Hisanaga, S., Tanaka, K., Murata, S., 2007. Rpn10-mediated degradation of ubiquitinated proteins is essential for mouse development. *Mol Cell Biol* 27**,** 6629-6638.

Hamilton, A.M., Oh, W.C., Vega-Ramirez, H., Stein, I.S., Hell, J.W., Patrick, G.N., Zito, K., 2012. Activity-dependent growth of new dendritic spines is regulated by the proteasome. *Neuron* 74**,** 1023-1030.

Hamilton, A.M., Zito, K., 2013. Breaking it down: the ubiquitin proteasome system in neuronal morphogenesis. *Neural Plast* 2013**,** 196848.

Hanna, J., Hathaway, N.A., Tone, Y., Crosas, B., Elsasser, S., Kirkpatrick, D.S., Leggett, D.S., Gygi, S.P., King, R.W., Finley, D., 2006. Deubiquitinating enzyme Ubp6 functions noncatalytically to delay proteasomal degradation. *Cell* 127**,** 99-111.

Hanna, R.A., Campbell, R.L., Davies, P.L., 2008. Calcium-bound structure of calpain and its mechanism of inhibition by calpastatin. *Nature* 456**,** 409-412.

Hanna, R.A., Garcia-Diaz, B.E., Davies, P.L., 2007. Calpastatin simultaneously binds four calpains with different kinetic constants. *FEBS Lett* 581**,** 2894-2898.

Hansen, K.B., Ogden, K.K., Yuan, H., Traynelis, S.F., 2014. Distinct functional and pharmacological properties of Triheteromeric GluN1/GluN2A/GluN2B NMDA receptors. *Neuron* 81**,** 1084-1096.

Haratake, K., Sato, A., Tsuruta, F., Chiba, T., 2016. KIAA0368-deficiency affects disassembly of 26S proteasome under oxidative stress condition. *J Biochem* 159**,** 609-618.

Hardingham, G.E., 2006. Pro-survival signalling from the NMDA receptor. *Biochem Soc Trans* 34**,** 936-938.

Hardingham, G.E., Bading, H., 2010. Synaptic versus extrasynaptic NMDA receptor signalling: implications for neurodegenerative disorders. *Nat Rev Neurosci* 11**,** 682-696.

Hardingham, G.E., Fukunaga, Y., Bading, H., 2002. Extrasynaptic NMDARs oppose synaptic NMDARs by triggering CREB shut-off and cell death pathways. *Nat Neurosci* 5**,** 405-414.

Hatton, C.J., Paoletti, P., 2005. Modulation of triheteromeric NMDA receptors by N-terminal domain ligands. *Neuron* 46**,** 261-274.

Hayakawa, K., Esposito, E., Wang, X., Terasaki, Y., Liu, Y., Xing, C., Ji, X., Lo, E.H., 2016. Transfer of mitochondria from astrocytes to neurons after stroke. *Nature* 535**,** 551-555.

Hayashi, T., Takada, K., Matsuda, M., 1992. Post-transient ischemia increase in ubiquitin conjugates in the early reperfusion. *Neuroreport* 3**,** 519-520.

Hendil, K.B., Hartmann-Petersen, R., Tanaka, K., 2002. 26S proteasomes function as stable entities. *J Mol Biol* 315**,** 627-636.

Hershko, A., Ciechanover, A., 1998. The ubiquitin system. *Annu Rev Biochem* 67**,** 425-479.

Hetz, C., Vitte, P.A., Bombrun, A., Rostovtseva, T.K., Montessuit, S., Hiver, A., Schwarz, M.K., Church, D.J., Korsmeyer, S.J., Martinou, J.C., Antonsson, B., 2005. Bax channel inhibitors prevent mitochondrion-mediated apoptosis and protect neurons in a model of global brain ischemia. *J Biol Chem* 280**,** 42960-42970.

Higuchi, M., Tomioka, M., Takano, J., Shirotani, K., Iwata, N., Masumoto, H., Maki, M., Itohara, S., Saido, T.C., 2005. Distinct mechanistic roles of calpain and caspase activation in neurodegeneration as revealed in mice overexpressing their specific inhibitors. *J Biol Chem* 280**,** 15229-15237.

Hochrainer, K., Jackman, K., Anrather, J., Iadecola, C., 2012. Reperfusion rather than ischemia drives the formation of ubiquitin aggregates after middle cerebral artery occlusion. *Stroke* 43**,** 2229-2235.

Hoege, C., Pfander, B., Moldovan, G.L., Pyrowolakis, G., Jentsch, S., 2002. RAD6-dependent DNA repair is linked to modification of PCNA by ubiquitin and SUMO. *Nature* 419**,** 135-141.

Hollmann, M., Hartley, M., Heinemann, S., 1991. Ca^{2+} permeability of KA-AMPA--gated glutamate receptor channels depends on subunit composition. *Science* 252**,** 851-853.

Hoyte, L., Barber, P.A., Buchan, A.M., Hill, M.D., 2004. The rise and fall of NMDA antagonists for ischemic stroke. *Curr Mol Med* 4**,** 131-136.

Hu, B.R., Janelidze, S., Ginsberg, M.D., Busto, R., Perez-Pinzon, M., Sick, T.J., Siesjo, B.K., Liu, C.L., 2001. Protein aggregation after focal brain ischemia and reperfusion. *J Cereb Blood Flow Metab* 21**,** 865-875.

Hu, B.R., Martone, M.E., Jones, Y.Z., Liu, C.L., 2000. Protein aggregation after transient cerebral ischemia. *J Neurosci* 20**,** 3191-3199.

Huang, Q., Wang, H., Perry, S.W., Figueiredo-Pereira, M.E., 2013. Negative regulation of 26S proteasome stability via calpain-mediated cleavage of Rpn10 subunit upon mitochondrial dysfunction in neurons. *J Biol Chem* 288**,** 12161-12174.

Huang, X., Luan, B., Wu, J., Shi, Y., 2016. An atomic structure of the human 26S proteasome. *Nat Struct Mol Biol* 23**,** 778-785.

Hung, A.Y., Sung, C.C., Brito, I.L., Sheng, M., 2010. Degradation of postsynaptic scaffold GKAP and regulation of dendritic spine morphology by the TRIM3 ubiquitin ligase in rat hippocampal neurons. *PLoS One* 5**,** e9842.

Huo, Y., Khatri, N., Hou, Q., Gilbert, J., Wang, G., Man, H.Y., 2015. The deubiquitinating enzyme USP46 regulates AMPA receptor ubiquitination and trafficking. *J Neurochem* 134**,** 1067-1080.

Iadecola, C., Anrather, J., 2011. The immunology of stroke: from mechanisms to translation. *Nat Med* 17**,** 796-808.

Ide, T., Takada, K., Qiu, J.H., Saito, N., Kawahara, N., Asai, A., Kirino, T., 1999. Ubiquitin stress response in postischemic hippocampal neurons under nontolerant and tolerant conditions. *J Cereb Blood Flow Metab* 19**,** 750-756.

Im, E., Chung, K.C., 2016. Precise assembly and regulation of 26S proteasome and correlation between proteasome dysfunction and neurodegenerative diseases. *BMB Rep* 49**,** 459-473.

Ishii, T., Moriyoshi, K., Sugihara, H., Sakurada, K., Kadotani, H., Yokoi, M., Akazawa, C., Shigemoto, R., Mizuno, N., Masu, M., et al., 1993. Molecular characterization of the family of the N-methyl-D-aspartate receptor subunits. *J Biol Chem* 268**,** 2836-2843.

Iwabuchi, M., Sheng, H., Thompson, J.W., Wang, L., Dubois, L.G., Gooden, D., Moseley, M., Paschen, W., Yang, W., 2014. Characterization of the ubiquitin-modified proteome regulated by transient forebrain ischemia. *J Cereb Blood Flow Metab* 34**,** 425-432.

Jang, M., Park, B.C., Lee, A.Y., Na, K.S., Kang, S., Bae, K.H., Myung, P.K., Chung, B.C., Cho, S., Lee, D.H., Park, S.G., 2007. Caspase-7 mediated cleavage of proteasome subunits during apoptosis. *Biochem Biophys Res Commun* 363**,** 388-394.

Jiang, X., Litkowski, P.E., Taylor, A.A., Lin, Y., Snider, B.J., Moulder, K.L., 2010. A role for the ubiquitin-proteasome system in activity-dependent presynaptic silencing. *J Neurosci* 30**,** 1798-1809.

Jin, J., Li, X., Gygi, S.P., Harper, J.W., 2007. Dual E1 activation systems for ubiquitin differentially regulate E2 enzyme charging. *Nature* 447**,** 1135-1138.

Johnson, J.W., Ascher, P., 1987. Glycine potentiates the NMDA response in cultured mouse brain neurons. *Nature* 325**,** 529-531.

Jonas, P., Burnashev, N., 1995. Molecular mechanisms controlling calcium entry through AMPA-type glutamate receptor channels. *Neuron* 15**,** 987-990.

Joshi, K.K., Chen, L., Torres, N., Tournier, V., Madura, K., 2011. A proteasome assembly defect in rpn3 mutants is associated with Rpn11 instability and increased sensitivity to stress. *J Mol Biol* 410**,** 383-399.

Ju, D., Xie, Y., 2004. Proteasomal degradation of RPN4 via two distinct mechanisms, ubiquitin-dependent and -independent. *J Biol Chem* 279**,** 23851-23854.

Jurd, R., Thornton, C., Wang, J., Luong, K., Phamluong, K., Kharazia, V., Gibb, S.L., Ron, D., 2008. Mind bomb-2 is an E3 ligase that ubiquitinates the N-methyl-D-aspartate receptor NR2B subunit in a phosphorylation-dependent manner. *J Biol Chem* 283**,** 301-310.

Kalejta, R.F., Shenk, T., 2003. Proteasome-dependent, ubiquitin-independent degradation of the Rb family of tumor suppressors by the human cytomegalovirus pp71 protein. *Proc Natl Acad Sci U S A* 100**,** 3263-3268.

Kamikubo, T., Hayashi, T., 1996. Changes in proteasome activity following transient ischemia. *Neurochem Int* 28**,** 209-212.

Kane, L.A., Lazarou, M., Fogel, A.I., Li, Y., Yamano, K., Sarraf, S.A., Banerjee, S., Youle, R.J., 2014. PINK1 phosphorylates ubiquitin to activate Parkin E3 ubiquitin ligase activity. *J Cell Biol* 205**,** 143-153.

Kannurpatti, S.S., Joshi, N.B., 1999. Energy metabolism and NAD-NADH redox state in brain slices in response to glutamate exposure and ischemia. *Metab Brain Dis* 14**,** 33-43.

Katchanov, J., Harms, C., Gertz, K., Hauck, L., Waeber, C., Hirt, L., Priller, J., von Harsdorf, R., Bruck, W., Hortnagl, H., Dirnagl, U., Bhide, P.G., Endres, M., 2001. Mild cerebral ischemia induces loss of cyclin-dependent kinase inhibitors and activation of cell cycle machinery before delayed neuronal cell death. *J Neurosci* 21**,** 5045-5053.

Katchanov, J., Waeber, C., Gertz, K., Gietz, A., Winter, B., Bruck, W., Dirnagl, U., Veh, R.W., Endres, M., 2003. Selective neuronal vulnerability following mild focal brain ischemia in the mouse. *Brain Pathol* 13**,** 452-464.

Kato, A., Rouach, N., Nicoll, R.A., Bredt, D.S., 2005. Activity-dependent NMDA receptor degradation mediated by retrotranslocation and ubiquitination. *Proc Natl Acad Sci U S A* 102**,** 5600-5605.

Kawamura, M., Nakajima, W., Ishida, A., Ohmura, A., Miura, S., Takada, G., 2005. Calpain inhibitor MDL 28170 protects hypoxic-ischemic brain injury in neonatal rats by inhibition of both apoptosis and necrosis. *Brain Res* 1037**,** 59-69.

Kawano, T., Morioka, M., Yano, S., Hamada, J., Ushio, Y., Miyamoto, E., Fukunaga, K., 2002. Decreased akt activity is associated with activation of forkhead transcription factor after transient forebrain ischemia in gerbil hippocampus. *J Cereb Blood Flow Metab* 22**,** 926-934.

Keller, J.N., Huang, F.F., Zhu, H., Yu, J., Ho, Y.S., Kindy, T.S., 2000. Oxidative stress-associated impairment of proteasome activity during ischemia-reperfusion injury. *J Cereb Blood Flow Metab* 20**,** 1467-1473.

Keller, J.N., Markesbery, W.R., 2000. Proteasome inhibition results in increased poly-ADP-ribosylation: implications for neuron death. *J Neurosci Res* 61**,** 436-442.

Khakh, B.S., Sofroniew, M.V., 2015. Diversity of astrocyte functions and phenotypes in neural circuits. *Nat Neurosci* 18**,** 942-952.

Khorchid, A., Ikura, M., 2002. How calpain is activated by calcium. *Nat Struct Biol* 9**,** 239-241.

Kim, C., Yun, N., Lee, Y.M., Jeong, J.Y., Baek, J.Y., Song, H.Y., Ju, C., Youdim, M.B., Jin, B.K., Kim, W.K., Oh, Y.J., 2013a. Gel-based protease proteomics for identifying the novel calpain substrates in dopaminergic neuronal cell. *J Biol Chem* 288**,** 36717-36732.

Kim, T., Mehta, S.L., Kaimal, B., Lyons, K., Dempsey, R.J., Vemuganti, R., 2016. Poststroke Induction of alpha-Synuclein Mediates Ischemic Brain Damage. *J Neurosci* 36**,** 7055-7065.

Kim, W., Bennett, E.J., Huttlin, E.L., Guo, A., Li, J., Possemato, A., Sowa, M.E., Rad, R., Rush, J., Comb, M.J., Harper, J.W., Gygi, S.P., 2011. Systematic and quantitative assessment of the ubiquitin-modified proteome. *Mol Cell* 44**,** 325-340.

Kim, Y.C., Li, X., Thompson, D., DeMartino, G.N., 2013b. ATP binding by proteasomal ATPases regulates cellular assembly and substrate-induced functions of the 26S proteasome. *J Biol Chem* 288**,** 3334-3345.

Kim, Y.C., Snoberger, A., Schupp, J., Smith, D.M., 2015. ATP binding to neighbouring subunits and intersubunit allosteric coupling underlie proteasomal ATPase function. *Nat Commun* 6**,** 8520.

Kimura, Y., Tanaka, K., 2010. Regulatory mechanisms involved in the control of ubiquitin homeostasis. *J Biochem* 147**,** 793-798.

Kirino, T., 1982. Delayed neuronal death in the gerbil hippocampus following ischemia. *Brain Res* 239**,** 57-69.

Kisselev, A.F., Akopian, T.N., Goldberg, A.L., 1998. Range of sizes of peptide products generated during degradation of different proteins by archaeal proteasomes. *J Biol Chem* 273**,** 1982-1989.

Kisselev, A.F., Akopian, T.N., Woo, K.M., Goldberg, A.L., 1999. The sizes of peptides generated from protein by mammalian 26 and 20S proteasomes. Implications for understanding the degradative mechanism and antigen presentation. *J Biol Chem* 274**,** 3363-3371.

Koh, J.Y., Goldberg, M.P., Hartley, D.M., Choi, D.W., 1990. Non-NMDA receptor-mediated neurotoxicity in cortical culture. *J Neurosci* 10**,** 693-705.

Köhler, A., Cascio, P., Leggett, D.S., Woo, K.M., Goldberg, A.L., Finley, D., 2001. The Axial Channel of the Proteasome Core Particle Is Gated by the Rpt2 ATPase and Controls Both Substrate Entry and Product Release. *Molecular Cell* 7**,** 1143-1152.

Komander, D., Clague, M.J., Urbe, S., 2009. Breaking the chains: structure and function of the deubiquitinases. *Nat Rev Mol Cell Biol* 10**,** 550-563.

Kostandy, B.B., 2012. The role of glutamate in neuronal ischemic injury: the role of spark in fire. *Neurol Sci* 33**,** 223-237.

Koulich, E., Li, X., DeMartino, G.N., 2008. Relative structural and functional roles of multiple deubiquitylating proteins associated with mammalian 26S proteasome. *Mol Biol Cell* 19**,** 1072-1082.

Kravchick, D.O., Karpova, A., Hrdinka, M., Lopez-Rojas, J., Iacobas, S., Carbonell, A.U., Iacobas, D.A., Kreutz, M.R., Jordan, B.A., 2016. Synaptonuclear messenger PRR7 inhibits c-Jun ubiquitination and regulates NMDA-mediated excitotoxicity. *EMBO J* 35**,** 1923-1934.

Kristian, T., Gido, G., Kuroda, S., Schutz, A., Siesjo, B.K., 1998. Calcium metabolism of focal and penumbral tissues in rats subjected to transient middle cerebral artery occlusion. *Exp Brain Res* 120**,** 503-509.

Kristian, T., Siesjo, B.K., 1998. Calcium in ischemic cell death. *Stroke* 29**,** 705-718.

Kumar, B., Kim, Y.C., DeMartino, G.N., 2010. The C terminus of Rpt3, an ATPase subunit of PA700 (19 S) regulatory complex, is essential for 26S proteasome assembly but not for activation. *J Biol Chem* 285**,** 39523-39535.

Kuryatov, A., Laube, B., Betz, H., Kuhse, J., 1994. Mutational analysis of the glycine-binding site of the NMDA receptor: structural similarity with bacterial amino acid-binding proteins. *Neuron* 12**,** 1291-1300.

Kutsuwada, T., Kashiwabuchi, N., Mori, H., Sakimura, K., Kushiya, E., Araki, K., Meguro, H., Masaki, H., Kumanishi, T., Arakawa, M., et al., 1992. Molecular diversity of the NMDA receptor channel. *Nature* 358**,** 36-41.

Kutsuwada, T., Sakimura, K., Manabe, T., Takayama, C., Katakura, N., Kushiya, E., Natsume, R., Watanabe, M., Inoue, Y., Yagi, T., Aizawa, S., Arakawa, M., Takahashi, T., Nakamura, Y., Mori, H., Mishina, M., 1996. Impairment of suckling response, trigeminal neuronal pattern formation, and hippocampal LTD in NMDA receptor epsilon 2 subunit mutant mice. *Neuron* 16**,** 333-344.

Lai, T.W., Zhang, S., Wang, Y.T., 2014. Excitotoxicity and stroke: identifying novel targets for neuroprotection. *Prog Neurobiol* 115**,** 157-188.

Lam, Y.A., Xu, W., DeMartino, G.N., Cohen, R.E., 1997. Editing of ubiquitin conjugates by an isopeptidase in the 26S proteasome. *Nature* 385**,** 737-740.

Lander, G.C., Estrin, E., Matyskiela, M.E., Bashore, C., Nogales, E., Martin, A., 2012. Complete subunit architecture of the proteasome regulatory particle. *Nature* 482**,** 186-191.

Latour, L.L., Kang, D.W., Ezzeddine, M.A., Chalela, J.A., Warach, S., 2004. Early blood-brain barrier disruption in human focal brain ischemia. *Ann Neurol* 56**,** 468-477.

Lau, C.G., Zukin, R.S., 2007. NMDA receptor trafficking in synaptic plasticity and neuropsychiatric disorders. *Nat Rev Neurosci* 8**,** 413-426.

Laube, B., Hirai, H., Sturgess, M., Betz, H., Kuhse, J., 1997. Molecular determinants of agonist discrimination by NMDA receptor subunits: analysis of the glutamate binding site on the NR2B subunit. *Neuron* 18**,** 493-503.

Lauwers, E., Jacob, C., Andre, B., 2009. K63-linked ubiquitin chains as a specific signal for protein sorting into the multivesicular body pathway. *J Cell Biol* 185**,** 493-502.

Le Tallec, B., Barrault, M.B., Guerois, R., Carre, T., Peyroche, A., 2009. Hsm3/S5b participates in the assembly pathway of the 19S regulatory particle of the proteasome. *Mol Cell* 33**,** 389-399.

Leal, G., Afonso, P.M., Salazar, I.L., Duarte, C.B., 2015. Regulation of hippocampal synaptic plasticity by BDNF. *Brain Res* 1621**,** 82-101.

Lee, B.H., Lee, M.J., Park, S., Oh, D.C., Elsasser, S., Chen, P.C., Gartner, C., Dimova, N., Hanna, J., Gygi, S.P., Wilson, S.M., King, R.W., Finley, D., 2010. Enhancement of proteasome activity by a small-molecule inhibitor of USP14. *Nature* 467**,** 179-184.

Lee, B.H., Lu, Y., Prado, M.A., Shi, Y., Tian, G., Sun, S., Elsasser, S., Gygi, S.P., King, R.W., Finley, D., 2016. USP14 deubiquitinates proteasome-bound substrates that are ubiquitinated at multiple sites. *Nature* 532**,** 398-401.

Lee, K.S., Frank, S., Vanderklish, P., Arai, A., Lynch, G., 1991. Inhibition of proteolysis protects hippocampal neurons from ischemia. *Proc Natl Acad Sci U S A* 88**,** 7233-7237.

Lee, M.J., Lee, B.H., Hanna, J., King, R.W., Finley, D., 2011a. Trimming of ubiquitin chains by proteasome-associated deubiquitinating enzymes. *Mol Cell Proteomics* 10**,** R110 003871.

Lee, S.Y., De la Mota-Peynado, A., Roelofs, J., 2011b. Loss of Rpt5 protein interactions with the core particle and Nas2 protein causes the formation of faulty proteasomes that are inhibited by Ecm29 protein. *J Biol Chem* 286**,** 36641-36651.

Lehmann, A., Janek, K., Braun, B., Kloetzel, P.M., Enenkel, C., 2002. 20S proteasomes are imported as precursor complexes into the nucleus of yeast. *J Mol Biol* 317**,** 401-413.

Li, L., Lundkvist, A., Andersson, D., Wilhelmsson, U., Nagai, N., Pardo, A.C., Nodin, C., Stahlberg, A., Aprico, K., Larsson, K., Yabe, T., Moons, L., Fotheringham, A., Davies, I., Carmeliet, P., Schwartz, J.P., Pekna, M., Kubista, M., Blomstrand, F., Maragakis, N., Nilsson, M., Pekny, M., 2008. Protective role of reactive astrocytes in brain ischemia. *J Cereb Blood Flow Metab* 28**,** 468-481.

Li, M., Sun, M., Cao, L., Gu, J.H., Ge, J., Chen, J., Han, R., Qin, Y.Y., Zhou, Z.P., Ding, Y., Qin, Z.H., 2014. A TIGAR-regulated metabolic pathway is critical for protection of brain ischemia. *J Neurosci* 34**,** 7458-7471.

Li, P.A., Howlett, W., He, Q.P., Miyashita, H., Siddiqui, M., Shuaib, A., 1998. Postischemic treatment with calpain inhibitor MDL 28170 ameliorates brain damage in a gerbil model of global ischemia. *Neurosci Lett* 247**,** 17-20.

Li, Q., Nakano, Y., Shang, J., Ohta, Y., Sato, K., Takemoto, M., Hishikawa, N., Yamashita, T., Abe, K., 2016. Temporal Profiles of Stress Protein Inductions after Focal Transient Ischemia in Mice Brain. *J Stroke Cerebrovasc Dis* 25**,** 2344-2351.

Li, W.L., Yu, S.P., Chen, D., Yu, S.S., Jiang, Y.J., Genetta, T., Wei, L., 2013. The regulatory role of NF-kappaB in autophagy-like cell death after focal cerebral ischemia in mice. *Neuroscience* 244**,** 16-30.

Lin, A., Hou, Q., Jarzylo, L., Amato, S., Gilbert, J., Shang, F., Man, H.Y., 2011. Nedd4-mediated AMPA receptor ubiquitination regulates receptor turnover and trafficking. *J Neurochem* 119**,** 27-39.

Lin, L., Chen, H., Zhang, Y., Lin, W., Liu, Y., Li, T., Zeng, Y., Chen, J., Du, H., Chen, R., Tan, Y., Liu, N., 2015. IL-10 Protects Neurites in Oxygen-Glucose-Deprived Cortical Neurons through the PI3K/Akt Pathway. *PLoS One* 10**,** e0136959.

Lipton, P., 1999. Ischemic cell death in brain neurons. *Physiol Rev* 79**,** 1431-1568.

Liu, B., Liao, M., Mielke, J.G., Ning, K., Chen, Y., Li, L., El-Hayek, Y.H., Gomez, E., Zukin, R.S., Fehlings, M.G., Wan, Q., 2006a. Ischemic insults direct glutamate receptor subunit 2-lacking AMPA receptors to synaptic sites. *J Neurosci* 26**,** 5309-5319.

Liu, C., Gao, Y., Barrett, J., Hu, B., 2010. Autophagy and protein aggregation after brain ischemia. *J Neurochem* 115**,** 68-78.

Liu, C.L., Ge, P., Zhang, F., Hu, B.R., 2005a. Co-translational protein aggregation after transient cerebral ischemia. *Neuroscience* 134**,** 1273-1284.

Liu, C.L., Martone, M.E., Hu, B.R., 2004. Protein ubiquitination in postsynaptic densities after transient cerebral ischemia. *J Cereb Blood Flow Metab* 24**,** 1219-1225.

Liu, C.W., Jacobson, A.D., 2013. Functions of the 19S complex in proteasomal degradation. *Trends Biochem Sci* 38**,** 103-110.

Liu, C.W., Li, X., Thompson, D., Wooding, K., Chang, T.L., Tang, Z., Yu, H., Thomas, P.J., DeMartino, G.N., 2006b. ATP binding and ATP hydrolysis play distinct roles in the function of 26S proteasome. *Mol Cell* 24**,** 39-50.

Liu, C.W., Strickland, E., Demartino, G.N., Thomas, P.J., 2005b. Recognition and processing of misfolded proteins by PA700, the 19S regulatory complex of the 26S proteasome. *Methods Mol Biol* 301**,** 71-81.

Liu, Y., Wong, T.P., Aarts, M., Rooyakkers, A., Liu, L., Lai, T.W., Wu, D.C., Lu, J., Tymianski, M., Craig, A.M., Wang, Y.T., 2007. NMDA receptor subunits have differential roles in mediating excitotoxic neuronal death both in vitro and in vivo. *J Neurosci* 27**,** 2846-2857.

Liu, Z., Cao, J., Gao, X., Ma, Q., Ren, J., Xue, Y., 2011. GPS-CCD: a novel computational program for the prediction of calpain cleavage sites. *PLoS One* 6**,** e19001.

Livnat-Levanon, N., Kevei, E., Kleifeld, O., Krutauz, D., Segref, A., Rinaldi, T., Erpapazoglou, Z., Cohen, M., Reis, N., Hoppe, T., Glickman, M.H., 2014. Reversible 26S proteasome disassembly upon mitochondrial stress. *Cell Rep* 7**,** 1371-1380.

Lobo, A.C., Gomes, J.R., Catarino, T., Mele, M., Fernandez, P., Inacio, A.R., Bahr, B.A., Santos, A.E., Wieloch, T., Carvalho, A.L., Duarte, C.B., 2011. Cleavage of the vesicular glutamate transporters under excitotoxic conditions. *Neurobiol Dis* 44**,** 292-303.

Lokireddy, S., Kukushkin, N.V., Goldberg, A.L., 2015. cAMP-induced phosphorylation of 26S proteasomes on Rpn6/PSMD11 enhances their activity and the degradation of misfolded proteins. *Proc Natl Acad Sci U S A* 112**,** E7176-7185.

Love, K.R., Catic, A., Schlieker, C., Ploegh, H.L., 2007. Mechanisms, biology and inhibitors of deubiquitinating enzymes. *Nat Chem Biol* 3**,** 697-705.

Luo, Y., Kuo, C.C., Shen, H., Chou, J., Greig, N.H., Hoffer, B.J., Wang, Y., 2009. Delayed treatment with a p53 inhibitor enhances recovery in stroke brain. *Ann Neurol* 65**,** 520-530.

Lussier, M.P., Herring, B.E., Nasu-Nishimura, Y., Neutzner, A., Karbowski, M., Youle, R.J., Nicoll, R.A., Roche, K.W., 2012. Ubiquitin ligase RNF167 regulates AMPA receptor-mediated synaptic transmission. *Proc Natl Acad Sci U S A* 109**,** 19426-19431.

Lussier, M.P., Nasu-Nishimura, Y., Roche, K.W., 2011. Activity-dependent ubiquitination of the AMPA receptor subunit GluA2. *J Neurosci* 31**,** 3077-3081.

Ma, H., Yang, H.Q., Takano, E., Lee, W.J., Hatanaka, M., Maki, M., 1993. Requirement of different subdomains of calpastatin for calpain inhibition and for binding to calmodulin-like domains. *J Biochem* 113**,** 591-599.

MacGregor, D.G., Avshalumov, M.V., Rice, M.E., 2003. Brain edema induced by in vitro ischemia: causal factors and neuroprotection. *J Neurochem* 85**,** 1402-1411.

Macrez, R., Ali, C., Toutirais, O., Le Mauff, B., Defer, G., Dirnagl, U., Vivien, D., 2011. Stroke and the immune system: from pathophysiology to new therapeutic strategies. *Lancet Neurol* 10**,** 471-480.

Maestre, C., Delgado-Esteban, M., Gomez-Sanchez, J.C., Bolanos, J.P., Almeida, A., 2008. Cdk5 phosphorylates Cdh1 and modulates cyclin B1 stability in excitotoxicity. *EMBO J* 27**,** 2736-2745.

Magnusson, K., Wieloch, T., 1989. Impairment of protein ubiquitination may cause delayed neuronal death. *Neurosci Lett* 96**,** 264-270.

Mahajan, S.S., Thai, K.H., Chen, K., Ziff, E., 2011. Exposure of neurons to excitotoxic levels of glutamate induces cleavage of the RNA editing enzyme, adenosine deaminase acting on RNA 2, and loss of GLUR2 editing. *Neuroscience* 189**,** 305-315.

Maki, M., Takano, E., Mori, H., Sato, A., Murachi, T., Hatanaka, M., 1987. All four internally repetitive domains of pig calpastatin possess inhibitory activities against calpains I and II. *FEBS Lett* 223**,** 174-180.

Manev, H., Favaron, M., Guidotti, A., Costa, E., 1989. Delayed increase of Ca^{2+} influx elicited by glutamate: role in neuronal death. *Mol Pharmacol* 36**,** 106-112.

Markgraf, C.G., Velayo, N.L., Johnson, M.P., McCarty, D.R., Medhi, S., Koehl, J.R., Chmielewski, P.A., Linnik, M.D., 1998. Six-hour window of opportunity for calpain inhibition in focal cerebral ischemia in rats. *Stroke* 29**,** 152-158.

Martinez-Sanchez, M., Striggow, F., Schroder, U.H., Kahlert, S., Reymann, K.G., Reiser, G., 2004. Na^{+} and Ca^{2+} homeostasis pathways, cell death and protection after oxygen-glucose-deprivation in organotypic hippocampal slice cultures. *Neuroscience* 128**,** 729-740.

Martorell-Riera, A., Segarra-Mondejar, M., Munoz, J.P., Ginet, V., Olloquequi, J., Perez-Clausell, J., Palacin, M., Reina, M., Puyal, J., Zorzano, A., Soriano, F.X., 2014. Mfn2 downregulation in excitotoxicity causes mitochondrial dysfunction and delayed neuronal death. *EMBO J* 33**,** 2388-2407.

Matos, C.A., Nobrega, C., Louros, S.R., Almeida, B., Ferreiro, E., Valero, J., Pereira de Almeida, L., Macedo-Ribeiro, S., Carvalho, A.L., 2016. Ataxin-3 phosphorylation decreases neuronal defects in spinocerebellar ataxia type 3 models. *J Cell Biol* 212**,** 465-480.

Matthews, E.A., Schoch, S., Dietrich, D., 2013. Tuning local calcium availability: cell-type-specific immobile calcium buffer capacity in hippocampal neurons. *J Neurosci* 33**,** 14431-14445.

Mayer, M.L., Westbrook, G.L., Guthrie, P.B., 1984. Voltage-dependent block by Mg^{2+} of NMDA responses in spinal cord neurones. *Nature* 309**,** 261-263.

McGinnis, K.M., Gnegy, M.E., Park, Y.H., Mukerjee, N., Wang, K.K., 1999. Procaspase-3 and poly(ADP)ribose polymerase (PARP) are calpain substrates. *Biochem Biophys Res Commun* 263**,** 94-99.

McIlwain, D.R., Berger, T., Mak, T.W., 2015. Caspase functions in cell death and disease. *Cold Spring Harb Perspect Biol* 7.

Mele, M., Aspromonte, M.C., Duarte, C.B., 2016. Downregulation of GABAA Receptor Recycling Mediated by HAP1 Contributes to Neuronal Death in In Vitro Brain Ischemia. *Mol Neurobiol*.

Mele, M., Ribeiro, L., Inacio, A.R., Wieloch, T., Duarte, C.B., 2014. GABA(A) receptor dephosphorylation followed by internalization is coupled to neuronal death in in vitro ischemia. *Neurobiol Dis* 65**,** 220-232.

Meller, R., 2009. The role of the ubiquitin proteasome system in ischemia and ischemic tolerance. *Neuroscientist* 15**,** 243-260.

Meller, R., Cameron, J.A., Torrey, D.J., Clayton, C.E., Ordonez, A.N., Henshall, D.C., Minami, M., Schindler, C.K., Saugstad, J.A., Simon, R.P., 2006. Rapid degradation of Bim by the ubiquitin-proteasome pathway mediates short-term ischemic tolerance in cultured neurons. *J Biol Chem* 281**,** 7429-7436.

Meller, R., Thompson, S.J., Lusardi, T.A., Ordonez, A.N., Ashley, M.D., Jessick, V., Wang, W., Torrey, D.J., Henshall, D.C., Gafken, P.R., Saugstad, J.A., Xiong, Z.G., Simon, R.P., 2008. Ubiquitin proteasome-mediated synaptic reorganization: a novel mechanism underlying rapid ischemic tolerance. *J Neurosci* 28**,** 50-59.

Melloni, E., Averna, M., Stifanese, R., De Tullio, R., Defranchi, E., Salamino, F., Pontremoli, S., 2006. Association of calpastatin with inactive calpain: a novel mechanism to control the activation of the protease? *J Biol Chem* 281**,** 24945-24954.

Melo, C.V., Okumoto, S., Gomes, J.R., Baptista, M.S., Bahr, B.A., Frommer, W.B., Duarte, C.B., 2013. Spatiotemporal resolution of BDNF neuroprotection against glutamate excitotoxicity in cultured hippocampal neurons. *Neuroscience* 237**,** 66-86.

Mengesdorf, T., Althausen, S., Mies, G., Olah, L., Paschen, W., 2002. Phosphorylation state, solubility, and activity of calcium/calmodulin-dependent protein kinase II alpha in transient focal ischemia in mouse brain. *Neurochem Res* 27**,** 477-484.

Mengual, E., Arizti, P., Rodrigo, J., Gimenez-Amaya, J.M., Castano, J.G., 1996. Immunohistochemical distribution and electron microscopic subcellular localization of the proteasome in the rat CNS. *J Neurosci* 16**,** 6331-6341.

Meyer, D.A., Torres-Altoro, M.I., Tan, Z., Tozzi, A., Di Filippo, M., DiNapoli, V., Plattner, F., Kansy, J.W., Benkovic, S.A., Huber, J.D., Miller, D.B., Greengard, P., Calabresi, P., Rosen, C.L., Bibb, J.A., 2014. Ischemic stroke injury is mediated by aberrant Cdk5. *J Neurosci* 34**,** 8259-8267.

Miao, S., Chen, R., Ye, J., Tan, G.H., Li, S., Zhang, J., Jiang, Y.H., Xiong, Z.Q., 2013. The Angelman syndrome protein Ube3a is required for polarized dendrite morphogenesis in pyramidal neurons. *J Neurosci* 33**,** 327-333.

Min, M., Mevissen, T.E., De Luca, M., Komander, D., Lindon, C., 2015. Efficient APC/C substrate degradation in cells undergoing mitotic exit depends on K11 ubiquitin linkages. *Mol Biol Cell* 26**,** 4325-4332.

Mir, S., Sen, T., Sen, N., 2014. Cytokine-induced GAPDH sulfhydration affects PSD95 degradation and memory. *Mol Cell* 56**,** 786-795.

Miyawaki, T., Ofengeim, D., Noh, K.M., Latuszek-Barrantes, A., Hemmings, B.A., Follenzi, A., Zukin, R.S., 2009. The endogenous inhibitor of Akt, CTMP, is critical to ischemia-induced neuronal death. *Nat Neurosci* 12**,** 618-626.

Moldoveanu, T., Gehring, K., Green, D.R., 2008. Concerted multi-pronged attack by calpastatin to occlude the catalytic cleft of heterodimeric calpains. *Nature* 456**,** 404-408.

Molinari, M., Maki, M., Carafoli, E., 1995. Purification of mu-calpain by a novel affinity chromatography approach. New insights into the mechanism of the interaction of the protease with targets. *J Biol Chem* 270**,** 14576-14581.

Montero, M., Nielsen, M., Ronn, L.C., Moller, A., Noraberg, J., Zimmer, J., 2007. Neuroprotective effects of the AMPA antagonist PNQX in oxygen-glucose deprivation in mouse hippocampal slice cultures and global cerebral ischemia in gerbils. *Brain Res* 1177**,** 124-135.

Monyer, H., Burnashev, N., Laurie, D.J., Sakmann, B., Seeburg, P.H., 1994. Developmental and regional expression in the rat brain and functional properties of four NMDA receptors. *Neuron* 12**,** 529-540.

Monyer, H., Sprengel, R., Schoepfer, R., Herb, A., Higuchi, M., Lomeli, H., Burnashev, N., Sakmann, B., Seeburg, P.H., 1992. Heteromeric NMDA receptors: molecular and functional distinction of subtypes. *Science* 256**,** 1217-1221.

Morimoto, T., Ide, T., Ihara, Y., Tamura, A., Kirino, T., 1996. Transient ischemia depletes free ubiquitin in the gerbil hippocampal CA1 neurons. *Am J Pathol* 148**,** 249-257.

Moskowitz, M.A., Lo, E.H., Iadecola, C., 2010. The science of stroke: mechanisms in search of treatments. *Neuron* 67**,** 181-198.

Murata, S., Yashiroda, H., Tanaka, K., 2009. Molecular mechanisms of proteasome assembly. *Nat Rev Mol Cell Biol* 10**,** 104-115.

Na, C.H., Jones, D.R., Yang, Y., Wang, X., Xu, Y., Peng, J., 2012. Synaptic protein ubiquitination in rat brain revealed by antibody-based ubiquitome analysis. *J Proteome Res* 11**,** 4722-4732.

Nag, D.K., Finley, D., 2012. A small-molecule inhibitor of deubiquitinating enzyme USP14 inhibits Dengue virus replication. *Virus Res* 165**,** 103-106.

Nakagawa, T., Yuan, J., 2000. Cross-talk between two cysteine protease families. Activation of caspase-12 by calpain in apoptosis. *J Cell Biol* 150**,** 887-894.

Nathan, J.A., Kim, H.T., Ting, L., Gygi, S.P., Goldberg, A.L., 2013. Why do cellular proteins linked to K63-polyubiquitin chains not associate with proteasomes? *EMBO J* 32**,** 552-565.

Neumar, R.W., Hagle, S.M., DeGracia, D.J., Krause, G.S., White, B.C., 1996. Brain mu-calpain autolysis during global cerebral ischemia. *J Neurochem* 66**,** 421-424.

Neumar, R.W., Meng, F.H., Mills, A.M., Xu, Y.A., Zhang, C., Welsh, F.A., Siman, R., 2001. Calpain activity in the rat brain after transient forebrain ischemia. *Exp Neurol* 170**,** 27-35.

Nguyen, D., Alavi, M.V., Kim, K.Y., Kang, T., Scott, R.T., Noh, Y.H., Lindsey, J.D., Wissinger, B., Ellisman, M.H., Weinreb, R.N., Perkins, G.A., Ju, W.K., 2011. A new vicious cycle involving glutamate excitotoxicity, oxidative stress and mitochondrial dynamics. *Cell Death Dis* 2**,** e240.

Nishitoh, H., Matsuzawa, A., Tobiume, K., Saegusa, K., Takeda, K., Inoue, K., Hori, S., Kakizuka, A., Ichijo, H., 2002. ASK1 is essential for endoplasmic reticulum stress-induced neuronal cell death triggered by expanded polyglutamine repeats. *Genes Dev* 16**,** 1345-1355.

Noga, M., Hayashi, T., 1996. Ubiquitin gene expression following transient forebrain ischemia. *Brain Res Mol Brain Res* 36**,** 261-267.

Noh, K.M., Yokota, H., Mashiko, T., Castillo, P.E., Zukin, R.S., Bennett, M.V., 2005. Blockade of calcium-permeable AMPA receptors protects hippocampal neurons against global ischemia-induced death. *Proc Natl Acad Sci U S A* 102**,** 12230-12235.

Noshita, N., Lewen, A., Sugawara, T., Chan, P.H., 2001. Evidence of phosphorylation of Akt and neuronal survival after transient focal cerebral ischemia in mice. *J Cereb Blood Flow Metab* 21**,** 1442-1450.

Nowak, L., Bregestovski, P., Ascher, P., Herbet, A., Prochiantz, A., 1984. Magnesium gates glutamate-activated channels in mouse central neurones. *Nature* 307**,** 462-465.

O'Hare, M.J., Kushwaha, N., Zhang, Y., Aleyasin, H., Callaghan, S.M., Slack, R.S., Albert, P.R., Vincent, I., Park, D.S., 2005. Differential roles of nuclear and cytoplasmic cyclin-dependent kinase 5 in apoptotic and excitotoxic neuronal death. *J Neurosci* 25**,** 8954-8966.

Obermeier, B., Daneman, R., Ransohoff, R.M., 2013. Development, maintenance and disruption of the blood-brain barrier. *Nat Med* 19**,** 1584-1596.

Oh, C., Park, S., Lee, E.K., Yoo, Y.J., 2013. Downregulation of ubiquitin level via knockdown of polyubiquitin gene Ubb as potential cancer therapeutic intervention. *Sci Rep* 3**,** 2623.

Olney, J.W., 1969. Brain lesions, obesity, and other disturbances in mice treated with monosodium glutamate. *Science* 164**,** 719-721.

Olsen, S.K., Lima, C.D., 2013. Structure of a ubiquitin E1-E2 complex: insights to E1-E2 thioester transfer. *Mol Cell* 49**,** 884-896.

Ono, Y., Saido, T.C., Sorimachi, H., 2016. Calpain research for drug discovery: challenges and potential. *Nat Rev Drug Discov*.

Ono, Y., Sorimachi, H., 2012. Calpains: an elaborate proteolytic system. *Biochim Biophys Acta* 1824**,** 224-236.

Opitz, T., Grooms, S.Y., Bennett, M.V., Zukin, R.S., 2000. Remodeling of alpha-amino-3-hydroxy-5-methyl-4-isoxazole-propionic acid receptor subunit composition in hippocampal neurons after global ischemia. *Proc Natl Acad Sci U S A* 97**,** 13360-13365.

Orlowski, M., Wilk, S., 2000. Catalytic activities of the 20S proteasome, a multicatalytic proteinase complex. *Arch Biochem Biophys* 383**,** 1-16.

Ostwald, K., Hayashi, M., Nakamura, M., Kawashima, S., 1994. Subcellular distribution of calpain and calpastatin immunoreactivity and fodrin proteolysis in rabbit hippocampus after hypoxia and glucocorticoid treatment. *J Neurochem* 63**,** 1069-1076.

Ouyang, Y.B., Tan, Y., Comb, M., Liu, C.L., Martone, M.E., Siesjo, B.K., Hu, B.R., 1999. Survival- and death-promoting events after transient cerebral ischemia: phosphorylation of Akt, release of cytochrome C and Activation of caspase-like proteases. *J Cereb Blood Flow Metab* 19**,** 1126-1135.

Ouyang, Y.B., Xu, L., Giffard, R.G., 2005. Geldanamycin treatment reduces delayed CA1 damage in mouse hippocampal organotypic cultures subjected to oxygen glucose deprivation. *Neurosci Lett* 380**,** 229-233.

Pal, G.P., De Veyra, T., Elce, J.S., Jia, Z., 2003. Crystal structure of a micro-like calpain reveals a partially activated conformation with low Ca^{2+} requirement. *Structure* 11**,** 1521-1526.

Paoletti, P., Bellone, C., Zhou, Q., 2013. NMDA receptor subunit diversity: impact on receptor properties, synaptic plasticity and disease. *Nat Rev Neurosci* 14**,** 383-400.

Papadia, S., Soriano, F.X., Leveille, F., Martel, M.A., Dakin, K.A., Hansen, H.H., Kaindl, A., Sifringer, M., Fowler, J., Stefovska, V., McKenzie, G., Craigon, M., Corriveau, R., Ghazal, P., Horsburgh, K., Yankner, B.A., Wyllie, D.J., Ikonomidou, C., Hardingham, G.E., 2008. Synaptic NMDA receptor activity boosts intrinsic antioxidant defenses. *Nat Neurosci* 11**,** 476-487.

Papadia, S., Stevenson, P., Hardingham, N.R., Bading, H., Hardingham, G.E., 2005. Nuclear Ca^{2+} and the cAMP response element-binding protein family mediate a late phase of activity-dependent neuroprotection. *J Neurosci* 25**,** 4279-4287.

Pathare, G.R., Nagy, I., Bohn, S., Unverdorben, P., Hubert, A., Korner, R., Nickell, S., Lasker, K., Sali, A., Tamura, T., Nishioka, T., Forster, F., Baumeister, W., Bracher, A., 2012. The proteasomal subunit Rpn6 is a molecular clamp holding the core and regulatory subcomplexes together. *Proc Natl Acad Sci U S A* 109**,** 149-154.

Patrick, G.N., Bingol, B., Weld, H.A., Schuman, E.M., 2003. Ubiquitin-mediated proteasome activity is required for agonist-induced endocytosis of GluRs. *Current Biology* 13**,** 2073-2081.

Patrick, G.N., Zukerberg, L., Nikolic, M., de la Monte, S., Dikkes, P., Tsai, L.H., 1999. Conversion of p35 to p25 deregulates Cdk5 activity and promotes neurodegeneration. *Nature* 402**,** 615-622.

Paul, S., Nairn, A.C., Wang, P., Lombroso, P.J., 2003. NMDA-mediated activation of the tyrosine phosphatase STEP regulates the duration of ERK signaling. *Nat Neurosci* 6**,** 34-42.

Pellegrini-Giampietro, D.E., Gorter, J.A., Bennett, M.V., Zukin, R.S., 1997. The GluR2 (GluR-B) hypothesis: Ca^{2+}-permeable AMPA receptors in neurological disorders. *Trends Neurosci* 20**,** 464-470.

Peng, P.L., Zhong, X., Tu, W., Soundarapandian, M.M., Molner, P., Zhu, D., Lau, L., Liu, S., Liu, F., Lu, Y., 2006. ADAR2-dependent RNA editing of AMPA receptor subunit GluR2 determines vulnerability of neurons in forebrain ischemia. *Neuron* 49**,** 719-733.

Peterson, D.W., Ando, D.M., Taketa, D.A., Zhou, H., Dahlquist, F.W., Lew, J., 2010. No difference in kinetics of tau or histone phosphorylation by CDK5/p25 versus CDK5/p35 in vitro. *Proc Natl Acad Sci U S A* 107**,** 2884-2889.

Peth, A., Besche, H.C., Goldberg, A.L., 2009. Ubiquitinated proteins activate the proteasome by binding to Usp14/Ubp6, which causes 20S gate opening. *Mol Cell* 36**,** 794-804.

Peth, A., Kukushkin, N., Bosse, M., Goldberg, A.L., 2013. Ubiquitinated proteins activate the proteasomal ATPases by binding to Usp14 or Uch37 homologs. *J Biol Chem* 288**,** 7781-7790.

Phillips, J.B., Williams, A.J., Adams, J., Elliott, P.J., Tortella, F.C., 2000. Proteasome inhibitor PS519 reduces infarction and attenuates leukocyte infiltration in a rat model of focal cerebral ischemia. *Stroke* 31**,** 1686-1693.

Pinto, M.J., Almeida, R.D., 2016. Puzzling out presynaptic differentiation. *J Neurochem*.(in press)

Ponnappan, S., Palmieri, M., Sullivan, D.H., Ponnappan, U., 2013. Compensatory increase in USP14 activity accompanies impaired proteasomal proteolysis during aging. *Mech Ageing Dev* 134**,** 53-59.

Pulsinelli, W.A., Brierley, J.B., Plum, F., 1982. Temporal profile of neuronal damage in a model of transient forebrain ischemia. *Ann Neurol* 11**,** 491-498.

Qiu, J.H., Asai, A., Chi, S., Saito, N., Hamada, H., Kirino, T., 2000. Proteasome inhibitors induce cytochrome c-caspase-3-like protease-mediated apoptosis in cultured cortical neurons. *J Neurosci* 20**,** 259-265.

Rami, A., Krieglstein, J., 1993. Protective effects of calpain inhibitors against neuronal damage caused by cytotoxic hypoxia in vitro and ischemia in vivo. *Brain Res* 609**,** 67-70.

Rauner, C., Kohr, G., 2011. Triheteromeric NR1/NR2A/NR2B receptors constitute the major N-methyl-D-aspartate receptor population in adult hippocampal synapses. *J Biol Chem* 286**,** 7558-7566.

Rehni, A.K., Singh, T.G., Behl, N., Arora, S., 2010. Possible involvement of ubiquitin proteasome system and other proteases in acute and delayed aspects of ischemic preconditioning of brain in mice. *Biol Pharm Bull* 33**,** 1953-1957.

Reinheckel, T., Sitte, N., Ullrich, O., Kuckelkorn, U., Davies, K.J., Grune, T., 1998. Comparative resistance of the 20S and 26S proteasome to oxidative stress. *Biochem J* 335 (Pt 3)**,** 637-642.

Roberts-Lewis, J.M., Savage, M.J., Marcy, V.R., Pinsker, L.R., Siman, R., 1994. Immunolocalization of calpain I-mediated spectrin degradation to vulnerable neurons in the ischemic gerbil brain. *J Neurosci* 14**,** 3934-3944.

Rogers, S., Wells, R., Rechsteiner, M., 1986. Amino acid sequences common to rapidly degraded proteins: the PEST hypothesis. *Science* 234**,** 364-368.

Rong, R., Yang, H., Rong, L., Wei, X., Li, Q., Liu, X., Gao, H., Xu, Y., Zhang, Q., 2016. Proteomic analysis of PSD-93 knockout mice following the induction of ischemic cerebral injury. *Neurotoxicology* 53**,** 1-11.

Rosenzweig, R., Bronner, V., Zhang, D., Fushman, D., Glickman, M.H., 2012. Rpn1 and Rpn2 coordinate ubiquitin processing factors at proteasome. *J Biol Chem* 287**,** 14659-14671.

Rosenzweig, R., Osmulski, P.A., Gaczynska, M., Glickman, M.H., 2008. The central unit within the 19S regulatory particle of the proteasome. *Nat Struct Mol Biol* 15**,** 573-580.

Rossi, D.J., Oshima, T., Attwell, D., 2000. Glutamate release in severe brain ischaemia is mainly by reversed uptake. *Nature* 403**,** 316-321.

Ruiz-Vela, A., Gonzalez de Buitrago, G., Martinez, A.C., 1999. Implication of calpain in caspase activation during B cell clonal deletion. *EMBO J* 18**,** 4988-4998.

Ruschak, A.M., Slassi, M., Kay, L.E., Schimmer, A.D., 2011. Novel proteasome inhibitors to overcome bortezomib resistance. *J Natl Cancer Inst* 103**,** 1007-1017.

Ryu, K.Y., Maehr, R., Gilchrist, C.A., Long, M.A., Bouley, D.M., Mueller, B., Ploegh, H.L., Kopito, R.R., 2007. The mouse polyubiquitin gene UbC is essential for fetal liver development, cell-cycle progression and stress tolerance. *EMBO J* 26**,** 2693-2706.

Saeki, Y., Kudo, T., Sone, T., Kikuchi, Y., Yokosawa, H., Toh-e, A., Tanaka, K., 2009. Lysine 63-linked polyubiquitin chain may serve as a targeting signal for the 26S proteasome. *EMBO J* 28**,** 359-371.

Sahtoe, D.D., Sixma, T.K., 2015. Layers of DUB regulation. *Trends Biochem Sci* 40**,** 456-467.

Saido, T.C., Yokota, M., Nagao, S., Yamaura, I., Tani, E., Tsuchiya, T., Suzuki, K., Kawashima, S., 1993. Spatial resolution of fodrin proteolysis in postischemic brain. *J Biol Chem* 268**,** 25239-25243.

Sakata, E., Bohn, S., Mihalache, O., Kiss, P., Beck, F., Nagy, I., Nickell, S., Tanaka, K., Saeki, Y., Forster, F., Baumeister, W., 2012. Localization of the proteasomal ubiquitin receptors Rpn10 and Rpn13 by electron cryomicroscopy. *Proc Natl Acad Sci U S A* 109**,** 1479-1484.

Sakimura, K., Kutsuwada, T., Ito, I., Manabe, T., Takayama, C., Kushiya, E., Yagi, T., Aizawa, S., Inoue, Y., Sugiyama, H., et al., 1995. Reduced hippocampal LTP and spatial learning in mice lacking NMDA receptor epsilon 1 subunit. *Nature* 373**,** 151-155.

Salazar, I.L., Caldeira, M.V., Curcio, M., Duarte, C.B., 2016. The Role of Proteases in Hippocampal Synaptic Plasticity: Putting Together Small Pieces of a Complex Puzzle. *Neurochem Res* 41**,** 156-182.

Santamaria, P.G., Finley, D., Ballesta, J.P., Remacha, M., 2003. Rpn6p, a proteasome subunit from Saccharomyces cerevisiae, is essential for the assembly and activity of the 26S proteasome. *J Biol Chem* 278**,** 6687-6695.

Sareen-Khanna, K., Papillon, J., Wing, S.S., Cybulsky, A.V., 2016. Role of the deubiquitinating enzyme ubiquitin-specific protease-14 in proteostasis in renal cells. *Am J Physiol Renal Physiol* 311**,** F1035-F1046.

Sattler, R., Xiong, Z., Lu, W.Y., MacDonald, J.F., Tymianski, M., 2000. Distinct roles of synaptic and extrasynaptic NMDA receptors in excitotoxicity. *J Neurosci* 20**,** 22-33.

Saver, J.L., Starkman, S., Eckstein, M., Stratton, S.J., Pratt, F.D., Hamilton, S., Conwit, R., Liebeskind, D.S., Sung, G., Kramer, I., Moreau, G., Goldweber, R., Sanossian, N., Investigators, F.-M., Coordinators, 2015. Prehospital use of magnesium sulfate as neuroprotection in acute stroke. *N Engl J Med* 372**,** 528-536.

Schad, E., Farkas, A., Jekely, G., Tompa, P., Friedrich, P., 2002. A novel human small subunit of calpains. *Biochem J* 362**,** 383-388.

Schielke, G.P., Kupina, N.C., Boxer, P.A., Bigge, C.F., Welty, D.F., Iadecola, C., 1999. The neuroprotective effect of the novel AMPA receptor antagonist PD152247 (PNQX) in temporary focal ischemia in the rat. *Stroke* 30**,** 1472-1477.

Schlesinger, D.H., Goldstein, G., Niall, H.D., 1975. The complete amino acid sequence of ubiquitin, an adenylate cyclase stimulating polypeptide probably universal in living cells. *Biochemistry* 14**,** 2214-2218.

Schoch, K.M., von Reyn, C.R., Bian, J., Telling, G.C., Meaney, D.F., Saatman, K.E., 2013. Brain injury-induced proteolysis is reduced in a novel calpastatin-overexpressing transgenic mouse. *J Neurochem* 125**,** 909-920.

Schreiber, J., Vegh, M.J., Dawitz, J., Kroon, T., Loos, M., Labonte, D., Li, K.W., Van Nierop, P., Van Diepen, M.T., De Zeeuw, C.I., Kneussel, M., Meredith, R.M., Smit, A.B., Van Kesteren, R.E., 2015. Ubiquitin ligase TRIM3 controls hippocampal plasticity and learning by regulating synaptic gamma-actin levels. *J Cell Biol* 211**,** 569-586.

Schreiner, P., Chen, X., Husnjak, K., Randles, L., Zhang, N., Elsasser, S., Finley, D., Dikic, I., Walters, K.J., Groll, M., 2008. Ubiquitin docking at the proteasome through a novel pleckstrin-homology domain interaction. *Nature* 453**,** 548-552.

Schubert, U., Anton, L.C., Gibbs, J., Norbury, C.C., Yewdell, J.W., Bennink, J.R., 2000. Rapid degradation of a large fraction of newly synthesized proteins by proteasomes. *Nature* 404**,** 770-774.

Schwarz, L.A., Hall, B.J., Patrick, G.N., 2010. Activity-dependent ubiquitination of GluA1 mediates a distinct AMPA receptor endocytosis and sorting pathway. *J Neurosci* 30**,** 16718-16729.

Schweitzer, A., Aufderheide, A., Rudack, T., Beck, F., Pfeifer, G., Plitzko, J.M., Sakata, E., Schulten, K., Forster, F., Baumeister, W., 2016. Structure of the human 26S proteasome at a resolution of 3.9 A. *Proc Natl Acad Sci U S A* 113**,** 7816-7821.

Scudder, S.L., Goo, M.S., Cartier, A.E., Molteni, A., Schwarz, L.A., Wright, R., Patrick, G.N., 2014. Synaptic strength is bidirectionally controlled by opposing activity-dependent regulation of Nedd4-1 and USP8. *J Neurosci* 34**,** 16637-16649.

Seyfried, D.M., Veyna, R., Han, Y., Li, K., Tang, N., Betts, R.L., Weinsheimer, S., Chopp, M., Anagli, J., 2001. A selective cysteine protease inhibitor is non-toxic and cerebroprotective in rats undergoing transient middle cerebral artery ischemia. *Brain Res* 901**,** 94-101.

Shang, F., Gong, X., Taylor, A., 1997. Activity of ubiquitin-dependent pathway in response to oxidative stress. Ubiquitin-activating enzyme is transiently up-regulated. *J Biol Chem* 272**,** 23086-23093.

Shi, Y., Chen, X., Elsasser, S., Stocks, B.B., Tian, G., Lee, B.H., Shi, Y., Zhang, N., de Poot, S.A., Tuebing, F., Sun, S., Vannoy, J., Tarasov, S.G., Engen, J.R., Finley, D., Walters, K.J., 2016a. Rpn1 provides adjacent receptor sites for substrate binding and deubiquitination by the proteasome. *Science* 351.

Shi, Y., Zhang, L., Pu, H., Mao, L., Hu, X., Jiang, X., Xu, N., Stetler, R.A., Zhang, F., Liu, X., Leak, R.K., Keep, R.F., Ji, X., Chen, J., 2016b. Rapid endothelial cytoskeletal reorganization enables early

blood-brain barrier disruption and long-term ischaemic reperfusion brain injury. *Nat Commun* 7**,** 10523.

Shin, S.M., Zhang, N., Hansen, J., Gerges, N.Z., Pak, D.T., Sheng, M., Lee, S.H., 2012. GKAP orchestrates activity-dependent postsynaptic protein remodeling and homeostatic scaling. *Nat Neurosci* 15**,** 1655-1666.

Shinkai-Ouchi, F., Koyama, S., Ono, Y., Hata, S., Ojima, K., Shindo, M., duVerle, D., Ueno, M., Kitamura, F., Doi, N., Takigawa, I., Mamitsuka, H., Sorimachi, H., 2016. Predictions of Cleavability of Calpain Proteolysis by Quantitative Structure-Activity Relationship Analysis Using Newly Determined Cleavage Sites and Catalytic Efficiencies of an Oligopeptide Array. *Mol Cell Proteomics* 15**,** 1262-1280.

Shringarpure, R., Grune, T., Mehlhase, J., Davies, K.J., 2003. Ubiquitin conjugation is not required for the degradation of oxidized proteins by proteasome. *J Biol Chem* 278**,** 311-318.

Silva, G.M., Finley, D., Vogel, C., 2015. K63 polyubiquitination is a new modulator of the oxidative stress response. *Nat Struct Mol Biol* 22**,** 116-123.

Smith, D.M., Chang, S.C., Park, S., Finley, D., Cheng, Y., Goldberg, A.L., 2007. Docking of the proteasomal ATPases' carboxyl termini in the 20S proteasome's alpha ring opens the gate for substrate entry. *Mol Cell* 27**,** 731-744.

Soares, L.M., De Vry, J., Steinbusch, H.W., Milani, H., Prickaerts, J., Weffort de Oliveira, R.M., 2016. Rolipram improves cognition, reduces anxiety- and despair-like behaviors and impacts hippocampal neuroplasticity after transient global cerebral ischemia. *Neuroscience* 326**,** 69-83.

Sokolova, V., Li, F., Polovin, G., Park, S., 2015. Proteasome Activation is Mediated via a Functional Switch of the Rpt6 C-terminal Tail Following Chaperone-dependent Assembly. *Sci Rep* 5**,** 14909.

Song, M., Yu, S.P., 2014. Ionic regulation of cell volume changes and cell death after ischemic stroke. *Transl Stroke Res* 5**,** 17-27.

Sorimachi, H., Hata, S., Ono, Y., 2011a. Calpain chronicle--an enzyme family under multidisciplinary characterization. *Proc Jpn Acad Ser B Phys Biol Sci* 87**,** 287-327.

Sorimachi, H., Hata, S., Ono, Y., 2011b. Impact of genetic insights into calpain biology. *J Biochem* 150**,** 23-37.

Sorimachi, H., Mamitsuka, H., Ono, Y., 2012. Understanding the substrate specificity of conventional calpains. *Biol Chem* 393**,** 853-871.

Spyracopoulos, L., 2016. The Proteasome: More Than a Means to an End. *Structure* 24**,** 1221-1223.

Stanika, R.I., Pivovarova, N.B., Brantner, C.A., Watts, C.A., Winters, C.A., Andrews, S.B., 2009. Coupling diverse routes of calcium entry to mitochondrial dysfunction and glutamate excitotoxicity. *Proc Natl Acad Sci U S A* 106**,** 9854-9859.

Stern, P., Behe, P., Schoepfer, R., Colquhoun, D., 1992. Single-channel conductances of NMDA receptors expressed from cloned cDNAs: comparison with native receptors. *Proc Biol Sci* 250**,** 271-277.

Storey, G.P., Opitz-Araya, X., Barria, A., 2011. Molecular determinants controlling NMDA receptor synaptic incorporation. *J Neurosci* 31**,** 6311-6316.

Strobl, S., Fernandez-Catalan, C., Braun, M., Huber, R., Masumoto, H., Nakagawa, K., Irie, A., Sorimachi, H., Bourenkow, G., Bartunik, H., Suzuki, K., Bode, W., 2000. The crystal structure of calcium-free human m-calpain suggests an electrostatic switch mechanism for activation by calcium. *Proc Natl Acad Sci U S A* 97**,** 588-592.

Sun, X.M., Butterworth, M., MacFarlane, M., Dubiel, W., Ciechanover, A., Cohen, G.M., 2004. Caspase activation inhibits proteasome function during apoptosis. *Mol Cell* 14**,** 81-93.

Swaney, D.L., Rodriguez-Mias, R.A., Villen, J., 2015. Phosphorylation of ubiquitin at Ser65 affects its polymerization, targets, and proteome-wide turnover. *EMBO Rep* 16**,** 1131-1144.

Swanson, G.T., Kamboj, S.K., Cull-Candy, S.G., 1997. Single-channel properties of recombinant AMPA receptors depend on RNA editing, splice variation, and subunit composition. *J Neurosci* 17**,** 58-69.

Szlanka, T., Haracska, L., Kiss, I., Deak, P., Kurucz, E., Ando, I., Viragh, E., Udvardy, A., 2003. Deletion of proteasomal subunit S5a/Rpn10/p54 causes lethality, multiple mitotic defects and overexpression of proteasomal genes in Drosophila melanogaster. *J Cell Sci* 116**,** 1023-1033.

Taglialatela, G., Kaufmann, J.A., Trevino, A., Perez-Polo, J.R., 1998. Central nervous system DNA fragmentation induced by the inhibition of nuclear factor kappa B. *Neuroreport* 9**,** 489-493.

Tai, H.C., Besche, H., Goldberg, A.L., Schuman, E.M., 2010. Characterization of the Brain 26S Proteasome and its Interacting Proteins. *Front Mol Neurosci* 3.

Takagi, K., Kim, S., Yukii, H., Ueno, M., Morishita, R., Endo, Y., Kato, K., Tanaka, K., Saeki, Y., Mizushima, T., 2012. Structural basis for specific recognition of Rpt1p, an ATPase subunit of 26S proteasome, by proteasome-dedicated chaperone Hsm3p. *J Biol Chem* 287**,** 12172-12182.

Takano, E., Ma, H., Yang, H.Q., Maki, M., Hatanaka, M., 1995. Preference of calcium-dependent interactions between calmodulin-like domains of calpain and calpastatin subdomains. *FEBS Lett* 362**,** 93-97.

Takano, E., Yumoto, N., Kannagi, R., Murachi, T., 1984. Molecular diversity of calpastatin in mammalian organs. *Biochem Biophys Res Commun* 122**,** 912-917.

Takano, J., Tomioka, M., Tsubuki, S., Higuchi, M., Iwata, N., Itohara, S., Maki, M., Saido, T.C., 2005. Calpain mediates excitotoxic DNA fragmentation via mitochondrial pathways in adult brains: evidence from calpastatin mutant mice. *J Biol Chem* 280**,** 16175-16184.

Thein, S., Tao-Cheng, J.H., Li, Y., Bayer, K.U., Reese, T.S., Dosemeci, A., 2014. CaMKII mediates recruitment and activation of the deubiquitinase CYLD at the postsynaptic density. *PLoS One* 9**,** e91312.

Thrower, J.S., Hoffman, L., Rechsteiner, M., Pickart, C.M., 2000. Recognition of the polyubiquitin proteolytic signal. *EMBO J* 19**,** 94-102.

Todi, S.V., Paulson, H.L., 2011. Balancing act: deubiquitinating enzymes in the nervous system. *Trends Neurosci* 34**,** 370-382.

Tomko, R.J., Jr., Hochstrasser, M., 2011. Incorporation of the Rpn12 subunit couples completion of proteasome regulatory particle lid assembly to lid-base joining. *Mol Cell* 44**,** 907-917.

Tomko, R.J., Jr., Hochstrasser, M., 2013. Molecular architecture and assembly of the eukaryotic proteasome. *Annu Rev Biochem* 82**,** 415-445.

Tompa, P., Buzder-Lantos, P., Tantos, A., Farkas, A., Szilagyi, A., Banoczi, Z., Hudecz, F., Friedrich, P., 2004. On the sequential determinants of calpain cleavage. *J Biol Chem* 279**,** 20775-20785.

Tompa, P., Mucsi, Z., Orosz, G., Friedrich, P., 2002. Calpastatin subdomains A and C are activators of calpain. *J Biol Chem* 277**,** 9022-9026.

Traynelis, S.F., Wollmuth, L.P., McBain, C.J., Menniti, F.S., Vance, K.M., Ogden, K.K., Hansen, K.B., Yuan, H., Myers, S.J., Dingledine, R., 2010. Glutamate receptor ion channels: structure, regulation, and function. *Pharmacol Rev* 62**,** 405-496.

Tsai, N.P., Wilkerson, J.R., Guo, W., Maksimova, M.A., DeMartino, G.N., Cowan, C.W., Huber, K.M., 2012. Multiple autism-linked genes mediate synapse elimination via proteasomal degradation of a synaptic scaffold PSD-95. *Cell* 151**,** 1581-1594.

Tsvetkov, P., Myers, N., Eliav, R., Adamovich, Y., Hagai, T., Adler, J., Navon, A., Shaul, Y., 2014. NADH binds and stabilizes the 26S proteasomes independent of ATP. *J Biol Chem* 289**,** 11272-11281.

Tu, J., Zhang, X., Zhu, Y., Dai, Y., Li, N., Yang, F., Zhang, Q., Brann, D.W., Wang, R., 2015. Cell-Permeable Peptide Targeting the Nrf2-Keap1 Interaction: A Potential Novel Therapy for Global Cerebral Ischemia. *J Neurosci* 35**,** 14727-14739.

Ullian, E.M., Barkis, W.B., Chen, S., Diamond, J.S., Barres, B.A., 2004. Invulnerability of retinal ganglion cells to NMDA excitotoxicity. *Mol Cell Neurosci* 26**,** 544-557.

Vaden, J.H., Bhattacharyya, B.J., Chen, P.C., Watson, J.A., Marshall, A.G., Phillips, S.E., Wilson, J.A., King, G.D., Miller, R.J., Wilson, S.M., 2015. Ubiquitin-specific protease 14 regulates c-Jun N-terminal kinase signaling at the neuromuscular junction. *Mol Neurodegener* 10**,** 3.

Vieira, M.M., Schmidt, J., Ferreira, J.S., She, K., Oku, S., Mele, M., Santos, A.E., Duarte, C.B., Craig, A.M., Carvalho, A.L., 2016. Multiple domains in the C-terminus of NMDA receptor GluN2B subunit contribute to neuronal death following in vitro ischemia. *Neurobiol Dis* 89**,** 223-234.

Vilchez, D., Boyer, L., Morantte, I., Lutz, M., Merkwirth, C., Joyce, D., Spencer, B., Page, L., Masliah, E., Berggren, W.T., Gage, F.H., Dillin, A., 2012a. Increased proteasome activity in human embryonic stem cells is regulated by PSMD11. *Nature* 489**,** 304-308.

Vilchez, D., Morantte, I., Liu, Z., Douglas, P.M., Merkwirth, C., Rodrigues, A.P., Manning, G., Dillin, A., 2012b. RPN-6 determines C. elegans longevity under proteotoxic stress conditions. *Nature* 489**,** 263-268.

Vosler, P.S., Gao, Y., Brennan, C.S., Yanagiya, A., Gan, Y., Cao, G., Zhang, F., Morley, S.J., Sonenberg, N., Bennett, M.V., Chen, J., 2011. Ischemia-induced calpain activation causes eukaryotic (translation) initiation factor 4G1 (eIF4GI) degradation, protein synthesis inhibition, and neuronal death. *Proc Natl Acad Sci U S A* 108**,** 18102-18107.

Waataja, J.J., Kim, H.J., Roloff, A.M., Thayer, S.A., 2008. Excitotoxic loss of post-synaptic sites is distinct temporally and mechanistically from neuronal death. *J Neurochem* 104**,** 364-375.

Waite, K.A., De-La Mota-Peynado, A., Vontz, G., Roelofs, J., 2016. Starvation Induces Proteasome Autophagy with Different Pathways for Core and Regulatory Particles. *J Biol Chem* 291**,** 3239-3253.

Wang, C.F., Huang, Y.S., 2012. Calpain 2 activated through N-methyl-D-aspartic acid receptor signaling cleaves CPEB3 and abrogates CPEB3-repressed translation in neurons. *Mol Cell Biol* 32**,** 3321-3332.

Wang, D., Zong, C., Koag, M.C., Wang, Y., Drews, O., Fang, C., Scruggs, S.B., Ping, P., 2011. Proteome dynamics and proteome function of cardiac 19S proteasomes. *Mol Cell Proteomics* 10**,** M110 006122.

Wang, F., Durfee, L.A., Huibregtse, J.M., 2013a. A cotranslational ubiquitination pathway for quality control of misfolded proteins. *Mol Cell* 50**,** 368-378.

Wang, K.K., 2000. Calpain and caspase: can you tell the difference? *Trends Neurosci* 23**,** 20-26.

Wang, N., Chen, W., Linsel-Nitschke, P., Martinez, L.O., Agerholm-Larsen, B., Silver, D.L., Tall, A.R., 2003. A PEST sequence in ABCA1 regulates degradation by calpain protease and stabilization of ABCA1 by apoA-I. *J Clin Invest* 111**,** 99-107.

Wang, Y., Briz, V., Chishti, A., Bi, X., Baudry, M., 2013b. Distinct roles for mu-calpain and m-calpain in synaptic NMDAR-mediated neuroprotection and extrasynaptic NMDAR-mediated neurodegeneration. *J Neurosci* 33**,** 18880-18892.

Wang, Y., Song, J.H., Denisova, J.V., Park, W.M., Fontes, J.D., Belousov, A.B., 2012. Neuronal gap junction coupling is regulated by glutamate and plays critical role in cell death during neuronal injury. *J Neurosci* 32**,** 713-725.

Weberruss, M.H., Savulescu, A.F., Jando, J., Bissinger, T., Harel, A., Glickman, M.H., Enenkel, C., 2013. Blm10 facilitates nuclear import of proteasome core particles. *EMBO J* 32**,** 2697-2707.

Wei, G., Yin, Y., Li, W., Bito, H., She, H., Mao, Z., 2012. Calpain-mediated degradation of myocyte enhancer factor 2D contributes to excitotoxicity by activation of extrasynaptic N-methyl-D-aspartate receptors. *J Biol Chem* 287**,** 5797-5805.

Weih, M., Schmitt, M., Gieche, J., Harms, C., Ruscher, K., Dirnagl, U., Grune, T., 2001. Proteolysis of oxidized proteins after oxygen-glucose deprivation in rat cortical neurons is mediated by the proteasome. *J Cereb Blood Flow Metab* 21**,** 1090-1096.

Weilinger, N.L., Lohman, A.W., Rakai, B.D., Ma, E.M., Bialecki, J., Maslieieva, V., Rilea, T., Bandet, M.V., Ikuta, N.T., Scott, L., Colicos, M.A., Teskey, G.C., Winship, I.R., Thompson, R.J., 2016. Metabotropic NMDA receptor signaling couples Src family kinases to pannexin-1 during excitotoxicity. *Nat Neurosci* 19**,** 432-442.

White, R.J., Reynolds, I.J., 1995. Mitochondria and Na^+/Ca^{2+} exchange buffer glutamate-induced calcium loads in cultured cortical neurons. *J Neurosci* 15**,** 1318-1328.

Widagdo, J., Chai, Y.J., Ridder, M.C., Chau, Y.Q., Johnson, R.C., Sah, P., Huganir, R.L., Anggono, V., 2015. Activity-Dependent Ubiquitination of GluA1 and GluA2 Regulates AMPA Receptor Intracellular Sorting and Degradation. *Cell Rep* 10**,** 783-795.

Wilkinson, K.D., Urban, M.K., Haas, A.L., 1980. Ubiquitin is the ATP-dependent proteolysis factor I of rabbit reticulocytes. *J Biol Chem* 255**,** 7529-7532.

Williams, A.J., Berti, R., Dave, J.R., Elliot, P.J., Adams, J., Tortella, F.C., 2004. Delayed treatment of ischemia/reperfusion brain injury: extended therapeutic window with the proteosome inhibitor MLN519. *Stroke* 35**,** 1186-1191.

Williams, A.J., Hale, S.L., Moffett, J.R., Dave, J.R., Elliott, P.J., Adams, J., Tortella, F.C., 2003. Delayed treatment with MLN519 reduces infarction and associated neurologic deficit caused by focal ischemic brain injury in rats via antiinflammatory mechanisms involving nuclear factor-kappaB activation, gliosis, and leukocyte infiltration. *J Cereb Blood Flow Metab* 23**,** 75-87.

Williams, A.J., Myers, T.M., Cohn, S.I., Sharrow, K.M., Lu, X.C., Tortella, F.C., 2005. Recovery from ischemic brain injury in the rat following a 10 h delayed injection with MLN519. *Pharmacol Biochem Behav* 81**,** 182-189.

Wojcik, C., 2002. Regulation of apoptosis by the ubiquitin and proteasome pathway. *J Cell Mol Med* 6**,** 25-48.

Wojcik, C., DeMartino, G.N., 2002. Analysis of Drosophila 26S proteasome using RNA interference. *J Biol Chem* 277**,** 6188-6197.

Wroge, C.M., Hogins, J., Eisenman, L., Mennerick, S., 2012. Synaptic NMDA receptors mediate hypoxic excitotoxic death. *J Neurosci* 32**,** 6732-6742.

Wyllie, D.J., Behe, P., Nassar, M., Schoepfer, R., Colquhoun, D., 1996. Single-channel currents from recombinant NMDA NR1a/NR2D receptors expressed in Xenopus oocytes. *Proc Biol Sci* 263**,** 1079-1086.

Wyllie, D.J., Livesey, M.R., Hardingham, G.E., 2013. Influence of GluN2 subunit identity on NMDA receptor function. *Neuropharmacology* 74**,** 4-17.

Xu, D., Shan, B., Lee, B.H., Zhu, K., Zhang, T., Sun, H., Liu, M., Shi, L., Liang, W., Qian, L., Xiao, J., Wang, L., Pan, L., Finley, D., Yuan, J., 2015. Phosphorylation and activation of ubiquitin-specific protease-14 by Akt regulates the ubiquitin-proteasome system. *Elife* 4**,** e10510.

Xu, D., Shan, B., Sun, H., Xiao, J., Zhu, K., Xie, X., Li, X., Liang, W., Lu, X., Qian, L., Yuan, J., 2016. USP14 regulates autophagy by suppressing K63 ubiquitination of Beclin 1. *Genes Dev* 30**,** 1718-1730.

Xu, J., Kurup, P., Zhang, Y., Goebel-Goody, S.M., Wu, P.H., Hawasli, A.H., Baum, M.L., Bibb, J.A., Lombroso, P.J., 2009a. Extrasynaptic NMDA receptors couple preferentially to excitotoxicity via calpain-mediated cleavage of STEP. *J Neurosci* 29**,** 9330-9343.

Xu, P., Duong, D.M., Seyfried, N.T., Cheng, D., Xie, Y., Robert, J., Rush, J., Hochstrasser, M., Finley, D., Peng, J., 2009b. Quantitative proteomics reveals the function of unconventional ubiquitin chains in proteasomal degradation. *Cell* 137**,** 133-145.

Xu, W., Wong, T.P., Chery, N., Gaertner, T., Wang, Y.T., Baudry, M., 2007. Calpain-mediated mGluR1alpha truncation: a key step in excitotoxicity. *Neuron* 53**,** 399-412.

Yamauchi, T., Sakurai, M., Abe, K., Matsumiya, G., Sawa, Y., 2008. Ubiquitin-mediated stress response in the spinal cord after transient ischemia. *Stroke* 39**,** 1883-1889.

Yang, H.Q., Ma, H., Takano, E., Hatanaka, M., Maki, M., 1994. Analysis of calcium-dependent interaction between amino-terminal conserved region of calpastatin functional domain and calmodulin-like domain of mu-calpain large subunit. *J Biol Chem* 269**,** 18977-18984.

Yano, S., Morioka, M., Fukunaga, K., Kawano, T., Hara, T., Kai, Y., Hamada, J., Miyamoto, E., Ushio, Y., 2001. Activation of Akt/protein kinase B contributes to induction of ischemic tolerance in the CA1 subfield of gerbil hippocampus. *J Cereb Blood Flow Metab* 21**,** 351-360.

Yao, T., Song, L., Xu, W., DeMartino, G.N., Florens, L., Swanson, S.K., Washburn, M.P., Conaway, R.C., Conaway, J.W., Cohen, R.E., 2006. Proteasome recruitment and activation of the Uch37 deubiquitinating enzyme by Adrm1. *Nat Cell Biol* 8**,** 994-1002.

Yao, X., Liu, J., McCabe, J.T., 2007. Ubiquitin and ubiquitin-conjugated protein expression in the rat cerebral cortex and hippocampus following traumatic brain injury (TBI). *Brain Res* 1182**,** 116-122.

Yao, X., Liu, J., McCabe, J.T., 2008. Alterations of cerebral cortex and hippocampal proteasome subunit expression and function in a traumatic brain injury rat model. *J Neurochem* 104**,** 353-363.

Ye, Y., Rape, M., 2009. Building ubiquitin chains: E2 enzymes at work. *Nat Rev Mol Cell Biol* 10**,** 755-764.

Yedidi, R.S., Fatehi, A.K., Enenkel, C., 2016. Proteasome dynamics between proliferation and quiescence stages of Saccharomyces cerevisiae. *Crit Rev Biochem Mol Biol***,** 1-16.

Yerbury, J.J., Ooi, L., Dillin, A., Saunders, D.N., Hatters, D.M., Beart, P.M., Cashman, N.R., Wilson, M.R., Ecroyd, H., 2016. Walking the tightrope: proteostasis and neurodegenerative disease. *J Neurochem* 137**,** 489-505.

Yi, J.J., Ehlers, M.D., 2007. Emerging roles for ubiquitin and protein degradation in neuronal function. *Pharmacol Rev* 59**,** 14-39.

Yokota, M., Saido, T.C., Tani, E., Kawashima, S., Suzuki, K., 1995. Three distinct phases of fodrin proteolysis induced in postischemic hippocampus. Involvement of calpain and unidentified protease. *Stroke* 26**,** 1901-1907.

Yokota, M., Tani, E., Tsubuki, S., Yamaura, I., Nakagaki, I., Hori, S., Saido, T.C., 1999. Calpain inhibitor entrapped in liposome rescues ischemic neuronal damage. *Brain Res* 819**,** 8-14.

Zadran, S., Jourdi, H., Rostamiani, K., Qin, Q., Bi, X., Baudry, M., 2010. Brain-derived neurotrophic factor and epidermal growth factor activate neuronal m-calpain via mitogen-activated protein kinase-dependent phosphorylation. *J Neurosci* 30**,** 1086-1095.

Zhang, F., Liu, C.L., Hu, B.R., 2006a. Irreversible aggregation of protein synthesis machinery after focal brain ischemia. *J Neurochem* 98**,** 102-112.

Zhang, L., Zhang, Z.G., Buller, B., Jiang, J., Jiang, Y., Zhao, D., Liu, X., Morris, D., Chopp, M., 2010. Combination treatment with VELCADE and low-dose tissue plasminogen activator provides potent neuroprotection in aged rats after embolic focal ischemia. *Stroke* 41**,** 1001-1007.

Zhang, L., Zhang, Z.G., Liu, X., Hozeska, A., Stagliano, N., Riordan, W., Lu, M., Chopp, M., 2006b. Treatment of embolic stroke in rats with bortezomib and recombinant human tissue plasminogen activator. *Thromb Haemost* 95**,** 166-173.

Zhang, L., Zhang, Z.G., Zhang, R.L., Lu, M., Adams, J., Elliott, P.J., Chopp, M., 2001. Postischemic (6-Hour) treatment with recombinant human tissue plasminogen activator and proteasome inhibitor PS-519 reduces infarction in a rat model of embolic focal cerebral ischemia. *Stroke* 32**,** 2926-2931.

Zhang, M., Li, W.B., Geng, J.X., Li, Q.J., Sun, X.C., Xian, X.H., Qi, J., Li, S.Q., 2007. The upregulation of glial glutamate transporter-1 participates in the induction of brain ischemic tolerance in rats. *J Cereb Blood Flow Metab* 27**,** 1352-1368.

Zhang, Q.G., Xu, Y.L., Li, H.C., Han, D., Zhang, G.Y., 2006c. NMDA receptor/L-VGCC-dependent expression and AMPA/KA receptor-dependent activation of c-Jun induced by cerebral ischemia in rat hippocampus. *Neurosci Lett* 398**,** 268-273.

Zhang, R., Xu, M., Wang, Y., Xie, F., Zhang, G., Qin, X., 2016. Nrf2-a Promising Therapeutic Target for Defensing Against Oxidative Stress in Stroke. *Mol Neurobiol*.

Zhang, S.J., Buchthal, B., Lau, D., Hayer, S., Dick, O., Schwaninger, M., Veltkamp, R., Zou, M., Weiss, U., Bading, H., 2011. A signaling cascade of nuclear calcium-CREB-ATF3 activated by synaptic NMDA receptors defines a gene repression module that protects against extrasynaptic NMDA receptor-induced neuronal cell death and ischemic brain damage. *J Neurosci* 31**,** 4978-4990.

Zhang, X., Yan, H., Yuan, Y., Gao, J., Shen, Z., Cheng, Y., Shen, Y., Wang, R.R., Wang, X., Hu, W.W., Wang, G., Chen, Z., 2013. Cerebral ischemia-reperfusion-induced autophagy protects against neuronal injury by mitochondrial clearance. *Autophagy* 9**,** 1321-1333.

Zhou, J., Du, T., Li, B., Rong, Y., Verkhratsky, A., Peng, L., 2015. Crosstalk Between MAPK/ERK and PI3K/AKT Signal Pathways During Brain Ischemia/Reperfusion. *ASN Neuro* 7.

Zhou, M., Baudry, M., 2006. Developmental changes in NMDA neurotoxicity reflect developmental changes in subunit composition of NMDA receptors. *J Neurosci* 26**,** 2956-2963.

Zhou, X., Ding, Q., Chen, Z., Yun, H., Wang, H., 2013. Involvement of the GluN2A and GluN2B subunits in synaptic and extrasynaptic N-methyl-D-aspartate receptor function and neuronal excitotoxicity. *J Biol Chem* 288**,** 24151-24159.

Zhou, Y., Danbolt, N.C., 2014. Glutamate as a neurotransmitter in the healthy brain. *J Neural Transm (Vienna)* 121**,** 799-817.

Zhou, Y., Takahashi, E., Li, W., Halt, A., Wiltgen, B., Ehninger, D., Li, G.D., Hell, J.W., Kennedy, M.B., Silva, A.J., 2007. Interactions between the NR2B receptor and CaMKII modulate synaptic plasticity and spatial learning. *J Neurosci* 27**,** 13843-13853.

Zhu, H., Yoshimoto, T., Imajo-Ohmi, S., Dazortsava, M., Mathivanan, A., Yamashima, T., 2012. Why are hippocampal CA1 neurons vulnerable but motor cortex neurons resistant to transient ischemia? *J Neurochem* 120**,** 574-585.

Ziv, I., Matiuhin, Y., Kirkpatrick, D.S., Erpapazoglou, Z., Leon, S., Pantazopoulou, M., Kim, W., Gygi, S.P., Haguenauer-Tsapis, R., Reis, N., Glickman, M.H., Kleifeld, O., 2011. A perturbed ubiquitin landscape distinguishes between ubiquitin in trafficking and in proteolysis. *Mol Cell Proteomics* 10**,** M111 009753.